

Small Molecule-Protein Interactions Exemplified on Short-Chain Dehydrogenases/Reductases

Inauguraldissertation

zur

Erlangung der Würde eines Doktors der Philosophie

vorgelegt der

Philosophisch-Naturwissenschaftlichen Fakultät

der Universität Basel

von

Katharina Richarda Beck,
aus Balzers, Fürstentum Liechtenstein

Basel, 2017

Originaldokument gespeichert auf dem Dokumentenserver der Universität Basel

edoc.unibas.ch



Dieses Werk ist lizenziert unter einer [Creative Commons Namensnennung-Nicht kommerziell 4.0 International Lizenz](https://creativecommons.org/licenses/by-nc/4.0/).

Genehmigt von der Philosophisch-Naturwissenschaftlichen Fakultät
auf Antrag von Prof. Dr. Alex Odermatt und Prof. Dr. Michael Arand

Basel, den 19.09.2017

Dekan
Prof. Dr. Martin Spiess

Table of content

1. Summary	4
2. Short-chain dehydrogenase/reductase superfamily	6
2.1. Published review articles:.....	8
2.1.1. Pharmacophore Models and Pharmacophore-Based Virtual Screening: Concepts and Applications Exemplified on Hydroxysteroid Dehydrogenases	8
2.1.2. Virtual screening applications in short-chain dehydrogenase/reductase research	43
3. Endocrine disrupting chemicals	67
3.1. 11 β -hydroxysteroid dehydrogenase type 2	67
3.1.1. Published article: Inhibition of 11 β -hydroxysteroid dehydrogenase 2 by the fungicides itraconazole and posaconazole	69
3.1.2. Discussion	81
3.2. <i>In vitro</i> testing systems – validation - limitations.....	85
3.2.1. Published article: Evaluation of tetrabromobisphenol A effects on human glucocorticoid and androgen receptors: a comparison of results from human- with yeast-based in vitro assays.....	87
3.2.2. Discussion	99
4. Substrate identification.....	103
4.1. 11 β -hydroxysteroid dehydrogenase type 1	103
4.1.1. Oxysterol metabolism.....	106
4.1.2. Human metabolome and lipid maps structure database screening	127
4.2. DHRS7	134
4.3. Carbonyl reductase 1.....	137
4.3.1. Published article: Carbonyl reductase 1 catalyses 20 β -reduction of glucocorticoids, modulating corticosteroid receptor activation and metabolic complications of obesity.....	138
4.4. Discussion	165
5. Appendix	169
6. Acknowledgement	173
7. References.....	174

1. Summary

The short-chain dehydrogenase/reductase (SDRs) family represents one of the largest enzyme superfamilies, with over 80 members in the human genome. Even though the human genome project has sequenced and mapped the entire human genome, the physiological functions of more than 70% of all SDRs are currently unexplored or insufficiently characterized. To start to fill this gap, the present thesis aimed to employ a combination of molecular modeling approaches and biological assessments for the identification and characterization of novel inhibitors and/or potential substrates of different SDRs.

Due to their involvement in steroid biosynthesis and metabolism, SDRs are potential targets of endocrine disrupting chemicals (EDCs). To test the use of pharmacophore-based virtual screening (VS) applications and subsequent *in vitro* evaluation of virtual hits for the identification and characterization of potential inhibitors, 11 β -hydroxysteroid dehydrogenase 2 (11 β -HSD2) was selected as an example. 11 β -HSD2 has an important role in the placenta by inactivating cortisol and protecting the fetus from high maternal glucocorticoid levels. An impaired placental 11 β -HSD2 function has been associated with altered fetal growth and angiogenesis as well as a higher risk for cardio-metabolic diseases in later life. Despite this vital function, 11 β -HSD2 is not covered in common off-target screening approaches. Several azole fungicides were identified as 11 β -HSD inhibitors amongst approved drugs by testing selected virtually retrieved hits for inhibition of cortisol to cortisone conversion in cell lysates expressing recombinant human 11 β -HSD2. Moreover, a significant structure-activity relationship between azole scaffold size, 11 β -HSD enzyme selectivity and potency was observed. The most potent 11 β -HSD2 inhibition was obtained for itraconazole (IC₅₀ 139 \pm 14 nM), for its active metabolite hydroxyitraconazole (IC₅₀ 223 \pm 31 nM), and for posaconazole (IC₅₀ 460 \pm 98 nM). Interestingly, substantially lower inhibitory 11 β -HSD2 activity of these compounds was detected using mouse and rat kidney homogenate preparations, indicating species-specific differences. Impaired placental 11 β -HSD2 function exerted by these compounds might, in addition to the known inhibition of P-glycoprotein efflux transport and cytochrome P450 enzymes, lead to locally elevated cortisol levels and thereby could affect fetal programming.

Successful employment of pharmacophore-based VS applications requires suitable and reliable *in vitro* validation strategies. Therefore, the following study addressed the re-evaluation of a potential EDC, the widely used flame retardant tetrabromobisphenol A (TBBPA), on glucocorticoid receptor (GR) and androgen receptor (AR) function. TBBPA was reported earlier in yeast-based reporter assays to potentially interfere with GR and moderately with AR function. Human HEK-293 cell-based reporter assays and cell-free receptor binding assays did not show any activity of TBBPA on GR function, which was supported by molecular docking calculations. The antiandrogenic effect, however, could be confirmed, although less pronounced than in the HEK-293 cell system. Nevertheless, the evaluation of the relevant concentrations of an EDC found in the human body is crucial for an appropriate safety assessment. Considering the rapid metabolism of TBBPA and the low concentrations observed in the human body, it is questionable whether relevant concentrations can be reached to cause harmful effects. Thus, it is vital to take the limitations of each testing system including the distinct sensitivities and specificities into account to avoid false positive or false negative results.

To extend the applications of *in silico* tools with demonstrated proof-of-concept, they were further employed to investigate novel substrate specificities for three different SDR members: the two multi-functional enzymes, 11 β -HSD1 and carbonyl reductase (CBR) 1 as well as the orphan enzyme DHRS7.

A role for 11 β -HSD1 in oxysterol metabolism by metabolizing 7-ketocholesterol (7kC) has already been described. However, in contrast to the known receptors for 7 α ,25-dihydroxycholesterol (7 α 25OHC), i.e. Epstein-Barr virus-induced gene 2 (EBI2), or 7 β ,27-dihydroxycholesterol (7 β 27OHC), i.e. retinoic acid related orphan receptor (ROR) γ , no endogenous receptor has been identified so far for 7kC or its metabolite 7 β -hydroxycholesterol. To explore the underlying biosynthetic pathways of such

dihydroxylated oxysterols, the role of 11 β -HSD1 in the generation of dihydroxylated oxysterols was investigated. For the first time, the stereospecific and seemingly irreversible oxoreduction of 7-keto,25-hydroxycholesterol (7k25OHC) and 7-keto,27-hydroxycholesterol (7k27OHC) to their corresponding 7 β -hydroxylated metabolites 7 β 25OHC and 7 β 27OHC by recombinant human 11 β -HSD1 could be demonstrated *in vitro* in intact HEK-293 cells. Furthermore, 7k25OHC and 7k27OHC were found to be potently inhibited the 11 β -HSD1-dependent oxoreduction of cortisone to cortisol. Molecular modeling experiments confirmed these results and suggested competition of 7k25OHC and 7k27OHC with cortisone in the enzyme binding pocket.

For a more detailed enzyme characterization, 11 β -HSD1 pharmacophore models were generated and employed for VS of the human metabolome database and the lipidmaps structure database. The VS yielded several hundred virtual hits, including the successful filtering of known substrates such as endogenous 11-ketoglucocorticoids, synthetic glucocorticoids, 7kC, and several bile acids known to inhibit the enzyme. Further hits comprised several eicosanoids including prostaglandins, leukotrienes, cyclopentenone isoprostanes, levuglandins or hydroxyeicosatetraenoic acids (HETEs) and compounds of the kynurenine pathway. The important role of these compounds as well as 11 β -HSD1 in inflammation emphasizes a potential association. However, further biological validation is of utmost necessity to explore a potential link.

The closest relative of 11 β -HSD1 is the orphan enzyme DHR7, which has been suggested to act as tumor suppressor. Among others, cortisone and 5 α -dihydrotestosterone have been identified as substrates of DHR7, although effects in functional assays could only be observed at high concentrations that may not be of physiological relevance. Hence, the existence of other yet unexplored substrates of DHR7 can be assumed, and the generation of homology models to study the structural features of the substrate binding site of DHR7 was employed. The predictivity of the constructed models is currently limited, due to a highly variable region comprising a part of the ligand binding site but particularly the entry of the binding pocket, and requires further optimizations. Nevertheless, the models generally displayed a cone-shaped binding site with a rather hydrophobic core. This may suggest larger metabolites to be converted by DHR7. Moreover, the flexible loops surrounding the binding pocket may lead to the induction of an induced fit upon ligand binding. However, further studies are crucial to confirm these findings.

CBR1 is well-known for its role in phase I metabolism of a variety of carbonyl containing xenobiotic compounds. Several endogenous substrates of CBR1 have been reported such as prostaglandins, S-nitrosoglutathione or lipid aldehydes. The physiological relevance of these endogenous substrates, however, is not fully understood. Thus, the physiological roles of CBR1 was further explored by identifying a novel function for CBR1 in the metabolism glucocorticoids. CBR1 was found to catalyze the conversion of cortisol into 20 β -dihydrocortisol (20 β -DHF), which was in turn detected as the major route of cortisol metabolism in horses and elevated in adipose tissue derived from obese horses, humans and mice. Additionally, 20 β -DHF was demonstrated as weak endogenous agonist of the GR, suggesting a novel pathway to modulate GR activation by CBR1-dependent protection against excessive GR activation in obesity.

In conclusion, this thesis emphasized the employment of molecular modeling approaches as an initial filter to identify toxicological relevant compound classes for the identification of potential EDCs and, moreover, as valuable tools to identify novel substrates of multifunctional SDRs and to unravel novel functions for the large majority of yet unexplored orphan SDR members, while carefully considering the limitations of this strategy.

2. Short-chain dehydrogenase/reductase superfamily

The family of short-chain dehydrogenases/reductases (SDRs) comprise more than 47,000 members, thus, representing one of the largest enzyme superfamilies [1]. SDRs are present in almost all domains of life, from archaea to bacteria, and eukaryota, with over 80 members described in the human genome [2, 3], emphasizing their significant and versatile role in distinct metabolic processes, such as the metabolism of steroid hormones, oxysterols, bile acids, fatty acid derivatives, prostaglandins, retinoids, amino acids, carbohydrates, and xenobiotics or redox sensor mechanisms [4].

SDRs generally share a low primary sequence identity of about 15-25% but they have common structural features. The basic three-dimensional core element conserved in all SDRs is the so-called Rossmann-fold, a common α/β -folding pattern composed of a central stranded parallel β -sheet with 6-7 strands flanked by 3-4 α -helices on each side. This structural feature displays the required scaffold for cofactor binding and includes a Tyr-(Xaa)₃-Lys motif crucial for the catalytic activity. The general topology of SDRs is illustrated in Figure 1, exemplified on 17 β -hydroxysteroid dehydrogenase type 1 (17 β -HSD1). The arrangement of the β -sheets has the following order: 3-2-1-4-5-6-7 with a long loop between strands 3 and 4, creating the binding site of the adenine ring of NAD(P)(H) [5]. This cavity includes a highly variable Gly-rich sequence (between the first strand the following helix), enabling the binding of the pyrophosphate group of the cofactor. The cofactor preference is dictated by the presence of either an acidic residue at the C-terminus after the second β -strand for NAD(H) or a basic residue for NADP(H) that interacts with the additional phosphate group [6, 7]. The majority of SDRs contain a catalytic triad/tetrad including a Tyr, Lys, Ser (and Asn) residue. The Tyr residue functions as catalytic base/acid donating or withdrawing a proton to or from the substrate, whereas the Lys residue forms a hydrogen bond (H-bond) with the nicotinamide ribose and thereby enhances the catalytic activity by lowering the pKa from the tyrosine hydroxyl. Additionally, the conserved Ser acts as stabilizing residue for the carbonyl substrate group. Although the Tyr residue in the catalytic center is found among the majority of SDRs, it is not rigidly conserved, indicated by divergent SDRs using a different mechanism [4]. This further gives rise to the strikingly broad mechanistic diversity of SDRs including the catalysis of carbonyl-alcohol oxidoreductions, isomerizations, decarboxylations, epimerizations, C=N reductions, enoyl-CoA reductions, dehydrations, and dehalogenation reactions. Interestingly, active site superimposition of SDRs and members of the family of aldo-keto reductases (AKRs) showed conserved Tyr and Lys residues in similar positions, even though AKRs structurally belong to the $(\alpha/\beta)_8$ or TIM barrel protein superfamily. This suggests convergent evolution of a common catalytic reaction mechanism [8].

Although, more than 15 years ago, the human genome project has achieved the accessibility of the entire human genome, the physiological roles of more than 70% of all SDRs are currently unknown or

inadequately characterized. To bridge this gap, *in silico* approaches could adopt a significant role, in the identification of substrates and modulators of such enzymes, even though many challenges remain, not only from the limited availability of structural information of many SDR members. Additionally, computational tools can also support and facilitate the identification of inhibitors, including potential therapeutic compounds but also toxic industrial chemicals and environmentally relevant hazardous compounds. Furthermore, due to the involvement of SDRs in steroid biosynthesis and metabolism, they represent potential sites for molecular initiating events of endocrine disrupting chemicals (EDCs). Therefore, the present thesis aimed to apply a combination of molecular modeling (including pharmacophore-based virtual screening and molecular docking) and biological assessment for the identification and characterization of novel inhibitors and/or potential substrates of different SDRs. A detailed overview of the efforts attempted in the field of virtual screening supported identification of bioactive molecules in SDR research and the accompanying limitations can be gained in the following two published review articles [9, 10].

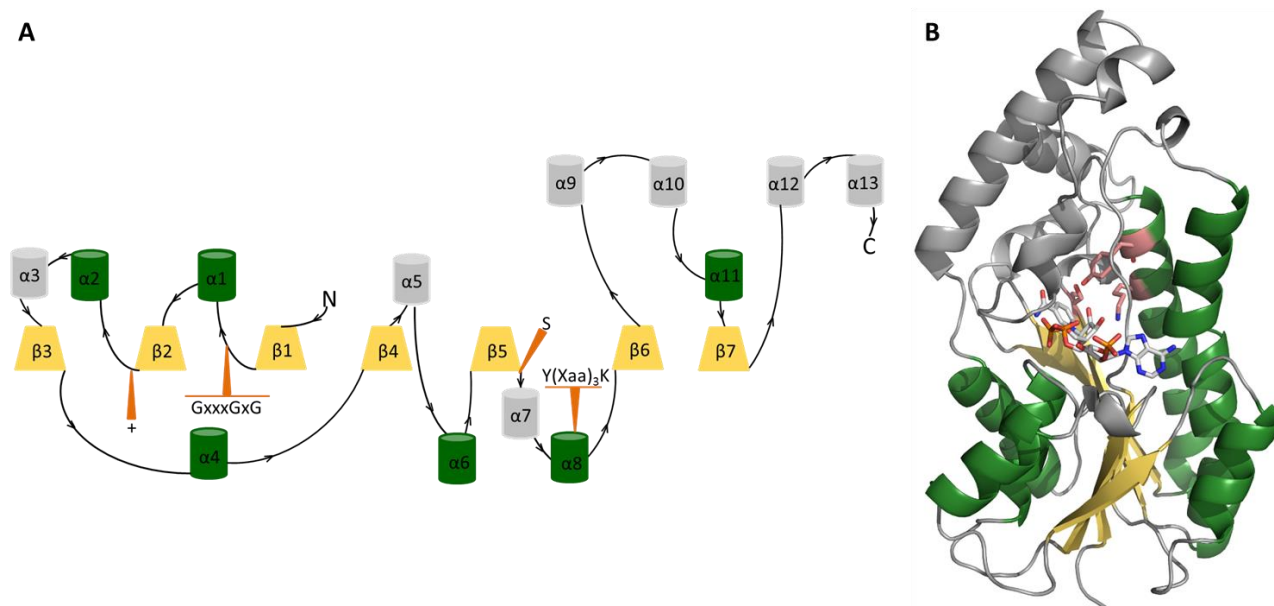


Figure 1. General 2D and 3D representation of SDR enzymes based on 17β-HSD1 as an example. (Figure adapted from Kaserer T and Beck KR et al., *Molecules* 2015 [10]). (A) 2D illustration of 17β-HSD1 (Protein database (PDB) entry 1EQU). Yellow squares depict β-sheets and barrels represent α-helices. Further structurally conserved regions (variable Gly-rich sequence and catalytic site) are highlighted in orange. The + illustrates in this case of 17β-HSD1 a positive charged residue at the C-terminus following the second β-strand essential for NADP(H) binding (an acidic residue would favor NAD(H) binding). (B) 3D depiction of 17β-HSD1 (PDB entry 1EQU) showing the same color code as the 2D representation. Several parallel stranded β-sheets (yellow), flanked by α-helices on both sides (green) build the Rossmann-fold. The Tyr-(Xaa)₃-Lys motif and the conserved Ser are highlighted in orange.

2.1. Published review articles:

2.1.1. Pharmacophore Models and Pharmacophore-Based Virtual Screening: Concepts and Applications Exemplified on Hydroxysteroid Dehydrogenases

Teresa Kaserer^{1,*}, Katharina R. Beck^{2,*}, Muhammad Akram¹, Alex Odermatt², Daniela Schuster¹, *Molecules*. 2015 Dec 19;20(12):22799-832

* These authors contributed equally to this work.

¹Institute of Pharmacy/Pharmaceutical Chemistry and Center for Molecular Biosciences Innsbruck (CMBI), Computer Aided Molecular Design Group, University of Innsbruck, Innrain 80/82, 6020 Innsbruck, Austria

²Swiss Center for Applied Human Toxicology and Division of Molecular and Systems Toxicology, Department of Pharmaceutical Sciences, Pharmazentrum, University of Basel, Klingelbergstrasse 50, 4056 Basel, Switzerland

Review

Pharmacophore Models and Pharmacophore-Based Virtual Screening: Concepts and Applications Exemplified on Hydroxysteroid Dehydrogenases

Teresa Kaserer ^{1,†}, Katharina R. Beck ^{2,†}, Muhammad Akram ¹, Alex Odermatt ^{2,*} and Daniela Schuster ^{1,*}

Received: 19 November 2015; Accepted: 9 December 2015; Published: 19 December 2015

Academic Editor: Peter Willett

¹ Institute of Pharmacy/Pharmaceutical Chemistry and Center for Molecular Biosciences Innsbruck (CMBI), Computer Aided Molecular Design Group, University of Innsbruck, Innrain 80/82, 6020 Innsbruck, Austria; Teresa.Kaserer@uibk.ac.at (T.K.); Muhammad.Akram@uibk.ac.at (M.A.)

² Swiss Center for Applied Human Toxicology and Division of Molecular and Systems Toxicology, Department of Pharmaceutical Sciences, Pharmazentrum, University of Basel, Klingelbergstrasse 50, 4056 Basel, Switzerland; Katharina.Beck@unibas.ch

* Correspondence: Alex.Odermatt@unibas.ch (A.O.); Daniela.Schuster@uibk.ac.at (D.S.); Tel.: +41-61-267-1530 (A.O.); +43-512-507-58253 (D.S.); Fax: +41-61-267-1515 (A.O.); +43-512-507-58299 (D.S.)

† These authors contributed equally to this work.

Abstract: Computational methods are well-established tools in the drug discovery process and can be employed for a variety of tasks. Common applications include lead identification and scaffold hopping, as well as lead optimization by structure-activity relationship analysis and selectivity profiling. In addition, compound-target interactions associated with potentially harmful effects can be identified and investigated. This review focuses on pharmacophore-based virtual screening campaigns specifically addressing the target class of hydroxysteroid dehydrogenases. Many members of this enzyme family are associated with specific pathological conditions, and pharmacological modulation of their activity may represent promising therapeutic strategies. On the other hand, unintended interference with their biological functions, e.g., upon inhibition by xenobiotics, can disrupt steroid hormone-mediated effects, thereby contributing to the development and progression of major diseases. Besides a general introduction to pharmacophore modeling and pharmacophore-based virtual screening, exemplary case studies from the field of short-chain dehydrogenase/reductase (SDR) research are presented. These success stories highlight the suitability of pharmacophore modeling for the various application fields and suggest its application also in future studies.

Keywords: pharmacophore; virtual screening; ligand protein interactions; hydroxysteroid dehydrogenase; oxidoreductase

1. Introduction

Pharmacophore Modeling

The concept of “pharmacophores” dates back to the late 19th century, when Paul Ehrlich suggested that specific groups within a molecule are responsible for its biological activity [1,2]. The pharmacophore definition, as currently used, was developed over time, with many researchers actively participating in the process (for a detailed history of pharmacophores, please refer to Güner and Bowen [2]). However, Schueler provided the basis for our modern understanding of a pharmacophore [2,3], which is defined by the International Union of Pure and Applied Chemistry

(IUPAC) as “the ensemble of steric and electronic features that is necessary to ensure the optimal supra-molecular interactions with a specific biological target structure and to trigger (or to block) its biological response” [4]. According to this definition, the interaction patterns of bioactive molecules with their targets are represented via a three-dimensional (3D) arrangement of abstract features that define interaction types rather than specific functional groups. These interaction types can, for example, include the formation of hydrogen bonds, charged interactions, metal interactions, or hydrophobic (H) and aromatic (AR) contacts (Figure 1). Besides that, many pharmacophore modeling programs allow for the addition of steric constraints. These so-called exclusion volumes (XVols) mimic the geometry of the binding pocket and prevent the mapping of compounds that would be inactive in the experimental assessment due to clashes with the protein surface. In its entirety, a pharmacophore model represents one binding mode of ligands with a specific target, as exemplified on 17 β -hydroxysteroid dehydrogenase (HSD) type 1 (Figure 1).

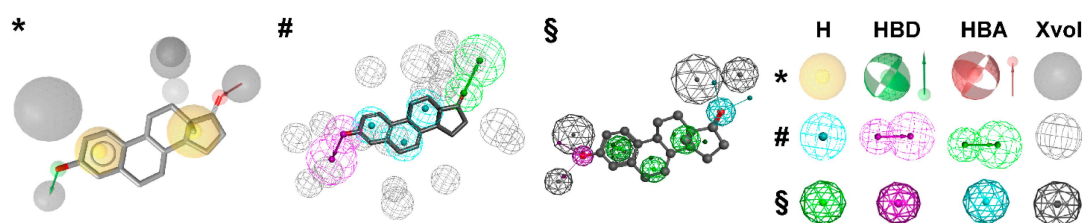


Figure 1. Pharmacophore models based on the estrogen equilin co-crystallized with 17 β -hydroxysteroid dehydrogenase type 1 (PDB entry 1EQU [5]) and generated with LigandScout [6] (*), Discovery Studio [7] (#), and Molecular Operating Environment (MOE) [8] (§). H, hydrophobic feature; HBD, hydrogen bond donor; HBA, hydrogen bond acceptor; XVols, exclusion volume.

Pharmacophore models can be generated using two different approaches (Figure 2) depending on the input data employed for model construction. In the structure-based approach, the interaction pattern of a molecule and its targets are directly extracted from experimentally determined ligand-target complexes (Figure 2A). An important source for these complexes, e.g., derived from NMR-spectroscopy or X-ray crystallography, represents the Protein Data Bank (PDB, www.pdb.org) [9]. To date (access date 2 November 2015), more than 113,000 macromolecular structures are stored in this online repository. However, not all of these structures were solved in a complex with a bound ligand, and in the case of induced fit, the binding of different ligands to an enzyme or receptor can lead to different interactions that are not covered by a single structure. To address this limitation, some pharmacophore modeling programs, e.g., Discovery Studio [7] and LigandScout [6], also provide tools to create pharmacophore models based exclusively on the topology of the binding site and in the absence of a ligand [10]. In Discovery Studio, for example, the binding site can be defined manually by selecting residues within the desired cavity or by applying implemented binding site identification tools. Once the binding site is defined, the program automatically calculates pharmacophore features based on the residues lining the active site. This initial ensemble of pharmacophore features can then be adapted to construct the final hypothesis [10]. In addition, structure-based pharmacophore models can also be generated with computationally derived ligand-target complexes. In the course of a docking run, known active compounds are fitted into the empty binding pocket of the target [11]. These docked binding poses can then directly be employed to extract the interaction patterns. For further refinement of the initial docking poses, molecular dynamics (MD) simulations can be conducted [12] prior to model generation.

In the course of ligand-based modeling, three-dimensional (3D) structures of two or more known active molecules are aligned and common pharmacophore features shared among these training set molecules are identified (Figure 2B). In a ligand-based approach, all of the common chemical features from the pharmacophore have to be presumed as essential, whereas in a structure-based approach, it can be considered whether a chemical feature of a molecule is directly involved in the ligand binding or not.

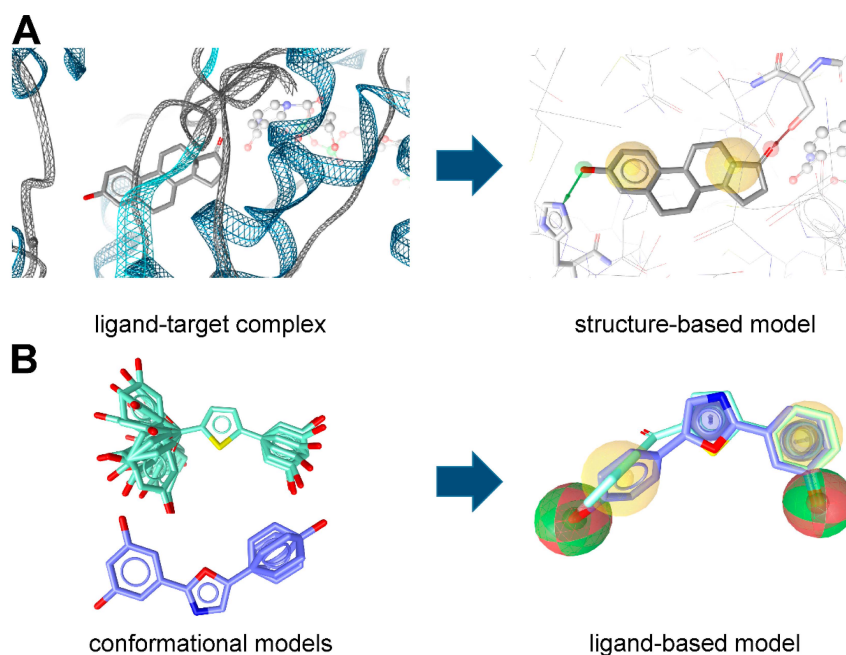


Figure 2. (A) Structure- and (B) ligand-based pharmacophore model generation with LigandScout. (A) Based on the complex of equilin bound to 17β -HSD1 (PDB entry 1EQU [5]), an initial pharmacophore model is created automatically; (B) Conformational models of known 17β -HSD1 ligands [13,14] are used to align the compounds and extract pharmacophore features they share.

Usually, datasets containing known active and inactive molecules are employed to assess the quality of the developed models. These datasets need to be designed carefully, because they largely influence the quality of the model and, accordingly, the success of the study. Only active molecules should be included, for which the direct interaction has been experimentally proven [15,16], e.g., by receptor binding or enzyme activity assays on isolated or recombinant proteins. Cell-based assays should be avoided in this context, because many factors other than interaction with the target can influence the results: Active compounds may potentially exert their effect via other mechanisms than the intended one, whereas on the other hand, inactive compounds may actually interact with the target, but due to poor pharmacokinetic properties, this cannot be detected. In addition, appropriate activity cut-offs need to be defined to avoid the inclusion of compounds with a low binding affinity and high EC_{50}/IC_{50} values (which may even be classified as “inactive”). Finally, the dataset should contain structurally diverse molecules [17] whenever possible. Preferably, experimentally confirmed inactive compounds should be included in the “inactives” dataset used for the theoretical validation [17,18]. Besides the original literature, several public compound repositories such as ChEMBL [19], Drugbank [20], or OpenPHACTS [21] can be explored for target-based activity data of compounds. In addition, several high-throughput screening (HTS) initiatives such as ToxCast [22], Tox21 [23], and PubChem Bioassay [24] provide a valuable resource for both active and inactive molecules. Whenever no or only a limited number of known inactive molecules are available, so-called decoys (compounds with unknown biological activity but assumed to be inactive) might be employed. These decoy-datasets need to be adapted for every target and should contain compounds with similar one-dimensional (1D) properties [25–27] but different topologies compared to the known active molecules. These properties can include the number of hydrogen bond donors (HBDs), the number of hydrogen bond acceptors (HBAs), the number of non-polar atoms [25], molecular weight, $\log P$, and the number of rotatable bonds [27]. The Directory of Useful Decoys, Enhanced (DUD-E) [28] provides a free service (<http://dude.docking.org>), where optimized decoys are generated based on the smiles codes of the uploaded active molecules. In general, a ratio of about 1:50 for the number of active molecules and decoys is recommended [28]. This should reflect the prospective screening

database, where usually only a few active molecules are also distributed among a vast amount of inactive molecules (Figure 3).

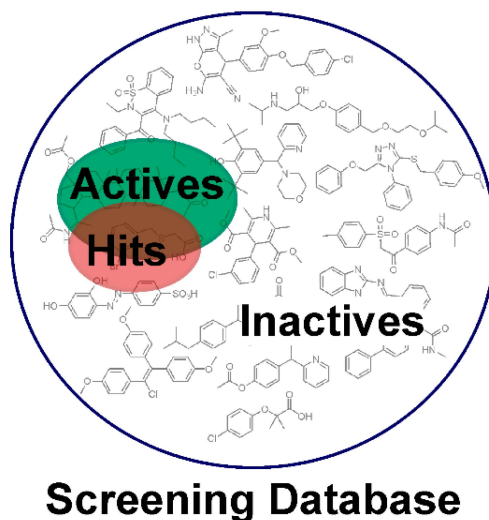


Figure 3. Enrichment of active molecules in the virtual hit list. Usually, the majority of compounds in a screening database are inactive molecules, while a small pool of bioactive molecules is contained. Pharmacophore-based virtual screening can help to enrich active molecules in the hit list compared to a random selection of test compounds.

The preliminary models generated with both approaches need further improvement in the majority of cases [16,29] to facilitate the recovery of the active molecules and concomitantly exclude the inactive compounds in the dataset from the hit list. Basic model refinement steps include the deletion or addition of pharmacophore features and adaptations concerning the feature weight and size. Selected features can also be defined as optional and, therefore, can but do not have to be mapped by a molecule. In addition, a user-defined number of omitted features can be specified in many pharmacophore modeling programs. More sophisticated modifications comprise the modification of feature definitions, *i.e.*, the functional groups covered by a pharmacophore feature.

The aim of pharmacophore-based virtual screening (VS) is to enrich active molecules in a screening database in the virtual hit list (Figure 3). Multiple quality metrics are available that help to evaluate the quality of the developed pharmacophore model, for example the enrichment factor [30] (the enrichment of active molecules compared to random selection), yield of actives (the percentage of active compounds in the virtual hit list), specificity (the ability to exclude inactive compounds) and sensitivity (the ability to identify active molecules), and the area under the curve of the Receiver Operating Characteristic plot (ROC-AUC) [31]. For detailed descriptions of commonly applied quality parameters we refer to earlier work [15,16,26,32]. The ultimate proof of a model's quality and value, *i.e.*, whether it is indeed capable of proposing novel active molecules, can, however, only be determined in a prospective experiment, as will be explained in more detail below. A workflow summarizing the individual steps of pharmacophore model generation and application is depicted in Figure 4.

As outlined below, refined, high quality pharmacophore models can then be employed for multiple tasks.

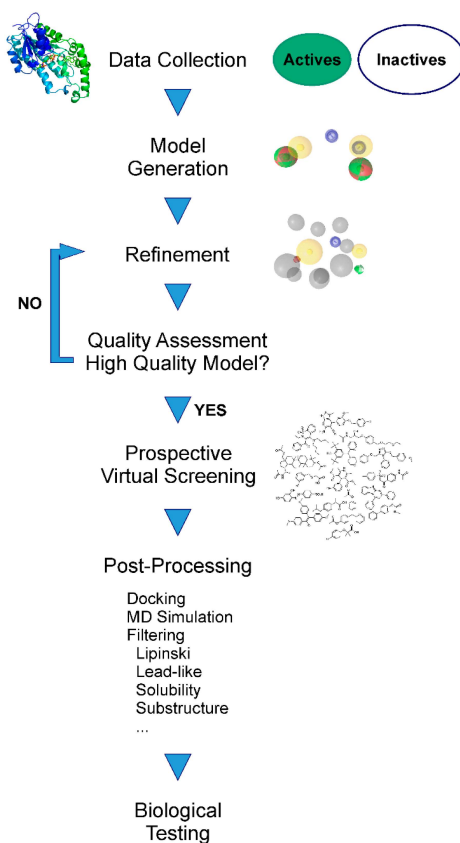


Figure 4. The different consecutive steps in pharmacophore model generation, refinement, and prospective application.

2. Applications of Pharmacophore-Based VS

In the course of a VS run, a pharmacophore model is screened against large chemical libraries, and molecules mapping the model are collected in a virtual hit list. These molecules fulfill the requirements of the model and therefore have a high likelihood to be active in the experimental testing. Accordingly, VS can be used to filter promising compounds out of large compound collections and enrich active molecules in chemical databases selected for experimental investigations. VS is considered a valuable support for classical HTS campaigns [33,34], because true positive hit rates are usually much higher than in those “random” testing strategies [35–37]. Reported hit rates from prospective pharmacophore-based virtual screening vary between individual studies, but are typically in the range of 5% to 40% (an excellent collection of prospective studies has been presented earlier [16]). On the other side, the hit rates of identifying active molecules upon random selection of test compounds are typically below 1% and have been described, for example, as 0.55% for glycogen synthase kinase-3 β [36], 0.075% for peroxisome proliferator-activated receptor (PPAR) γ [38], and 0.021% for protein tyrosine phosphatase-1B [37].

2.1. Drug Discovery

Pharmacophore-based VS is widely applied in different steps of the drug discovery process and facilitates the initial selection of compound classes as well as the optimization of compound properties as outlined below.

2.1.1. Lead Identification

The most common application of pharmacophore-based virtual screening concerns lead identification, the so-called cherry-picking approach. Virtual screening is often deployed in these

projects to prioritize molecules for testing and minimizing the number of compounds to be investigated in biological screens. The ultimate aim is the identification of novel lead compounds for a specific disease-related target, which can be developed into drug candidates for the treatment of the intended disease, with numerous studies during the last years describing such applications [39–44]. For example, Ha *et al.* reported the discovery of novel ligands for the chemokine receptor CXCR2 by using a ligand-based pharmacophore modeling approach [45]. In the course of a pharmacophore-based virtual screening for novel histamine H₃ receptor antagonists, Lepailleur *et al.* identified novel compounds additionally binding to the 5HT₄ receptor [46]. Both activities were considered beneficial for the treatment of Alzheimer's disease and the authors were the first to report compounds with this dual mechanism of action [46].

2.1.2. Structure-Activity Relationships

As mentioned in the introduction, a pharmacophore model represents the putative binding mode of active molecules to their target. It therefore describes the crucial functionalities required for a compound's activity. A pharmacophore model is trained to discriminate between active and inactive molecules (in the best case even between members of the same chemical series), which makes it highly valuable for establishing structure-activity relationships (SARs). Differences in the experimentally observed biological activities of a set of compounds can be rationalized based on the presence/absence of chemical groups, represented by pharmacophore features, in the respective molecules. SARs can be established during model building, thereby elucidating the underlying mechanisms for the (absent) biological activity. For example, Ferreira *et al.* employed pharmacophore models to elucidate important features responsible for the interaction of compounds with the P-glycoprotein drug binding site [47]. Previous studies suggested a crucial role for a nitrogen atom in the modulators; however, active constituents from *Euphorbia* species isolated in-house did not contain such a moiety. The authors generated multiple refined pharmacophore models and evaluated them against a dataset of literature-derived modulators, the in-house collection, and inactive molecules. Their final model highlighted the important role of hydrophobic contacts and the presence of a HBA feature for P-glycoprotein modulators and showed that mapping of the most active compounds was also preserved when a further HBA/HBD feature was added [47]. In addition, pharmacophore models can be employed to reflect previously elucidated SARs for the identification of novel bioactive molecules. In 2002, Flohr *et al.* used the endogenous peptide urotensin II and synthetic analogues to experimentally identify interactions that are crucial for binding to the urotensin II receptor [48]. Based on the established SAR, pharmacophore models were built and employed to screen a chemical library containing small drug-like compounds. Subsequent experimental testing of the virtual hits led to the identification of six novel scaffold classes, which, importantly, contained non-peptidic molecules [48].

2.1.3. Scaffold Hopping

A pharmacophore feature describes abstract chemical functionalities rather than specific functional groups. Additionally, pharmacophore models only demand local functional similarity of active compounds and virtual hits at 3D locations essential for biological activity. Therefore, there are no specifications concerning the actual two-dimensional (2D) structures of mapping compounds. Although the composition of a pharmacophore model is influenced by the 2D structure of the molecules employed for model generation and refinement, it still allows for mapping of structurally distinct hits. This makes pharmacophore modeling broadly applicable for the investigation of molecules originating from a diverse chemical space such as natural products and synthetic compounds. Importantly, it also allows for the identification of novel scaffolds that have not been associated with the target of interest before, a strategy that is called scaffold hopping. An earlier review extensively discussed pharmacophore modeling in the context of scaffold hopping [49]. A recent study employed pharmacophore modeling for the discovery of novel transient receptor potential vanilloid type 1 channel ligands [50]. Although the initial hits only weakly interacted with the target, they represent an

interesting starting point for further chemical optimization. Such studies mostly emphasized novel chemical scaffolds and retrieved low similarity scores compared to the highly active compounds in the theoretical validation dataset [50].

Scaffold hopping is certainly relevant for the pharmaceutical industry that needs to explore compounds which are not yet covered by intellectual property issues. Of relevance for the general public, scaffold hopping facilitates the identification of chemicals with only limited available data. This is often the case for environmental pollutants and chemicals from consumer products that are often not drug-like by their nature.

2.1.4. Selectivity Profiling

For some projects, it may be of the utmost importance to identify compounds that selectively modulate the activity of one or more isoforms of an enzyme (family) to trigger the desired biological effect. For example, steroidal core structures are frequently found in endogenous and exogenous bioactive compounds; however, these compounds often lack selectivity. To identify selective compounds, specific chemical substitutions leading to additional hydrophobic or ionic interactions and hydrogen bonds have to be implemented. It has to be emphasized that these specific chemical modifications allow for distinguishing between the enzyme of interest and its related enzymes.

For example, 17 β -HSD1 inhibitors are promising drug candidates for the treatment of hormone-sensitive breast cancer as well as endometriosis because they block the activation of estrone to the highly potent endogenous estrogen receptor (ER) agonist estradiol [51–53]. On the other side, the converse reaction, (*i.e.*, inactivation of estradiol) mediated via 17 β -HSD2, should not be blocked by these molecules. Ideally, bioassays of all relevant members within a given protein family would be employed to assess a compound's selectivity. Additionally, proteins sharing structural similarity in the domain that contains the ligand binding pocket rather than sequence similarity should be considered in the selectivity assessment of compounds [54,55]. Thus, a huge number of proteins need to be covered in this resource- and time-consuming approach. In a first step, parallel screening using a large collection of pharmacophores, covering the most relevant proteins, allows for an initial characterization of a compound's activity profile and facilitates the prioritization of the bioassays to be chosen for further biological analyses.

However, selectivity may not be limited to different isoforms. As exemplified by a study from Guasch *et al.*, it can even address the biological effect exerted via the same target [56]. The authors focused on the exclusive discovery of novel PPAR γ partial agonists. The retrieval of full agonists was avoided to prevent the side effects accompanying full receptor activation. For this purpose, a pharmacophore model for full agonists (called the anti-pharmacophore) was generated and used to remove all potential full agonists from the screening database. In the second step, a partial agonist pharmacophore model was applied to identify potential partial agonists in the compound library. After several additional filtering steps, eight compounds were finally subjected to biological testing and five of them could be confirmed as novel PPAR γ ligands displaying partial agonistic effects [56].

2.1.5. Combination with Other Techniques

Pharmacophore models are also often used together with other methods to further increase the number of active molecules in the hit list *via* the application of a consensus approach. Commonly employed combinations comprise docking, shape-based modeling, and MD simulation.

In addition, a number of filters are available that help to limit the virtual hits to those with the desired properties and eliminate unwanted actions or molecules. Probably the most prominent filter represents the Lipinski's, describing properties that are shared by approved and orally administered drugs [57]. In particular, these comprise a number of ≤ 5 HBDs, ≤ 10 HBAs, a molecular weight of ≤ 500 , and a cLogP ≤ 5 . Since all descriptors are either five or a multiple of five, Lipinski *et al.* referred to it as the "rule of five". Although the rule of five was initially developed to predict the oral bioavailability of molecules, it is also widely applied as a general drug-like filter. Veber *et al.* suggested two other

criteria for the oral bioavailability of compounds: First, compounds should have a number of ≤ 10 rotatable bonds and, second, either a polar surface area of $\leq 140 \text{ \AA}^2$ or ≤ 12 HBAs and HBDs [58].

In analogy to Lipinski's rule of five, Congreve *et al.* introduced the "rule of three" for the identification of promising hit compounds in fragment-based drug discovery [59]. Their analysis revealed that most of the small compounds that were successfully optimized to potent lead-like candidates had a molecular weight of ≤ 300 , a number of HBDs ≤ 3 , a number of HBAs ≤ 3 , and a $\text{cLogP} \leq 3$ [59].

More recently, a substructure filter was developed to identify highly problematic compounds that notoriously produce false positive assay read-outs [60]. Baell and Holloway analyzed high-throughput testing results and observed that a group of molecules were prone to unspecifically interfere with some experimental test systems. The subsequently developed substructure filter can help to detect these pan-assay-interference compounds (PAINS) [60] prior to spending time and resources in investigating and optimizing such molecules [61].

Multiple of these methods and filters can be included as well. As an example, Noha *et al.* employed a variety of computational techniques in a sequential manner to identify novel inhibitors of microsomal prostaglandin E_2 synthase-1 [62]. The workflow included multiple prefilters, among them also the Lipinski filter, a pharmacophore-based virtual screening procedure, and molecular docking. Out of the 17 molecules finally selected for testing, two showed good activity in the experimental assay, and two further had moderate effects. Temml *et al.* used a combination of pharmacophore- and shape-based virtual screening to identify novel liver X receptor agonists [44]. In their study mentioned above [56], Guasch *et al.* not only applied pharmacophore models, but also a multistep protocol comprised of electrostatic and shape similarity and molecular docking to identify novel PPAR γ partial agonists.

2.2. The Short-Chain Dehydrogenase/Reductase Superfamily

The short-chain dehydrogenase/reductase (SDR) enzyme family are nicotinamide adenine dinucleotide NAD (phosphate (P))-dependent enzymes sharing a common core structure of up to seven parallel stranded β -sheets flanked by three to four α -helices on each side, the so-called Rossmann fold, for NAD(P) binding and a catalytic center characterized by a Tyr-(Xaa) $_3$ -Lys motif. This motif is often found in combination with a conserved serine residue that stabilizes the orientation of the bound substrate (Figure 5) [63]. SDRs typically share a low sequence identity between 20%–30%, but with considerable structural similarity in the core domain.

The SDR family contains HSDs that play key roles in adrenal and gonadal steroidogenesis as well as in the metabolism of steroids in peripheral tissues [64]. Some of these HSDs are considered as promising therapeutic targets for the treatment of estrogen- and androgen-dependent diseases such as osteoporosis, endometriosis, and breast and prostate cancer, and other enzymes gained interest regarding the treatment of corticosteroid-related diseases such as diabetes, visceral obesity and dyslipidemia, atherosclerosis, wound healing, glaucoma, neurodegenerative disease, and cognitive impairment [53,65–67].

The development of specific SDR inhibitors needs to take into account the structural similarity of the various SDR enzymes in order to exclude the inhibition of members causing adverse effects, so-called off-targets. Suitable enzyme activity assays are fundamental for selectivity testing of potential inhibitors. Koch *et al.* proposed that structural similarity rather than primary sequence similarity should be chosen as the criterion for whether a certain chemical affects the activity of a related enzyme [54]. Therefore, the closest structurally related enzymes should be included for selectivity testing—using pharmacophore models and cell-based assays. Another application of the modeling approaches is the identification of toxic xenobiotics including industrial and environmentally relevant chemicals [68–70]. The role of several SDRs in xenobiotics metabolism and in steroid synthesis and metabolism makes them prone as targets for endocrine disruption [71–76].

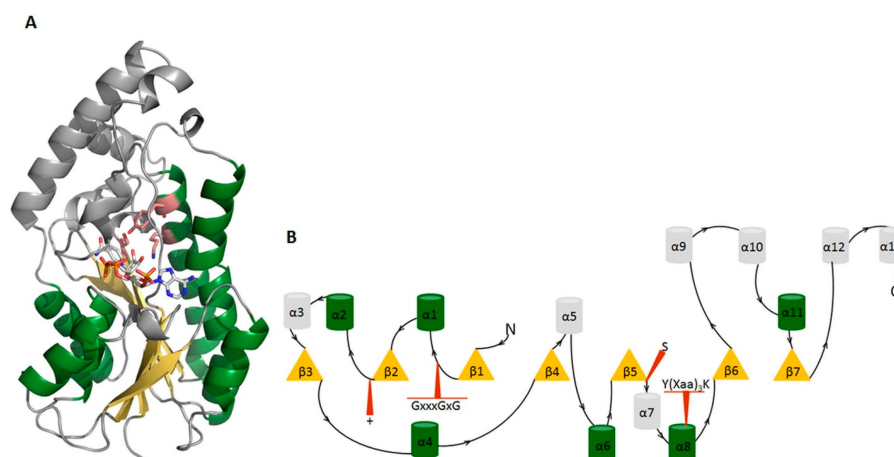


Figure 5. The general structure of SDR enzymes exemplified on 17 β -HSD1 (PDB entry 1EQU [5]). (A) The Rossmann fold consists of parallel stranded β -sheets (yellow), which are flanked by α -helices on both sides (green). This structural domain forms the binding site of the co-factor NADP $^{+}$. The residues Tyr155 and Lys159 of the Tyr-(Xaa)3-Lys motif as well as the conserved Ser142 are highlighted in rose; (B) 2D depiction of 17 β -HSD1 (PDB entry 1EQU). Yellow triangles display β -sheets and barrel symbols α -helices. Apart from the Rossmann fold, structurally conserved regions are highlighted in red. The conserved glycine-rich motif GxxxGxG is important for cofactor binding and the + indicates a positive charged residue crucial for cofactor (NADP $^{+}$) stabilization.

3. Examples from the SDR Family

3.1. 11 β -Hydroxysteroid Dehydrogenase Type 1

The two isoenzymes of 11 β -HSD catalyze the interconversion of the biologically inactive cortisone and the active cortisol (Figure 6). The 11 β -HSD1 is ubiquitously expressed and mediates the regeneration of active glucocorticoids [77,78], whereas 11 β -HSD2 catalyzes the inactivation of glucocorticoids mainly in the kidney, colon and placenta. There is evidence for beneficial effects of 11 β -HSD1 inhibition in the metabolic syndrome [79–87], atherosclerosis [88–91], osteoporosis [66,92], glaucoma [93–95], cognitive functions [96–100], skin aging [101], and wound healing [102,103]. Thus, inhibition of 11 β -HSD1 has substantial therapeutic potential for glucocorticoid-related diseases. Numerous 11 β -HSD1 inhibitors have already been identified and some have reached the clinical phase, but to date still no 11 β -HSD1 inhibitor is on the market [104]. Although structural variety is prevalent among the 11 β -HSD1 inhibitors, the crystal structures are rather similar [105]. Nevertheless, the observed differences are useful in selecting a structure for further *in silico* evaluations. To date, 27 human, four mouse, and three guinea pig 11 β -HSD1 crystal structures are accessible through the PDB; however, there is currently no 3D structure of human 11 β -HSD1 in-complex with a substrate available. In addition, structural information about 11 β -HSD2 is entirely missing.

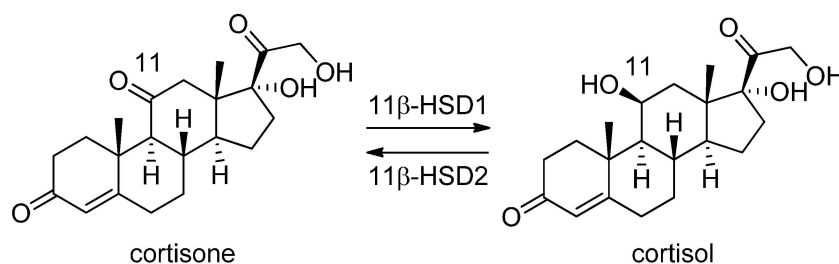


Figure 6. Interconversion of cortisone and cortisol catalyzed by the 11 β -HSD enzymes.

Schuster and Maurer *et al.* [106] were the first to introduce pharmacophore models for the identification of novel classes of 11 β -HSD1 inhibitors. As there was no X-ray crystal structure of 11 β -HSD1 available at the beginning of their study, they employed two ligand-based pharmacophore models as VS tools. Depending on the 11 β -HSD activity of the training compounds used for the model generation, a model for 11 β -HSD1-selective (Figure 7A) and one for nonselective 11 β -HSD inhibitors (Figure 7B), preferably targeting 11 β -HSD2, were developed. These models identified compounds resembling the structure of the known unselective 11 β -HSD inhibitor glycyrrhethinic acid (GA), steroid-like compounds, and novel structural classes. A comparison of the training set compounds used for the generation of the 11 β -HSD1-selective and the 11 β -HSD-nonselective pharmacophore models with the compounds from the VS showed similar inhibition profiles towards 11 β -HSD1 and 11 β -HSD2.

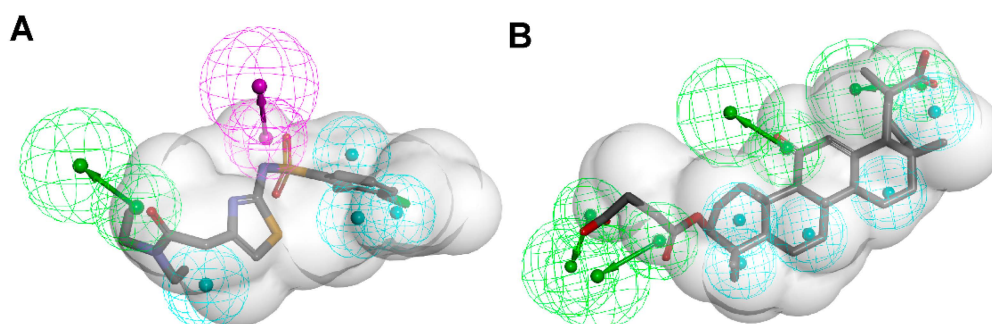


Figure 7. The selective (A) and nonselective (B) 11 β -HSD1 pharmacophore models reported in the study by Schuster and Maurer [106]. The training compounds CAS 376638-65-2 (A) and carbenoxolone (B) are aligned to the models. The 11 β -HSD1-selective model consisted of four H features (blue), one HBA (green) and one HBD (magenta) feature and a shape restriction. The nonselective 11 β -HSD model contained five H, four HBA features and also a shape restriction.

Testing the inhibitory potential of their VS hits, Schuster and Maurer *et al.* determined biological activities for human 11 β -HSD1, 11 β -HSD2, 17 β -HSD1 and 17 β -HSD2 [106]. Out of 30 tested compounds, seven inhibited 11 β -HSD1 activity by more than 70% at 10 μ M and only three showed reasonable selectivity over the other tested enzymes.

The potential of the selective 11 β -HSD1 ligand-based pharmacophore model obtained by Schuster and Maurer *et al.* [106] was further evaluated by Hofer *et al.* [107]. VS and subsequent lead optimization by classical bioisosteric studies revealed a class of selective 11 β -HSD1 inhibitors bearing an arylsulfonylpiperazine scaffold. Docking studies, performed to rationalize the biological data, showed good alignment of all active compounds with the co-crystallized ligand, belonging to the same chemical scaffold. This structure-based approach further validated the ligand-based pharmacophore model.

Rollinger *et al.* used the same pharmacophore model as a query for the screening of a database consisting of constituents from medicinal plants, in order to identify natural compounds selectively inhibiting 11 β -HSD1 [108]. The chemical class of triterpenoids displayed one of the dominating chemical scaffolds in the virtual hit list. Earlier investigations led to the assumption that extracts from the anti-diabetic medical plant loquat (*Eriobotrya japonica*) dose-dependently and preferentially inhibit 11 β -HSD1 over 11 β -HSD2 [109]. Therefore, the virtual screening hit corosolic acid, a known constituent of *E. japonica*, was tested and identified as potent inhibitor of human 11 β -HSD1 with an IC₅₀ of 810 nM [108]. Subsequent bioassay-guided phytochemical analyses revealed further secondary metabolites from the triterpenoid ursane type as 11 β -HSD1 inhibitors with IC₅₀ in the micromolar range. Importantly, a mixture of the constituents with moderate inhibitory activities displayed an additive effect. This is a common observation in phytotherapy, where a mixture of constituents is often responsible for the therapeutic effect. Docking studies for binding mode prediction suggested a flipped binding mode, where these triterpenoids would not interact with the catalytic amino acids but

with Thr124 and Tyr177 (Figure 8). Based on the most active compounds, a pharmacophore model was generated that enriched active molecules on the top of the hit list and successfully reflected the substructures important for binding. Additionally, this study demonstrates a further application in the drug discovery process—finding inhibitors from natural origins.

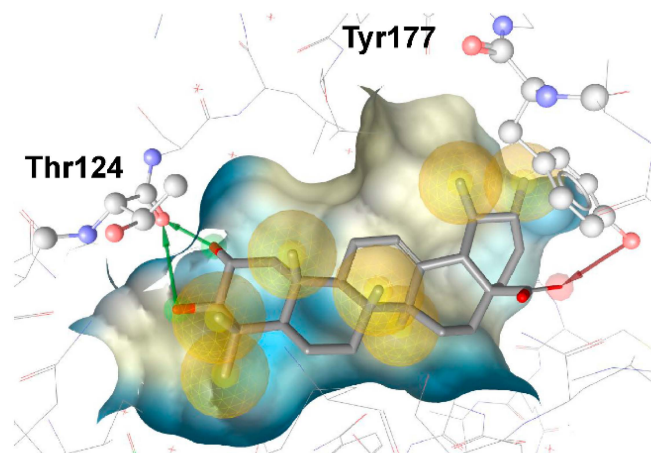


Figure 8. The docking pose of the potent inhibitor corosolic acid in the binding pocket of 11 β -HSD1 (PDB entry 2BEL [110]) suggests interactions with Thr124 and Tyr177.

Considering the ongoing search for novel 11 β -HSD1 inhibitors, high predictivity and performance of pharmacophores are essential. Thus, to maintain high quality standards, pharmacophore models have to be continuously re-evaluated and improved. Vuorinen *et al.* [29] performed a refinement study of the 11 β -HSD pharmacophore models previously described by Schuster and Maurer *et al.* [106] and Kratschmar *et al.* [78]. In a first step, the selective 11 β -HSD1 model was refined by exchanging a chemical feature and removing shape restriction using literature data. Whereas the unrefined model was only able to recognize two out of 14 test compounds, the refined model found 13. Subsequent prospective VS and biological testing revealed better performance of the refined model. However, although the refinement improved the sensitivity of the model and more active compounds were found, it decreased specificity and also more inactive compounds fitted into the model. Adding a shape restriction, following newly identified selective 11 β -HSD1 inhibitors, increased specificity, whereas the sensitivity remained the same. For additional testing of the model quality on a different dataset, literature-based validation was performed with structurally diverse compounds, which had not been used in the model development. Specificity was increased, whereas sensitivity decreased. This illustrates that improvement of model quality is accompanied by balancing the specificity and sensitivity of a model. Refinement of the 11 β -HSD2-selective model was equally conducted. Since there is no 3D structure of 11 β -HSD2 available and only a few selective, mainly triterpenoid scaffold-based 11 β -HSD2 inhibitors are known, the 11 β -HSD2 model data are biased. They were, however, able to improve 11 β -HSD2 model quality, and novel active scaffolds selectively inhibiting both 11 β -HSD1 (Figure 9A) and 11 β -HSD2 (Figure 9B) were discovered [29].

Using the refined 11 β -HSD1 model, Vuorinen *et al.* applied a VS to filter a database consisting of constituents from medicinal plants to identify potential 11 β -HSD1 inhibitors focusing on triterpenoids present in *Pistacia lentiscus* (*P. lentiscus*), so-called mastic gum that is used in traditional Greek medicine for the treatment of diabetes [111]. The VS hit list contained eight hits of *P. lentiscus* constituents. The two main constituents of mastic gum, masticadienonic acid and isomasticadienonic acid, were chosen for further biological evaluation. Both compounds were shown to selectively inhibit 11 β -HSD1 over 11 β -HSD2 with IC₅₀ values of 2.51 μ M for masticadienonic acid and 1.94 μ M for isomasticadienonic acid, respectively. Examination of the whole resin's activity revealed half the IC₅₀ value of the single molecules, suggesting an additive inhibitory effect. Thus, the hypothesis of 11 β -HSD1 involvement in the antidiabetic activity of mastic gum was supported. Analyzing the binding orientation of the

two substances by docking revealed interactions comparable to that of the co-crystallized ligand carbenoxolone, suggesting a competitive binding mode. Thus, the refined pharmacophore model has proven its ability to identify novel 11 β -HSD1 inhibitors from natural sources.

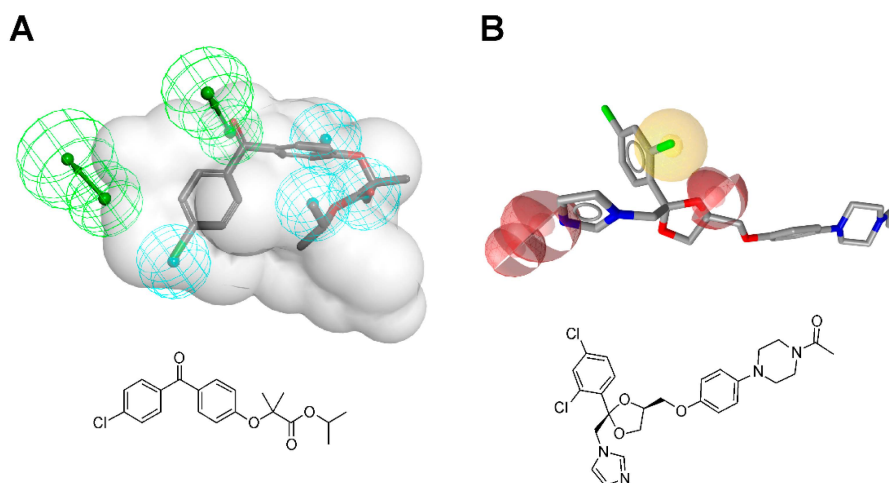


Figure 9. Both the refined 11 β -HSD1 (A) and 11 β -HSD2 (B) model identified novel scaffolds [29]. The inhibitor fenofibrate maps the 11 β -HSD1 model (A) and ketoconazole matches the 11 β -HSD2 model (B). Both models were screened with one omitted feature. The 2D structures of the novel inhibitors are depicted underneath the alignments.

Yang *et al.* performed a study using different 11 β -HSD1 crystal structures in order to identify synthetic 11 β -HSD1 inhibitors [112]. They applied a combined approach of molecular docking and ligand-based pharmacophore modeling. For virtual docking calculations the crystal structure 1XU9 [113] and the program DOCK4.0 [114] were used to screen a commercial compound database. The 3000 compounds with the highest docking score were selected for a second docking run using Glide [115]. Additionally, a ligand-based pharmacophore model for selective 11 β -HSD1 inhibitors was constructed using Catalyst 4.10 [116], which was used for screening the 3000 compounds with the Best Flexible Search mode. Compounds with high docking and good fit score were further evaluated by filtering for drug likeness and finally selected for biological testing on human and mouse 11 β -HSD1. Importantly, other studies showed significant species-specific variability in the potency of various 11 β -HSD1 inhibitors, indicating significant differences in the 3D organization of the hydrophobic substrate-binding pocket of human and mouse 11 β -HSD1 [117,118]. Due to this issue, the tested compounds showed different inhibition profiles for the mouse and human enzyme. Eleven out of 121 tested compounds inhibited the human 11 β -HSD1 with IC₅₀ values of 0.26–14.6 μ M, whereas six molecules inhibited the mouse 11 β -HSD1 with IC₅₀ values of 0.48–12.49 μ M. Two substances displayed overlapping hits with IC₅₀ for the human 11 β -HSD1 of 0.69 μ M and 3.57 μ M and for the mouse isoenzyme of 0.48 μ M and 2.09 μ M, respectively. In order to test the selectivity over 11 β -HSD2 for subsequent animal studies, only compounds inhibiting mouse 11 β -HSD1 were tested for the inhibition of mouse 11 β -HSD2. All compounds selectively inhibited 11 β -HSD1. Nevertheless, selectivity assessment needs to include human 11 β -HSD2 and, ideally, other SDRs. Cross-species activity would be the optimal situation for preclinical evaluation in the development of novel drug candidates.

A consecutive *in silico* study of Yang *et al.* includes virtual screening with 11 β -HSD1 structure-based pharmacophore models and subsequent docking for hit selection [119]. Compounds chosen in the docking process were able to form hydrogen bonds with the amino acids Tyr183 and Ser170 from the catalytic triade. Nine out of 56 enzymatically tested compounds exhibited dose-dependent and selective inhibition of human 11 β -HSD1 with IC₅₀ values between 0.85–7.98 μ M and six substances inhibited the mouse 11 β -HSD1 with IC₅₀ values between 0.44 μ M and 8.48 μ M.

Four substances inhibited both isoenzymes with similar IC_{50} values. In contrast, during their first 11β -HSD1 *in silico* study, Yang *et al.* identified 11 out of 121 tested compounds from the same database as actives against 11β -HSD1, with IC_{50} values between 0.26–14.6 μ M [113]. Four of the identified 11β -HSD1 inhibitors incorporate an arylsulfamido scaffold, an already reported scaffold to inhibit 11β -HSD1 [118]. Besides, three new scaffolds were identified as displayed in Figure 10.

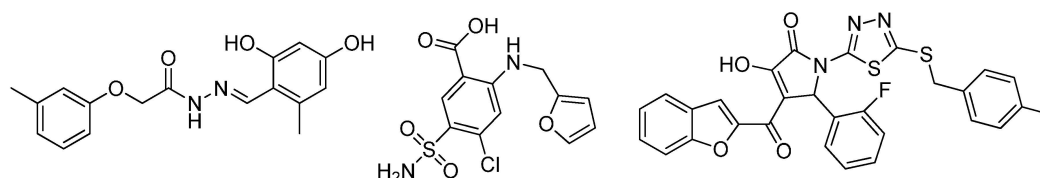


Figure 10. The three new identified scaffolds by Yang *et al.* [119].

Table 1 summarizes the pharmacophore-based virtual screening studies and illustrates the scaffold-hopping of the different 11β -HSD1 inhibitors.

3.1.1. 17β -Hydroxysteroid Dehydrogenase Type 1

To date, 14 different human 17β -hydroxysteroid dehydrogenase (17β -HSD) enzymes have been reported, all of which except the aldo-keto reductase (AKR) member 17β -HSD5 (AKR1C3) belong to the SDR family [120]. The 17β -HSDs essentially regulate the local metabolism and activity of estrogens and androgens (Figure 11).

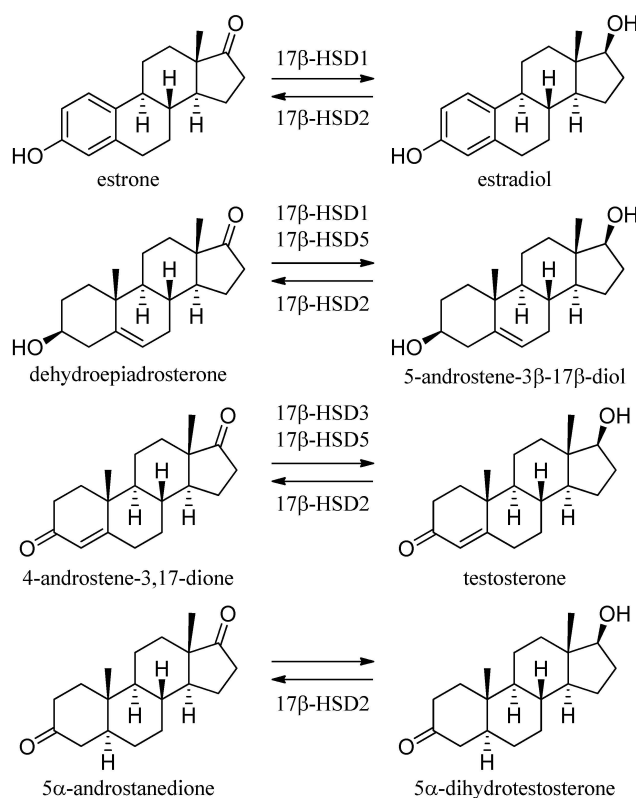


Figure 11. 17β -HSDs involved in sex steroid metabolism.

Table 1. 11 β -HSD1 pharmacophore-based virtual screening studies summarized.

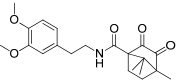
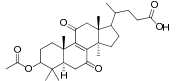
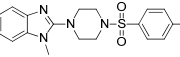
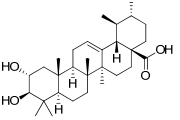
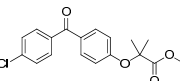
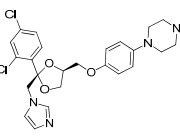
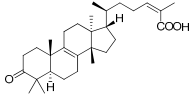
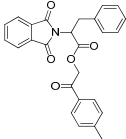
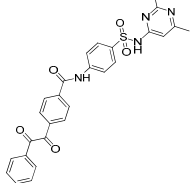
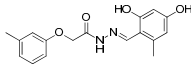
Reference Study Aim	Pharmacophore Model	Database Used for VS	Hits				Biological Testing		
			Most Active Hit	Number of Virtual Hits	Tested <i>in Vitro</i>	Actives	Assay	IC ₅₀	Selectivity
Schuster and Maurer <i>et al.</i> [106] <i>11β-HSD1 inhibitors</i>	Ligand-based using Catalyst	Asinex Gold and Platinum, Bionet 2003, ChemBridge DBS, Clab and IDC, Enamine 03, Interbioscreen 03		16/20304	15	2	Lysate	2.03 and 7.59 μ M	Against 11 β -HSD2, 17 β -HSD1, and 17 β -HSD2
	11 β -HSD1 selective (4 H, 1 HBA, 1 HBD, and shape restriction)	nat and syn, Maybridge 2003, NCI, Specs 09 03		107/1776579	15	5	Lysate	11 β -HSD1 0.144–2.81 μ M 11 β -HSD2 0.06–3.95 μ M	Most of them against 17 β -HSD1 and 17 β -HSD2
Hofer <i>et al.</i> [107] <i>Lead optimization</i>	11 β -HSD1 selective from Schuster and Maurer <i>et al.</i> [106]	In-house database		-	-	-	Lysate	0.7 μ M	Against 11 β -HSD2
Rollinger <i>et al.</i> [108] Natural compounds inhibiting 11 β -HSD1	11 β -HSD1 selective from Schuster and Maurer <i>et al.</i> [106]	DIOS (Natural products in-house database)	 corosolic acid	172	1	1	Lysate	0.81 μ M	Against 11 β -HSD2
Vuorinen <i>et al.</i> [29] <i>Refinement study</i>	Refined models from Schuster and Maurer <i>et al.</i> [106] Using Discovery Studio	In-house database, DIOS	 fenofibrate	463	9	3	Lysate	Considered as active if remaining enzyme activity \leq 55% at test substance concentration of 20 μ M or \leq 65% at test substance concentration of 10 μ M 5%–40%	Two preferentially inhibited 11 β -HSD2, one was unselective
	11 β -HSD1 selective								
	11 β -HSD2 selective	In-house database, Specs, Maybridge	 ketoconazole	444	25	2			
11 β -HSD unselective	EDC, In-house database			38	4		36%–49% Enzyme rest activity	Two preferentially inhibited 11 β -HSD1 one preferentially inhibited 11 β -HSD2	

Table 1. Cont.

Reference Study Aim	Pharmacophore Model	Database Used for VS	Hits		Biological Testing				
			Most Active Hit	Number of Virtual Hits	Tested <i>in Vitro</i>	Actives	Assay	IC ₅₀	Selectivity
Vuorinen <i>et al.</i> [112] <i>Mode of action study</i>	Refined 11β-HSD1 model from Vuorinen <i>et al.</i> [29]	DIOS		305/6702	2	2	Lysate	1.94 μM and 2.15 μM	Against 11β-HSD2
Yang <i>et al.</i> [113] <i>11β-HSD1 inhibitors</i>	Ligand-based Using Catalyst (4 H, 1 HBA, 1 AR)	SPECS	 Active against human 11β-HSD1  Active against human and mouse 11β-HSD1	3000 Selected by docking (these 3000 were fitted in the pharmacophore model)	121 (39 out of docking and 82 from pharmacophore modeling)	11	Scintillation proximity assay	Human 11β-HSD1 0.26–14.6 μM Nine compounds Mouse 11β-HSD1 0.48–12.49 μM	Only tested against mouse 11β-HSD2 not tested toward the human 11β-HSD2
Yang <i>et al.</i> [119] <i>11β-HSD1 inhibitors</i>	Two structure-based models using LigandScout (PDB code 2IRW) (3 H, 1HBD, 1 HBA)	SPECS		1000 Selected for each model	56	Nine human and six mouse	Scintillation proximity assay	Human 11β-HSD1 0.85–7.98 μM Mouse 11β-HSD1 0.44–8.48 μM	Against 11β-HSD2

The enzyme 17 β -HSD1 catalyzes the NADP (H)-dependent reduction of the weak estrogen estrone to the potent estradiol and to a minor extent of dehydroepiandrosterone (DHEA) to 5-androstene-3 β ,17 β -diol [121]. 17 β -HSD1 is predominantly expressed in the human placenta, ovaries, and mammary gland, and is of major importance for the peripheral and gonadal estradiol synthesis [122]. Several studies provide evidence for the association of 17 β -HSD1 with breast cancer [123–125], endometriosis [52,126], endometrial cancer [127] and uterine leiomyoma [128].

Despite the recently increasing numbers of reported 17 β -HSD1 inhibitors, still no compound reached clinical trials. To date, more than 20 crystal structures have been published. The binding pocket of 17 β -HSD1 is an elongated hydrophobic tunnel, with key roles for Leu149, Val225, Phe226, and Phe259, and polar areas at each end formed by His221 and Glu282 on one side and the catalytically essential residues Ser142 and Tyr155 on the other side. The active site is limited by a flexible loop (amino acids 188–201), which is not well resolved in the crystal structures (Figure 12) [13].

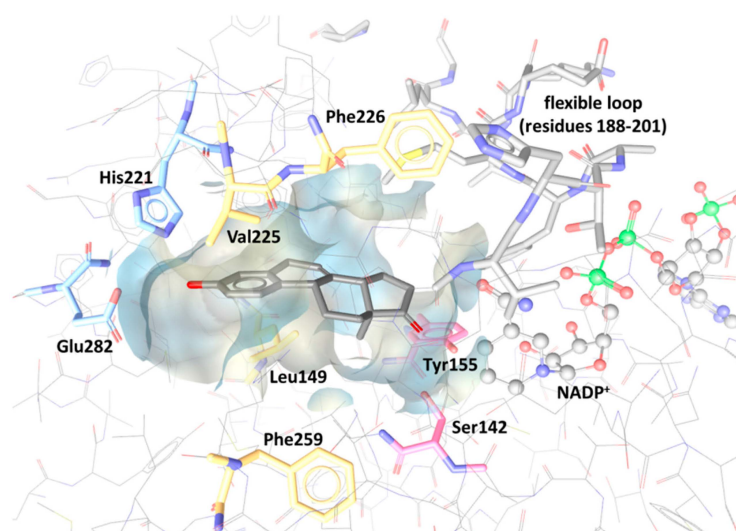


Figure 12. Shape binding site of 17 β -HSD1 with equilin as co-crystallized ligand, key residues, a flexible loop and the cofactor NADP⁺ (PDB 1EQU).

In 2001, Hoffren *et al.* were the first to report structure-based pharmacophore models for the discovery of 17 β -HSD1 inhibitors [129]. The pharmacophore models were validated to specifically recognize compounds possessing the structural and chemical features of steroids and flavonoids. Coumestrol displayed the most potent 17 β -HSD1 inhibiting activity among the test compounds used for model validation. However, coumestrol also inhibited 17 β -HSD5 and is, therefore, not selective [130]. Unfortunately, the virtual hits were not confirmed by biological validation [129].

To support the development of therapeutic inhibitors, database creation for pharmacophore model validation should focus on selective inhibitors to increase model selectivity and sensitivity. Since steroidal inhibitors and natural phytoestrogens, including flavonoids, often exhibit cross-reactivity with other enzymes and hormone receptors involved in the steroidogenesis, non-steroidal scaffolds are more favorable for virtual screening and drug development. However, although highly selective inhibitors are needed for many therapeutic applications, polyvalent inhibitors acting on synergistic pathways may be advantageous in some situations.

The 17 β -HSD1 can be inhibited by several modes: competing reversibly and irreversibly with the natural substrate for its binding site, competing with NADP(H) for its binding site at the Rossmann fold or occupying the ligand and the cofactor binding site by so-called hybrid compounds consisting of a steroidal core and extended side-chains of NADP(H) moieties [131,132]. Since only crystal structures containing steroidal inhibitors were available at that time, Schuster and Nashev *et al.* generated structure-based pharmacophore models based on steroidal inhibitors [133]. They developed two pharmacophore models, representing, on one hand, reversible competitive inhibitors based on the

steroidal core equilin (Figure 13A) and, on the other hand, hybrid inhibitors (Figure 13B). Whereas the first model was suggested to be suitable as a general screening tool, expecting many false positive hits, the hybrid model was more restrictive due to the unique scaffold of the underlying hybrid inhibitors. VS and subsequent *in vitro* validation of 14 selected compounds from the virtual hit list revealed, amongst others, two nonsteroidal hits with IC_{50} of 5.7 μ M and 19 μ M, respectively. As mentioned above, the SDR enzymes share substantial structural similarity. For selectivity assessment, 11 β -HSD1, 11 β -HSD2, 17 β -HSD2, 17 β -HSD3 and the AKR 17 β -HSD5 were tested. Two additional inhibitors were selective. One was a steroidal compound with an IC_{50} of 3.8 μ M for 11 β -HSD1 and 47 μ M for 17 β -HSD1, and one a nonsteroidal 11 β -HSD1 inhibitor with IC_{50} of 6.2 μ M and comparable activity on 17 β -HSD3. These observations emphasize the importance of including structurally related enzymes for selectivity assessment. In addition to the biological selectivity assessment, Schuster and Nashev *et al.* applied pharmacophore models of structurally related enzymes as an alternative strategy to identify unspecific inhibitors [133]. These pharmacophores should act as initial filters to eliminate compounds with a low degree of selectivity that may exhibit off-target effects. Screening the compounds identified as actives for 11 β -HSD1 with their previously established selective 11 β -HSD1 pharmacophore model resulted in retrieving one hit [106]. By deleting the shape restriction, the second hit was found as well and, at the same time, showed higher best fit values than an inactive compound. Thus, screening of pharmacophore models of related enzymes may facilitate the discrimination of selective and nonselective inhibitors and the virtual hit selection for *in vitro* testing, similar to the study by Guasch *et al.* described above [56].

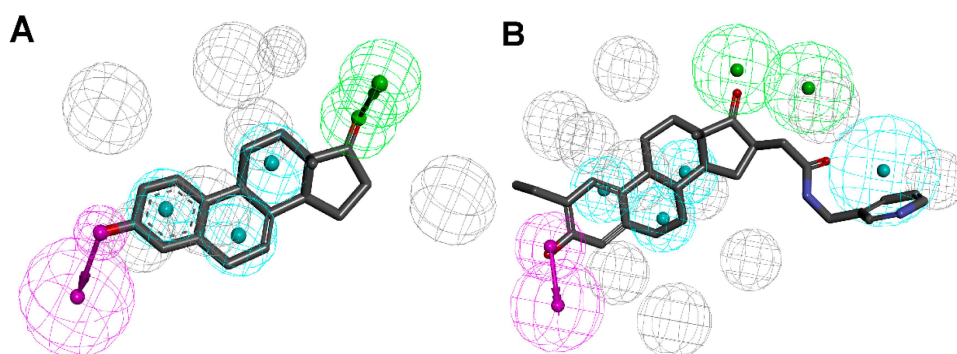


Figure 13. (A) 17 β -HSD1 model based on the equilin crystal structure (PDB entry 1EQU [5]); (B) The potent inhibitor STX 1040 maps the hybrid 17 β -HSD1 pharmacophore model [133].

For pharmacophore model generation, Sparado *et al.* [134] superimposed five 17 β -HSD1 crystal structures, covering most of the chemical space occupied by the co-crystallized ligands. Performing a VS of an in-house compound library led to the identification of one virtual hit with moderate inhibitory activity against 17 β -HSD1. Application of the rigidification strategy, scaffold hopping and further SAR analysis resulted in two far more potent benzothiazole-scaffold-bearing inhibitors with IC_{50} in cell lysates of 44 and 243 nM, respectively. Both hits were selective against 17 β -HSD2. Furthermore, the less active compound still potently inhibited estrogen formation, with a comparable IC_{50} value to the lysates, in a human cell model endogenously expressing 17 β -HSD1. The more potent compound showed pronounced affinity to bind to ER α and ER β . Depending on whether binding to ER α and ER β results in agonistic or antagonistic effects, this could cause beneficial or adverse effects. Interestingly, although the two hits differ only in a carbonyl and amide bridge, respectively, binding mode investigations by docking showed a 180° flipped orientation of the two molecules (Figure 14). The observation of a flipped binding mode was also discovered for corosolic acid and other triterpenoides in the binding pocket of 11 β -HSD1 as described earlier [108]. A follow-up lead optimization study to improve activity and selectivity of the two compounds for *in vivo* applications, without the help of molecular modeling techniques, led to the discovery of two new lead compounds [135]. They showed selectivity over 17 β -HSD2, no ER binding and promising activity in the intact cell model.

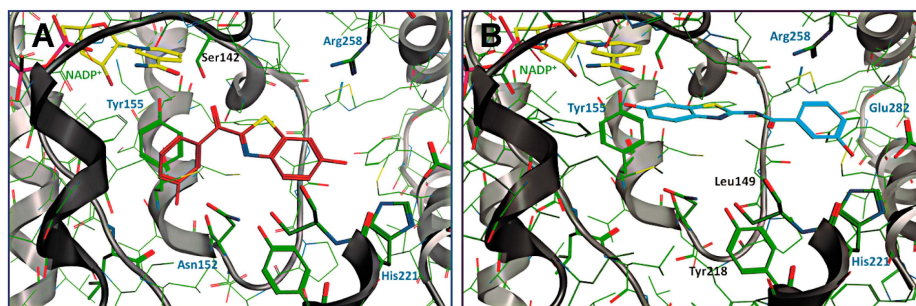


Figure 14. 17 β -HSD1 in complex with the two hits from Sparado *et al.* [134], (doi:10.1371/journal.pone.0029252.g010, doi:10.1371/journal.pone.0029252.g011) showing a 180° flipped orientation. IC₅₀ values of 44 nM (A) and 243 nM (B).

Table 2 shows a summary of the prospective pharmacophore-based virtual screening studies and illustrates the scaffold-hopping potential for 17 β -HSD1 inhibitors.

Structure-based and ligand-based pharmacophore modeling was performed by Karkola *et al.* [136]. They generated four pharmacophore models with different methods based on a crystal structure, a relaxed crystal structure, alignment of thienopyrimidinone inhibitors, and a docked complex of 17 β -HSD1 with a potent inhibitor. By VS, they found several compounds fitting into the active site of 17 β -HSD1 without determining the activity of the hits. However, to validate these hits as 17 β -HSD1 inhibitors, biological testing is needed. In addition, they could apply their differently generated pharmacophore models to calculate selectivity and sensitivity.

3.1.2. 17 β -Hydroxysteroid Dehydrogenase Type 2

The oxidative inactivation of estradiol to estrone is predominantly catalyzed by 17 β -HSD2. Additionally, 17 β -HSD2 is capable of converting testosterone into 4-androstene-3,17-dione (androstenedione), 5 α -dihydrotestosterone (DHT) into 5 α -androstenedione, 5-androstene-3 β ,17 β -diol to DHEA, and 20 α -dihydroprogesterone into progesterone using the cofactor NAD⁺ [137,138]. The 17 β -HSD2 is expressed in various tissues such as bone, placenta, endometrium, breast, uterus, prostate, stomach, small intestine, and colon epithelium [139,140]. The current treatment options for osteoporosis bear several limitations. Since 17 β -HSD2 is expressed in osteoblasts, its inhibition may provide a new approach to treat osteoporosis by increasing the local availability of estradiol.

Since 17 β -HSD2 contains an N-terminal transmembrane anchor, the experimental 3D structure determination remains a challenge and, to date, still no crystal structure is available. Due to this lack, Vuorinen *et al.* constructed three ligand-based pharmacophore models as virtual screening filters [141]. Virtual hit-testing in a cell-free assay revealed seven out of 29 compounds with IC₅₀ values against 17 β -HSD2 ranging between 0.24 μ M and 33 μ M. Most of the active compounds represented phenylbenzene-sulfonamides and -sulfonates. With the new structural classes of 17 β -HSD2 inhibitors, they performed a SAR study using two different approaches: first, by a 2D similarity search without fitting the compounds into the pharmacophore models, and second, using a pharmacophore model for VS. From the 2D search, one out of 16 compounds inhibited 17 β -HSD2 with an IC₅₀ of 3.3 μ M, whereas the VS showed five out of 14 compounds with IC₅₀ between 1–15 μ M. Selectivity of all active compounds was tested against inhibition of 17 β -HSD1, 17 β -HSD3, 11 β -HSD1, and 11 β -HSD2. The activity data of the phenylbenzene-sulfonamide and -sulfonate inhibitors revealed a phenolic hydroxyl group with hydrogen bond donor functionality, which was important for 17 β -HSD2 inhibition. This feature was confirmed by a ligand-based pharmacophore model that was developed based on several of the newly identified active compounds (Figure 15). Furthermore, to improve the initial pharmacophore model, a refinement database was created, including the original test set compounds and the newly identified inhibitors as well as the inactive compounds. The specificity of the model was increased by adding exclusion volumes. This approach is an important step to enhance a model's ability to enrich active compounds from a database.

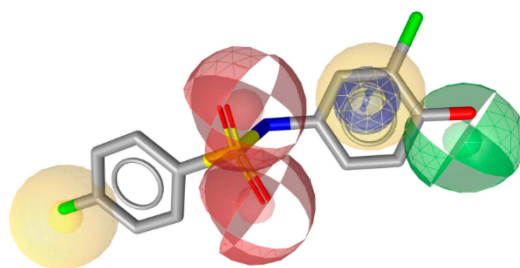


Figure 15. The selective 17 β -HSD2 model contains a HBD feature (green sphere), which is important for 17 β -HSD2 inhibitors such as the newly identified phenylbenzene-sulfonamide derivative 13 [141].

3.1.3. 17 β -Hydroxysteroid Dehydrogenase Type 3

The 17 β -HSD3 is almost exclusively expressed in the testes and catalyzes the reduction of androstenedione to testosterone in the presence of NADPH [142]. Although 17 β -HSD3 is mainly found in the testes, there is evidence for 17 β -HSD3 mRNA up-regulation in prostate cancer [143]. Co-expression of 17 β -HSD5, catalyzing the same reaction, might limit the therapeutic efficacy of 17 β -HSD3 inhibitors and a combined treatment with inhibitors against both enzymes should be envisaged.

The enzyme is anchored through an N-terminal transmembrane domain to the endoplasmic reticulum, and, like 17 β -HSD2, its catalytic domain faces the cytoplasmic compartment [144,145]. As for 17 β -HSD2, there is still no crystal structure available for the membrane protein 17 β -HSD3.

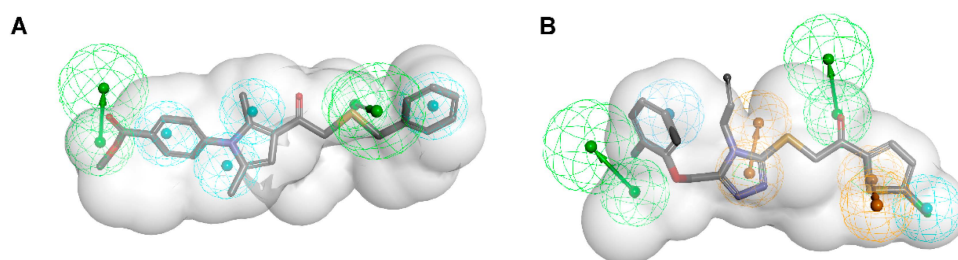


Figure 16. (A) The novel 17 β -HSD3 inhibitor 1–7 was identified with the steroid-based model consisting of two HBAs (green) and four H features (blue); (B) The non-selective inhibitor 2-2 mapped the nonsteroid-based 17 β -HSD3 model containing two HBAs, two AR (orange), one H and one H-AR feature [146].

Two ligand-based pharmacophore models, based on steroidal and nonsteroidal 17 β -HSD3 inhibitors, were developed by Schuster *et al.* [146] (Figure 16). These ligand-based models supported the observations by Vicker *et al.* of a highly hydrophobic active site of 17 β -HSD3 [147]. The models were then used to screen eight commercial databases and the hit list was further filtered prior to the selection of hits. Enzymatic tests showed that, from the steroid-based model, two out of 15 tested substances inhibited 17 β -HSD3, with one also inhibiting 17 β -HSD1 [146]. At the same time, three other compounds inhibiting the AKR 17 β -HSD5 were identified. The 17 β -HSD5 is a multifunctional enzyme and, like 17 β -HSD3, catalyzes the conversion of androstenedione into testosterone. The most potent compound was not selective and also inhibited 11 β -HSD1 and 11 β -HSD2. Similar results were obtained with the nonsteroidal model. The nonsteroidal model and its training compounds displayed several overlapping features with the lead compound identified earlier by Vicker *et al.* [147]; thus, the examination of their compounds for 17 β -HSD5 inhibitory activity would be interesting. These observations again emphasize the importance of including structurally related enzymes, independently of their enzymatic classes, for selectivity profiling. A summary of the 17 β -HSD3 pharmacophore-based virtual screening study presented by Schuster *et al.* is provided in Table 3.

Table 2. 17 β -HSD1 pharmacophore-based virtual screening studies summarized.

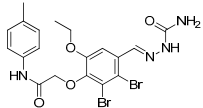
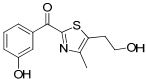
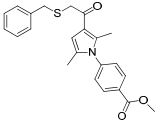
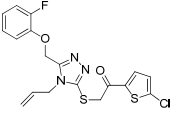
Reference Study Aim	Pharmacophore Model	Database Used for VS	Hits			Biological Testing			
			Most Active Hit	Number of Virtual Hits	Tested <i>in Vitro</i>	Actives	Assay	IC ₅₀	Selectivity
Schuster and Nashev <i>et al.</i> [133] 17 β -HSD1 inhibitors	Structure-based Using LigandScout and Catalyst 115R model (4 H, 2HBA, 2 HBD) Based on a hybrid inhibitor	NCI, SPECS		1559/340042	14	4, IC ₅₀ < 50 μ M	Lysates	5.7–47 μ M	Selective over 17 β -HSD2, 17 β -HSD3, 17 β -HSD5 and 11 β -HSD1, except one compound, which was not selective towards 17 β -HSD5 and 11 β -HSD1. However, one compound inhibited 17 β -HSD3 and 11 β -HSD1 but not 17 β -HSD1 and another compound inhibited 11 β -HSD1 only.
Sparado <i>et al.</i> [134] 17 β -HSD1 inhibitors and lead optimization	Ligand-based By superimposing co-crystallized ligands using MOE (5 H, 3 HBA, 1 HBD, 1 AR)	In-house database		-/37	-	1	Cell-free	34% Enzyme inhibition with 10 μ M test compounds	Selectivity of optimized compounds tested against 17 β -HSD2 and ER α and ER β

Table 3. Summary of the 17 β -HSD3 pharmacophore-based virtual screening study.

Reference Study Aim	Pharmacophore Model	Database Used for VS	Hits			Biological Testing			
			Most Active Hit	Number of Hits after Filtering	Tested <i>in Vitro</i>	Actives	Assay	Enzyme Inhibition	Selectivity
Schuster <i>et al.</i> [146] 17 β -HSD3 inhibitors	Ligand-based Using Catalyst	Asinex Gold and Platinum, ChemBridge, Enamine, IF-Labs, Maybridge, Specs, Vitas-M		3921/1712102	15	2	Lysates	Inhibition >40% with 2 μ M test compounds as threshold 41.3% and 50.8%	Selective over 17 β -HSD2, 17 β -HSD4, 17 β -HSD7, 11 β -HSD1, and 11 β -HSD2, acceptable selectivity over 17 β -HSD1 and 17 β -HSD5. However, several hits inhibited 17 β -HSD5 more potently than 17 β -HSD3
	Model 1: steroidal training compounds (four H, two HBA)			8190/1712102	16	2		55.6% and 57.5%	Selective over 17 β -HSD2, 17 β -HSD4, 17 β -HSD7, and 11 β -HSD2, acceptable selectivity over 17 β -HSD1. One hit was not selective over 17 β -HSD5 and the other not over 11 β -HSD1. However, several hits inhibited 17 β -HSD5 more potently than 17 β -HSD3

3.2. Applications in Toxicology

3.2.1. Anti-Target Screening

Although the actual virtual screening process is analogous to lead identification, anti-target screening pursues a different aim. Lead identification focuses on the discovery of ligands for therapeutically relevant targets, whereas anti-target screening aims at predicting the interaction of molecules with macromolecules mediating potentially harmful effects (so-called anti-targets). These investigations support the identification of (serious) adverse events already at an early stage in drug development. This strategy is powerful, as recently shown by Kratz *et al.* [148], who successfully applied pharmacophore models to identify inhibitors of the human ether-a-go-go-related gene (hERG) potassium channel, thereby predicting the cardiotoxic potential of the investigated molecules [148].

3.2.2. Parallel Screening

Parallel screening represents an extension to lead identification and anti-target screening protocols. It investigates not a single target but a whole collection of macromolecules with the aim of obtaining activity profiles of compounds of interest in order to prioritize further investigation. Thus, the focus of this technique shifts from the target of interest to the compound of interest, which is screened against a collection of pharmacophores, representing a plethora of different targets. Parallel screening has the potential to identify macromolecular interaction partners of the investigated molecule, thereby providing novel insight into its biological activities. These activities may include beneficial (*i.e.*, therapeutic) and harmful (*i.e.*, toxic) effects. Therefore, the results support the evaluation of a compound both with regard to the occurrence of adverse events and potential novel application fields (whenever this aspect represents the main aim of the parallel screening, this technique is also referred to as drug repurposing or drug repositioning). In the attempt to explore the biological activity of leoligin, a lignan isolated from the alpine plant Edelweiss (*Leontopodium alpinum*), the compound was screened against the Inte:Ligand pharmacophore collection in the course of a parallel screening [149]. Among the proposed targets, wascholesteryl ester transfer protein (CETP), a target involved in lipoprotein metabolism, was shown to be activated by leoligin in subsequent experimental testing. On the other side, leoligin was also predicted to inhibit the cytochrome P450 (CYP) isoforms 1A2, 2C9, and 3A4 [150], which are involved in the metabolic clearance of exogenous compounds. While it was not active on CYP1A2, it was a weak inhibitor on CYP2C9, and a sub-micromolar IC₅₀ was determined for CYP3A4 [150]. Inhibition of CYP enzymes can cause severe drug-drug interactions that may lead to serious adverse effects and eventually require the termination of a drug development project. Accordingly, both potentially beneficial (CETP activation) and potentially harmful (CYP inhibition) effects can be detected during a parallel screening.

3.2.3. Examples

There is a great demand for improved methods for the safety assessment of man-made chemicals released into the environment [68,151]. Endocrine-disrupting chemicals (EDCs) are exogenous substances interfering with hormone synthesis, metabolism and/or hormonal regulation, thereby adversely affecting human health by contributing to developmental and reproductive disorders, cardio-metabolic diseases, cancer, and immune-related diseases and psychiatric disorders [152]. EDCs include substances used in agriculture, industrial production, dyes, food preservatives, or body care products and cosmetics. Several SDRs are essentially involved in the control of the local availability of active glucocorticoids, androgens and estrogens, and these enzymes should therefore be considered in the assessment of potential EDCs. *In silico* tools are well established in the drug discovery process; however, they can also display a valuable part in the identification of new EDCs or the mechanism of action of known EDCs [68].

Nashev and Vuorinen *et al.* [70] reported a pharmacophore-based virtual screening using a ligand-based 11 β -HSD pharmacophore model preferentially focusing on 11 β -HSD2 [106]. The 11 β -HSD2

protects the mineralocorticoid receptor (MR) from activation by cortisol and renders specificity for the much less abundant aldosterone to activate this receptor. Genetic defects of this enzyme cause the syndrome of apparent mineralocorticoid excess (AME), characterized by hypokalemia, hypernatremia, and severe hypertension [153,154]. In addition, placental 11 β -HSD2 protects the fetus from enhanced maternal cortisol exposure [155,156]. Therefore, disrupting corticosteroid action by EDCs can be expected to cause substantial adverse health effects. VS of an EDC database predicted 29 compounds fitting into the model of which five hits were selected for biological evaluation. Two compounds were found to inhibit 11 β HSD2, the silane coupling agent AB110873 and the antibiotic lasalocid, with IC₅₀ values of 6.1 μ M and 14 μ M, respectively. The silane AB110873 is widely used as a rubber additive for the production of tires, mechanical goods, or shoe soles and lasalocid is used as a feed additive for the prevention of infections in the breeding of chicken and turkeys. Docking studies were implemented to understand the binding mode of AB110873 in 11 β -HSD2 (Figure 17) and MR.

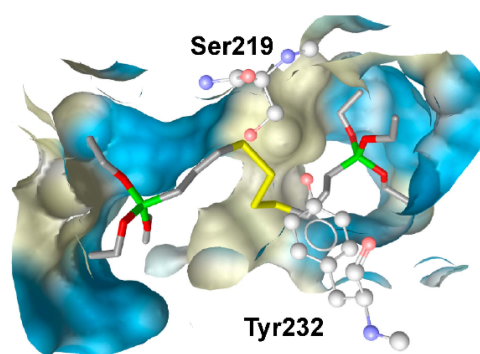


Figure 17. Docking of silane into the homology model of 11 β -HSD2 [78] suggests hydrogen bond interactions with Ser219 and Tyr232 [70].

Genetic defects resulting in 17 β -HSD3 deficiency cause 46,XY disorder of sex development [142,157,158]. Inhibition of 17 β -HSD3 activity by EDCs might reduce plasma testosterone levels, thereby interfering with male sexual development and contributing to male reproductive disorders. To identify potential EDCs inhibiting 17 β -HSD3, Nashev and Schuster *et al.* generated a ligand-based pharmacophore model [74]. VS of an EDC database predicted several organic UV filters containing a benzophenone as a bioactive chemical scaffold. UV filters are a structurally diverse class of chemicals widely used in sunscreens and cosmetics as well as plastic additives. *In vitro* testing of selected virtual hits and similar environmentally relevant derivatives led to the identification of benzophenone-1 (BP-1) as the most potent 17 β -HSD3 inhibitor with an IC₅₀ of 1.05 μ M in intact cells. BP-2,3-benzylidene camphor (3-BC) and 4-methylbenzylidene camphor (4-MBC) moderately inhibited 17 β -HSD3 with IC₅₀ values between 10.7 μ M and 33.3 μ M, but showed substantial inhibitory activity on 17 β -HSD2 with IC₅₀ between 5.9 μ M and 10.3 μ M. Importantly, the most active compound, BP-1, as well as 3-BC and 4-MBC were not included in the initial virtual hit list but added to the biological testing due to their use as UV filters. Hence, VS displays an initial filter for the identification of potential EDC compound classes and aims at prioritizing the compounds to be included for biological investigations. In analogy to the drug discovery process, it is important to test structurally related enzymes in order to know whether they are affected by a given EDC. Importantly, major metabolites should also be included in the analysis. For example, BP-3 showed no activity against 17 β -HSD3, but it is demethylated *in vivo* to the potent inhibitor BP-1 [159]. To explain the differential inhibitory activities of the tested UV filters, Schuster and Nashev conducted pharmacophore-based SAR studies, suggesting that the ether group on BP-3 and BP-8 instead of a hydroxyl group on BP-1 and BP-2 was the reason for the loss of activity of BP-3 and BP-8 (Figure 18). To further study the toxicological relevance of 17 β -HSD3 inhibition by BP-1, concentrations reached *in vivo*, especially in the testes, need to be determined.

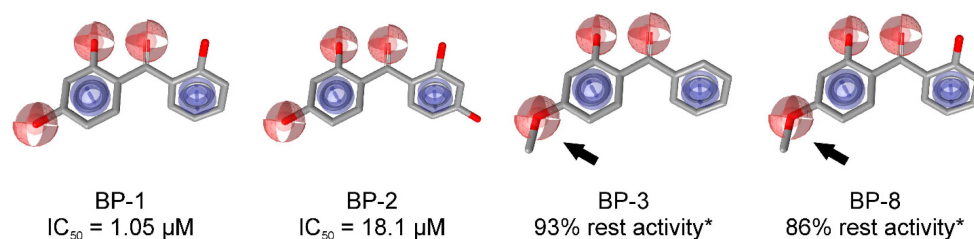


Figure 18. SAR analysis revealed that the etherification of the hydroxyl group (as indicated by the arrows) was responsible for the loss of activity observed for BP-3 and BP-8 [74]. *Remaining enzyme activity at a compound concentration of 20 μM compared to vehicle control.

4. Limitations

As with every method, pharmacophore modeling and pharmacophore-based virtual screening also have their limits. A recent study compared the performances of two pharmacophore modeling programs, LigandScout and Discovery Studio, on the identification of novel cyclooxygenase inhibitors [160]. Intriguingly, although both programs succeeded in the identification of novel bioactive molecules, the virtual hit lists retrieved with the two tools were highly complementary. It is of note that not a single overlap in the hit lists was observed, even when the identical crystal structure of a ligand-target complex was employed for model generation. This illustrates that neither of the two programs was capable of comprehensively covering the active space and that models from different programs need to be combined whenever a more complete retrieval of active molecules is required. The authors suggested that the reasons for this finding may be found in the different screening algorithms and feature definitions deployed by the programs.

Feature definitions can be improved in general, as highlighted by the treatment of halogens. Some pharmacophore modeling programs consider halogens solely as hydrophobic moieties in the default settings [7,8,161]. LigandScout, in addition, matches fluorine to HBA features [6]. In 2013, a study by Sirimulla *et al.* [162] revealed that in many ligand-target complexes, halogens participate in strong halogen bond formation, e.g., with aromatic rings, and thereby considerably contribute to the interaction between the ligand and the target. These types of interactions, although often employed by medicinal chemists to improve the binding affinity of compounds [162], are not yet implemented in common pharmacophore-based virtual screening tools.

A major limitation, not only for pharmacophore modeling but for virtual screening tools in general, is the fact that the quality of a pharmacophore model critically depends on the data employed for model generation, refinement, and theoretical validation. Many public data repositories are available that can be explored to build a model. However, caution is required as, apparently, parts of the data are erroneous. Fourches *et al.* investigated six different datasets, and after curation, up to 10% of the original structures were removed [163]. Besides several other preventive measures, the authors suggest to include a final manual inspection step to check the structures of the input compounds. We fully support this recommendation and would even go one step further: Not only the structures of the compounds included in the modeling dataset need to be critically evaluated, but also the annotated biological data. This starts with inclusion/exclusion criteria for appropriate/inappropriate testing systems applied to determine the biological activity of a compound (for example, data obtained from intact cell assays or from animal tissue preparations are of limited use for human enzyme models), the application of suitable activity cut-offs (distinguishing between specific and unspecific effects, depending on the investigated target), and ends at a critical comparison with the original literature as errors can also happen during the transfer of data to depositories. These procedures may be quite elaborate; nevertheless, they are crucial for the generation of high quality models and every modeler is well advised to carefully review the data on which the models are based.

Another limitation is a lack of compounds confirmed as inactive for a specific target. Results on proven inactives for model validation are often not accessible because, unfortunately, negative

results are rarely published. The information from confirmed inactive compounds is important for the balancing between selectivity and sensitivity of a model during the validation step. In the drug development process, restrictive models are required because, finally, only one or a few lead compounds are selected for further optimization steps, whereas in a toxicology screening, it is important to correctly find preferably all of the potentially harmful substances. Albeit considerably more successful than random screening, the success rate of VS may still be a limiting factor for toxicological projects. However, it has the ability to identify structural compound classes that then can be further evaluated. Obviously, the database used for VS might be self-limiting as not all potential active compounds are included.

One caveat of pharmacophore modeling is that a modeler needs to be aware of concerns about detailed interaction patterns of the active compounds in the dataset. Although high quality experimental data confirming their binding and activity may be available for these ligands, the exact binding site is still not clearly defined for most of them. Many molecules may occupy a similar yet slightly different part of the binding pocket, e.g., compared to the co-crystallized ligand in an X-ray crystallographic complex employed for model generation. Accordingly, the interaction patterns may differ. This factor is even more pronounced in ligands affecting the function of a protein by binding to allosteric sites, disrupting conformational changes, or interfering with post-translational modifications. Similar concerns also apply for the experimental validation of the *in silico* predictions, as it is, in the end, often not known whether the newly identified compounds indeed exert the predicted binding mode [164]. An X-ray crystal structure of the ligand-target complex would provide the ultimate confirmation of the exact interaction patterns; however, 3D structure resolution of transmembrane proteins by crystallization remains difficult. Several SDRs belong to this class of proteins such as, for instance, 11 β HSD2, 17 β HSD2, and 17 β HSD3. For these proteins, structure-based pharmacophore modeling is currently not possible, and homology modeling remains challenging due to the low sequence similarity of SDRs. However, for these cases, ligand-based pharmacophore modeling displays an elegant solution.

Pharmacophore-based VS proved to be a powerful tool to support drug discovery and development, especially concerning the enrichment of active molecules among test compounds. Nevertheless, expectations concerning the results of VS need to remain realistic. Although sometimes potent compounds are discovered via VS, the majority of virtual hits usually display only weak activity. For this concern, the initial virtual hits from VS should be considered similar to initial experimental hits discovered in a HTS campaign, which also require further chemical optimization steps to develop to potential drug candidates [164].

5. Conclusions

The current work summarizes prospective pharmacophore-based studies conducted in the field of steroid biology, with special focus on SDRs, and highlights success stories reported in this area. Pharmacophore models are suitable to address a wide range of issues relevant for both drug discovery and toxicology. This is of special relevance for SDRs, because members of this target class are both associated with therapeutic value (e.g., 17 β -HSD1 inhibition for the treatment of hormone-sensitive cancers) and toxicological liabilities (disruption of 11 β -HSD2 actions). Although the method itself still has room for improvement as pointed out in the “Limits” section, the caveats associated with pharmacophore modeling largely also apply for other virtual screening techniques. In addition, in case of a lack of available structural data on macromolecular targets, ligand-based modeling strategies offer a useful alternative. The identification of structurally diverse molecules may, to a certain extent, be restricted to the data employed for model generation and refinement. However, the extraction of crucial interactions and their representation via abstract chemical features proved to be a powerful approach to step beyond the initial chemical space. As highlighted in this review, pharmacophore-based VS is a valuable scaffold-hopping tool. Importantly, this allows for the application of pharmacophore-based virtual screening also for compound classes that do not fall into the category of “small drug-like

compounds” or whose properties differ from that of synthetic compounds: For example, natural products provide a vast resource for bioactive compounds that can be exploited for therapeutic purposes. On the other hand, the *in silico*-driven investigation of environmental chemicals, which often chemically differ from drug-like molecules, facilitates the rapid identification of potentially harmful compounds that need to be prioritized for experimental evaluation. Given the many application fields of pharmacophore-based virtual screening and the successful examples summarized in this review, an increasing number of studies, also in the field of SDR research, can be expected in the future.

Acknowledgments: We are grateful for financial support from the Austrian Science Fund (FWF, project P26782 “Safety of environmental chemicals”. A.O. was supported as Chair for Molecular and Systems Toxicology by the Novartis Research Foundation.

Author Contributions: Teresa Kaserer, Katharina R. Beck, Muhammad Akram, Alex Odermatt and Daniela Schuster were involved in literature search, data analysis and interpretation, and writing of the manuscript.

Conflicts of Interest: The authors declare no conflict of interest.

Abbreviations

The following abbreviations are used in this manuscript:

3-BC	3-benzylidene camphor
4-MBC	4-methylbenzylidene camphor
AKR	aldo-keto reductase
AME	apparent mineralocorticoid excess
AR	aromatic features
BP	benzophenone
CETP	cholesterylester transfer protein
CYP	cytochrome P450
DHEA	dehydroepiandrosterone
DHT	5 α -dihydrotestosterone
DUD-E	Directory of Useful Decoys, Enhanced
EDCs	endocrine disrupting chemicals
ER	estrogen receptor
GA	glycyrrhetic acid
H	hydrophobic feature
HBA	hydrogen bond acceptor
HBD	hydrogen bond donor
hERG	human ether-a-go-go related gene
HSD	hydroxysteroid dehydrogenase
HTS	high-throughput screening
IUPAC	International Union of Pure and Applied Chemistry
MD	molecular dynamics
MOE	Molecular Operating Environment
MR	mineralocorticoid receptor
NADP	nicotinamide adenine dinucleotide phosphate
PAINS	Pan-Assay Interference Compounds
PDB	Protein Data Bank
PPAR γ	peroxisome proliferator-activated receptor γ
ROC-AUC	area under the receiver operating characteristics curve
SAR	structure-activity relationship
SDR	short-chain dehydrogenase/reductase

VS	virtual screening
XVols	exclusion volumes

References

1. Ehrlich, P. Über die constitution des diphtheriegiftes. *Deutsch. Med. Wochschr.* **1898**, *24*, 597–600. [[CrossRef](#)]
2. Güner, O.F.; Bowen, J.P. Setting the record straight: The origin of the pharmacophore concept. *J. Chem. Inf. Model.* **2014**, *54*, 1269–1283. [[CrossRef](#)] [[PubMed](#)]
3. Schueler, F.W. *Chemobiodynamics and Drug Design*; McGraw-Hill: New York, NY, USA, 1960.
4. Wermuth, G.; Ganellin, C.R.; Lindberg, P.; Mitscher, L.A. Glossary of terms used in medicinal chemistry (iupac recommendations 1998). *Pure Appl. Chem.* **1998**, *70*, 1129–1143. [[CrossRef](#)]
5. Sawicki, M.W.; Erman, M.; Puranen, T.; Vihko, P.; Ghosh, D. Structure of the ternary complex of human 17 β -hydroxysteroid dehydrogenase type 1 with 3-hydroxyestra-1,3,5,7-tetraen-17-one (equilin) and NADP⁺. *Proc. Natl. Acad. Sci. USA* **1999**, *96*, 840–845. [[CrossRef](#)] [[PubMed](#)]
6. Wolber, G.; Langer, T. Ligandscout: 3-D pharmacophores derived from protein-bound ligands and their use as virtual screening filters. *J. Chem. Inf. Model.* **2005**, *45*, 160–169. [[CrossRef](#)] [[PubMed](#)]
7. Dassault Systèmes BIOVIA. *Discovery Studio Modeling Environment*; Dassault Systèmes: San Diego, CA, USA, 2015.
8. *Molecular Operating Environment (MOE)*; Chemical Computing Group Inc.: Montreal, QC, Canada, 2015.
9. Berman, H.; Westbrook, J.; Feng, Z.; Gilliland, G.; Bhat, T.; Weissig, H.; Shindyalov, I.; Bourne, P. The Protein Data Bank. *Nucleic Acids Res.* **2000**, *28*, 235–242. [[CrossRef](#)] [[PubMed](#)]
10. Sutter, J.; Li, J.; Maynard, A.J.; Goupil, A.; Luu, T.; Nadassy, K. New features that improve the pharmacophore tools from accelrys. *Curr. Comput.-Aided Drug Des.* **2011**, *7*, 173–180. [[CrossRef](#)] [[PubMed](#)]
11. Kitchen, D.B.; Decornez, H.; Furr, J.R.; Bajorath, J. Docking and scoring in virtual screening for drug discovery: Methods and applications. *Nat. Rev. Drug Discov.* **2004**, *3*, 935–949. [[CrossRef](#)] [[PubMed](#)]
12. Shen, J.; Zhang, W.; Fang, H.; Perkins, R.; Tong, W.; Hong, H. Homology modeling, molecular docking, and molecular dynamics simulations elucidated alpha-fetoprotein binding modes. *BMC Bioinform.* **2013**, *14* (Suppl. 14), S6.
13. Bey, E.; Marchais-Oberwinkler, S.; Kruchten, P.; Frotscher, M.; Werth, R.; Oster, A.; Algül, O.; Neugebauer, A.; Hartmann, R.W. Design, synthesis and biological evaluation of bis(hydroxyphenyl) azoles as potent and selective non-steroidal inhibitors of 17 β -hydroxysteroid dehydrogenase type 1 (17 β -HSD1) for the treatment of estrogen-dependent diseases. *Bioorg. Med. Chem.* **2008**, *16*, 6423–6435. [[CrossRef](#)] [[PubMed](#)]
14. Oster, A.; Hinsberger, S.; Werth, R.; Marchais-Oberwinkler, S.; Frotscher, M.; Hartmann, R.W. Bicyclic substituted hydroxyphenylmethanones as novel inhibitors of 17 β -hydroxysteroid dehydrogenase type 1 (17 β -hsd1) for the treatment of estrogen-dependent diseases. *J. Med. Chem.* **2010**, *53*, 8176–8186. [[CrossRef](#)] [[PubMed](#)]
15. Akram, M.; Kaserer, T.; Schuster, D. Pharmacophore modeling and screening. In *In silico Drug Discovery and Design: Theory, Methods, Challenges and Applications*; Cavasotto, C., Ed.; CRC Press: Boca Raton, FL, USA, 2015; pp. 123–153.
16. Vuorinen, A.; Schuster, D. Methods for generating and applying pharmacophore models as virtual screening filters and for bioactivity profiling. *Methods* **2015**, *71*, 113–134. [[CrossRef](#)] [[PubMed](#)]
17. Lagarde, N.; Zagury, J.-F.; Montes, M. Benchmarking data sets for the evaluation of virtual ligand screening methods: Review and perspectives. *J. Chem. Inf. Model.* **2015**, *55*, 1297–1307. [[CrossRef](#)] [[PubMed](#)]
18. Heikamp, K.; Bajorath, J. Comparison of confirmed inactive and randomly selected compounds as negative training examples in support vector machine-based virtual screening. *J. Chem. Inf. Model.* **2013**, *53*, 1595–1601. [[CrossRef](#)] [[PubMed](#)]
19. Gaulton, A.; Bellis, L.J.; Bento, A.P.; Chambers, J.; Davies, M.; Hersey, A.; Light, Y.; McGlinchey, S.; Michalovich, D.; Al-Lazikani, B.; et al. ChEMBL: A large-scale bioactivity database for drug discovery. *Nucleic Acids Res.* **2011**, *40*, D1100–D1107. [[CrossRef](#)] [[PubMed](#)]
20. Wishart, D.S.; Knox, C.; Guo, A.C.; Shrivastava, S.; Hassanali, M.; Stothard, P.; Chang, Z.; Woolsey, J. Drugbank: A comprehensive resource for in silico drug discovery and exploration. *Nucleic Acids Res.* **2006**, *34*, D668–D672. [[CrossRef](#)] [[PubMed](#)]

21. Williams, A.J.; Harland, L.; Groth, P.; Pettifer, S.; Chichester, C.; Willighagen, E.L.; Evelo, C.T.; Blomberg, N.; Ecker, G.; Goble, C.; *et al.* Open phacts: Semantic interoperability for drug discovery. *Drug Discov. Today* **2012**, *17*, 1188–1198. [[CrossRef](#)] [[PubMed](#)]
22. Dix, D.J.; Houck, K.A.; Martin, M.T.; Richard, A.M.; Setzer, R.W.; Kavlock, R.J. The toxcast program for prioritizing toxicity testing of environmental chemicals. *Toxicol. Sci.* **2007**, *95*, 5–12. [[CrossRef](#)] [[PubMed](#)]
23. Kavlock, R.J.; Austin, C.P.; Tice, R.R. Toxicity testing in the 21st century: Implications for human health risk assessment. *Risk Anal.* **2009**, *29*, 485–487. [[CrossRef](#)] [[PubMed](#)]
24. Wang, Y.; Xiao, J.; Suzek, T.O.; Zhang, J.; Wang, J.; Zhou, Z.; Han, L.; Karapetyan, K.; Dracheva, S.; Shoemaker, B.A.; *et al.* Pubchem’s bioassay database. *Nucleic Acids Res.* **2012**, *40*, D400–D412. [[CrossRef](#)] [[PubMed](#)]
25. Verdonk, M.L.; Berdini, V.; Hartshorn, M.J.; Mooij, W.T.M.; Murray, C.W.; Taylor, R.D.; Watson, P. Virtual screening using protein–ligand docking: Avoiding artificial enrichment. *J. Chem. Inf. Comput. Sci.* **2004**, *44*, 793–806. [[CrossRef](#)] [[PubMed](#)]
26. Kirchmair, J.; Markt, P.; Distinto, S.; Wolber, G.; Langer, T. Evaluation of the performance of 3d virtual screening protocols: Rmsd comparisons, enrichment assessments, and decoy selection—What can we learn from earlier mistakes? *J. Comput. Aided Mol. Des.* **2008**, *22*, 213–228. [[CrossRef](#)] [[PubMed](#)]
27. Huang, N.; Shoichet, B.K.; Irwin, J.J. Benchmarking sets for molecular docking. *J. Med. Chem.* **2006**, *49*, 6789–6801. [[CrossRef](#)] [[PubMed](#)]
28. Mysinger, M.M.; Carchia, M.; Irwin, J.J.; Shoichet, B.K. Directory of useful decoys, enhanced (DUD-E): Better ligands and decoys for better benchmarking. *J. Med. Chem.* **2012**, *55*, 6582–6594. [[CrossRef](#)] [[PubMed](#)]
29. Vuorinen, A.; Nashev, L.G.; Odermatt, A.; Rollinger, J.M.; Schuster, D. Pharmacophore model refinement for 11 β -xhydroysteroid dehydrogenase inhibitors: Search for modulators of intracellular glucocorticoid concentrations. *Mol. Inf.* **2014**, *33*, 15–25. [[CrossRef](#)]
30. Güner, F.; Henry, R. Metric for analyzing hit-lists and pharmacophores. In *Pharmacophore Perception, Development, and Use in Drug Design*; Güner, O.F., Ed.; International University Line: La Jolla, CA, USA, 2000; pp. 193–212.
31. Triballeau, N.; Acher, F.; Brabet, I.; Pin, J.-P.; Bertrand, H.-O. Virtual screening workflow development guided by the “receiver operating characteristic” curve approach. Application to high-throughput docking on metabotropic glutamate receptor subtype 4. *J. Med. Chem.* **2005**, *48*, 2534–2547. [[CrossRef](#)] [[PubMed](#)]
32. Braga, R.C.; Andrade, C.H. Assessing the performance of 3d pharmacophore models in virtual screening: How good are they? *Curr. Top. Med. Chem.* **2013**, *13*, 1127–1138. [[CrossRef](#)] [[PubMed](#)]
33. Bajorath, J. Integration of virtual and high-throughput screening. *Nat. Rev. Drug Discov.* **2002**, *1*, 882–894. [[CrossRef](#)] [[PubMed](#)]
34. Tanrikulu, Y.; Krüger, B.; Proschak, E. The holistic integration of virtual screening in drug discovery. *Drug Discov. Today* **2013**, *18*, 358–364. [[CrossRef](#)] [[PubMed](#)]
35. Schuster, D.; Spetea, M.; Music, M.; Rief, S.; Fink, M.; Kirchmair, J.; Schütz, J.; Wolber, G.; Langer, T.; Stuppner, H.; *et al.* Morphinans and isoquinolines: Acetylcholinesterase inhibition, pharmacophore modeling, and interaction with opioid receptors. *Bioorganic Med. Chem.* **2010**, *18*, 5071–5080. [[CrossRef](#)] [[PubMed](#)]
36. Polgár, T.; Baki, A.; Szendrei, G.L.; Keserű, G.M. Comparative virtual and experimental high-throughput screening for glycogen synthase kinase-3 β inhibitors. *J. Med. Chem.* **2005**, *48*, 7946–7959. [[CrossRef](#)] [[PubMed](#)]
37. Doman, T.N.; McGovern, S.L.; Witherbee, B.J.; Kasten, T.P.; Kurumbail, R.; Stallings, W.C.; Connolly, D.T.; Shoichet, B.K. Molecular docking and high-throughput screening for novel inhibitors of protein tyrosine phosphatase-1b. *J. Med. Chem.* **2002**, *45*, 2213–2221. [[CrossRef](#)] [[PubMed](#)]
38. Wu, B.; Gao, J.; Wang, M. Development of a complex scintillation proximity assay for high throughput screening of ppar[γ] modulators. *Acta Pharmacol. Sin.* **2005**, *26*, 339–344. [[CrossRef](#)] [[PubMed](#)]
39. Murgueitio, M.S.; Henneke, P.; Glossmann, H.; Santos-Sierra, S.; Wolber, G. Prospective virtual screening in a sparse data scenario: Design of small-molecule tlr2 antagonists. *ChemMedChem* **2014**, *9*, 813–822. [[CrossRef](#)] [[PubMed](#)]
40. Krautscheid, Y.; Senning, C.J.Å.; Sartori, S.B.; Singewald, N.; Schuster, D.; Stuppner, H. Pharmacophore modeling, virtual screening, and *in vitro* testing reveal haloperidol, eprazinone, and fenbutrazate as neurokinin receptors ligands. *J. Chem. Inf. Model.* **2014**, *54*, 1747–1757. [[CrossRef](#)] [[PubMed](#)]

41. Joung, J.Y.; Lee, H.Y.; Park, J.; Lee, J.-Y.; Chang, B.H.; No, K.T.; Nam, K.-Y.; Hwang, J.S. Identification of novel rab27a/melanophilin blockers by pharmacophore-based virtual screening. *Appl. Biochem. Biotechnol.* **2014**, *172*, 1882–1897. [[CrossRef](#)] [[PubMed](#)]
42. Lu, P.; Wang, Y.; Ouyang, P.K.; She, J.; He, M. 3d-qsar based pharmacophore modeling and virtual screening for identification of novel g protein-coupled receptor 40 agonists. *Curr. Comput.-Aided Drug Des.* **2015**, *11*, 51–56. [[CrossRef](#)] [[PubMed](#)]
43. Singh, N.; Tiwari, S.; Srivastava, K.K.; Siddiqi, M.I. Identification of novel inhibitors of mycobacterium tuberculosis pknG using pharmacophore based virtual screening, docking, molecular dynamics simulation, and their biological evaluation. *J. Chem. Inf. Model.* **2015**, *55*, 1120–1129. [[CrossRef](#)] [[PubMed](#)]
44. Temml, V.; Voss, C.V.; Dirsch, V.M.; Schuster, D. Discovery of new liver x receptor agonists by pharmacophore modeling and shape-based virtual screening. *J. Chem. Inf. Model.* **2014**, *54*, 367–371. [[CrossRef](#)] [[PubMed](#)]
45. Ha, H.; Debnath, B.; Odde, S.; Bensman, T.; Ho, H.; Beringer, P.M.; Neamati, N. Discovery of novel cxcr2 inhibitors using ligand-based pharmacophore models. *J. Chem. Inf. Model.* **2015**, *55*, 1720–1738. [[CrossRef](#)] [[PubMed](#)]
46. Lepailleur, A.; Freret, T.; Lemaître, S.; Boulouard, M.; Dauphin, F.; Hirschberger, A.; Dulin, F.; Lesnard, A.; Bureau, R.; Rault, S. Dual histamine h3r/serotonin 5-ht4r ligands with anti-amnesic properties: Pharmacophore-based virtual screening and polypharmacology. *J. Chem. Inf. Model.* **2014**, *54*, 1773–1784. [[CrossRef](#)] [[PubMed](#)]
47. Ferreira, R.J.; dos Santos, D.J.V.A.; Ferreira, M.-J.U.; Guedes, R.C. Toward a better pharmacophore description of p-glycoprotein modulators, based on macrocyclic diterpenes from euphorbia species. *J. Chem. Inf. Model.* **2011**, *51*, 1315–1324. [[CrossRef](#)] [[PubMed](#)]
48. Flohr, S.; Kurz, M.; Kostenis, E.; Brkovich, A.; Fournier, A.; Klabunde, T. Identification of nonpeptidic urotensin ii receptor antagonists by virtual screening based on a pharmacophore model derived from structure–activity relationships and nuclear magnetic resonance studies on urotensin ii. *J. Med. Chem.* **2002**, *45*, 1799–1805. [[CrossRef](#)] [[PubMed](#)]
49. Hessler, G.; Baringhaus, K.-H. The scaffold hopping potential of pharmacophores. *Drug Discov. Today Technol.* **2010**, *7*, e263–e269. [[CrossRef](#)] [[PubMed](#)]
50. Goldmann, D.; Pakfeifer, P.; Hering, S.; Ecker, G.F. Novel scaffolds for modulation of trpv1 identified with pharmacophore modeling and virtual screening. *Future Med. Chem.* **2015**, *7*, 243–256. [[CrossRef](#)] [[PubMed](#)]
51. Ayan, D.; Maltais, R.; Roy, J.; Poirier, D. A new nonestrogenic steroidal inhibitor of 17beta-hydroxysteroid dehydrogenase type i blocks the estrogen-dependent breast cancer tumor growth induced by estrone. *Mol. Cancer Ther.* **2012**, *11*, 2096–2104. [[CrossRef](#)] [[PubMed](#)]
52. Delvoux, B.; D’Hooghe, T.; Kyama, C.; Koskimies, P.; Hermans, R.J.; Dunselman, G.A.; Romano, A. Inhibition of type 1 17beta-hydroxysteroid dehydrogenase impairs the synthesis of 17beta-estradiol in endometriosis lesions. *J. Clin. Endocr. Metab.* **2014**, *99*, 276–284. [[CrossRef](#)] [[PubMed](#)]
53. Marchais-Oberwinkler, S.; Henn, C.; Moller, G.; Klein, T.; Negri, M.; Oster, A.; Spadaro, A.; Werth, R.; Wetzel, M.; Xu, K.; *et al.* 17beta-hydroxysteroid dehydrogenases (17beta-hsds) as therapeutic targets: Protein structures, functions, and recent progress in inhibitor development. *J. Steroid Biochem. Mol. Biol.* **2011**, *125*, 66–82. [[CrossRef](#)] [[PubMed](#)]
54. Koch, M.A.; Wittenberg, L.O.; Basu, S.; Jeyaraj, D.A.; Gourzoulidou, E.; Reinecke, K.; Odermatt, A.; Waldmann, H. Compound library development guided by protein structure similarity clustering and natural product structure. *Proc. Natl. Acad. Sci. USA* **2004**, *101*, 16721–16726. [[CrossRef](#)] [[PubMed](#)]
55. Koch, M.A.; Schuffenhauer, A.; Scheck, M.; Wetzel, S.; Casaulta, M.; Odermatt, A.; Ertl, P.; Waldmann, H. Charting biologically relevant chemical space: A structural classification of natural products (scomp). *Proc. Natl. Acad. Sci. USA* **2005**, *102*, 17272–17277. [[CrossRef](#)] [[PubMed](#)]
56. Guasch, L.; Sala, E.; Castell-Auví, A.; Cedó, L.; Liedl, K.R.; Wolber, G.; Muehlbacher, M.; Mulero, M.; Pinent, M.; Ardévol, A.; *et al.* Identification of pargamma partial agonists of natural origin (i): Development of a virtual screening procedure and *in vitro* validation. *PLoS ONE* **2012**, *7*, e50816. [[CrossRef](#)] [[PubMed](#)]
57. Lipinski, C.A.; Lombardo, F.; Dominy, B.W.; Feeney, P.J. Experimental and computational approaches to estimate solubility and permeability in drug discovery and development settings. *Adv. Drug Deliv. Rev.* **1997**, *23*, 3–25. [[CrossRef](#)]
58. Veber, D.F.; Johnson, S.R.; Cheng, H.-Y.; Smith, B.R.; Ward, K.W.; Kopple, K.D. Molecular properties that influence the oral bioavailability of drug candidates. *J. Med. Chem.* **2002**, *45*, 2615–2623. [[CrossRef](#)] [[PubMed](#)]

59. Congreve, M.; Carr, R.; Murray, C.; Jhoti, H. A “rule of three” for fragment-based lead discovery? *Drug Discov. Today* **2003**, *8*, 876–877. [[CrossRef](#)]
60. Baell, J.B.; Holloway, G.A. New substructure filters for removal of pan assay interference compounds (pains) from screening libraries and for their exclusion in bioassays. *J. Chem. Med.* **2010**, *53*, 2719–2740. [[CrossRef](#)] [[PubMed](#)]
61. Baell, J.; Walters, M.A. Chemistry: Chemical con artists foil drug discovery. *Nature* **2014**, *513*, 481–483. [[CrossRef](#)] [[PubMed](#)]
62. Noha, S.M.; Fischer, K.; Koeberle, A.; Garscha, U.; Werz, O.; Schuster, D. Discovery of novel, non-acidic mPGES-1 inhibitors by virtual screening with a multistep protocol. *Bioorganic Med. Chem.* **2015**, *23*, 4839–4845. [[CrossRef](#)] [[PubMed](#)]
63. Kavanagh, K.L.; Jornvall, H.; Persson, B.; Oppermann, U. Medium- and short-chain dehydrogenase/reductase gene and protein families: The SDR superfamily: Functional and structural diversity within a family of metabolic and regulatory enzymes. *Cell. Mol. Life Sci.* **2008**, *65*, 3895–3906. [[CrossRef](#)] [[PubMed](#)]
64. Miller, W.L.; Auchus, R.J. The molecular biology, biochemistry, and physiology of human steroidogenesis and its disorders. *Endocr. Rev.* **2011**, *32*, 81–151. [[CrossRef](#)] [[PubMed](#)]
65. Yang, S.Y.; He, X.Y.; Isaacs, C.; Dobkin, C.; Miller, D.; Philipp, M. Roles of 17 β -hydroxysteroid dehydrogenase type 10 in neurodegenerative disorders. *J. Steroid Biochem. Mol. Biol.* **2014**, *143*, 460–472. [[CrossRef](#)] [[PubMed](#)]
66. Gathercole, L.L.; Lavery, G.G.; Morgan, S.A.; Cooper, M.S.; Sinclair, A.J.; Tomlinson, J.W.; Stewart, P.M. 11 β -hydroxysteroid dehydrogenase 1: Translational and therapeutic aspects. *Endocr. Rev.* **2013**, *34*, 525–555. [[CrossRef](#)] [[PubMed](#)]
67. Luu-The, V. Assessment of steroidogenesis and steroidogenic enzyme functions. *J. Steroid Biochem. Mol. Biol.* **2013**, *137*, 176–182. [[CrossRef](#)] [[PubMed](#)]
68. Vuorinen, A.; Odermatt, A.; Schuster, D. *In silico* methods in the discovery of endocrine disrupting chemicals. *J. Steroid Biochem. Mol. Biol.* **2013**, *137*, 18–26. [[CrossRef](#)] [[PubMed](#)]
69. Vitku, J.; Starka, L.; Bicikova, M.; Hill, M.; Heracek, J.; Sosvorova, L.; Hampl, R. Endocrine disruptors and other inhibitors of 11 β -hydroxysteroid dehydrogenase 1 and 2: Tissue-specific consequences of enzyme inhibition. *J. Steroid Biochem. Mol. Biol.* **2016**, *155*, 207–216. [[CrossRef](#)] [[PubMed](#)]
70. Nashev, L.G.; Vuorinen, A.; Praxmarer, L.; Chantong, B.; Cereghetti, D.; Winiger, R.; Schuster, D.; Odermatt, A. Virtual screening as a strategy for the identification of xenobiotics disrupting corticosteroid action. *PLoS ONE* **2012**, *7*, e46958. [[CrossRef](#)] [[PubMed](#)]
71. Odermatt, A.; Nashev, L.G. The glucocorticoid-activating enzyme 11 β -hydroxysteroid dehydrogenase type 1 has broad substrate specificity: Physiological and toxicological considerations. *J. Steroid Biochem. Mol. Biol.* **2010**, *119*, 1–13. [[CrossRef](#)] [[PubMed](#)]
72. Maser, E.; Oppermann, U.C. Role of type-1 11 β -hydroxysteroid dehydrogenase in detoxification processes. *Eur. J. Biochem.* **1997**, *249*, 365–369. [[CrossRef](#)] [[PubMed](#)]
73. Maser, E. Xenobiotic carbonyl reduction and physiological steroid oxidoreduction. The pluripotency of several hydroxysteroid dehydrogenases. *Biochem. Pharmacol.* **1995**, *49*, 421–440. [[CrossRef](#)]
74. Nashev, L.G.; Schuster, D.; Laggner, C.; Sodha, S.; Langer, T.; Wolber, G.; Odermatt, A. The uv-filter benzophenone-1 inhibits 17 β -hydroxysteroid dehydrogenase type 3: Virtual screening as a strategy to identify potential endocrine disrupting chemicals. *Biochem. Pharmacol.* **2010**, *79*, 1189–1199. [[CrossRef](#)] [[PubMed](#)]
75. Yuan, K.; Zhao, B.; Li, X.W.; Hu, G.X.; Su, Y.; Chu, Y.; Akingbemi, B.T.; Lian, Q.Q.; Ge, R.S. Effects of phthalates on 3 β -hydroxysteroid dehydrogenase and 17 β -hydroxysteroid dehydrogenase 3 activities in human and rat testes. *Chem.-Biol. Interact.* **2012**, *195*, 180–188. [[CrossRef](#)] [[PubMed](#)]
76. Zhao, B.; Chu, Y.; Hardy, D.O.; Li, X.K.; Ge, R.S. Inhibition of 3 β - and 17 β -hydroxysteroid dehydrogenase activities in rat leydig cells by perfluorooctane acid. *J. Steroid Biochem. Mol. Biol.* **2009**, *118*, 13–17. [[CrossRef](#)] [[PubMed](#)]
77. Chapman, K.; Holmes, M.; Seckl, J. 11 β -hydroxysteroid dehydrogenases: Intracellular gate-keepers of tissue glucocorticoid action. *Physiol. Rev.* **2013**, *93*, 1139–1206. [[CrossRef](#)] [[PubMed](#)]
78. Kratschmar, D.V.; Vuorinen, A.; Da Cunha, T.; Wolber, G.; Classen-Houben, D.; Doblhoff, O.; Schuster, D.; Odermatt, A. Characterization of activity and binding mode of glycyrrhetic acid derivatives inhibiting 11 β -hydroxysteroid dehydrogenase type 2. *J. Steroid Biochem. Mol. Biol.* **2011**, *125*, 129–142. [[CrossRef](#)] [[PubMed](#)]

79. Kannisto, K.; Pietilainen, K.H.; Ehrenborg, E.; Rissanen, A.; Kaprio, J.; Hamsten, A.; Yki-Jarvinen, H. Overexpression of 11 β -hydroxysteroid dehydrogenase-1 in adipose tissue is associated with acquired obesity and features of insulin resistance: Studies in young adult monozygotic twins. *J. Clin. Endocrinol. Metab.* **2004**, *89*, 4414–4421. [[CrossRef](#)] [[PubMed](#)]
80. Kotelevtsev, Y.; Holmes, M.C.; Burchell, A.; Houston, P.M.; Schmolli, D.; Jamieson, P.; Best, R.; Brown, R.; Edwards, C.R.; Seckl, J.R.; *et al.* 11beta-hydroxysteroid dehydrogenase type 1 knockout mice show attenuated glucocorticoid-inducible responses and resist hyperglycemia on obesity or stress. *Proc. Natl. Acad. Sci. USA* **1997**, *94*, 14924–14929. [[CrossRef](#)] [[PubMed](#)]
81. Lindsay, R.S.; Wake, D.J.; Nair, S.; Bunt, J.; Livingstone, D.E.; Permana, P.A.; Tataranni, P.A.; Walker, B.R. Subcutaneous adipose 11 β -hydroxysteroid dehydrogenase type 1 activity and messenger ribonucleic acid levels are associated with adiposity and insulinemia in pima indians and caucasians. *J. Clin. Endocrinol. Metab.* **2003**, *88*, 2738–2744. [[CrossRef](#)] [[PubMed](#)]
82. Masuzaki, H.; Paterson, J.; Shinyama, H.; Morton, N.M.; Mullins, J.J.; Seckl, J.R.; Flier, J.S. A transgenic model of visceral obesity and the metabolic syndrome. *Science* **2001**, *294*, 2166–2170. [[CrossRef](#)] [[PubMed](#)]
83. Masuzaki, H.; Yamamoto, H.; Kenyon, C.J.; Elmquist, J.K.; Morton, N.M.; Paterson, J.M.; Shinyama, H.; Sharp, M.G.; Fleming, S.; Mullins, J.J.; *et al.* Transgenic amplification of glucocorticoid action in adipose tissue causes high blood pressure in mice. *J. Clin. Investig.* **2003**, *112*, 83–90. [[CrossRef](#)] [[PubMed](#)]
84. Paterson, J.M.; Morton, N.M.; Fievet, C.; Kenyon, C.J.; Holmes, M.C.; Staels, B.; Seckl, J.R.; Mullins, J.J. Metabolic syndrome without obesity: Hepatic overexpression of 11 β -hydroxysteroid dehydrogenase type 1 in transgenic mice. *Proc. Natl. Acad. Sci. USA* **2004**, *101*, 7088–7093. [[CrossRef](#)] [[PubMed](#)]
85. Paulmyer-Lacroix, O.; Boullu, S.; Oliver, C.; Alessi, M.C.; Grino, M. Expression of the mRNA coding for 11 β -hydroxysteroid dehydrogenase type 1 in adipose tissue from obese patients: An *in situ* hybridization study. *J. Clin. Endocrinol. Metab.* **2002**, *87*, 2701–2705. [[CrossRef](#)] [[PubMed](#)]
86. Rask, E.; Walker, B.R.; Soderberg, S.; Livingstone, D.E.; Eliasson, M.; Johnson, O.; Andrew, R.; Olsson, T. Tissue-specific changes in peripheral cortisol metabolism in obese women: Increased adipose 11 β -hydroxysteroid dehydrogenase type 1 activity. *J. Clin. Endocrinol. Metab.* **2002**, *87*, 3330–3336. [[CrossRef](#)] [[PubMed](#)]
87. Valsamakis, G.; Anwar, A.; Tomlinson, J.W.; Shackleton, C.H.; McTernan, P.G.; Chetty, R.; Wood, P.J.; Banerjee, A.K.; Holder, G.; Barnett, A.H.; *et al.* 11 β -hydroxysteroid dehydrogenase type 1 activity in lean and obese males with type 2 diabetes mellitus. *J. Clin. Endocrinol. Metab.* **2004**, *89*, 4755–4761. [[CrossRef](#)] [[PubMed](#)]
88. Kipari, T.; Hadoke, P.W.; Iqbal, J.; Man, T.Y.; Miller, E.; Coutinho, A.E.; Zhang, Z.; Sullivan, K.M.; Mitic, T.; Livingstone, D.E.; *et al.* 11 β -hydroxysteroid dehydrogenase type 1 deficiency in bone marrow-derived cells reduces atherosclerosis. *FASEB J.* **2013**, *27*, 1519–1531. [[CrossRef](#)] [[PubMed](#)]
89. Hermanowski-Vosatka, A.; Balkovec, J.M.; Cheng, K.; Chen, H.Y.; Hernandez, M.; Koo, G.C.; Le Grand, C.B.; Li, Z.; Metzger, J.M.; Mundt, S.S.; *et al.* 11 β -HSD1 inhibition ameliorates metabolic syndrome and prevents progression of atherosclerosis in mice. *J. Exp. Med.* **2005**, *202*, 517–527. [[CrossRef](#)] [[PubMed](#)]
90. Garcia, R.A.; Search, D.J.; Lupisella, J.A.; Ostrowski, J.; Guan, B.; Chen, J.; Yang, W.P.; Truong, A.; He, A.; Zhang, R.; *et al.* 11 β -hydroxysteroid dehydrogenase type 1 gene knockout attenuates atherosclerosis and *in vivo* foam cell formation in hyperlipidemic apoe^{-/-} mice. *PLoS ONE* **2013**, *8*, e53192. [[CrossRef](#)] [[PubMed](#)]
91. Luo, M.J.; Thieringer, R.; Springer, M.S.; Wright, S.D.; Hermanowski-Vosatka, A.; Plump, A.; Balkovec, J.M.; Cheng, K.; Ding, G.J.; Kawka, D.W.; *et al.* 11 β -HSD1 inhibition reduces atherosclerosis in mice by altering proinflammatory gene expression in the vasculature. *Physiol. Genom.* **2013**, *45*, 47–57. [[CrossRef](#)] [[PubMed](#)]
92. Wu, L.; Qi, H.; Zhong, Y.; Lv, S.; Yu, J.; Liu, J.; Wang, L.; Bi, J.; Kong, X.; Di, W.; *et al.* 11 β -hydroxysteroid dehydrogenase type 1 selective inhibitor bvt.2733 protects osteoblasts against endogenous glucocorticoid induced dysfunction. *Endocr. J.* **2013**, *60*, 1047–1058. [[CrossRef](#)] [[PubMed](#)]
93. Rauz, S.; Cheung, C.M.; Wood, P.J.; Coca-Prados, M.; Walker, E.A.; Murray, P.I.; Stewart, P.M. Inhibition of 11 β -hydroxysteroid dehydrogenase type 1 lowers intraocular pressure in patients with ocular hypertension. *QJM* **2003**, *96*, 481–490. [[CrossRef](#)] [[PubMed](#)]
94. Rauz, S.; Walker, E.A.; Shackleton, C.H.; Hewison, M.; Murray, P.I.; Stewart, P.M. Expression and putative role of 11 β -hydroxysteroid dehydrogenase isozymes within the human eye. *Investig. Ophthalmol. Visual Sci.* **2001**, *42*, 2037–2042.

95. Anderson, S.; Carreiro, S.; Quenzer, T.; Gale, D.; Xiang, C.; Gukasyan, H.; Lafontaine, J.; Cheng, H.; Krauss, A.; Prasanna, G. In vivo evaluation of 11 β -hydroxysteroid dehydrogenase activity in the rabbit eye. *J. Ocul. Pharmacol. Ther.* **2009**, *25*, 215–222. [[CrossRef](#)] [[PubMed](#)]
96. Sooy, K.; Webster, S.P.; Noble, J.; Binnie, M.; Walker, B.R.; Seckl, J.R.; Yau, J.L. Partial deficiency or short-term inhibition of 11 β -hydroxysteroid dehydrogenase type 1 improves cognitive function in aging mice. *J. Neurosci.* **2010**, *30*, 13867–13872. [[CrossRef](#)] [[PubMed](#)]
97. Yau, J.L.; McNair, K.M.; Noble, J.; Brownstein, D.; Hibberd, C.; Morton, N.; Mullins, J.J.; Morris, R.G.; Cobb, S.; Seckl, J.R. Enhanced hippocampal long-term potentiation and spatial learning in aged 11 β -hydroxysteroid dehydrogenase type 1 knock-out mice. *J. Neurosci.* **2007**, *27*, 10487–10496. [[CrossRef](#)] [[PubMed](#)]
98. Yau, J.L.; Noble, J.; Seckl, J.R. 11 β -hydroxysteroid dehydrogenase type 1 deficiency prevents memory deficits with aging by switching from glucocorticoid receptor to mineralocorticoid receptor-mediated cognitive control. *J. Neurosci.* **2011**, *31*, 4188–4193. [[CrossRef](#)] [[PubMed](#)]
99. Sooy, K.; Noble, J.; McBride, A.; Binnie, M.; Yau, J.L.; Seckl, J.R.; Walker, B.R.; Webster, S.P. Cognitive and disease-modifying effects of 11 β -hydroxysteroid dehydrogenase type 1 inhibition in male tg2576 mice, a model of Alzheimer's disease. *Endocrinology* **2015**, *156*, 4592–4603. [[CrossRef](#)] [[PubMed](#)]
100. Mohler, E.G.; Browman, K.E.; Roderwald, V.A.; Cronin, E.A.; Markosyan, S.; Scott Bitner, R.; Strakhova, M.I.; Drescher, K.U.; Hornberger, W.; Rohde, J.J.; *et al.* Acute inhibition of 11 β -hydroxysteroid dehydrogenase type-1 improves memory in rodent models of cognition. *J. Neurosci.* **2011**, *31*, 5406–5413. [[CrossRef](#)] [[PubMed](#)]
101. Tiganescu, A.; Tahrani, A.A.; Morgan, S.A.; Otranto, M.; Desmouliere, A.; Abrahams, L.; Hassan-Smith, Z.; Walker, E.A.; Rabbitt, E.H.; Cooper, M.S.; *et al.* 11 β -hydroxysteroid dehydrogenase blockade prevents age-induced skin structure and function defects. *J. Clin. Investig.* **2013**, *123*, 3051–3060. [[CrossRef](#)] [[PubMed](#)]
102. Tiganescu, A.; Hupe, M.; Uchida, Y.; Mauro, T.; Elias, P.M.; Holleran, W.M. Increased glucocorticoid activation during mouse skin wound healing. *J. Endocrinol.* **2014**, *221*, 51–61. [[CrossRef](#)] [[PubMed](#)]
103. Youm, J.K.; Park, K.; Uchida, Y.; Chan, A.; Mauro, T.M.; Holleran, W.M.; Elias, P.M. Local blockade of glucocorticoid activation reverses stress- and glucocorticoid-induced delays in cutaneous wound healing. *Wound Repair Regen.* **2013**, *21*, 715–722. [[CrossRef](#)] [[PubMed](#)]
104. Scott, J.S.; Goldberg, F.W.; Turnbull, A.V. Medicinal chemistry of inhibitors of 11 β -hydroxysteroid dehydrogenase type 1 (11 β -HSD1). *J. Med. Chem.* **2014**, *57*, 4466–4486. [[CrossRef](#)] [[PubMed](#)]
105. Thomas, M.P.; Potter, B.V. Crystal structures of 11 β -hydroxysteroid dehydrogenase type 1 and their use in drug discovery. *Future Med. Chem.* **2011**, *3*, 367–390. [[CrossRef](#)] [[PubMed](#)]
106. Schuster, D.; Maurer, E.M.; Laggner, C.; Nashev, L.G.; Wilckens, T.; Langer, T.; Odermatt, A. The discovery of new 11 β -hydroxysteroid dehydrogenase type 1 inhibitors by common feature pharmacophore modeling and virtual screening. *J. Med. Chem.* **2006**, *49*, 3454–3466. [[CrossRef](#)] [[PubMed](#)]
107. Hofer, S.; Kratschmar, D.V.; Scherthanner, B.; Vuorinen, A.; Schuster, D.; Odermatt, A.; Easmon, J. Synthesis and biological analysis of benzazol-2-yl piperazine sulfonamides as 11 β -hydroxysteroid dehydrogenase 1 inhibitors. *Bioorg. Med. Chem. Lett.* **2013**, *23*, 5397–5400. [[CrossRef](#)] [[PubMed](#)]
108. Rollinger, J.M.; Kratschmar, D.V.; Schuster, D.; Pfisterer, P.H.; Gumy, C.; Aubry, E.M.; Brandstötter, S.; Stuppner, H.; Wolber, G.; Odermatt, A. 11 β -hydroxysteroid dehydrogenase 1 inhibiting constituents from *eriobotrya japonica* revealed by bioactivity-guided isolation and computational approaches. *Bioorganic Med. Chem.* **2010**, *18*, 1507–1515. [[CrossRef](#)] [[PubMed](#)]
109. Gumy, C.; Thurnbichler, C.; Aubry, E.M.; Balazs, Z.; Pfisterer, P.; Baumgartner, L.; Stuppner, H.; Odermatt, A.; Rollinger, J.M. Inhibition of 11 β -hydroxysteroid dehydrogenase type 1 by plant extracts used as traditional antidiabetic medicines. *Fitoterapia* **2009**. [[CrossRef](#)] [[PubMed](#)]
110. Wu, X.; Kavanagh, K.; Svensson, S.; Elleby, B.; Hult, M.; Von Delft, F.; Marsden, B.; Jornvall, H.; Abrahmsen, L.; Oppermann, U. Structure of human 11 β -hydroxysteroid dehydrogenase in complex with nadp and carbenoxolone. *PDB Entry 2BEL* **2004**. [[CrossRef](#)]
111. Vuorinen, A.; Seibert, J.; Papageorgiou, V.P.; Rollinger, J.M.; Odermatt, A.; Schuster, D.; Assimopoulou, A.N. Pistacia lentiscus oleoresin: Virtual screening and identification of masticadienonic and isomasticadienonic acids as inhibitors of 11 β -hydroxysteroid dehydrogenase 1. *Planta Med.* **2015**, *81*, 525–532. [[CrossRef](#)] [[PubMed](#)]

112. Yang, H.; Dou, W.; Lou, J.; Leng, Y.; Shen, J. Discovery of novel inhibitors of 11 β -hydroxysteroid dehydrogenase type 1 by docking and pharmacophore modeling. *Bioorg. Med. Chem. Lett.* **2008**, *18*, 1340–1345. [[CrossRef](#)] [[PubMed](#)]
113. Hosfield, D.J.; Wu, Y.; Skene, R.J.; Hilgers, M.; Jennings, A.; Snell, G.P.; Aertgeerts, K. Conformational flexibility in crystal structures of human 11 β -hydroxysteroid dehydrogenase type i provide insights into glucocorticoid interconversion and enzyme regulation. *J. Biol. Chem.* **2005**, *280*, 4639–4648. [[CrossRef](#)] [[PubMed](#)]
114. Ewing, T.J.A.; Makino, S.; Skillman, A.G.; Kuntz, I.D. DOCK 4.0: Search strategies for automated molecular docking of flexible molecule databases. *J. Comput.-Aided Mol. Des.* **2001**, *15*, 411–428. [[CrossRef](#)] [[PubMed](#)]
115. Friesner, R.A.; Banks, J.L.; Murphy, R.B.; Halgren, T.A.; Klicic, J.J.; Mainz, D.T.; Repasky, M.P.; Knoll, E.H.; Shaw, D.E.; Shelley, M.; *et al.* Glide: A new approach for rapid, accurate docking and scoring. 1. Method and assessment of docking accuracy. *J. Med. Chem.* **2004**, *47*, 1739–1749. [[CrossRef](#)] [[PubMed](#)]
116. *Catalyst Version 4.10*; Accelrys Software Inc.: San Diego, CA, USA, 2005.
117. Arampatzis, S.; Kadereit, B.; Schuster, D.; Balazs, Z.; Schweizer, R.A.; Frey, F.J.; Langer, T.; Odermatt, A. Comparative enzymology of 11 β -hydroxysteroid dehydrogenase type 1 from six species. *J. Mol. Endocrinol.* **2005**, *35*, 89–101. [[CrossRef](#)] [[PubMed](#)]
118. Barf, T.; Vallgarda, J.; Emond, R.; Haggstrom, C.; Kurz, G.; Nygren, A.; Larwood, V.; Mosialou, E.; Axelsson, K.; Olsson, R.; *et al.* Arylsulfonamidothiazoles as a new class of potential antidiabetic drugs. Discovery of potent and selective inhibitors of the 11beta-hydroxysteroid dehydrogenase type 1. *J. Med. Chem.* **2002**, *45*, 3813–3815. [[CrossRef](#)] [[PubMed](#)]
119. Yang, H.; Shen, Y.; Chen, J.; Jiang, Q.; Leng, Y.; Shen, J. Structure-based virtual screening for identification of novel 11 β -HSD1 inhibitors. *Eur. J. Med. Chem.* **2009**, *44*, 1167–1171. [[CrossRef](#)] [[PubMed](#)]
120. Moeller, G.; Adamski, J. Integrated view on 17 β -hydroxysteroid dehydrogenases. *Mol. Cell. Endocrinol.* **2009**, *301*, 7–19. [[CrossRef](#)] [[PubMed](#)]
121. Poirier, D. Inhibitors of 17 β -hydroxysteroid dehydrogenases. *Curr. Med. Chem.* **2003**, *10*, 453–477. [[CrossRef](#)] [[PubMed](#)]
122. Lukacik, P.; Kavanagh, K.L.; Oppermann, U. Structure and function of human 17 β -hydroxysteroid dehydrogenases. *Mol. Cell. Endocrinol.* **2006**, *248*, 61–71. [[CrossRef](#)] [[PubMed](#)]
123. Jansson, A. 17 β -hydroxysteroid dehydrogenase enzymes and breast cancer. *J. Steroid Biochem. Mol. Biol.* **2009**, *114*, 64–67. [[CrossRef](#)] [[PubMed](#)]
124. Oduwole, O.O.; Li, Y.; Isomaa, V.V.; Mantyniemi, A.; Pulkka, A.E.; Soini, Y.; Vihko, P.T. 17 β -hydroxysteroid dehydrogenase type 1 is an independent prognostic marker in breast cancer. *Cancer Res.* **2004**, *64*, 7604–7609. [[CrossRef](#)] [[PubMed](#)]
125. Miyoshi, Y.; Ando, A.; Shiba, E.; Taguchi, T.; Tamaki, Y.; Noguchi, S. Involvement of up-regulation of 17 β -hydroxysteroid dehydrogenase type 1 in maintenance of intratumoral high estradiol levels in postmenopausal breast cancers. *Int. J. Cancer* **2001**, *94*, 685–689. [[CrossRef](#)] [[PubMed](#)]
126. Smuc, T.; Pucelj, M.R.; Sinkovec, J.; Husen, B.; Thole, H.; Rizner, T.L. Expression analysis of the genes involved in estradiol and progesterone action in human ovarian endometriosis. *Gynecol. Endocrinol.* **2007**, *23*, 105–111. [[CrossRef](#)] [[PubMed](#)]
127. Cornel, K.M.; Kruitwagen, R.F.; Delvoux, B.; Visconti, L.; van de Vijver, K.K.; Day, J.M.; van Gorp, T.; Hermans, R.J.; Dunselman, G.A.; Romano, A. Overexpression of 17 β -hydroxysteroid dehydrogenase type 1 increases the exposure of endometrial cancer to 17 β -estradiol. *J. Clin. Endocrinol. Metab.* **2012**, *97*, E591–E601. [[CrossRef](#)] [[PubMed](#)]
128. Kasai, T.; Shozu, M.; Murakami, K.; Segawa, T.; Shinohara, K.; Nomura, K.; Inoue, M. Increased expression of type i 17 β -hydroxysteroid dehydrogenase enhances *in situ* production of estradiol in uterine leiomyoma. *J. Clin. Endocrinol. Metab.* **2004**, *89*, 5661–5668. [[CrossRef](#)] [[PubMed](#)]
129. Hoffren, A.M.; Murray, C.M.; Hoffmann, R.D. Structure-based focusing using pharmacophores derived from the active site of 17 β -hydroxysteroid dehydrogenase. *Curr. Pharm. Des.* **2001**, *7*, 547–566. [[CrossRef](#)] [[PubMed](#)]
130. Krazeisen, A.; Breitling, R.; Moller, G.; Adamski, J. Phytoestrogens inhibit human 17 β -hydroxysteroid dehydrogenase type 5. *Mol. Cell. Endocrinol.* **2001**, *171*, 151–162. [[CrossRef](#)]
131. Berube, M.; Poirier, D. Synthesis of simplified hybrid inhibitors of type 1 17 β -hydroxysteroid dehydrogenase via cross-metathesis and sonogashira coupling reactions. *Org. Lett.* **2004**, *6*, 3127–3130. [[CrossRef](#)] [[PubMed](#)]

132. Fournier, D.; Poirier, D.; Mazumdar, M.; Lin, S.X. Design and synthesis of bisubstrate inhibitors of type 1 17 β -hydroxysteroid dehydrogenase: Overview and perspectives. *Eur. J. Med. Chem.* **2008**, *43*, 2298–2306. [[CrossRef](#)] [[PubMed](#)]
133. Schuster, D.; Nashev, L.G.; Kirchmair, J.; Laggner, C.; Wolber, G.; Langer, T.; Odermatt, A. Discovery of nonsteroidal 17 β -hydroxysteroid dehydrogenase 1 inhibitors by pharmacophore-based screening of virtual compound libraries. *J. Med. Chem.* **2008**, *51*, 4188–4199. [[CrossRef](#)] [[PubMed](#)]
134. Spadaro, A.; Negri, M.; Marchais-Oberwinkler, S.; Bey, E.; Frotscher, M. Hydroxybenzothiazoles as new nonsteroidal inhibitors of 17 β -hydroxysteroid dehydrogenase type 1 (17 β -HSD1). *PLoS ONE* **2012**, *7*, e29252. [[CrossRef](#)] [[PubMed](#)]
135. Spadaro, A.; Frotscher, M.; Hartmann, R.W. Optimization of hydroxybenzothiazoles as novel potent and selective inhibitors of 17 β -HSD1. *J. Med. Chem.* **2012**, *55*, 2469–2473. [[CrossRef](#)] [[PubMed](#)]
136. Karkola, S.; Alho-Richmond, S.; Wahala, K. Pharmacophore modelling of 17 β -HSD1 enzyme based on active inhibitors and enzyme structure. *Mol. Cell. Endocrinol.* **2009**, *301*, 225–228. [[CrossRef](#)] [[PubMed](#)]
137. Wu, L.; Einstein, M.; Geissler, W.M.; Chan, H.K.; Elliston, K.O.; Andersson, S. Expression cloning and characterization of human 17 β -hydroxysteroid dehydrogenase type 2, a microsomal enzyme possessing 20 α -hydroxysteroid dehydrogenase activity. *J. Biol. Chem.* **1993**, *268*, 12964–12969. [[PubMed](#)]
138. Puranen, T.J.; Kurkela, R.M.; Lakkakorpi, J.T.; Poutanen, M.H.; Itaranta, P.V.; Melis, J.P.; Ghosh, D.; Vihko, R.K.; Vihko, P.T. Characterization of molecular and catalytic properties of intact and truncated human 17 β -hydroxysteroid dehydrogenase type 2 enzymes: Intracellular localization of the wild-type enzyme in the endoplasmic reticulum. *Endocrinology* **1999**, *140*, 3334–3341. [[CrossRef](#)] [[PubMed](#)]
139. Dong, Y.; Qiu, Q.Q.; Debear, J.; Lathrop, W.F.; Bertolini, D.R.; Tamburini, P.P. 17 β -hydroxysteroid dehydrogenases in human bone cells. *J. Bone Miner. Res.* **1998**, *13*, 1539–1546. [[CrossRef](#)] [[PubMed](#)]
140. Vihko, P.; Isomaa, V.; Ghosh, D. Structure and function of 17 β -hydroxysteroid dehydrogenase type 1 and type 2. *Mol. Cell. Endocrinol.* **2001**, *171*, 71–76. [[CrossRef](#)]
141. Vuorinen, A.; Engeli, R.; Meyer, A.; Bachmann, F.; Griesser, U.J.; Schuster, D.; Odermatt, A. Ligand-based pharmacophore modeling and virtual screening for the discovery of novel 17 β -hydroxysteroid dehydrogenase 2 inhibitors. *J. Med. Chem.* **2014**, *57*, 5995–6007. [[CrossRef](#)] [[PubMed](#)]
142. Geissler, W.M.; Davis, D.L.; Wu, L.; Bradshaw, K.D.; Patel, S.; Mendonca, B.B.; Elliston, K.O.; Wilson, J.D.; Russell, D.W.; Andersson, S. Male pseudohermaphroditism caused by mutations of testicular 17 β -hydroxysteroid dehydrogenase 3. *Nat. Genet.* **1994**, *7*, 34–39. [[CrossRef](#)] [[PubMed](#)]
143. Koh, E.; Noda, T.; Kanaya, J.; Namiki, M. Differential expression of 17 β -hydroxysteroid dehydrogenase isozyme genes in prostate cancer and noncancer tissues. *Prostate* **2002**, *53*, 154–159. [[CrossRef](#)] [[PubMed](#)]
144. Legeza, B.; Balazs, Z.; Nashev, L.G.; Odermatt, A. The microsomal enzyme 17 β -hydroxysteroid dehydrogenase 3 faces the cytoplasm and uses NADPH generated by glucose-6-phosphate dehydrogenase. *Endocrinology* **2013**, *154*, 205–213. [[CrossRef](#)] [[PubMed](#)]
145. Tsachaki, M.; Birk, J.; Egert, A.; Odermatt, A. Determination of the topology of endoplasmic reticulum membrane proteins using redox-sensitive green-fluorescence protein fusions. *Biochim. Biophys. Acta* **2015**, *1853*, 1672–1682. [[CrossRef](#)] [[PubMed](#)]
146. Schuster, D.; Kowalik, D.; Kirchmair, J.; Laggner, C.; Markt, P.; Aebischer-Gumy, C.; Strohle, F.; Moller, G.; Wolber, G.; Wilckens, T.; *et al.* Identification of chemically diverse, novel inhibitors of 17 β -hydroxysteroid dehydrogenase type 3 and 5 by pharmacophore-based virtual screening. *J. Steroid Biochem. Mol. Biol.* **2011**, *125*, 148–161. [[CrossRef](#)] [[PubMed](#)]
147. Vicker, N.; Sharland, C.M.; Heaton, W.B.; Gonzalez, A.M.; Bailey, H.V.; Smith, A.; Springall, J.S.; Day, J.M.; Tutill, H.J.; Reed, M.J.; *et al.* The design of novel 17 β -hydroxysteroid dehydrogenase type 3 inhibitors. *Mol. Cell. Endocrinol.* **2009**, *301*, 259–265. [[CrossRef](#)] [[PubMed](#)]
148. Kratz, J.M.; Schuster, D.; Edtbauer, M.; Saxena, P.; Mair, C.E.; Kirchebner, J.; Matuszczak, B.; Baburin, I.; Hering, S.; Rollinger, J.M. Experimentally validated herg pharmacophore models as cardiotoxicity prediction tools. *J. Chem. Inf. Model.* **2014**, *54*, 2887–2901. [[CrossRef](#)] [[PubMed](#)]
149. Duwensee, K.; Schwaiger, S.; Tancevski, I.; Eller, K.; van Eck, M.; Markt, P.; Linder, T.; Stanzl, U.; Ritsch, A.; Patsch, J.R.; *et al.* Leoligin, the major lignan from edelweiss, activates cholesteryl ester transfer protein. *Atherosclerosis* **2011**, *219*, 109–115. [[CrossRef](#)] [[PubMed](#)]

150. Kaserer, T.; Höferl, M.; Müller, K.; Elmer, S.; Ganzera, M.; Jäger, W.; Schuster, D. *In silico* predictions of drug-drug interactions caused by cyp1a2, 2c9, and 3a4 inhibition—A comparative study of virtual screening performance. *Mol. Inf.* **2015**, *34*, 431–457. [[CrossRef](#)]
151. Blumberg, B.; Iguchi, T.; Odermatt, A. Endocrine disrupting chemicals. *J. Steroid Biochem. Mol. Biol.* **2011**, *127*, 1–3. [[CrossRef](#)] [[PubMed](#)]
152. Hampl, R.; Kubatova, J.; Starka, L. Steroids and endocrine disruptors—history, recent state of art and open questions. *J. Steroid Biochem. Mol. Biol.* **2016**, *155*, 217–223. [[CrossRef](#)] [[PubMed](#)]
153. Mune, T.; Rogerson, F.M.; Nikkila, H.; Agarwal, A.K.; White, P.C. Human hypertension caused by mutations in the kidney isozyme of 11 β -hydroxysteroid dehydrogenase. *Nat. Genet.* **1995**, *10*, 394–399. [[CrossRef](#)] [[PubMed](#)]
154. Wilson, R.C.; Harbison, M.D.; Krozowski, Z.S.; Funder, J.W.; Shackleton, C.H.L.; Hanauskeabel, H.M.; Wei, J.Q.; Hertecant, J.; Moran, A.; Neiberger, R.E.; *et al.* Several homozygous mutations in the gene for 11 β -hydroxysteroid dehydrogenase type-2 in patients with apparent mineralocorticoid excess. *J. Clin. Endocrinol. Metab.* **1995**, *80*, 3145–3150. [[PubMed](#)]
155. Lindsay, R.S.; Lindsay, R.M.; Edwards, C.R.; Seckl, J.R. Inhibition of 11 β -hydroxysteroid dehydrogenase in pregnant rats and the programming of blood pressure in the offspring. *Hypertension* **1996**, *27*, 1200–1204. [[CrossRef](#)] [[PubMed](#)]
156. Nyirenda, M.J.; Lindsay, R.S.; Kenyon, C.J.; Burchell, A.; Seckl, J.R. Glucocorticoid exposure in late gestation permanently programs rat hepatic phosphoenolpyruvate carboxykinase and glucocorticoid receptor expression and causes glucose intolerance in adult offspring. *J. Clin. Investig.* **1998**, *101*, 2174–2181. [[CrossRef](#)] [[PubMed](#)]
157. Boehmer, A.L.; Brinkmann, A.O.; Sandkuijl, L.A.; Halley, D.J.; Niermeijer, M.F.; Andersson, S.; de Jong, F.H.; Kayserili, H.; de Vroede, M.A.; Otten, B.J.; *et al.* 17 β -hydroxysteroid dehydrogenase-3 deficiency: Diagnosis, phenotypic variability, population genetics, and worldwide distribution of ancient and de novo mutations. *J. Clin. Endocrinol. Metab.* **1999**, *84*, 4713–4721. [[CrossRef](#)] [[PubMed](#)]
158. Phelan, N.; Williams, E.L.; Cardamone, S.; Lee, M.; Creighton, S.M.; Rumsby, G.; Conway, G.S. Screening for mutations in 17 β -hydroxysteroid dehydrogenase and androgen receptor in women presenting with partially virilised 46,xy disorders of sex development. *Eur. J. Endocrinol.* **2015**, *172*, 745–751. [[CrossRef](#)] [[PubMed](#)]
159. Wang, L.; Kannan, K. Characteristic profiles of benzonphenone-3 and its derivatives in urine of children and adults from the United States and China. *Environ. Sci. Technol.* **2013**, *47*, 12532–12538. [[CrossRef](#)] [[PubMed](#)]
160. Temml, V.; Kaserer, T.; Kutil, Z.; Landa, P.; Vanek, T.; Schuster, D. Pharmacophore modelling for cyclooxygenase-1 and 2 inhibitors with ligandscout in comparison to discovery studio. *Future Med. Chem.* **2014**, *6*, 1869–1881. [[CrossRef](#)] [[PubMed](#)]
161. Dixon, S.; Smondjrev, A.; Knoll, E.; Rao, S.; Shaw, D.; Friesner, R. Phase: A new engine for pharmacophore perception, 3D QSAR model development, and 3D database screening: 1. Methodology and preliminary results. *J. Comput.-Aided Mol. Des.* **2006**, *20*, 647–671. [[CrossRef](#)] [[PubMed](#)]
162. Sirimulla, S.; Bailey, J.B.; Vegesna, R.; Narayan, M. Halogen interactions in protein-ligand complexes: Implications of halogen bonding for rational drug design. *J. Chem. Inf. Model.* **2013**, *53*, 2781–2791. [[CrossRef](#)] [[PubMed](#)]
163. Fourches, D.; Muratov, E.; Tropsha, A. Trust, but verify: On the importance of chemical structure curation in cheminformatics and qsar modeling research. *J. Chem. Inf. Model.* **2010**, *50*, 1189–1204. [[CrossRef](#)] [[PubMed](#)]
164. Scior, T.; Bender, A.; Tresadern, G.; Medina-Franco, J.L.; Martínez-Mayorga, K.; Langer, T.; Cuanalo-Contreras, K.; Agrafiotis, D.K. Recognizing pitfalls in virtual screening: A critical review. *J. Chem. Inf. Model.* **2012**, *52*, 867–881. [[CrossRef](#)] [[PubMed](#)]



© 2015 by the authors; licensee MDPI, Basel, Switzerland. This article is an open access article distributed under the terms and conditions of the Creative Commons by Attribution (CC-BY) license (<http://creativecommons.org/licenses/by/4.0/>).

2.1.2. Virtual screening applications in short-chain dehydrogenase/reductase research

Katharina R. Beck^a, Teresa Kaserer^b, Daniela Schuster^b, Alex Odermatt^a, *J Steroid Biochem Mol Biol.* 2017 Jul;171:157-177.

^aSwiss Center for Applied Human Toxicology and Division of Molecular and Systems Toxicology, Department of Pharmaceutical Sciences, Pharmazentrum, University of Basel, Klingelbergstrasse 50, 4056 Basel, Switzerland

^bInstitute of Pharmacy/Pharmaceutical Chemistry and Center for Molecular Biosciences Innsbruck (CMBI), Computer Aided Molecular Design Group, University of Innsbruck, Innrain 80/82, 6020 Innsbruck, Austria



Review

Virtual screening applications in short-chain dehydrogenase/reductase research

Katharina R. Beck^a, Teresa Kaserer^b, Daniela Schuster^{b,*}, Alex Odermatt^{a,*}^aSwiss Center for Applied Human Toxicology and Division of Molecular and Systems Toxicology, Department of Pharmaceutical Sciences, University of Basel, Klingelbergstrasse 50, 4056 Basel, Switzerland^bInstitute of Pharmacy/Pharmaceutical Chemistry and Center for Molecular Biosciences Innsbruck (CMBI), Computer Aided Molecular Design Group, University of Innsbruck, Innrain 80/82, 6020 Innsbruck, Austria

ARTICLE INFO

Article history:

Received 28 December 2016
 Received in revised form 6 March 2017
 Accepted 8 March 2017
 Available online 9 March 2017

Keywords:

Short-chain dehydrogenase/reductase
 Hydroxysteroid dehydrogenase
 Drug development
 Endocrine disrupting chemicals
 Virtual screening

ABSTRACT

Several members of the short-chain dehydrogenase/reductase (SDR) enzyme family play fundamental roles in adrenal and gonadal steroidogenesis as well as in the metabolism of steroids, oxysterols, bile acids, and retinoids in peripheral tissues, thereby controlling the local activation of their cognate receptors. Some of these SDRs are considered as promising therapeutic targets, for example to treat estrogen-/androgen-dependent and corticosteroid-related diseases, whereas others are considered as anti-targets as their inhibition may lead to disturbances of endocrine functions, thereby contributing to the development and progression of diseases. Nevertheless, the physiological functions of about half of all SDR members are still unknown. In this respect, *in silico* tools are highly valuable in drug discovery for lead molecule identification, in toxicology screenings to facilitate the identification of hazardous chemicals, and in fundamental research for substrate identification and enzyme characterization. Regarding SDRs, computational methods have been employed for a variety of applications including drug discovery, enzyme characterization and substrate identification, as well as identification of potential endocrine disrupting chemicals (EDC). This review provides an overview of the efforts undertaken in the field of virtual screening supported identification of bioactive molecules in SDR research. In addition, it presents an outlook and addresses the opportunities and limitations of computational modeling and *in vitro* validation methods.

© 2017 Elsevier Ltd. All rights reserved.

Contents

1. Introduction	158
1.1. The short-chain dehydrogenase/reductase (SDR) superfamily	158
1.2. Computer-aided drug design	158
2. Examples from the SDR family	159
2.1. Drug development	159
2.1.1. 11 β -hydroxysteroid dehydrogenase type 1	159

Abbreviations: 3-BC, 3-benzylidene camphor; 4-MBC, 4-methylbenzylidene camphor; A β , amyloid- β ; ABAD, A β -binding alcohol dehydrogenase; AD, Alzheimer's disease; AI, aromatase inhibitor; AKR, aldo-keto reductase; AME, apparent mineralocorticoid excess; AR, androgen receptor; Aro, aromatic feature; BP, benzophenone; CBR, carbonyl reductase; CYP, cytochrome P450; DAS1, dual aromatase-sulfatase inhibitor; DHEA, dehydroepiandrosterone; DHT, 5 α -dihydrotestosterone; EDCs, endocrine disrupting chemicals; ER, estrogen receptor; FXR, farnesoid X receptor; GA, glycyrrhetic acid; GPCR, G-protein-coupled receptor; GR, glucocorticoid receptor; H6PDH, Hexose-6-phosphate dehydrogenase; H, hydrophobic feature HBA hydrogen bond acceptor; HBD, hydrogen bond donor; hERG, human ether-a-go-go related gene; HSD, hydroxysteroid dehydrogenase; HTS, high-throughput screening; LDH, lactate dehydrogenase; MR, mineralocorticoid receptor; MD, molecular dynamics; MOE, Molecular Operating Environment; NI, negatively ionizable; PAINS, Pan-Assay Interference Compounds; PI, positively ionizable; PDB, Protein Data Bank; PR, progesterone receptor; ROS, reactive oxygen species; SAR, structure-activity relationship; SDR, short-chain dehydrogenase/reductase; SERM, selective estrogen receptor modulator; SPA, scintillation proximity assay; STS, steroid sulfatase; Tc, Tanimoto coefficient; TRL, tropinone reductase-like; UDCA, ursodeoxycholic acid; UFSRAT, Ultra-fast recognition with atom types; VS, virtual screening; XVols, exclusion volumes.

* Correspondence authors.

E-mail addresses: Daniela.Schuster@uibk.ac.at (D. Schuster), Alex.Odermatt@unibas.ch (A. Odermatt).<http://dx.doi.org/10.1016/j.jsbmb.2017.03.008>

0960-0760/© 2017 Elsevier Ltd. All rights reserved.

2.1.2.	17 β -hydroxysteroid dehydrogenase type 1	163
2.1.3.	17 β -hydroxysteroid dehydrogenase type 2	165
2.1.4.	17 β -hydroxysteroid dehydrogenase type 3	166
2.2.	Enzyme characterization and substrate identification	167
2.2.1.	17 β -hydroxysteroid dehydrogenase type 10	167
2.2.2.	17 β -hydroxysteroid dehydrogenase type 14	168
2.2.3.	Application of structural modeling for substrate identification	168
2.3.	Virtual screening applications in toxicology focusing on SDRs	169
2.4.	Limitations	170
2.4.1.	Computational applications	170
2.4.2.	Biological validation	171
3.	Conclusion	172
	Conflicts of interest	172
	Acknowledgements	172
	References	172

1. Introduction

1.1. The short-chain dehydrogenase/reductase (SDR) superfamily

The SDR enzyme family consists of over 47,000 members found in archaea, bacteria, and eukaryota, with more than 80 members identified in the human genome [1]. They share a common core structure, the so-called Rossmann-fold, consisting of up to seven stranded parallel β -sheets flanked by three α -helices on each side. This core structure is crucial for NAD(P)(H) binding and includes a Tyr-(Xaa)₃-Lys motif essential for the catalytic center. The conserved Tyr residue acts as a catalytic amino acid promoting the proton transfer by the support of a hydrogen bond between Lys and nicotinamide ribose, which lowers the pK_a of the Tyr [2]. The catalytic center is frequently occurring with a conserved Ser residue, stabilizing the bound substrate. Despite this substantial structural similarity, SDRs generally share low sequence identity of 20–30%. In addition to the classic SDRs, consisting of one globular structure, there are extended forms with additional domains fused to the N- or C-terminus [3].

SDRs are catalyzing carbonyl-alcohol oxidoreduction, isomerization, decarboxylation, epimerization, C=N reduction, enoyl-CoA reduction, dehydration, and dehalogenation reactions. They are involved in the metabolism of a wide range of molecules, including steroid hormones, oxysterols, bile acids, prostaglandins, retinoids, fatty acids, amino acids, sugars, and various xenobiotics [3]. Probably the most extensively studied SDRs are hydroxysteroid dehydrogenases (HSDs) with key roles in adrenal and gonadal steroidogenesis, including 3 β -HSDs and 17 β -HSDs, as well as enzymes with 3 α -HSD, 11 β -HSD and 17 β -HSD activities catalyzing the metabolism of steroids in peripheral tissues and thereby controlling local steroid hormone action [4]. Generally, 3 α -HSDs are assigned to the family of aldo-keto reductases (AKR); however, several SDRs are reported to have 3 α -HSD activity such as 17 β -HSD6, 17 β -HSD10 or members of the retinol dehydrogenase (RODH) subfamily [5,6].

Some of these HSDs are investigated as potential therapeutic targets for estrogen- and androgen-dependent diseases such as osteoporosis, endometriosis, and breast and prostate cancer or corticosteroid-related diseases such as dyslipidemia, visceral obesity and diabetes, wound healing, atherosclerosis, osteoporosis, glaucoma, neurodegenerative disease, and cognitive impairment [7–13].

The similarity of the core structure of various SDRs needs to be taken into account when developing specific inhibitors to avoid the inhibition of other members causing off-target effects. In this respect, a major challenge remains the identification of the substrates and functions of “orphan” enzymes with yet unknown substrates and physiological functions. Approximately 50% of the

SDRs have been poorly or not investigated so far, although some of these orphan enzymes have been associated with diseases [14–17]. Molecular modeling and virtual screening (VS) approaches can not only facilitate the identification of selective inhibitors by excluding molecules that bind to off-targets, but they may also support the identification of substrates for orphan enzymes [18]. Another application of the modeling approach includes the identification of toxic industrial and environmentally relevant chemicals [19–21]. Due to their involvement in steroid biosynthesis and metabolism, SDRs represent potential sites for molecular initiating events of endocrine disrupting chemicals (EDCs) [22–27].

1.2. Computer-aided drug design

Besides experimental methods, a plethora of computational techniques is available to support the identification of novel bioactive molecules in the context of both drug discovery and toxicology. The majority of these techniques rely on the concept of similarity introduced by Johnson and Maggiora, based on the assumption that similar compounds exert similar bioactivities [28]. Computational models can be generated based on the properties of known active compounds (preferably in comparison to known inactive molecules) to search for similar compounds in large chemical databases in the course of a VS. For example, 2D similarity-based methods (Fig. 1A) can employ molecular fingerprints to represent the 2D structure of molecules. The degree of similarity among the molecules is then determined with similarity coefficients, most prominently among them the Tanimoto coefficient (Tc) [29,30].

Structure-based pharmacophore models (Fig. 1B) use a higher degree of abstraction, as they solely represent the interaction patterns between a ligand and its macromolecular target. According to IUPAC, pharmacophore models are defined as “the ensemble of steric and electronic features that is necessary to ensure the optimal supra-molecular interactions with a specific biological target and to trigger (or block) its biological response” [31]. These features do not describe specific functional groups, but the type of interactions these chemical functionalities can be involved in. For example, many pharmacophore modeling tools include hydrogen bond donor (HBD) and acceptor (HBA), hydrophobic (H), positively (PI) or negatively (NI) ionizable, and aromatic (Aro) features in their default settings [32–35]. In addition, some types of steric constraints, either shape or exclusion volumes (XVols) (or both) are commonly available. XVols for example can be added to mimic the binding site and to prevent the mapping of compounds that would clash with the binding site and therefore be inactive. The shape of a known active molecule can also be added to a model to restrict the virtual hits to those with similar volumes and geometries compared to the initial training

compound. A scoring function is then employed to calculate how well a compound geometrically fits a pharmacophore model. Widely used pharmacophore modeling programs include Phase (Schrödinger Inc.), DS Catalyst (Biovia), LigandScout (Inte:Ligand GmbH), Molecular Operating Environment (MOE), and others (as reviewed in [36]).

Shape-based methods (Fig. 1C) in principle rely on the shape similarity between a query compound and the molecules under investigation to prioritize compounds for biological testing. Additionally, many shape-based modeling tools provide the option to include chemical information such as pharmacophore features [37,38] (also referred to as color features in ROCS [39,40]), atom types as in Phase Shape [41], or electrostatic potentials in ShaEP [42] to improve the performance of the shape model. Similar to pharmacophore modeling, scoring functions are employed to determine the degree of shape overlay and, if applicable, the extent to which a compound fulfills additional requirements of the model.

Other than the methods mentioned so far, docking does not rely on the concept of similarity, but rather aims to calculate the free binding energy between a macromolecular target and potential ligands. For this purpose, the molecules under investigation are placed within the empty binding pocket of the target, which needs to be defined by the user prior to docking. Each created docking pose is then evaluated with a score estimating the binding energy [43], thus predicting the likelihood of binding (Fig. 1D). For a comprehensive description of docking and scoring as well as frequently used programs, a recent work by Sotriffer is recommended [44]. In some docking programs, also the flexibility of amino acids in the binding site is considered, e.g. in GOLD [45].

The *in silico* methods described in this section have also been employed for the investigation of SDRs. Successful application

examples for selected SDRs are described in detail in the following sections.

2. Examples from the SDR family

2.1. Drug development

2.1.1. 11 β -hydroxysteroid dehydrogenase type 1

The inactive glucocorticoid cortisone is converted to the biologically active cortisol by 11 β -hydroxysteroid dehydrogenase type 1 (11 β -HSD1) using NADPH as cofactor (Fig. 2). 11 β -HSD1 is expressed in tissues such as liver, adipose tissue, adrenals, skeletal muscle, skin, pancreas, hippocampus, as well as in macrophages [46,47]. The reverse reaction is catalyzed by 11 β -HSD2, thereby ensuring mineralocorticoid receptor (MR) activation by aldosterone in kidney and colon as well as fetal protection in the placenta from excess amounts of maternal glucocorticoids [48]. Transgenic mice selectively overexpressing 11 β -HSD1 in the adipose tissue develop metabolic syndrome including insulin-resistant diabetes, hyperlipidemia, hypertension, and visceral obesity [49,50], whereas hepatic overexpression of 11 β -HSD1 caused metabolic syndrome without obesity [51]. Enhanced 11 β -HSD1 expression can also be detected in adipose tissue of obese patients and in skeletal muscles of diabetic patients [52–56]. In contrast, 11 β -HSD1 knock-out mice were found to be resistant against the development of diet- or stress-induced diabetes [57], suggesting pharmacological inhibition of this enzyme as a therapeutic option for metabolic diseases. Furthermore, inhibition of 11 β -HSD1 showed favorable therapeutic effects in wound healing [58,59], skin aging [60], osteoporosis [8,61], atherosclerosis [62–65], glaucoma [66–68], and cognitive functions [69–73]. Although various 11 β -HSD1

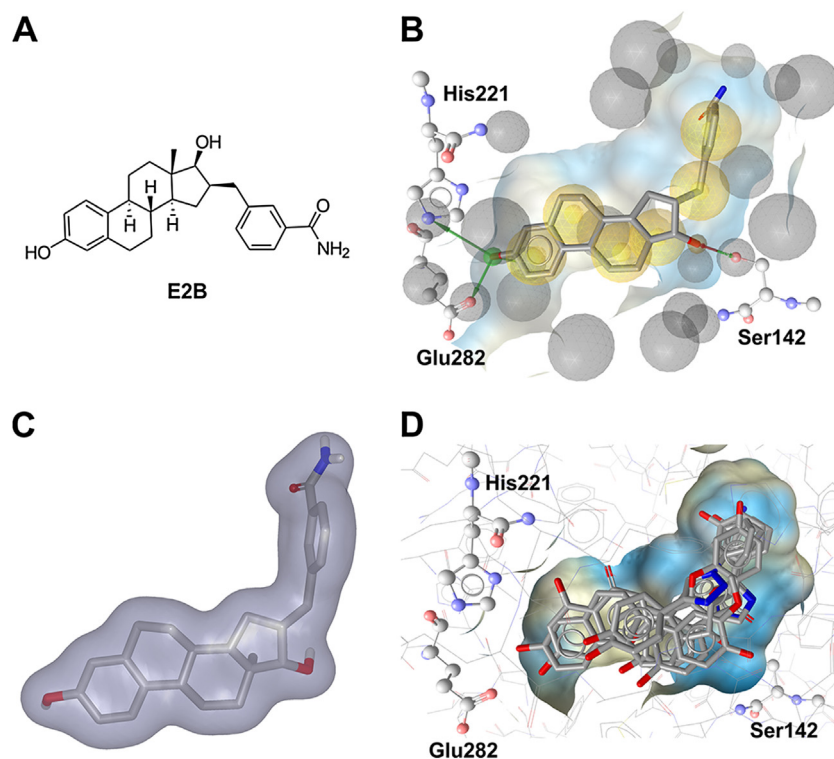


Fig. 1. Principles of commonly applied virtual screening tools exemplified on the crystal structure of 17 β -HSD1 in complex with a steroidal inhibitor. (A) Based on the 2D structure of the inhibitor (the estradiol analogue E2B, 3-[3',17' β -dihydroxyestra-1',3',5'(10')-trien-16' β -methyl]benzamide, PDB code 3HB5 [211]), structurally similar compounds can be retrieved from a compound database in the course of a 2D similarity-based search. (B) A pharmacophore model can be created based on the ligand-target interactions patterns in the crystal complex. Exclusion volumes (XVols, gray spheres) can be added on residues lining the binding site, thereby mimicking the steric constraints of the pocket. Red arrows: HBA, green arrows: HBD, yellow spheres: H features. (C) The shape of the inhibitor defines the 3D space in which other active chemicals may fit. (D) Diverse compounds from a chemical database docked into the binding pocket of 17 β -HSD1. (For interpretation of the references to colour in this figure legend, the reader is referred to the web version of this article.)

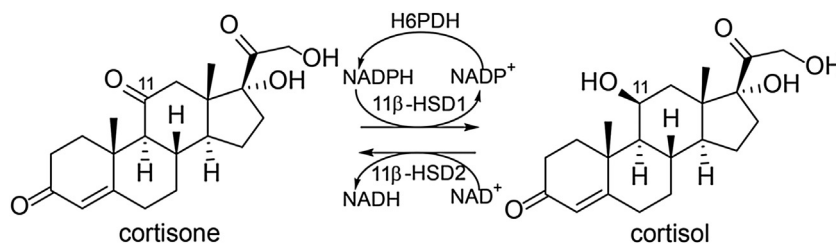


Fig. 2. Conversion of cortisone to cortisol by 11β-HSD1 using NADPH, supplied by hexose-6-phosphate dehydrogenase (H6PDH), and oxidation of cortisol to cortisone catalyzed by 11β-HSD2 using NAD⁺ as cofactor.

inhibitors have been reported and a few also have entered clinical trials, no 11β-HSD1 inhibitor has reached the market so far [74]. Structural variety is prevailing between the different 11β-HSD1 inhibitors; nevertheless, the crystalized protein structures are comparable [75]. However, for selection of a protein structure for *in silico* evaluations, the detected dissimilarities upon ligand binding should be considered. The protein data bank (PDB) currently contains 29 human, 5 mouse, and 3 guinea-pig 11β-HSD1 crystal structures. To date, only X-ray crystal structures in complex with inhibitors but not with a substrate are accessible for the human isoenzyme. In contrast, no crystal structure of 11β-HSD2 is available to date.

Schuster et al. first reported the use of pharmacophore modeling to identify structurally new classes of 11β-HSD1 inhibitors [76]. To perform VS of different databases, they designed two ligand-based multi-feature pharmacophore models as the 11β-HSD1 protein structure was not experimentally resolved at the beginning of their study. They classified their pharmacophore models according to the 11β-HSD activity of the training compounds employed for the model generation as 11β-HSD1-selective and 11β-HSD non-selective. The virtual hits found by the pharmacophore models contained steroid-like compounds, the known unselective 11β-HSD inhibitor glycyrrhetic acid (GA), related triterpenoids, and novel structural classes. The *in vitro* 11β-HSD1 and 11β-HSD2 inhibition profile of the active VS hits showed similar selectivities as the training set compounds used for the 11β-HSD1-selective and the 11β-HSD-unselective pharmacophore model construction.

Suitable enzyme activity assays are fundamental for selectivity testing of potential inhibitors. Regarding 11β-HSD1 inhibitors, 11β-HSD2 is usually chosen as counter screen because cross-inhibition of 11β-HSD2 would cause cortisol-induced MR activation in the kidney, resulting in hypertension. Taking into account that the different SDR family members share considerable structural similarity, but rather low primary sequence similarity, other enzymes such as 3β-HSDs and 17β-HSDs should be included in the selectivity assessment of 11β-HSD1 inhibitors.

By determining the biological activities in HEK-293 cell lysates or intact cells expressing human recombinant 11β-HSD1, 11β-HSD2, 17β-HSD1 or 17β-HSD2, Schuster et al. tested the potency and selectivity of their VS hits [76]. 11β-HSD1 activity was inhibited by more than 70% at 10 μM by 7 out of 30 tested compounds, but only 3 of them displayed reasonable selectivity over the other tested SDRs. This is not surprising as some of the unselective hits belonged to the class of triterpenoids resembling GA. The authors observed similar kinetic parameters for the three 11β-HSD1-selective chemicals in differentiated mouse adipocytes and myotubes, metabolically relevant tissues endogenously expressing 11β-HSD1. Other studies showed significant species-specific variability in the potency of various 11β-HSD1 inhibitors [77–79], indicating significant differences in the 3D organization of the hydrophobic substrate-binding pocket of human and mouse 11β-HSD1. Thus, species-specific variability must be considered

and the use of suitable human cell lines endogenously expressing 11β-HSD1 is indicated.

Glucocorticoids are recognized by several different proteins during synthesis (CYP11B1), distribution (cortisol-binding globulin, transport proteins such as P-glycoprotein), peripheral metabolism (11β-HSDs), receptor action (MR, glucocorticoid receptor (GR)), and degradation (5β-reductase, CYP3A4). These proteins recognize some common structural features and inhibitors of 11β-HSD1 might therefore bind to other glucocorticoid recognizing proteins as well. To address this, Schuster et al. tested their most active hits in GR- and MR-dependent reporter gene assays. Reduced tissue-specific glucocorticoid reactivation and therefore blockade of the GR-mediated gene expression are responsible for the therapeutic effects of an 11β-HSD1 inhibitor. The ability of an 11β-HSD1 inhibitor to also act as a GR or MR antagonist would rather enhance its therapeutic benefit by reducing GR-dependent stimulation of hepatic gluconeogenesis and decreasing cortisol-mediated MR activation in macrophages. Their most active compound showed only weak GR and MR antagonistic effects, with a 6–10-fold preference for 11β-HSD1 inhibition and can therefore be used as starting point for further investigations.

The selective 11β-HSD1 pharmacophore model generated by Schuster et al. [76] was further used to assess its potential to identify new lead structures for 11β-HSD1 inhibitor development [80]. Enzymatic testing of the virtual hits led to the discovery of an 11β-HSD1 inhibitor with an IC₅₀ of 4.8 μM. Lead optimization studies revealed arylsulfonylpiperazine scaffolds as a new class of selective 11β-HSD1 inhibitors.

This pharmacophore model was additionally employed to search for selective 11β-HSD1 inhibitors derived from constituents of medicinal plants [81]. The virtual hit list contained to a large extent scaffolds from the chemical class of triterpenoids such as corosolic acid. This is a known constituent of *Eriobotrya japonica*, which is used in the traditional Chinese medicine as antidiabetic treatment. An earlier study, investigating the potential of extracts from traditionally used antidiabetic medical plants to inhibit 11β-HSD1 activity, found leaf extracts of *E. japonica* preferentially inhibiting 11β-HSD1 over 11β-HSD2 [82]. Thus, the VS hit corosolic acid was tested for inhibition of the human 11β-HSD enzymes in a lysate-based assay and revealed selective inhibition of 11β-HSD1 with an IC₅₀ of 810 nM. In order to discover additional secondary metabolites inhibiting 11β-HSD1, bioassay-guided phytochemical analyses were implemented. These investigations led to the identification of several molecules from the triterpenoid ursane type with IC₅₀ between 1.9 and 17.4 μM. However, an enhanced 11β-HSD1 inhibitory activity could be detected by mixtures of these moderately active compounds. Additive effects of constituent mixtures are a common finding in phytotherapy and often explain their therapeutic effect. Binding mode prediction performed by docking studies indicated a flipped interaction pattern of the triterpenoids with interactions to Thr124 and Tyr177 instead of the catalytic residues. The identification of 11β-HSD1 inhibitors in traditionally used antidiabetic medical plants

indicated a possible mode of action – a further application field for pharmacophore modeling.

Further studies using the 11 β -HSD pharmacophore models from Schuster et al. [76] for model refinement [83] and subsequently as screening tool for 11 β -HSD1 inhibitor identification among constituents of the traditionally used Greek medical plant *Pistacia lentiscus* [84], are described in the Supplementary information.

For the identification of new 11 β -HSD1 inhibitors Miguet et al. [85] developed a homology model to predict the 3D structure of 11 β -HSD1. Structure-based VS of a reference database composed of molecules with known activities towards 11 β -HSD1 was used to validate the model showing its ability to discriminate between 11 β -HSD1 inhibitors. The reference database included 19 11 β -HSD1 inhibitors, 3 weak inhibitors, 3 non-inhibitors, and 2 substrates. To distinguish between virtual hits based on activity data of a reference database, it would be advantageous if the different activity categories would be more equal. Scoring calculations were further used as numerical cut-offs, filtering the virtual hit list after VS of a natural molecules database. As in the meantime, the first experimentally derived 11 β -HSD1 X-ray structure became available, the results derived from the homology model were confirmed by molecular modeling based on the crystallographic structure. Several hits of the VS belonged to the flavonoids, with 2 hits already known as 11 β -HSD1 inhibitors. The remaining candidates were not enzymatically tested, and, unfortunately, no follow up evaluation of these hits was reported.

Yang et al. combined ligand-based pharmacophore modeling and molecular docking for the identification of synthetic 11 β -HSD1 inhibitors [86]. In a virtual docking approach, the SPECS database was screened and the 3000 compounds with the highest docking score were selected for a second, more computationally expensive docking calculation. Furthermore, a ligand-based pharmacophore model on the basis of three selective 11 β -HSD1 inhibitors was generated and used as a query to additionally filter the 3000 selected compounds. High fit and docking scores, as well as drug likeness were selection criteria for compounds to be further biologically tested for their activity on human and mouse 11 β -HSDs. Therefore, a scintillation proximity assay (SPA) was performed using microsomes prepared from HEK-293 cells stably expressing human and mouse 11 β -HSD1 or 11 β -HSD2, respectively. Significant differences in the inhibitory potential of the compounds were observed when comparing their activities against human and mouse 11 β -HSD1. Whereas 11 out of 121 tested compounds revealed IC₅₀ values of 0.26–14.6 μ M against the human enzyme, 6 substances showed IC₅₀ values between 0.48–12.49 μ M against the mouse enzyme. Among these inhibitors, only two displayed overlapping activity for human and mouse 11 β -HSD1 with IC₅₀ values of 0.69 μ M and 3.57 μ M, and 0.48 μ M and 2.09 μ M, respectively. In regard to subsequent animal studies, selectivity over 11 β -HSD2 was tested only for the mouse isoenzyme and just for compounds inhibiting mouse 11 β -HSD1. Selectivity was ensured; however, appropriate selectivity determination requires at least the inclusion of human 11 β -HSD2, and ideally also other SDRs. The ideal case for preclinical assessments in drug development would include cross-species activity. Importantly, significant species-specific differences regarding the potency of diverse 11 β -HSD1 inhibitors have previously been reported, implying critical variability in the 3D conformation of the active site of human and mouse 11 β -HSD1 [77–79].

In a consecutive study, Yang et al. successfully used 11 β -HSD1 structure-based pharmacophore models as initial screening tools, followed by a docking approach for hit selection [87]. Only compounds interacting with the catalytic residues Tyr183 and Ser170 were chosen after the docking evaluation for further biological assessment. In contrast to their earlier study where they

found 11 out of 121 hits as inhibitors for the human 11 β -HSD1 [86], 9 out of 56 tested compounds displayed selective and dose-dependent 11 β -HSD1 inhibition with IC₅₀ values of 0.85–7.98 μ M. The mouse enzyme was inhibited by 6 compounds with IC₅₀ values between 0.44 μ M and 8.48 μ M, of which 4 inhibited human and mouse 11 β -HSD1 with comparable IC₅₀ values.

Shape-based screening combined with fast rigid docking was applied by Xia et al. to find 11 β -HSD1 inhibitors [88]. The 1000 best ranked compounds of each screening were combined for further ligand-flexible docking calculations. By manual inspection of the top 200 molecules in the final hit list, 70 structurally diverse molecules were chosen for biological testing by SPA, of which 14 compounds inhibited 11 β -HSD1 by more than 50% at 1 μ M, 8 of them had IC₅₀ values \leq 100 nM, and 3 inhibitors already being reported [89–91]. In addition, by analyzing the binding mode conformations, a new hydrophobic sub-pocket was discovered. However, the interacting residues of this sub-pocket were not described, although this would further support inhibitor development. During the validation of this finding with a molecule fitting into this pocket, a novel scaffold was identified that inhibited 11 β -HSD1 with an IC₅₀ of 45 nM. Selectivity over 11 β -HSD2 was only verified for the two compounds with the most favorable ADME prediction profiles. However, since pharmacokinetics can be improved after lead identification, it would be of interest to obtain selectivity information for all 11 β -HSD1 inhibitors. Moreover, to improve further study designs, it would be important to know the difference between the hit rates of shape-based screening and rigid docking. In an independent, subsequently performed study, Xia et al. designed a new class of derivatives of 1-arylsulfonyl piperidine-3-carboxamides using medicinal chemistry tools [92]. For lead structure selection and following animal studies, the compounds were tested against mouse and human 11 β -HSD1 and 11 β -HSD2. They found a large lipophilic group at the amino moiety as favorable for cross-species potency. Unfortunately, they did not mention if this bulky lipophilic group also targets their previously identified hydrophobic sub-pocket, which could be interesting for further inhibitor development studies.

A similar approach was performed by Lagos et al. who used shape-based query hypotheses as a filter during a structure-based VS process [93]. Steroidal compounds were excluded from the query in order to avoid similarity of the virtual hits with this scaffold type. Top scored compounds were visually analyzed for their binding features and selected for testing in cell-based assays. For this purpose, they used the liposarcoma-derived adipose cell line LS14, differentiated into adipocytes and endogenously expressing 11 β -HSD1 [94]. Of 39 compounds tested, two selectively inhibited 11 β -HSD1 over 11 β -HSD2 with IC₅₀ values around 5 μ M. Selectivity over 11 β -HSD2 was also tested in differentiated LS14 cells, although its expression was marginal. However, the use of an intact cell-based testing system as an initial biological assessment tool has the disadvantage that the compounds do not have direct access to their target and the ranking of the obtained biological activities cannot be used to draw conclusions on the performance of the VS approach.

Shave et al. employed another method containing shape-based calculations but without the need for any detailed structural information of the target [95]. They used Ultra-fast Recognition with Atom Types (UFRAT), an algorithm that considers the shape and the electrostatics of atoms to score and retrieve candidate molecules capable to make similar interactions to those of the supplied query. The non-selective 11 β -HSD1 inhibitor carbenoxolone was used to generate the query. VS of a database against the query resulted in a hit list of the most similar compounds. Biological testing was implemented against 11 β -HSD1 reductase and dehydrogenase activity. Out of 26 tested compounds, 4 inhibited the reductase activity in a SPA cell-based assay with IC₅₀

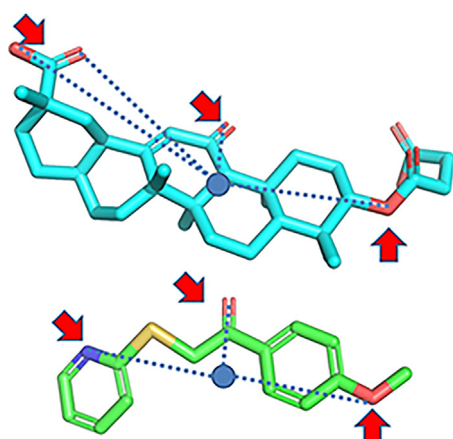


Fig. 3. Carbenoxolone (top) and hit molecule with a preserved key pattern of atoms involved in hydrogen bonding [95].

values between 0.067 and 11.3 μM and the dehydrogenase activity of recombinant human 11 β -HSD1 protein with K_i^{app} of 26–248 μM . Interestingly, the top virtual hits displayed totally different scaffolds compared to the query molecule but showed similarity to already known 11 β -HSD1 inhibitors (Fig. 3). Thus, UFSRAT has demonstrated its ability for scaffold hopping during the VS screening process. However, the query molecule carbenoxolone is an unselective 11 β -HSD inhibitor, exhibiting activity against 11 β -HSD1 and 11 β -HSD2. For this reason, biological testing of the selected virtual hits against 11 β -HSD2 would be required for further development of these compounds. Moreover, choosing a selective 11 β -HSD1 inhibitor as a query molecule for the UFSRAT algorithm may even improve the success of this approach.

A number of adamantane-containing selective 11 β -HSD1 inhibitors have been reported [96]. Tice et al. used them to generate models of the 11 β -HSD1 binding site with the help of a proprietary structure-based drug design program of Vitae Pharmaceuticals called Contour [97]. The most satisfactory poses were selected, and based on them a medicinal chemistry program was initiated to improve potency, selectivity, and physical properties, supported by additional modeling. This led to the identification of a class of spirocyclic ureas selectively inhibiting 11 β -HSD1 with IC_{50} values in the lower nanomolar range.

Using the same drug design platform Contour, Xu et al. developed a novel class of 11 β -HSD1 inhibitors by incorporating a 1,3-oxazinan-2-one ring system [98]. Prior to the medicinal chemistry program, the available 11 β -HSD1 X-ray structures were examined and a template compound bearing a 1,3-oxazinan-2-one ring docked into the 2BEL structure of 11 β -HSD1. Subsequently, more than 5000 molecules were designed *in silico* by adding

fragments directly to the template compound. Structure-based drug design and lead compound optimization studies revealed a highly potent 11 β -HSD1 inhibitor with IC_{50} values of 0.8 nM using recombinant human 11 β -HSD1 in a microsomal preparation of CHO cells and 2.5 nM in differentiated human adipocytes. Testing inhibitory activity against 11 β -HSD2, 17 β -HSD1, 3 β -HSD2, and three CYP isoenzymes showed >1000-fold selectivity for 11 β -HSD1. The same results were observed when examining its potential to bind to GR, MR, FXR or hERG. In regard to subsequently performed animal studies, pharmacokinetic parameters were measured in several species. In addition, distribution into mouse adipose tissue could be observed with proportional plasma concentrations levels and three times higher concentrations in the liver. However, due to the poor potency against mouse 11 β -HSD1, but comparable activity towards human and cynomolgus monkey 11 β -HSD1, the latter species was selected as *in vivo* model for 11 β -HSD1 inhibition. Oral administration, after suppression of endogenous plasma glucocorticoid levels with dexamethasone and challenge with cortisone 21-acetate after 5 h of compound administration, revealed reduced cortisol production by 85% compared to the vehicle control. However, the authors described no further details how the animal study was conducted as for instance the number of animals used. As they aimed to specifically target the adipose tissue, this measurement only provides data about the overall 11 β -HSD1 activity. Therefore, they determined in a consecutive preclinical characterization study the inhibitory activity of their lead compound *ex vivo* in cynomolgus monkey and human adipose tissue [99]. Remarkably, the enzyme inhibition was minor in cynomolgus monkey tissue and 30-fold less pronounced in human adipose tissue compared to cultured differentiated preadipocytes. They proposed the high lipophilic nature of the compound and therefore its uptake and sequestration into lipid droplets as a possible reason for this observation. Based on these investigations, they established a modified assay strategy for lead compound identification, newly including analysis in human and non-human primate adipose tissue. This approach led to the identification of a new 11 β -HSD1 inhibitor candidate, of which toxicological assessment was introduced in regard to Phase I clinical studies. An adapted, more general version of this testing cascade is shown in the biological limitation section.

Several different computational methods have been applied to discover new selective 11 β -HSD1 inhibitors and successfully identified structurally diverse virtual hits in biological assays as potential lead compounds for further drug development. However, computer-aided drug design is also advantageous for lead optimization. In order to improve selectivity, potency and pharmacokinetic parameters of initially discovered 11 β -HSD1 inhibitors, several groups implemented scaffold hopping and structure-activity relationship (SAR) studies on the basis of docking studies [100–105]. Following chemical synthesis the same

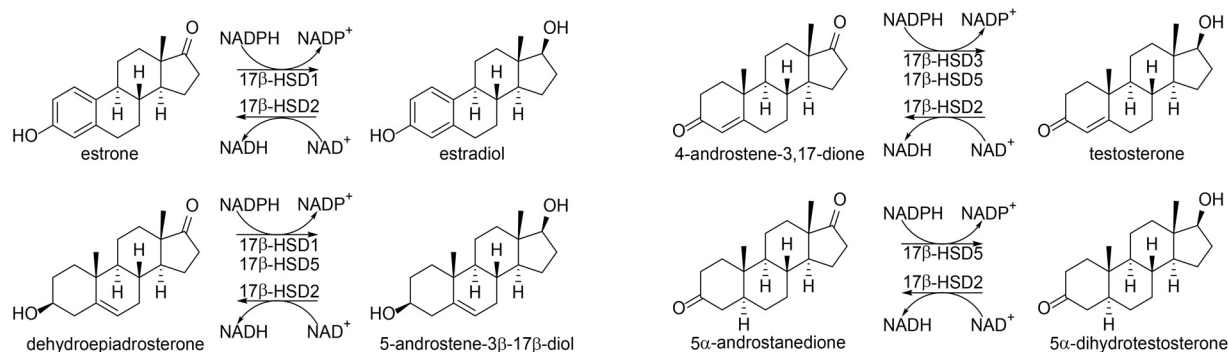


Fig. 4. Selected 17 β -HSDs involved in estrogen and androgen steroid metabolism.

approach is often also used for binding mode explanations [106–108].

2.1.2. 17 β -hydroxysteroid dehydrogenase type 1

To date, 14 different human 17 β -hydroxysteroid dehydrogenase (17 β -HSD) enzymes, belonging to the SDR family with the exception of the aldo-keto reductase AKR1C3 (17 β -HSD5), have been described [109]. Several of the 17 β -HSDs are essentially involved in the local metabolism of estrogens and androgens, thereby controlling ER and AR signaling in a tissue- and cell-dependent manner (Fig. 4).

17 β -HSD1 reduces in an NADPH-dependent reaction the weak estrogen estrone to the potent estradiol. It also catalyzes the conversion of dehydroepiandrosterone (DHEA) to 5-androstene-3 β ,17 β -diol [110]. The human placenta, ovaries, and mammary gland are the predominant expression sites of 17 β -HSD1 and therefore of considerable relevance for the gonadal and peripheral synthesis of estradiol [111]. Studies demonstrating a correlation of 17 β -HSD1 mRNA expression levels and poor breast cancer prognosis [112–114] suggest the local inhibition of estradiol biosynthesis by targeting 17 β -HSD1 as a promising therapeutic strategy against breast cancer, especially in postmenopausal women, where estradiol originates mainly from extragonadal sites. Importantly, *in vivo* studies found a reduction in tumor size in mice stimulated with exogenous estrone after co-treatment with specific 17 β -HSD1 inhibitors [115,116]. In addition, high 17 β -HSD1 expression levels were shown to be associated with endometriosis [117,118], endometrial cancer [119], and uterine leiomyoma [120], offering additional therapeutic opportunities.

Although the number of reported 17 β -HSD1 inhibitors is increasing, to date no compound made it into clinical trials. Currently, over 20 crystal structures of the 17 β -HSD1 protein have been published. The binding pocket consists of an elongated hydrophobic channel, formed by Leu149, Val225, Phe226, and Phe259, and hydrophilic residues at each end allowing interactions with the catalytic essential residues Ser142 and Tyr155 on one side and His221 and Glu282 on the other side. A flexible loop (amino acids 188–201) in the crystal structure, which compromises the exact definition of the substrate binding pocket and therefore influences the predictivity of VS studies, is not well resolved [121] (Fig. 5).

Hoffrén et al. were the first to describe structure-based pharmacophore models for the discovery of 17 β -HSD1 inhibitors [122]. They validated their pharmacophore models with molecules bearing the structural and chemical features of steroids and

flavonoids. The most potent training compound applied in the model validation was coumestrol. However, coumestrol also displays inhibitory activity against 17 β -HSD5 and is not selective for 17 β -HSD1, which needs to be taken into account in model and hit validation [123]. The selectivity and sensitivity of a pharmacophore model strongly depend on the compounds selected for its generation and validation. Ideally, if available, selective inhibitors are chosen for model development. Thus, because phytoestrogens and steroidal scaffolds frequently display cross-reactivity against other enzymes and receptors involved in steroid action, non-steroidal structures are preferred, not only for the modeling and validation, but also as lead structures to increase selectivity. Since the VS hits from Hoffrén et al. were not validated by biological testing, no further information is available on the selectivity of the pharmacophore model as well as on the identified hits.

Even though selective inhibitors are usually chosen for therapeutic applications, polyvalent inhibitors with synergistic beneficial effects may be advantageous in some circumstances. Chanplakorn et al. reported a significant increase of estrogen sulfatase and 17 β -HSD1 expression after neoadjuvant therapy with aromatase inhibitors (AIs) in postmenopausal women suffering from estrogen receptor- α (ER α)-positive breast cancer [124]. They proposed that the observed expression changes are a result of compensatory responses to estrogen depletion in breast carcinoma tissue. To prevent the compensatory estradiol production triggered by chronic treatment with AIs, Dual Aromatase-Sulfatase Inhibitors (DASI) have been developed as an alternative to administration of a combination of drugs for each target [125–127]. Aromatase catalyzes the conversion of 4-androstene-3,7-dione to estrone, which is then conjugated by estrogen sulfotransferase to estrone sulfate that can serve as a storage upon hydrolysis in breast cancer tissue by steroid sulfatase (STS), and further reduction by 17 β -HSD1 leads to estradiol production. Thus, hormone-dependent breast cancer might be more effectively treated using a polyvalent drug. Designing these DASIs, Woo et al. integrated the inhibitory STS pharmacophore into the scaffold search for AIs, allowing minimal structural changes to preserve aromatase inhibition [128]. Thus, the use of specific inhibitors for each relevant target as well as inhibitors with activities against synergistic targets represents a promising approach to prevent the development of resistance.

Focusing exclusively on 17 β -HSD1, inhibitors can target several sites including reversible and irreversible inhibition of the binding of the substrate, of the cofactor NADPH at the Rossmann-fold, or both by so-called hybrid compounds (Fig. 6) consisting of a steroidal core and extended side chains to occupy the cofactor binding site [129,130].

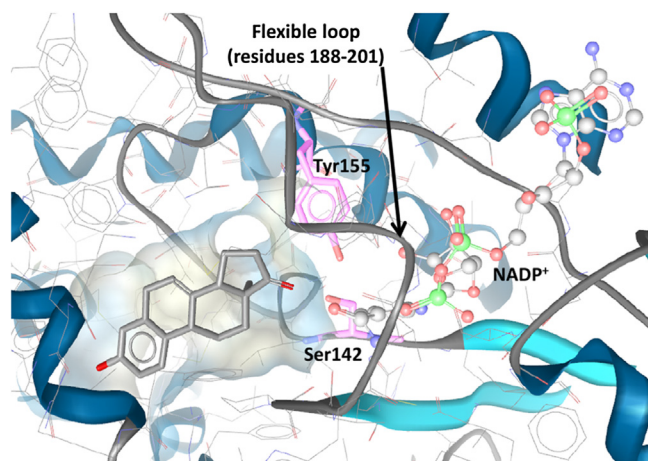


Fig. 5. Substrate binding pocket of 17 β -HSD1 with the co-crystallized ligand equilin (PDB 1EQU), catalytic key residues (Ser142 and Tyr155), a flexible loop (residues 188–201) and NADPH⁺.

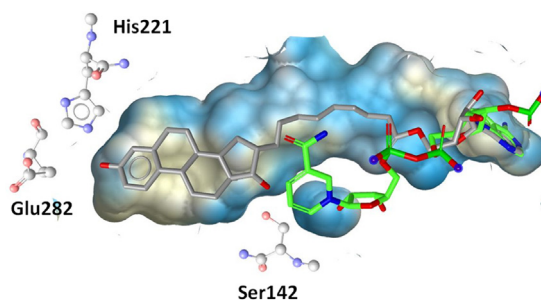


Fig. 6. The hybrid inhibitor EM1745 (gray) occupies both the steroid and the cofactor (green) binding site in 17 β -HSD1 (PDB entry 115R). The co-factor conformation was taken from the PDB entry 3HB5. (For interpretation of the references to colour in this figure legend, the reader is referred to the web version of this article.)

Due to the lack of 17 β -HSD1 X-ray structures co-crystallized with nonsteroidal inhibitors, Schuster et al. constructed two structure-based pharmacophore models based on crystal structures containing steroidal inhibitors in order to find new nonsteroidal 17 β -HSD1 inhibitor scaffolds [131]. Whereas one model was developed based on the steroidal scaffold equilin and expected to be an appropriate general screening tool, yielding a higher number of false positive and unselective hits, the second model was constructed based on a hybrid inhibitor, suggested to be more restrictive because of the underlying unique scaffold. *In vitro* testing of 14 selected virtual hits led to the identification of two nonsteroidal, selective 17 β -HSD1 inhibitors with moderate activities (IC₅₀ 5.7 μ M and 19 μ M). Selectivity was tested against 17 β -HSD2, 17 β -HSD3, the AKR 17 β -HSD5, 11 β -HSD1, and 11 β -HSD2, additionally revealing a nonsteroidal and a steroidal 11 β -HSD1 inhibitor (IC₅₀ 6.2 μ M and 3.8 μ M, respectively) and a nonsteroidal 17 β -HSD3 inhibitor (IC₅₀ 19 μ M). These results emphasize the relevance of including several structurally related enzymes for selectivity evaluation. To increase the exclusion rate of compounds potentially causing off-target effects, Schuster et al. tested an alternative approach using pharmacophore models of structurally related enzymes [131]. Using these models as additional filters to exclude compounds with a low degree of selectivity enriched the virtual hit list with more selective compounds and therefore reduced the efforts for laborious biological testing. They applied their previously constructed selective 11 β -HSD1 pharmacophore model for a VS of the scaffolds identified as 11 β -HSD1 inhibitors [76]. The nonsteroidal 11 β -HSD1 inhibitor mentioned above was identified as hit, and it was also found when removing the shape restriction. Therefore, applying nonrestrictive pharmacophore models of related enzymes as additional filter tools can assist the selection of virtual hits for biological testing by eliminating promiscuous inhibitors.

Regarding the structural similarity of different proteins, Brown et al. demonstrated inhibition of human lactate dehydrogenase (LDH) and of 17 β -HSD1 by binding of gossypol derivatives to the Rossmann fold [132]. Thus, on one hand structural conservation provides a basis for lead compounds targeting several related proteins but on the other hand it raises concerns about their selectivity. Brown et al. did not test their gossypol derivatives against other SDRs. Since gossypol was also found to inhibit 3 β -HSD1, 17 β -HSD3 [133], and 11 β -HSD2 [134], testing of the gossypol derivatives against other structurally related enzymes will be crucial.

To create a pharmacophore model and define the ligand-protein interactions for both, the ligand and the active site of the protein, Sparado et al. [135] superimposed five 17 β -HSD1 X-ray structures. VS of a small in-house compound library and experimental validation of the hits in a cell-free assay led to the identification of a moderately active 17 β -HSD1 inhibitor. Further SAR analysis, including scaffold hopping and rigidification, resulted in two benzothiazole-scaffold bearing 17 β -HSD1 inhibitors with IC₅₀ values of 44 and 243 nM, respectively. The subsequent selectivity testing not only consisted of an assay for the related enzyme 17 β -HSD2, but also for the ER α and ER β . Depending on whether a compound also binds to ER α and/or ER β and acts as agonist or antagonist, different effects on ER-mediated signaling can be expected. Both compounds showed selectivity over 17 β -HSD2 but differences regarding their binding affinities against both ERs. The more potent compound displayed considerable affinity to bind to ER α and ER β , whereas the less active compound was marginally active against both ERs. Further biological evaluation in a human cell system endogenously expressing 17 β -HSD1 (T47-D cells) revealed potent inhibition of estrogen formation with an IC₅₀ of 245 nM for the less active compound. Moreover, docking investigations revealed a 180° flipped orientation of the two

compounds, although they differ only in a carbonyl and an amide-bridge, respectively. As described earlier, a flipped binding orientation was also observed for corosolic acid and other triterpenes inhibiting 11 β -HSD1 [81]. To improve the activity and selectivity for *in vivo* use of their two 17 β -HSD1 inhibitors, Sparado et al. conducted a follow-up optimization study [136]. SAR experiments led to the identification of two new lead compounds, which were highly active against 17 β -HSD1 with IC₅₀ values in a cell-free assay of 27 nM and 13 nM and in T47-D cells of 258 nM and 37 nM, respectively. Both inhibitors were selective over 17 β -HSD2 and ER α / β . Furthermore, the potency of the inhibitors was tested against marmoset 17 β -HSD1 and 17 β -HSD2 as the marmoset monkey can be used as an animal model for endometriosis. The lead compounds almost completely inhibited 17 β -HSD1 at 50 nM when tested in marmoset placenta microsomes. However, the compounds were less selective towards marmoset 17 β -HSD2 compared to the human enzymes (50 nM of the compounds inhibited marmoset 17 β -HSD2 activity by 51% and 40%, respectively).

Pharmacophore modeling using structure-based and ligand-based concepts were also applied by Karkola et al. [137]. Four different approaches using docking, alignment of known inhibitors, molecular dynamics (MD) simulation, and automated model generation on the basis of a 17 β -HSD1 crystal structure were implemented. VS led to the discovery of several potential 17 β -HSD1 inhibitors; however, their biological activities were not determined. Biological testing of these hits would allow validating them as 17 β -HSD1 inhibitors and could provide information on the selectivity and sensitivity of the different pharmacophore models.

Starčević et al. [138] performed a virtual high-throughput screening based on the 3D structure of 17 β -HSD1 in complex with equilin. The database was pre-filtered to reduce it to compounds with similar size and shape as estrone. Concerning the large scaffold of hybrid inhibitors, this approach may bias the VS and its hit list, and potentially active hits may be missed. During the visual inspection of the virtual hit list, compounds with potential estrogenic effects such as steroids, flavonoids, or other phytoestrogens were eliminated. Of 18 enzymatically tested substances, three compounds bearing the central scaffold of aurones, a 2-benzylidenebenzofuran-3(2H)-one structure, showed potent inhibition with IC₅₀ values in the lower nanomolar range (Fig. 7). Additionally, one hit was an already known 17 β -HSD1 inhibitor, thus validating the approach. However, a 2D similarity search with

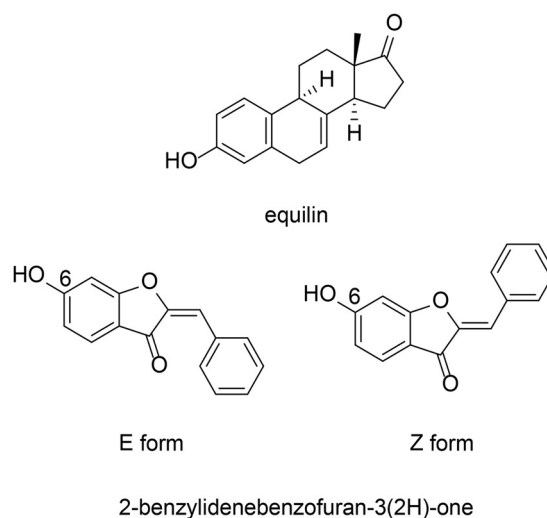


Fig. 7. Equilin and E respectively Z form of 2-benzylidenebenzofuran-3(2H)-one structure.

the aurone derivatives as queries identified no new 17β -HSD1 inhibitors. A SAR analysis revealed the presence of a 6-OH group as essential for potent 17β -HSD1 inhibition by 2-benzylidenebenzofuran-3(2H)-ones. Docking studies suggested that these inhibitors occupy an ideal orientation in the active site by forming triple hydrogen bonds with the catalytic residues Ser142 and Tyr155 and the cofactor.

A docking approach was also applied by Frotscher et al. [139], who studied the 3D architecture of 17β -HSD1 in complex with estradiol for important chemical features involved in the protein-ligand interactions to design steroid mimetics with nonsteroidal scaffolds. These inhibitors should contain two polar groups with 11 Å distance in between to imitate the A-ring and the D-ring and a flat conformation similar to the steroids. In addition, they discovered two residues in the active site, Tyr218 and Ser222, which are not directly involved in steroid binding but may display promising new interaction partners for the development of new inhibitors. Accordingly, phenyltetralone, phenyl-naphthalene, phenylquinoline, and phenylindole scaffolds were chosen for a medicinal chemistry program with scaffold hopping and SAR analysis based on biological analysis with 17β -HSD1 and 17β -HSD2. Docking and MD simulations thereby helped to reveal the molecular interactions of the synthesized compounds with the protein. This led to the discovery of a (hydroxyphenyl)naphthalene derivative as potent 17β -HSD1 inhibitor with selectivity towards 17β -HSD2, ER α , and ER β . Moreover, pharmacokinetic studies demonstrated Caco-2 penetration, low inhibitory effects on the most important hepatic CYP enzymes, and moderate metabolic stability in rat liver microsomes. For optimization of inhibitory activity, selectivity and pharmacokinetic properties, novel substituted 6-phenyl-2-naphthols were synthesized [140]. Molecular modeling supported SAR and binding mode explanation. The new lead compound showed improved overall properties and can be further tested *in vivo*. The inhibitory activity was tested only against human 17β -HSD1. Thus, prior to animal experiments, possible species-specific differences should be considered.

In a follow-up project, Marchais-Oberwinkler et al. [141] performed a SAR study to optimize the 17β -HSD1 pharmacophore of Frotscher et al. [139] (Fig. 8). The study highlights the restricted flexibility of the active site of 17β -HSD1. Therefore, the enzyme might not be able to adjust its geometry upon inhibitor binding. Targeting the polar ends of the active site, the positions of the hydroxyl groups of the (hydroxyphenyl)naphthalene derivatives were optimized in order to allow formation of hydrogen bonds. By the introduction of a hydrophobic core, the inhibitors are stabilized in the hydrophobic tunnel of the enzyme. Furthermore, biological results and modeling studies indicated that the amino acids Tyr218 and Ser222, characterized by Frotscher et al. as potential

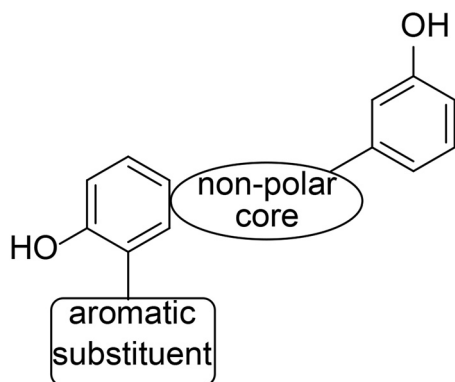


Fig. 8. Revised pharmacophore for 17β -HSD1 inhibitors (adapted from Marchais-Oberwinkler et al. [141]).

interaction partners [139], are unlikely to form hydrogen bonds with this class of inhibitors. Available space with potential π - π interactions close to position 1 of the naphthalene ring may be exploited by introducing an aromatic substituent.

Applying a similar strategy of a ligand- and structure-based drug design mimicking steroids, Bey et al. identified bis(hydroxyphenyl) azoles as potent 17β -HSD1 inhibitors [121]. Different azoles and hydroxyl substitutions were synthesized and evaluated for activity and selectivity. Thereby, a 2,5-disubstituted oxazole displayed the most potent inhibitory effects with good selectivity and pharmacokinetic properties. Further structural optimization resulted in enhanced IC₅₀ values in the low nanomolar range, high selectivity profiles, and good pharmacokinetic properties [142]. Interestingly, compared to the (hydroxyphenyl)naphthalene class of 17β -HSD1 inhibitors, the active bis(hydroxyphenyl) azoles were predicted to form hydrogen bonds with Tyr218.

The approach of identifying new 17β -HSD1 inhibitors by structure-based drug design was applied by several groups and led to the discovery of 17β -HSD1 inhibitors based on 2-substitutions of estrone and D-homo-estrone [143] and on pyrimidinones [144]. This strategy is commonly used in medicinal chemistry for optimization of known inhibitors and lead compounds in a rational manner. Thus, VS offers an inexpensive and rapid approach to identify novel compounds and helps to enrich compounds within a set of similar compounds from the same scaffold [145].

2.1.3. 17β -hydroxysteroid dehydrogenase type 2

17β -HSD2 catalyzes the NAD⁺-dependent conversion of the active estradiol into the weak estrogen estrone. Moreover, 17β -HSD2 is able to convert testosterone to 4-androstene-3,17-dione (androstenedione), 5 α -dihydrotestosterone (DHT) to 5 α -androstenedione, 5-androstene-3 β ,17 β -diol to DHEA, and 20 α -dihydroprogesterone to progesterone (Fig. 4) [146,147]. Several tissues such as bone, endometrium, uterus, breast, placenta, stomach, small intestine, and colon epithelium express 17β -HSD2 [148,149]. In the placenta, 17β -HSD2 protects the fetus from maternal androgens and estrogens. Decreased levels of estrogens in postmenopausal women and androgens in elderly men result in an imbalance between bone formation and bone loss, ultimately causing osteoporosis [150]. Among the most frequent pharmacological interventions in Europe against osteoporosis is the administration of bisphosphonates and selective estrogen-receptor modulators (SERMs) [151]. However, both treatment options have limitations and there is a great demand for novel therapies. Especially SERMs are associated with an increased risk for cardiovascular complications. Since 17β -HSD2 is expressed in osteoblasts, its inhibition may provide a new approach to treat osteoporosis by increasing local estradiol availability. This strategy is supported by an *in vivo* study in ovariectomized cynomolgus monkeys, where oral administration of a 17β -HSD2 inhibitor led to maintenance of bone formation and strength [152]. Nevertheless, as increased estradiol concentrations can also be related to severe disorders such as endometriosis or breast cancer, it may be important to design 17β -HSD2 inhibitors that exclusively act in bone tissue. Thus, the application route of these inhibitors might be a major challenge to overcome.

Because of the lack of 17β -HSD2 crystal structures, Vuorinen et al. applied ligand-based pharmacophore modeling to find novel inhibitors [153]. Biological testing of the VS hits in a cell-free assay revealed 7 out of 29 tested compounds (of initially 202,906 compounds subjected to *in silico* screening) with IC₅₀ values between 0.24 μ M and 33 μ M. Among the active compounds, phenylbenzene-sulfonamides and -sulfonates displayed the main class of structural scaffolds. In addition, a search for structurally similar molecules was performed using this new class of 17β -HSD2 inhibitors. With a simple 2D similarity search, one (IC₅₀ of 3.3 μ M)

out of 16 compounds was found to inhibit 17 β -HSD2. In parallel, the pharmacophore model was refined, used for VS, and 14 derivatives were biologically tested. Among them, 5 hits revealed IC₅₀ values between 1 and 15 μ M. Although the compounds used for pharmacophore model generation were selective against 17 β -HSD1, the selectivity of the newly identified 17 β -HSD2 inhibitors remains to be determined. The active inhibitor-derivatives were tested for their selectivity against 17 β -HSD1, 17 β -HSD3, 11 β -HSD1, and 11 β -HSD2. Only one of the overall 13 discovered inhibitors showed activity against 17 β -HSD1 (IC₅₀ 18 μ M), being still 18 times more active against 17 β -HSD2. Unfortunately, the most potent 17 β -HSD2 inhibitor (IC₅₀ 0.24 μ M) was also active against 17 β -HSD3 (IC₅₀ 8.5 μ M) and 11 β -HSD1 (IC₅₀ 2.1 μ M). Two compounds were equipotent against 17 β -HSD2 and 11 β -HSD1 and two substances showed even higher inhibitory activity against 17 β -HSD3 than 17 β -HSD2. However, all tested compounds were selective against 11 β -HSD2. In addition, the specificity of the initial pharmacophore model was improved by creating a refinement database including the original training compounds, the newly discovered active compounds, as well as the inactive substances. Thus, the ability of the model was enhanced to find active hits from a database.

Wetzel et al. [154] used the findings from their previous 17 β -HSD1 inhibitor study [155] for the development of a new class of 17 β -HSD2 inhibitors. Their former project was based on a structure- and ligand-based design strategy including docking of two potent heterocyclic substituted biphenylol 17 β -HSD1 inhibitors and evaluation of their interaction pattern in the active site of the enzyme. A three-point pharmacophore model built the basis for a medicinal chemistry inhibitor design concept. One of the most promising 17 β -HSD1 inhibitors (IC₅₀ 8 nM) showed 48-fold selectivity against 17 β -HSD2 (IC₅₀ 382 nM) in cell-free lysate assays. Nevertheless, this compound was selected by Wetzel et al. as starting point for 17 β -HSD2 activity optimization experiments in order to gain selectivity against 17 β -HSD1. However, considerably more potent 17 β -HSD2 inhibitors with lower selectivity factors toward 17 β -HSD1 were obtained as well. Unfortunately, the authors did not provide a reason for their particular selection of the starting compound. Structural optimization led to the discovery of bicyclic substituted hydroxyphenylmethanone derivatives as a new class of 17 β -HSD2 inhibitors. The most promising compound displayed 13-fold selectivity over 17 β -HSD1 with an IC₅₀ value of 101 nM.

2.1.4. 17 β -hydroxysteroid dehydrogenase type 3

17 β -HSD3 reduces androstenedione to testosterone using as cofactor NADPH. It is almost exclusively expressed in the testis [156]. The rare autosomal recessive disorder 46, XY disorder of sex development (also known as male pseudohermaphroditism) emphasizes the importance of 17 β -HSD3 for testosterone production [157,158]. 17 β -HSD3 deficiency leads to impaired masculinization of male external genitalia and the affected individuals are born with female or ambiguous external genitalia [159]. However, even though 17 β -HSD3 is predominantly expressed in testis, it was reported that 17 β -HSD3 mRNA was upregulated in prostate cancer [160]. Importantly, Day et al. recently reported that treatment with specific 17 β -HSD3 inhibitors significantly decreased androgen-dependent growth of xenografts expressing 17 β -HSD3 in castrated mice [161]. The therapeutic efficacy of 17 β -HSD3 inhibitors might be limited by the coexpression of 17 β -HSD5 (AKR1C3), which catalyzes the same reaction and is expressed in prostate cancer [162,163]. Therefore, a combined treatment targeting both enzymes should be envisaged. Like 17 β -HSD2, 17 β -HSD3 is anchored to the endoplasmic reticulum membrane by an N-terminal transmembrane domain, and its catalytic domain faces the cytoplasmic compartment [164,165]. For both membrane proteins experimentally derived 3D structures are still not available.

Thus, Vicker et al. built a homology model, validated by known 17 β -HSD3 inhibitors, to support structure-based drug design [166]. Homology models depict the active site not as accurate as crystal structure-derived models. However, used in a docking approach, it allows for a prediction of an inhibitor's interactions with the active site and helps to uncover the chemical features that are important for its activity. The established 17 β -HSD3 homology model revealed the highly hydrophobic nature of the active site. Potential interactions include π - π interactions of aromatic rings with Phe205 and other hydrophobic interactions with residues such as Val213, Ile148, Phe151, Trp153, and Leu252. The homology model was then used for docking-based VS. Biological testing in a cell-based assay revealed a novel lead compound with an IC₅₀ of 770 nM for 17 β -HSD3, with selectivity over 17 β -HSD1 and 17 β -HSD2. Docking into the homology model and subsequent scaffold hopping, considering potential interactions with the active site, led to the discovery of new compounds, with the most potent inhibitor showing an IC₅₀ of 200 nM in intact cells of human origin (Fig. 9). The activity of this 17 β -HSD3 inhibitor was further confirmed in an

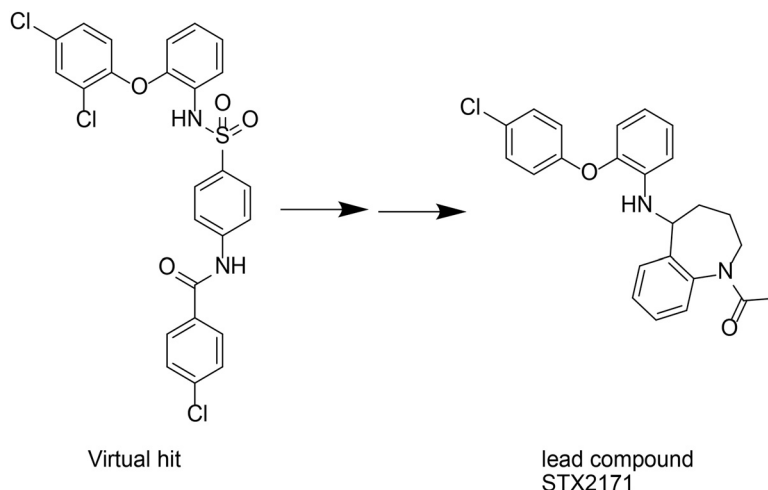


Fig. 9. Virtual screening hit compared to 17 β -HSD3 inhibitor STX2171 found by Vicker et al. [166].

in vivo hormone-dependent prostate cancer model, where castrated mice showed significantly decreased androgen-dependent growth of tumor xenografts expressing human 17 β -HSD3 [161]. Moreover, significantly lowered plasma testosterone levels were observed in treated mice.

The hydrophobic character of the active site of 17 β -HSD3 described by Vicker et al. was further supported by two ligand-based pharmacophore models generated by Schuster et al. [167]. One model was based on steroidal and another one on nonsteroidal 17 β -HSD3 inhibitors as different interaction patterns might be established within the binding pocket. After the screening of several databases and an additional *in silico* filtering approach, the selected virtual hits were tested in a cell-based assay for 17 β -HSD3 inhibition. In addition, specificity was tested against 17 β -HSD1, 17 β -HSD2, 17 β -HSD4, 17 β -HSD5, 17 β -HSD7, 11 β -HSD1, and 11 β -HSD2. Two out of 15 tested compounds found by the steroid-based pharmacophore model and 2 out of 16 hits form the non-steroidal model showed >40% inhibition of 17 β -HSD3 at 2 μ M of test substance. Of the tested compounds, 3 derived from the steroidal and 5 from the non-steroidal model revealed 2–4 fold more potent inhibition against 17 β -HSD5 (AKR1C3) than 17 β -HSD3. Furthermore, one 17 β -HSD3 inhibitor displayed equipotent activity to 17 β -HSD5 and even stronger inhibition against 11 β -HSD1, whereas as a second 17 β -HSD3 inhibitor was capable to inhibit 17 β -HSD1. These investigations again emphasize the importance of an expanded selectivity profiling including structurally and functionally related enzymes.

2.2. Enzyme characterization and substrate identification

Although the sequence of the human genome has been solved and all genes are accessible, to date the physiological role of more than half of all SDR members still remains unknown or poorly examined. *In silico* approaches assist not only in the process of lead compound identification during drug development for well-characterized enzymes, but can also support the deorphanization and characterization of enzymes in order to explore their physiological functions and to identify additional drug targets.

2.2.1. 17 β -hydroxysteroid dehydrogenase type 10

The homotetrameric single domain multifunctional enzyme 17 β -HSD10 has diverse substrate specificity and, in healthy tissues, is located in mitochondria [168,169]. 17 β -HSD10 is expressed in various regions of the brain, the liver, heart, kidney, and gonads. In addition to its promiscuous substrate spectrum, it was shown that proteins and peptides such as the Alzheimer's disease (AD) related amyloid- β (A β) peptide or ER α can bind to 17 β -HSD10, thereby inhibiting its activity [170]. 17 β -HSD10 contains a unique β -hairpin structure at residues 102–107, which is distinct from all other NAD⁺-dependent SDRs and thought to be the recognition site for A β [171,172]. Thus, 17 β -HSD10 is also known as A β binding alcohol dehydrogenase (ABAD). The inhibition of 17 β -HSD10 by ER α binding seems to be estrogen-dependent [173], and high levels of intracellular estradiol disrupt the described interaction and the released unbound 17 β -HSD10 then was suggested to convert estradiol to estrone. However, regarding its mitochondrial localization it remains to be demonstrated that interaction of 17 β -HSD10 with A β and ER α indeed occurs under patho-physiological conditions. Furthermore, 17 β -HSD10 has been proposed to catalyze the oxidation of steroid modulators of GABA(A) receptors [174]. Thus, clearly further research is needed to elucidate the physiological substrates and interactions of this enzyme. Nevertheless, altered 17 β -HSD10 function can be found in patients suffering from AD, certain cognitive disabilities, multiple sclerosis, and in chemotherapy-resistant osteosarcoma patients showing an overexpression of 17 β -HSD10 [170].

In order to understand the molecular basis of the substrate promiscuity of human 17 β -HSD10, Nordling et al. [175] generated a homology model and performed docking experiments with known substrates to examine structure–function relationships. The active site was found to be a wide cleft, consisting of mainly hydrophobic residues and containing at the bottom of the pocket a polar region with the highly conserved catalytic triad Ser155, Tyr168, and Lys172. For the docking calculations different steroids were selected to simulate the following site- and stereo-specific enzyme activities: 3 α -OH to 3-oxo conversion and 17 β -OH dehydrogenase activity. 17 β -HSD activity was mimicked with optimal distances and geometry for estradiol, testosterone, DHT, and 3 β -androstenediol. Five- α reduced steroids such as 3 α ,5 α -androstane, 17-one revealed ideal hydrogen bond distances to Tyr168, Ser155, and NAD⁺ for 3 α -HSD activity. In contrast, 3 β -hydroxylated compounds or 5 β -reduced steroids such as the bile acid ursodeoxycholic acid (UDCA) showed inappropriate distances to Ser155 (>4 Å), therefore restricting the oxidation reaction. However, in an expanded follow-up study including kinetic measurements, they found 17 β -HSD10 acting as 7 β -hydroxysteroid dehydrogenase for the bile acids UDCA and isoUDCA, respectively [176]. To explain this novel substrate specificity on both equatorial and axial positions of the steroidal compounds, they generated again a homology model, this time based on the orthologous rat crystal structure (PDB entry 1E6W [177]), whereas the model of the former study was obtained using the related 7 α -HSD (PDB entry 1FMC [178]). Interestingly, the observed molecular distances for isoUDCA to the catalytic triad were identical for the hydroxyl group of Tyr and the C4 atom of NAD⁺, but decreased in this docking application from 4.26 Å to 2.1 Å. Unfortunately, the exact pose of isoUDCA and therefore the parts of the substrate involved in the interaction, was not displayed for both approaches. This might clarify structural differences of the homology models and may explain the observed distance difference. In addition to the 7 β -hydroxysteroid dehydrogenase activity of 17 β -HSD10, they detected novel activities, namely the oxidation of 20 β - and 21-hydroxyl groups in C₂₁ steroids such as glucocorticoids.

Although homology models are not as precise as high-resolution X-ray structures, they represent a valuable basis for the analysis of substrate recognition and specificity. Furthermore, the 17 β -HSD10 crystal structure resolved by Kissinger et al. [172] almost entirely confirmed the hydrophobic residues predicted by the homology model generated by Nordling et al. to be involved in substrate binding [175].

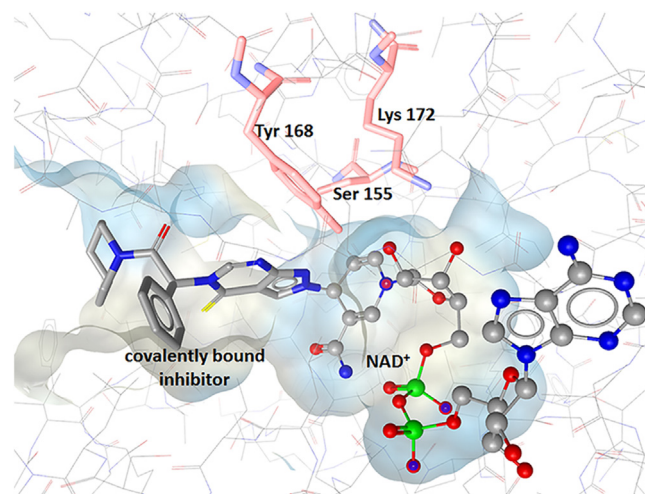


Fig. 10. Binding pocket of 17 β -HSD10 with residues of the catalytic triad and co-crystallized ligand covalently bound to NAD⁺ (PDB 1U7T).

To analyze the role of 17 β -HSD10 in AD pathogenesis and as part of a structure-based drug design process, Kissinger et al. crystallized the human 17 β -HSD10 in complex with NAD⁺ and a small molecule inhibitor (PDB 1U7T) (Fig. 10). In line with Nordling et al., they described the substrate binding pocket as flexible and highly hydrophobic cleft, supporting the multi-substrate specificity of the enzyme. Superimposition with the rat enzyme, for which already three resolved protein structures were available, showed very similar overall chain fold [177]. Interestingly, the inhibitor was found to form covalent adducts with the bound cofactor NAD⁺. Although the human protein structure was successfully resolved, no molecular modeling studies for substrate or inhibitor identification were implemented so far.

2.2.2. 17 β -hydroxysteroid dehydrogenase type 14

The physiological functions of 17 β -HSD14 still remain unclear. Expression analysis revealed a cytoplasmic localization of 17 β -HSD14 with high expression in liver, placenta, and brain, but absence in steroidogenic tissues such as testis and ovary [179]. In contrast, Sivik et al. [180] reported intense 17 β -HSD14 immunohistochemical staining patterns in breast, ovary, and testis. The observed discrepancy may be due to differences in antibody specificity; thus, further confirmatory expression studies are necessary.

Lukacik et al. provided structural and functional information building a basis for the deorphanization of this enzyme and leading to the renaming of the *DHRS10* gene to *HSD17B14* [179]. The resolution of the 17 β -HSD14 holo enzyme crystal structure represented a major achievement to deduce functional consequences. Besides the typically conserved regions of SDRs, such as the Rossmann-fold or the catalytic triad consisting of Ser141, Tyr154, and Lys158, the active site of 17 β -HSD14 displayed a deep and broad hydrophobic cleft. An *in vitro* substrate screening using purified recombinant 17 β -HSD14 and including 50 different steroids comprising androgens, estrogens, progestin, glucocorticoids, bile acids and oxysterols revealed rather low catalytic turnover of estradiol and 5-androstene-3 β ,17 β -diol using NAD⁺ as cofactor. Non-saturable kinetics were found for testosterone. Docking calculations for structural comparison of estradiol binding within 17 β -HSD1 and other 17 β -HSDs showed a comparatively loose binding of estradiol in the active site cleft of 17 β -HSD14. However, this extensive and open active cleft may also be due to lack of a co-crystallized substrate in the X-ray structure, and substrate binding might result in an induced fit. Evidence for an induced fit upon cofactor binding was recently provided by Bertolotti and Braun et al., who resolved the crystal structure of 17 β -HSD14 as the holo form with NAD⁺ and as ternary complexes with estrone and the first nonsteroidal inhibitor of 17 β -HSD14 [181]. The residues 189–212 were found to form a flexible loop adopting a closed conformation in the presence of cofactor and reducing the size of the active site. The geometry of the active site in the ternary complexes with the inhibitor or estrone bound showed the same closed state delimiting an elongated, conical shaped binding site with the catalytic triade at the apex of the cone and a solvent-exposed opening site. However, estrone was found in an atypical binding pose with the A-ring next to the nicotinamide structure of the cofactor and forming an H-bond with Tyr154 of the catalytic triade instead of the actual reaction position 17. Furthermore, the position 17 itself was not observed to introduce any other interaction. Chemical modification of this inhibitor scaffold applying a ligand-based approach led to the identification of five new 17 β -HSD14 inhibitors with K_i values in the lower nanomolar range [182]. The 17 β -HSD14 crystal structure determination in complex with these new inhibitors revealed a highly similar binding mode compared to previously reported nonsteroidal 17 β -HSD14 inhibitor.

2.2.3. Application of structural modeling for substrate identification

Favia et al. [183] introduced a molecular docking protocol to identify candidate substrates for 27 SDR members with resolved X-ray structures and known catalytic function. The enzymes included oxidoreductases, lyases, and isomerases, whereby half of the proteins were from bacterial organisms and half from eukaryotes. They docked the known substrates and products together with >900 human metabolites from the KEGG pathway metabolite database to each protein. In two thirds of all cases, the actual known substrate or product was found within the top 5% of all docked compounds. For the remaining third, allowing full flexibility of the side chains enhanced the rate of recognition of their natural substrates. However, increasing the degrees of freedom is not a practicable solution for docking of large libraries as it also increases the required computational time and capacity. Nevertheless, rigidity of a docking calculation can result in an increased rate of false negative and false positive hits. A closer look at the 2D structural similarity of the top-ranking compounds to the substrate revealed rather weak correlation. Metabolites resembling the natural substrate were indeed identified; however, only some of the top-ranking compounds showed reasonable correlation of the similarity with the docking rank. This may be explained by the large hydrophobic binding pockets and induced fit, allowing the enzyme to bind various molecules, an essential property of multi-functional SDR enzymes. In addition, Favia et al. clustered the substrates into steroids, small polar molecules, coenzyme A derivatives, nucleotide sugars, and others, and investigated whether the use of representatives of each structural class might provide similar information on substrate preferences of an enzyme as the whole dataset. Even though they found that the rank of a group representative correlated well with the mean rank of the corresponding cluster, this approach seemed to be too abstract for substrate identification calculations. The diversity within a cluster is important as it covers structurally related compounds with great affinity variations; thus defining a class representative will decrease the ability to identify potential candidate substrates.

In this respect, Hermann et al. conducted a structure-based docking study on a selection of high-energy intermediate forms of potential substrates for the amidohydrolase superfamily member Tm0936, and they were able to predict three substrates with substantial catalytic rate constants [184]. Their study was based on two important facts: first the X-ray structure was already resolved, and second the number of possible catalytic reactions could be reduced to a limited set of mechanistically associated conversions. For this approach to be successful, it seems crucial to already have some information on the mechanistic details of the enzyme. Regarding SDRs, they show very broad substrate diversity, making it difficult to restrict possible substrates to a specific subclass of molecules. A pharmacophore-based VS approach for substrate identification of enzymes not belonging to the SDR family where no prior knowledge about the binding site of a protein is necessary was employed by Mallipeddi and Joshi et al. [185]. Detailed description of this study can be found in the Supplementary information. However, all of the above mentioned studies validated their approaches by modeling known substrates and they did not include a subsequent *in vitro* evaluation of the substrate-like compounds.

Reinhardt et al. examined tropinone reductase-like SDRs (TRLs) of the Brassicaceae *Cochlearia officinalis* and the closely related *Arabidopsis thaliana* *in silico* and *in vitro* for their catalytic capacities due to the uncertainty of their denomination and biological function [186]. Two TRLs sharing 79% sequence identity and one sharing 61% identity with a known tropinone reductase were chosen for homology modeling, substrate docking and *in vitro* validation. Although tropinone was successfully docked in a favorable position into the binding pockets of all three enzymes,

none of them was able to reduce tropinone or nitrogen-containing analogues *in vitro*. A more detailed investigation of the substrate binding sites revealed a small and hydrophobic pocket, where compounds with a charged nitrogen atom can hardly be accepted as substrates. Therefore, small lipophilic carbonyl compounds were used for further docking applications, in which they were predicted as substrates. Biological testing confirmed these *in silico* predictions, even though highly different kinetic characteristics were obtained. These results enabled them to generate pharmacophore models to identify further substrates by VS of small compound libraries. The resulting hit list was again docked into the binding sites to evaluate for keto or aldehyde functions in the reactive position. The four scaffolds recognized by all of the pharmacophore models were selected for biological assays. All three TRLs reduced the four compounds *in vitro*, however, with different kinetics. Thus, this pharmacophore-based approach succeeded in the identification of new substrates. This study also emphasizes the importance of *in vitro* testing of hits from VS when using models based on reference proteins sharing high sequence identity. Especially small scaffolds may easily adopt a favorable docking pose without acting as a substrate. Nevertheless, VS techniques for substrate identification are always dependent on the available database. A potential substrate can only be found if contained in the database. Another limitation of pharmacophore models is that only compounds matching the defined chemical features are retrieved. If a model contains one feature more or less than a potential substrate, it will not be found in the virtual hit list. Hence, applying this approach for substrate identification should rather include open models, retrieving a higher number of hits.

Another example of rather unusually high sequence identity (71%) among SDRs can be found for carbonyl reductases (CBR) 1 and CBR3. CBR1 has a role in phase I metabolism of a wide range of carbonyl containing xenobiotics, and it also catalyzes the conversion of some endogenous substrates including prostaglandins, steroids, and lipid aldehydes, although the physiological role in converting these endogenous substrates requires further research. In contrast, the function of CBR3 has not yet been extensively characterized [187]. Pilka et al. established an *in vitro* substrate profile for CBR3 that they then used for an *in silico* structure-activity relationship comparison with CBR1 [188]. The results revealed a much narrower substrate spectrum for CBR3 compared with CBR1. Orthoquinones, isatin-like compounds, and oracin were the only tested substrates shared between the two enzymes. None of the endogenous substrates of CBR1 served as substrate of CBR3. The resolution of a CBR3 crystal structure, substrate docking calculations, and site-directed mutagenesis studies allowed them to identify residues that are critical for substrate recognition and enzyme conformation. Although CBR1 and CBR3 share high sequence similarity, their active sites differ in regard to shape, size, and surface properties. A major difference lies in a short segment of the substrate binding loop containing Trp229 and Ala235 in CBR1 and Pro230 and Asp236 at analogous positions in CBR3, respectively. Thus, a large hydrophobic barrier is formed in CBR1 by Trp229, in contrast to a rather open binding pocket with an additional charge contributed by Asp236 in CBR3. Furthermore, Met141 and Gln142 in the active site of CBR1 and CBR3, respectively, had significantly different effects on the catalytic activity, although the residues are of similar size. The observations of this study were further supported by El-Hawari et al. [189]. Thus, CBR3 clearly has a substrate spectrum distinct from that of CBR1.

CBR1 shares 27% sequence identity with the fruit-fly *Drosophila melanogaster* carbonyl reductase sniffer, which was reported to prevent age-related neurodegeneration [190]. The mechanism underlying the role of sniffer in neurodegeneration remains incompletely understood. To study the substrate binding site of sniffer and obtain hints towards potential physiological substrates,

Sgraja et al. resolved the crystal structure of sniffer in complex with NAD⁺ [191]. The structure revealed that the dinucleotide-binding site and the substrate-binding loop adopt similar conformations compared with porcine and human CBR1. Compared to other SDRs, the substrate-binding loop is shorter in all three enzymes. For most SDRs, this loop remains disordered until the substrate has bound. However, in the sniffer protein this loop adopts a well-defined conformation even in the absence of a bound substrate. Crystallization of the sniffer protein in complex with an artificial substrate such as 9,10-phenanthrenequinone, p-nitrobenzaldehyde, or menadione, which were described earlier as sniffer substrates, was not successful. Thus, these compounds were computationally docked into the binding site after crystallization. Plausible docking poses could be found for 9,10-phenanthrenequinone and menadione. The previously mentioned tryptophane residue corresponding to position 229 in the human enzyme seems to be highly conserved and was also found to be involved in substrate binding in the sniffer protein. Furthermore, the observed binding modes led the authors to suggest that the unoccupied space in the binding pocket should allow binding of larger substrate molecules such as steroids or prostaglandins. In this respect, Martin et al. recently showed that sniffer is able to catalyze the NADPH-dependent reduction of the lipid peroxidation product 4-oxonon-2-enal into the less reactive 4-hydroxynon-2-enal, thereby providing a possible explanation for the mechanism of protection from oxidative stress in *Drosophila melanogaster* [192].

2.3. Virtual screening applications in toxicology focusing on SDRs

Molecular modeling applications are not only useful for substrate and lead compound identification, but they can also facilitate the identification of hazardous chemicals in predicting interactions of compounds with so-called anti-targets that may lead to severe adverse health effects. Although the different applications pursue distinct goals, the actual computational algorithm distinguishes not between screening of a drug candidate, potential substrate or hazardous compound. There are only few VS reports focusing on SDRs and toxicological questions so far, and they will be introduced briefly.

A large number of exogenous substances such as dyes, food additives, body care products and cosmetics, as well as chemicals used for industrial production or agriculture are produced and placed on the market every year, often with insufficient safety assessment. Hazard characterization and risk evaluation of synthetic chemicals on human health and the environment are important for safety management strategies; and in this respect the interference of xenobiotics with the endocrine system may cause harmful effects and is a topic of high actual interest [19,193]. These so-called endocrine disrupting chemicals (EDCs) can disturb hormone synthesis, metabolism, and hormonal signaling, thereby potentially contributing to major diseases.

Nuclear steroid receptors such as ER, AR, MR, GR, and progesterone receptor (PR) are among the most extensively investigated targets for EDC action. However, biosynthesis and peripheral metabolism essentially impact on tissue- and cell-specific regulation of steroid levels and action. Several SDRs are involved in the local interconversion of inactive and active steroid metabolites, and it is important to include them in the evaluation of potential EDCs. Covering all these potential enzymes and receptors for biological testing represents a major challenge. Computational approaches can be highly useful in a first step to identify new EDCs and to gain insights into the mechanism of action, thus helping to prioritize the chemicals for further biological evaluation [19].

In such a proof of concept study, Vuorinen et al. aimed at identifying potential EDCs inhibiting 11 β -HSD2, which converts

the potent glucocorticoid cortisol into the inactive cortisone, thereby protecting MR from excessive cortisol [21]. Elevated MR activation by glucocorticoids due to 11 β -HSD2 disruption or congenital deficiency causes the syndrome of apparent mineralocorticoid excess (AME), characterized by severe hypertension, hypokalemia, and hypernatremia [194,195]. 11 β -HSD2 is also expressed in non-mineralocorticoid target tissues such as the placenta, where it ensures fetal protection from maternal glucocorticoids [196,197]. Impaired 11 β -HSD2 function has been associated with altered fetal growth, impaired angiogenesis, and a higher risk for cardio-metabolic and neuropsychiatric disorders in later life [198,199]. Thus, Nashev et al. applied a ligand-based 11 β -HSD pharmacophore model for VS of a database containing putative EDCs [21]. In total, 29 hit compounds virtually matched with the chemical features of the model, of which 5 substances were tested in a cell-free assay for 11 β -HSD1 and 11 β -HSD2 inhibition. AB110873, a silane-coupling agent used as rubber additive, and the antibiotic lasalocid, applied in chicken and turkey breeding, were thereby found to inhibit 11 β HSD2 activity (IC₅₀ 6.1 μ M and 14 μ M, respectively). Besides 11 β -HSD2 inhibition, the silane AB110873 showed concentration-dependent MR activation, which resulted in enhanced interleukin-6 (IL-6) expression and mitochondrial reactive oxygen species (ROS) production in macrophages exposed to this compound. Docking studies were implemented to understand the binding mode of AB110873. Interestingly, AB110873 adopted the same hydrophobic interactions as aldosterone and in addition occupied a hydrophobic side pocket of the receptor. A newly generated structure-based MR pharmacophore recognized AB110873 as a hit, demonstrating the ability to find compounds with quite different, non-steroidal scaffolds. However, regarding risk assessment, it remains to be shown whether relevant concentrations of these substances can be observed in the human body, especially in industry workers producing and processing them.

The importance of 17 β -HSD3 during male sexual development is highlighted by specific defects in HSD17B3, leading to 46, XY disorder of sex development [143–145]. Inhibition of 17 β -HSD3 activity during early development until puberty by EDCs might lower plasma testosterone levels, thereby disturbing the masculinization process and contributing to male reproductive disorders. For this purpose, Nashev et al. developed a ligand-based pharmacophore model to search for 17 β -HSD3 inhibitors from a database containing putative EDCs [19]. VS revealed several benzophenones (Fig. 11) used as UV-filters in cosmetics,

sunscreens, and as plastic additives. Upon biological testing of selected virtual hits and structurally similar derivatives that are environmentally relevant in intact cells, benzophenone-1 (BP-1) was found to be the most potent 17 β -HSD3 inhibitor with an IC₅₀ value of 1.05 μ M. Moderate inhibition with IC₅₀ between 5.9 μ M and 10.3 μ M were found for BP-2, 3-benzylidene camphor (3-BC) and 4-methylbenzylidene camphor (4-MBC). Notably, BP-1, 3-BC and 4-MBC were not found as virtual hits but were included in the *in vitro* testing because of their structural similarity to the initially identified UV-filter hits. In addition to 17 β -HSD3, the related SDRs 17 β -HSD2 and 11 β -HSD1 were also inhibited by these UV-filter chemicals (17 β -HSD2: IC₅₀ for BP-2, 3-BC and 4-MBC of 10.0 μ M, 6.3 μ M and 5.8 μ M; 11 β -HSD1: IC₅₀ for BP-2, 3-BC and 4-MBC of 12.2 μ M, 2.3 μ M and 2.9 μ M, respectively), emphasizing the need to include several related SDRs for the safety assessment of these chemicals.

As benzophenones may be regarded as steroid mimetics, they may directly bind to nuclear steroid receptors. Therefore, the investigated UV-filter chemicals were also tested for direct effects on the androgen receptor (AR). Several UV-filters antagonized the AR, with BP-1, BP-2, and BP-3 displaying the most potent activities with IC₅₀ values between 2.2 μ M and 5.7 μ M. These results emphasize that VS as initial filtering tool for the discovery of active compound classes can aid the identification of EDCs. Additionally, as metabolites can be equally or even more active than their parent substances, major metabolites should be included in safety analyses. For example, whilst benzophenone-3 (BP-3) displayed no inhibitory activity against 17 β -HSD3, it is rapidly demethylated *in vivo* to the potent 17 β -HSD3 inhibitor BP-1 [200]. Of note, pharmacophore-based SAR studies, implemented to analyze the differences in the activities of the tested UV-filters on 17 β -HSD3, indicated that the loss of activity of BP-3 was due to the ether group. Nevertheless, for the risk assessment, the concentrations of BP-1 reached *in vivo* in the testes need to be determined in order to assess the relevance of 17 β -HSD3 inhibition.

2.4. Limitations

2.4.1. Computational applications

Despite the many reported success stories, *in silico* approaches for the identification of chemicals binding to a cognate protein are facing several challenges. The predictive power of VS workflows is determined by the quality of the data underlying the model or workflow. Thus, the biological data of the training and test compounds used for model generation and validation must be critically evaluated [201]. The following aspects should therefore be considered: the biological data should be based on suitable *in vitro* testing systems employed for activity determination (i.e. purified protein or cell lysates allowing for a direct access of a given chemical to the corresponding protein), activity cut-offs to exclude unspecific effects, use of suitable positive and negative controls, consideration of species differences (i.e. data and model must be for the same species), and verification of the original references when using compound databases. The majority of these issues is equally important for the biological validation of virtual hits, to guarantee a correct subsequent model refinement. Hence, they are discussed in more detail below. These issues refer not only to compounds determined as active, but also to confirm inactive molecules. These data are scarce because proven inactive compounds for a specific target, i.e. negative results, are rarely reported. Compounds confirmed as inactive can provide valuable insights into unwanted properties that cannot be tolerated for a compound to interact with a macromolecular target. In addition, they can help estimating and adjusting the selectivity and sensitivity of an *in silico* workflow. Rather restrictive models are often employed in the drug development process to find few

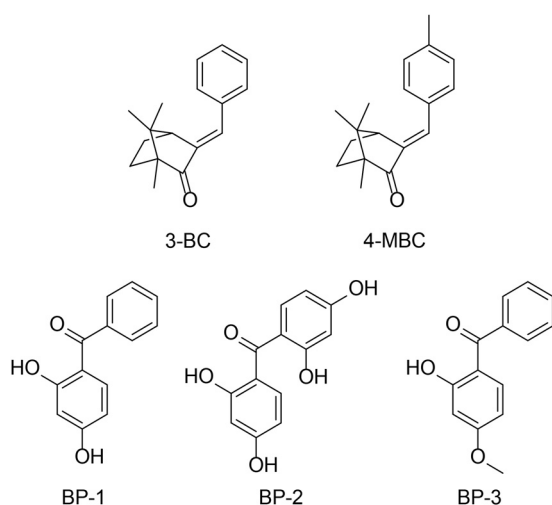


Fig. 11. Benzophenones (BP-1, BP-2, BP-3), 3-benzylidene camphor (3-BC), and 4-methylbenzylidene camphor (4-MBC).

potential drug candidates and keep the number of false positive virtual hits low. In contrast, toxicological applications aim to identify all conceivably harmful substances and can accept lower VS hit rates. Additionally, most *in silico* workflows were generated with drug-like compounds where a lot of data may already be available. Toxicologically relevant molecules such as environmental chemicals occupy a different chemical space, for which a workflow was not optimized. Nevertheless, the identification of structural compound classes acting on a given target, which are then further biologically evaluated, can yield important information for the prioritization of follow-on experiments.

For many members of the SDR family, structural information is currently not or only partially available. For example, many available crystal structures are not including the cofactor, and several SDRs bear a transmembrane binding anchor that is usually not covered in the crystal structures. The experimental 3D resolution of these membrane proteins still remains challenging as is the alternative approach of homology modeling due to the low sequence similarity among SDRs. The lack of suitable x-ray crystallographic data thus limits structure-guided design strategies for several SDR family members. Alternatively, ligand-based methods can be applied to target these molecules.

Different computational programs can generate different VS results even when the same chemical library and protein structural information are used, and each approach by its own yields valuable results [202,203]. Thus, combining different computational programs may be crucial for substrate identification or toxicological approaches, where a more complete recovery of the active compounds is needed [204]. Another drawback in the VS process, especially for substrate identification purposes, represents the fact that the available chemical databases are not fully representative. While a lot of databases containing small drug-like compounds are available (e.g. ChEMBL [205]), less data is easily accessible for endogenous substrates or environmental chemicals. The gaining knowledge of existing metabolites and extending existing databases such as the human metabolome database [206], will improve future VS applications aiming at substrate identification.

Regarding successful VS applications, *in silico* tools should not be seen as isolated approaches, but rather as complementary to experimental techniques. Thus, the biological validation of virtual hits using appropriate *in vitro* testing systems is of utmost importance and will therefore be discussed in detail in the following section.

2.4.2. Biological validation

As mentioned above, biological assays are essential to validate virtual hits. To avoid biased results, the limitations of the *in vitro* testing systems should be known and considered for data interpretation. The enzyme activity analysis of selected virtual hits has to be conducted under cell-free conditions (i.e. purified protein or lysates expressing the protein in an environment with very low background). Equally important is the appropriate selection of the assay detection technology. Compounds can be regarded as false positive due to interference issues with the assay signaling (for example autofluorescence of certain compounds for fluorescence detectors). Data obtained from intact cells can only be used to verify active hits but do not allow appropriate ranking of hits with different activities, nor does it allow exclusion of inactive molecules. Whereas a test compound has direct access to its target in cell-free systems, a compound's concentration in intact cells depends on the presence of transport proteins, intracellular binding proteins, as well as metabolizing enzymes. Thus, negative results in cell-based assays do not allow drawing unambiguous conclusions about the biological activity of a virtual hit. Moreover, results from cell-based assays can be influenced by parameters such as passage number of a cell line and therefore different expression levels, conditions of cell

handling, and medium composition. Similarly, problems may be evident in preparation of cell lysates and protein purification, where different handling can lead to different activity of an enzyme preparation. Thus, ideally data on a series of compounds should be obtained with the same material. Using the same procedure and inclusion of appropriate positive and negative controls facilitates comparison with results obtained other studies. Nevertheless, upon initial confirmation, active hits need further comprehensive biological characterization including selectivity assessment, analysis of species-specific differences and *in vivo* pharmacodynamics and pharmacokinetics.

Although the members of the SDR family share considerable structural similarity, the primary sequence similarity is rather low. Koch et al. [207] proposed that structural similarity rather than primary sequence similarity should be chosen as criterion for whether a certain chemical affects the activity of a related enzyme. Therefore, the closest structurally related enzymes should be included for selectivity testing. Because of the high number of orphan SDRs, the function and substrate specificity of the closest relatives of a given enzyme are often unknown and no suitable assay read-outs for selectivity assessment are available. Thus, deorphanization of SDRs is important to improve the physiological understanding of these enzymes and to discover potentially novel drug or anti-drug targets.

The lack of assay read-outs for testing potential substrates to deorphanize enzymes hampers the attempt of substrate identifications. Unlike other protein families, SDRs do not share a common activity element that can be used as read-out. For instance, the activation of G protein coupled-receptors (GPCRs) involves well-described steps that can be monitored, such as the accumulation of second messengers. This allows for the detection of specific changes upon receptor activation [208]. SDRs, however, are enzymes with a remarkably broad substrate specificity, which impedes the monitoring of activation-specific changes.

Species-specific variabilities have been reported for inhibitors and substrates of different HSDs [77,79,209]. These observations suggested significant differences in the 3D conformations of the enzymes from different species. During the drug development process, a lead compound ideally inhibits the human enzyme as well as the orthologue of the species (usually rodents) in which the preclinical or safety studies are conducted. However, Möller et al. compared the activities of 17 β -HSD1 inhibitors in different species and found that the most potent inhibitors of the human enzyme lacked inhibition of the rodent enzymes [209]. Moreover, they were not able to predict the species-specific effects by molecular docking calculations. In this regard, an initial enzymatic assay including only the orthologue of the subsequently used animal model species would miss potential inhibitors for human applications. Abdelsamie et al. performed structural optimization studies to enhance the potency of a 17 β -HSD1 inhibitor against the rodent enzyme and performed docking and homology modeling applications to elucidate the interspecies differences [210]. The observed species-specific protein-ligand interactions might offer valuable information for the design of new inhibitors.

Achieving tissue-specific enzyme inhibition can be important for therapeutic applications in order to reduce potential side effects. Therefore, a compound should be tested in suitable *in vitro* and *in vivo* testing systems to elucidate its tissue distribution. Moreover, regarding toxicological studies, tissue distribution and accumulation studies could help to assess the potential of compounds acting as EDCs. In this context, Hamilton et al. developed a test cascade for the development of 11 β -HSD1 inhibitors as described above [99]. To summarize the limitations involved in the biological validation of virtual hits described in this review and to provide a potential solution approach, we adapted the former cascade to a more general screening strategy (Fig. 12).

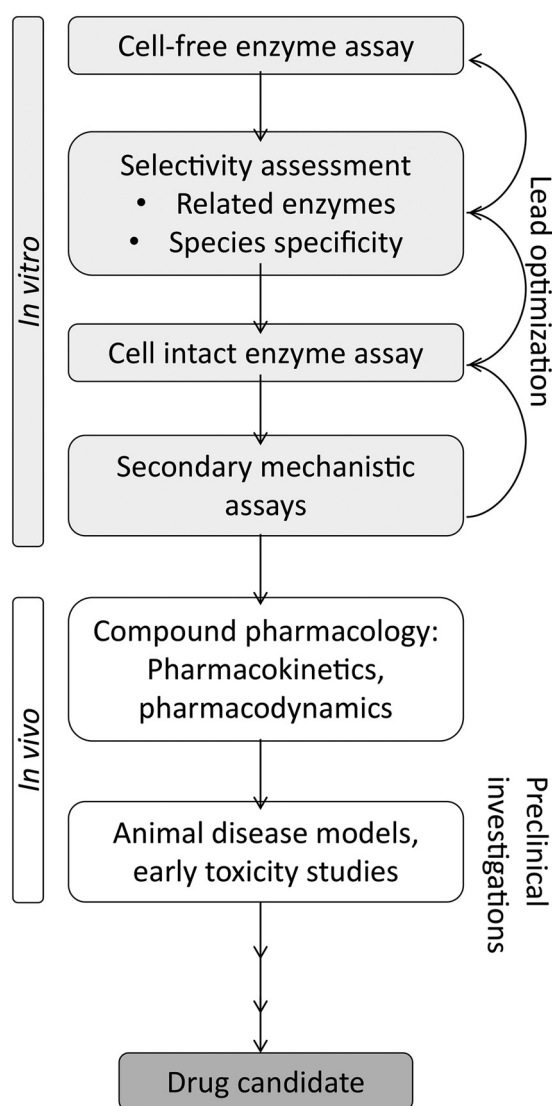


Fig. 12. Potential screening strategy for biological validation of *in silico* derived hits.

3. Conclusion

Computational tools offer a rational, cost-effective addition to large high-throughput screening (HTS) studies by enriching virtual hits from large databases applying target-specific filters. They can be employed in various application fields such as lead compound identification during drug development, toxicological screenings including EDC assessment, but also for substrate identification and enzyme characterization. This review highlights the efforts made in these areas for the family of SDRs, particularly focusing on HSDs. Several SDRs are involved in steroid synthesis and metabolism as well as in the metabolism of xenobiotics, suggesting that these enzymes may be susceptible to endocrine disruption. *In silico* design for therapeutic 11 β -HSD1 and 17 β -HSD1 inhibitors comprise the majority of studies conducted. Only few studies investigated HSDs as EDC targets and applied VS tools as pre-filter to identify compound classes rather than specific substances. Regarding the large number of orphan SDRs, new methods are required for substrate identification, where computational approaches could offer valuable support. However, these investigations into SDRs are rather at the beginning, and need to be extended.

For the appropriate application of *in silico* tools and subsequent biological validation of virtual hits, careful consideration of the limitations of the individual approaches is crucial. The reported successful studies including computational and biological analyses of SDRs raise the expectations of increasing numbers of studies performed in this area.

Conflicts of interest

The authors declare no conflict of interest.

Acknowledgements

We are grateful for financial support by the Swiss National Science Foundation (No 31003A-159454 to A.O.), the Austrian Science Fund (FWF, project P26782 "Safety of environmental chemicals" to D.S.), and the Swiss Center for Applied Human Toxicology and the Swiss Federal Office of Public Health (to A.O.). A. O. was supported as Chair for Molecular and Systems Toxicology by the Novartis Research Foundation. D.S. holds an Ingeborg Hochmaier Professorship of the University of Innsbruck.

Appendix A. Supplementary data

Supplementary data associated with this article can be found, in the online version, at <http://dx.doi.org/10.1016/j.jsbmb.2017.03.008>.

References

- [1] Y. Kallberg, U. Oppermann, B. Persson, Classification of the short-chain dehydrogenase/reductase superfamily using hidden Markov models, *FEBS J.* 277 (2010) 2375–2386.
- [2] D.J. Hosfield, Y. Wu, R.J. Skene, M. Hilgers, A. Jennings, G.P. Snell, K. Aertgeerts, Conformational flexibility in crystal structures of human 11 β -hydroxysteroid dehydrogenase type 1 provide insights into glucocorticoid interconversion and enzyme regulation, *J. Biol. Chem.* 280 (2005) 4639–4648.
- [3] K.L. Kavanagh, H. Jornvall, B. Persson, U. Oppermann, Medium- and short-chain dehydrogenase/reductase gene and protein families: the SDR superfamily: functional and structural diversity within a family of metabolic and regulatory enzymes, *Cell. Mol. Life Sci.* 65 (2008) 3895–3906.
- [4] W.L. Miller, R.J. Auchus, The molecular biology, biochemistry, and physiology of human steroidogenesis and its disorders, *Endocr. Rev.* 32 (2011) 81–151.
- [5] T.M. Penning, D.R. Bauman, Y. Jin, T.L. Rizner, Identification of the molecular switch that regulates access of 5 α -DHT to the androgen receptor, *Mol. Cell. Endocrinol.* (2007) 77–82 265–266.
- [6] J.L. Mohler, M.A. Titus, S. Bai, B.J. Kennerley, F.B. Lih, K.B. Tomer, E.M. Wilson, Activation of the androgen receptor by intratumoral bioconversion of androstenediol to dihydrotestosterone in prostate cancer, *Cancer Res.* 71 (2011) 1486–1496.
- [7] S.Y. Yang, X.Y. He, C. Isaacs, C. Dobkin, D. Miller, M. Philipp, Roles of 17 β -hydroxysteroid dehydrogenase type 10 in neurodegenerative disorders, *J. Steroid Biochem. Mol. Biol.* 143 (2014) 460–472.
- [8] L.L. Gathercole, G.G. Lavery, S.A. Morgan, M.S. Cooper, A.J. Sinclair, J.W. Tomlinson, P.M. Stewart, 11 β -hydroxysteroid dehydrogenase 1: translational and therapeutic aspects, *Endocr. Rev.* 34 (2013) 525–555.
- [9] V. Luu-The, Assessment of steroidogenesis and steroidogenic enzyme functions, *J. Steroid Biochem. Mol. Biol.* 137 (2013) 176–182.
- [10] S. Marchais-Oberwinkler, C. Henn, G. Moller, T. Klein, M. Negri, A. Oster, A. Spadaro, R. Werth, M. Wetzel, K. Xu, M. Frotscher, R.W. Hartmann, J. Adamski, 17 β -Hydroxysteroid dehydrogenases (17 β -HSDs) as therapeutic targets: protein structures, functions, and recent progress in inhibitor development, *J. Steroid Biochem. Mol. Biol.* 125 (2011) 66–82.
- [11] P.W. Hadoke, T. Kipari, J.R. Seckl, K.E. Chapman, Modulation of 11 β -hydroxysteroid dehydrogenase as a strategy to reduce vascular inflammation, *Curr. Atheroscler. Rep.* 15 (2013) 320.
- [12] T.M. Penning, Human hydroxysteroid dehydrogenases and pre-receptor regulation: insights into inhibitor design and evaluation, *J. Steroid Biochem. Mol. Biol.* 125 (2011) 46–56.
- [13] D. Sun, M. Wang, Z. Wang, Small molecule 11 β -hydroxysteroid dehydrogenase type 1 inhibitors, *Curr. Top. Med. Chem.* 11 (2011) 1464–1475.
- [14] J.K. Seibert, L. Quagliata, C. Quintavalle, T.G. Hammond, L. Terracciano, A. Odermatt, A role for the dehydrogenase DHR57 (SDR34C1) in prostate cancer, *Cancer Medicine* 4 (2015) 1717–1729.
- [15] D. Kowalik, F. Haller, J. Adamski, G. Moeller, In search for function of two human orphan SDR enzymes: hydroxysteroid dehydrogenase like 2 (HSDL2)

- and short-chain dehydrogenase/reductase-orphan (SDR-O), *J. Steroid Biochem. Mol. Biol.* 117 (2009) 117–124.
- [16] A. Kitamoto, T. Kitamoto, T. Nakamura, Y. Ogawa, M. Yoneda, H. Hyogo, H. Ochi, S. Mizusawa, T. Ueno, K. Nakao, A. Sekine, K. Chayama, A. Nakajima, K. Hotta, Association of polymorphisms in GCKR and TRIB1 with nonalcoholic fatty liver disease and metabolic syndrome traits, *Endocr. J.* 61 (2014) 683–689.
- [17] X. Chen, M. Yamamoto, K. Fujii, Y. Nagahama, T. Ooshio, B. Xin, Y. Okada, H. Furukawa, Y. Nishikawa, Differential reactivation of fetal/neonatal genes in mouse liver tumors induced in cirrhotic and non-cirrhotic conditions, *Cancer Sci.* 106 (2015) 972–981.
- [18] G.V. Dhoke, Y. Ensari, M.D. Davari, A.J. Ruff, U. Schwaneberg, M. Bocola, What's my substrate? computational function assignment of QM/AMM paraiposilis ADH5 by genome database search, virtual screening, and QM/MM calculations, *J. Chem. Inf. Model.* 56 (2016) 1313–1323.
- [19] A. Vuorinen, A. Odermatt, D. Schuster, In silico methods in the discovery of endocrine disrupting chemicals, *J. Steroid Biochem. Mol. Biol.* 137 (2013) 18–26.
- [20] J. Vitku, L. Starka, M. Bicikova, M. Hill, J. Heracek, L. Sosvorova, R. Hampl, Endocrine disruptors and other inhibitors of 11 β -hydroxysteroid dehydrogenase 1 and 2: tissue-specific consequences of enzyme inhibition, *J. Steroid Biochem. Mol. Biol.* 155 (2016) 207–216.
- [21] L.G. Nashev, A. Vuorinen, L. Praxmarer, B. Chantong, D. Cereghetti, R. Winiger, D. Schuster, A. Odermatt, Virtual screening as a strategy for the identification of xenobiotics disrupting corticosteroid action, *PLoS One* 7 (2012) e46958.
- [22] A. Odermatt, L.G. Nashev, The glucocorticoid-activating enzyme 11 β -hydroxysteroid dehydrogenase type 1 has broad substrate specificity: physiological and toxicological considerations, *J. Steroid Biochem. Mol. Biol.* 119 (2010) 1–13.
- [23] E. Maser, U.C. Oppermann, Role of type -1 11 β -hydroxysteroid dehydrogenase in detoxification processes, *Eur. J. Biochem.* 249 (1997) 365–369.
- [24] E. Maser, Xenobiotic carbonyl reduction and physiological steroid oxidoreduction. The pluripotency of several hydroxysteroid dehydrogenases, *Biochem. Pharmacol.* 49 (1995) 421–440.
- [25] L.G. Nashev, D. Schuster, C. Laggner, S. Sodha, T. Langer, G. Wolber, A. Odermatt, The UV-filter benzophenone-1 inhibits 17 β -hydroxysteroid dehydrogenase type 3: virtual screening as a strategy to identify potential endocrine disrupting chemicals, *Biochem. Pharmacol.* 79 (2010) 1189–1199.
- [26] K. Yuan, B. Zhao, X.W. Li, G.X. Hu, Y. Su, Y. Chu, B.T. Akingbemi, Q.Q. Lian, R.S. Ge, Effects of phthalates on 3 β -hydroxysteroid dehydrogenase and 17 β -hydroxysteroid dehydrogenase 3 activities in human and rat testes, *Chem.-Biol. Interact.* 195 (2012) 180–188.
- [27] B. Zhao, Y. Chu, D.O. Hardy, X.K. Li, R.S. Ge, Inhibition of 3 β - and 17 β -hydroxysteroid dehydrogenase activities in rat Leydig cells by perfluorooctane acid, *J. Steroid Biochem. Mol. Biol.* 118 (2009) 13–17.
- [28] M.A. Johnson, G.M. Maggiora, Concepts and Applications of Molecular Similarity, Wiley, New York, 1990.
- [29] T.T. Tanimoto, IBM Internal Report 17th Nov., 1957.
- [30] P. Jaccard, Distribution de la flore alpine dans le bassin des Dranses et dans quelques régions voisines, *Bull. Soc. Vaud. Sci. Nat.* 37 (1901) 241–272.
- [31] G. Wermuth, C.R. Ganellin, P. Lindberg, L.A. Mitscher, Glossary of terms used in medicinal chemistry (IUPAC Recommendations, Pure Appl. Chem. 70 (1998) 1129–1143.
- [32] G. Wolber, T. Langer, LigandScout: 3-D pharmacophores derived from protein-bound ligands and their use as virtual screening filters, *J. Chem. Inf. Model.* 45 (2005) 160–169.
- [33] Discovery Studio Modeling Environment, Dassault Systèmes BIOVIA, San Diego: Dassault Systèmes.
- [34] S.L. Dixon, A.M. Smondyrev, E.H. Knoll, S.N. Rao, D.E. Shaw, R.A. Friesner, PHASE: a new engine for pharmacophore perception, 3D QSAR model development, and 3D database screening: 1. Methodology and preliminary results, *J. Comput. Aided Mol. Des.* 20 (2006) 647–671.
- [35] C.C.G. Inc, Molecular Operating Environment (MOE), C.C.G. Inc., 1010 Sherbooke St. West, Suite #910, Montreal, QC, Canada, H 3A 2R7, 2015.
- [36] M.K. Akram, T. Kaserer, D. Schuster, Pharmacophore modeling and pharmacophore-based virtual screening, in: C.N. Cavasotto (Ed.), In silico drug discovery and design. Theory, Methods, Challenges, and Applications, CRC Press, Boca Raton, FL, 2016, pp. 123–154.
- [37] X. Liu, H. Jiang, H. Li, SHAFTS: a hybrid approach for 3D molecular similarity calculation. 1. Method and assessment of virtual screening, *J. Chem. Inf. Model.* 51 (2011) 2372–2385.
- [38] W. Lu, X. Liu, X. Cao, M. Xue, K. Liu, Z. Zhao, X. Shen, H. Jiang, Y. Xu, J. Huang, H. Li, SHAFTS: a hybrid approach for 3D molecular similarity calculation. 2. prospective case study in the discovery of diverse p90 ribosomal S6 protein kinase 2 inhibitors to suppress cell migration, *J. Med. Chem.* 54 (2011) 3564–3574.
- [39] vROCS, OpenEye Scientific Software, Santa FE, NM, pp. <http://www.eyesopen.com>.
- [40] P.C. Hawkins, A.G. Skillman, A. Nicholls, Comparison of shape-Matching and docking as virtual screening tools, *J. Med. Chem.* 50 (2007) 74–82.
- [41] G.M. Sastry, S.L. Dixon, W. Sherman, Rapid shape-based ligand alignment and virtual screening method based on atom/feature-pair similarities and volume overlap scoring, *J. Chem. Inf. Model.* 51 (2011) 2455–2466.
- [42] M.J. Vainio, J.S. Puranen, M.S. Johnson, ShaEP: molecular overlay based on shape and electrostatic potential, *J. Chem. Inf. Model.* 49 (2009) 492–502.
- [43] D.B. Kitchen, H. Decornez, J.R. Furr, J. Bajorath, Docking and scoring in virtual screening for drug discovery: methods and applications, *Nat. Rev. Drug Discov.* 3 (2004) 935–949.
- [44] C.A. Sotriffer, Protein-Ligand docking: from basic principles to advanced applications, in: C.N. Cavasotto (Ed.), In Silico Drug Discovery and Design. Theory, Methods, Challenges, and Applications, CRC Press, Boca Raton, FL, 2016, pp. 155–188.
- [45] G. Jones, P. Willett, R.C. Glen, A.R. Leach, R. Taylor, Development and validation of a genetic algorithm for flexible docking, *J. Mol. Biol.* 267 (1997) 727–748.
- [46] K. Chapman, M. Holmes, J. Seckl, 11 β -hydroxysteroid dehydrogenases: intracellular gate-keepers of tissue glucocorticoid action, *Physiol. Rev.* 93 (2013) 1139–1206.
- [47] A. Odermatt, D.V. Kratschmar, Tissue-specific modulation of mineralocorticoid receptor function by 11 β -hydroxysteroid dehydrogenases: an overview, *Mol. Cell. Endocrinol.* 350 (2012) 168–186.
- [48] P.C. White, T. Mune, A.K. Agarwal, 11 β -hydroxysteroid dehydrogenase and the syndrome of apparent mineralocorticoid excess, *Endocr. Rev.* 18 (1997) 135–156.
- [49] H. Masuzaki, J. Paterson, H. Shinyama, N.M. Morton, J.J. Mullins, J.R. Seckl, J.S. Flier, A transgenic model of visceral obesity and the metabolic syndrome, *Science* 294 (2001) 2166–2170.
- [50] H. Masuzaki, H. Yamamoto, C.J. Kenyon, J.K. Elmquist, N.M. Morton, J.M. Paterson, H. Shinyama, M.G. Sharp, S. Fleming, J.J. Mullins, J.R. Seckl, J.S. Flier, Transgenic amplification of glucocorticoid action in adipose tissue causes high blood pressure in mice, *J. Clin. Invest.* 112 (2003) 83–90.
- [51] J.M. Paterson, N.M. Morton, C. Fievet, C.J. Kenyon, M.C. Holmes, B. Staels, J.R. Seckl, J.J. Mullins, Metabolic syndrome without obesity: hepatic overexpression of 11 β -hydroxysteroid dehydrogenase type 1 in transgenic mice, *Proc. Natl. Acad. Sci. U. S. A.* 101 (2004) 7088–7093.
- [52] R.S. Lindsay, D.J. Wake, S. Nair, J. Bunt, D.E. Livingstone, P.A. Permana, P.A. Tataranni, B.R. Walker, Subcutaneous adipose 11 β -hydroxysteroid dehydrogenase type 1 activity and messenger ribonucleic acid levels are associated with adiposity and insulinemia in Pima Indians and Caucasians, *J. Clin. Endocrinol. Metab.* 88 (2003) 2738–2744.
- [53] G. Valsamakis, A. Anwar, J.W. Tomlinson, C.H. Shackleton, P.G. McTernan, R. Chetty, P.J. Wood, A.K. Banerjee, G. Holder, A.H. Barnett, P.M. Stewart, S. Kumar, 11 β -hydroxysteroid dehydrogenase type 1 activity in lean and obese males with type 2 diabetes mellitus, *J. Clin. Endocrinol. Metab.* 89 (2004) 4755–4761.
- [54] E. Rask, B.R. Walker, S. Soderberg, D.E. Livingstone, M. Eliasson, O. Johnson, R. Andrew, T. Olsson, Tissue-specific changes in peripheral cortisol metabolism in obese women: increased adipose 11 β -hydroxysteroid dehydrogenase type 1 activity, *J. Clin. Endocrinol. Metab.* 87 (2002) 3330–3336.
- [55] O. Paulmyer-Lacroix, S. Boullu, C. Oliver, M.C. Alessi, M. Grino, Expression of the mRNA coding for 11 β -hydroxysteroid dehydrogenase type 1 in adipose tissue from obese patients: an in situ hybridization study, *J. Clin. Endocrinol. Metab.* 87 (2002) 2701–2705.
- [56] K. Kannisto, K.H. Pietiläinen, E. Ehrenborg, A. Rissanen, J. Kaprio, A. Hamsten, H. Yki-Jarvinen, Overexpression of 11 β -hydroxysteroid dehydrogenase-1 in adipose tissue is associated with acquired obesity and features of insulin resistance: studies in young adult monozygotic twins, *J. Clin. Endocrinol. Metab.* 89 (2004) 4414–4421.
- [57] Y. Kotelevtsev, M.C. Holmes, A. Burchell, P.M. Houston, D. Schmolli, P. Jamieson, R. Best, R. Brown, C.R. Edwards, J.R. Seckl, J.J. Mullins, 11 β -hydroxysteroid dehydrogenase type 1 knockout mice show attenuated glucocorticoid-inducible responses and resist hyperglycemia on obesity or stress, *Proc. Natl. Acad. Sci. U. S. A.* 94 (1997) 14924–14929.
- [58] A. Tiganescu, M. Hupe, Y. Uchida, T. Mauro, P.M. Elias, W.M. Holleran, Increased glucocorticoid activation during mouse skin wound healing, *J. Endocrinol.* 221 (2014) 51–61.
- [59] J.K. Youm, K. Park, Y. Uchida, A. Chan, T.M. Mauro, W.M. Holleran, P.M. Elias, Local blockade of glucocorticoid activation reverses stress- and glucocorticoid-induced delays in cutaneous wound healing, *Wound Repair Regen.* 21 (2013) 715–722.
- [60] A. Tiganescu, A.A. Tahrani, S.A. Morgan, M. Otranto, A. Desmouliere, L. Abrahams, Z. Hassan-Smith, E.A. Walker, E.H. Rabbitt, M.S. Cooper, K. Amrein, G.G. Lavery, P.M. Stewart, 11 β -hydroxysteroid dehydrogenase blockade prevents age-induced skin structure and function defects, *J. Clin. Invest.* 123 (2013) 3051–3060.
- [61] L. Wu, H. Qi, Y. Zhong, S. Lv, J. Yu, J. Liu, L. Wang, J. Bi, X. Kong, W. Di, J. Zha, F. Liu, G. Ding, 11 β -hydroxysteroid dehydrogenase type 1 selective inhibitor BVT.2733 protects osteoblasts against endogenous glucocorticoid induced dysfunction, *Endocr. J.* 60 (2013) 1047–1058.
- [62] T. Kipari, P.W. Hadoke, J. Iqbal, T.Y. Man, E. Miller, A.E. Coutinho, Z. Zhang, K.M. Sullivan, T. Mitic, D.E. Livingstone, C. Schrecker, K. Samuel, C.I. White, M.A. Bouhrel, G. Chinetti-Gbaguidi, B. Staels, R. Andrew, B.R. Walker, J.S. Savill, K.E. Chapman, J.R. Seckl, 11 β -hydroxysteroid dehydrogenase type 1 deficiency in bone marrow-derived cells reduces atherosclerosis, *FASEB J.* 27 (2013) 1519–1531.
- [63] A. Hermanowski-Vosatka, J.M. Balkovec, K. Cheng, H.Y. Chen, M. Hernandez, G.C. Koo, C.B. Le Grand, Z. Li, J.M. Metzger, S.S. Mundt, H. Noonan, C.N. Nunes, S.H. Olson, B. Pikounis, N. Ren, N. Robertson, J.M. Schaeffer, K. Shah, M.S. Springer, A.M. Strack, M. Strowski, K. Wu, T. Wu, J. Xiao, B.B. Zhang, S.D. Wright, R. Thieringer, 11-(HSD1) inhibition ameliorates metabolic syndrome

- and prevents progression of atherosclerosis in mice, *J. Exp. Med.* 202 (2005) 517–527.
- [64] R.A. Garcia, D.J. Search, J.A. Lupisella, J. Ostrowski, B. Guan, J. Chen, W.P. Yang, A. Truong, A. He, R. Zhang, M. Yan, S.E. Hellings, P.S. Gargalovic, C.S. Ryan, L.M. Watson, R.A. Langish, P.A. Shipkova, N.L. Carson, J.R. Taylor, R. Yang, G.C. Psaltis, T.W. Harrity, J.A. Robl, D.A. Gordon, 11 β -hydroxysteroid dehydrogenase type 1 gene knockout attenuates atherosclerosis and in vivo foam cell formation in hyperlipidemic apoE(-)/(-) mice, *PLoS One* 8 (2013) e53192.
- [65] M.J. Luo, R. Thieringer, M.S. Springer, S.D. Wright, A. Hermanowski-Vosatka, A. Plump, J.M. Balkovec, K. Cheng, G.J. Ding, D.W. Kawka, G.C. Koo, C.B. Grand, Q. Luo, M.M. Maletic, L. Malkowitz, K. Shah, I. Singer, S.T. Waddell, K.K. Wu, J. Yuan, J. Zhu, S. Stepaniants, X. Yang, P.Y. Lum, I.M. Wang, 11 β -HSD1 inhibition reduces atherosclerosis in mice by altering proinflammatory gene expression in the vasculature, *Physiol. Genomics* 45 (2013) 47–57.
- [66] S. Rauz, C.M. Cheung, P.J. Wood, M. Coca-Prados, E.A. Walker, P.I. Murray, P.M. Stewart, Inhibition of 11 β -hydroxysteroid dehydrogenase type 1 lowers intraocular pressure in patients with ocular hypertension, *QJM* 96 (2003) 481–490.
- [67] S. Rauz, E.A. Walker, C.H. Shackleton, M. Hewison, P.I. Murray, P.M. Stewart, Expression and putative role of 11 β -hydroxysteroid dehydrogenase isozymes within the human eye, *Invest. Ophthalmol. Vis. Sci.* 42 (2001) 2037–2042.
- [68] S. Anderson, S. Carreiro, T. Quenzer, D. Gale, C. Xiang, H. Gukasyan, J. Lafontaine, H. Cheng, A. Krauss, G. Prasanna, In vivo evaluation of 11 β -hydroxysteroid dehydrogenase activity in the rabbit eye, *J. Ocul. Pharmacol. Ther.* 25 (2009) 215–222.
- [69] K. Sooy, S.P. Webster, J. Noble, M. Binnie, B.R. Walker, J.R. Seckl, J.L. Yau, Partial deficiency or short-term inhibition of 11 β -hydroxysteroid dehydrogenase type 1 improves cognitive function in aging mice, *J. Neurosci.* 30 (2010) 13867–13872.
- [70] J.L. Yau, K.M. McNair, J. Noble, D. Brownstein, C. Hibberd, N. Morton, J.J. Mullins, R.G. Morris, S. Cobb, J.R. Seckl, Enhanced hippocampal long-term potentiation and spatial learning in aged 11 β -hydroxysteroid dehydrogenase type 1 knock-out mice, *J. Neurosci.* 27 (2007) 10487–10496.
- [71] J.L. Yau, J. Noble, J.R. Seckl, 11 β -hydroxysteroid dehydrogenase type 1 deficiency prevents memory deficits with aging by switching from glucocorticoid receptor to mineralocorticoid receptor-mediated cognitive control, *J. Neurosci.* 31 (2011) 4188–4193.
- [72] E.G. Mohler, K.E. Browman, V.A. Roderwald, E.A. Cronin, S. Markosyan, R. Scott Bitner, M.I. Strakhova, K.U. Drescher, W. Hornberger, J.J. Rohde, M.E. Brune, P.B. Jacobson, L.E. Rueter, Acute inhibition of 11 β -hydroxysteroid dehydrogenase type-1 improves memory in rodent models of cognition, *J. Neurosci.* 31 (2011) 5406–5413.
- [73] K. Sooy, J. Noble, A. McBride, M. Binnie, J.L. Yau, J.R. Seckl, B.R. Walker, S.P. Webster, Cognitive and disease-modifying effects of 11 β -hydroxysteroid dehydrogenase type 1 inhibition in male tg2576 mice, a model of alzheimer's disease, *Endocrinology* 156 (2015) 4592–4603.
- [74] J.S. Scott, F.W. Goldberg, A.V. Turnbull, Medicinal chemistry of inhibitors of 11 β -hydroxysteroid dehydrogenase type 1 (11(-HSD1)), *J. Med. Chem.* 57 (2014) 4466–4486.
- [75] M.P. Thomas, B.V. Potter, Crystal structures of 11 β -hydroxysteroid dehydrogenase type 1 and their use in drug discovery, *Future Med. Chem.* 3 (2011) 367–390.
- [76] D. Schuster, E.M. Maurer, C. Laggner, L.G. Nashev, T. Wilckens, T. Langer, A. Odermatt, The discovery of new 11 β -hydroxysteroid dehydrogenase type 1 inhibitors by common feature pharmacophore modeling and virtual screening, *J. Med. Chem.* 49 (2006) 3454–3466.
- [77] S. Arampatzis, B. Kadereit, D. Schuster, Z. Balazs, R.A. Schweizer, F.J. Frey, T. Langer, A. Odermatt, Comparative enzymology of 11 β -hydroxysteroid dehydrogenase type 1 from six species, *J. Mol. Endocrinol.* 35 (2005) 89–101.
- [78] T. Barf, J. Vallgarda, R. Emond, C. Haggstrom, G. Kurz, A. Nygren, V. Larwood, E. Mosialou, K. Axelsson, R. Olsson, L. Engblom, N. Edling, Y. Ronquist-Nii, B. Ohman, P. Alberts, L. Abrahmsen, Arylsulfonamidothiazoles as a new class of potential antidiabetic drugs. Discovery of potent and selective inhibitors of the 11 β -hydroxysteroid dehydrogenase type 1, *J. Med. Chem.* 45 (2002) 3813–3815.
- [79] M. Hult, N. Shafqat, B. Elleby, D. Mitschke, S. Svensson, M. Forsgren, T. Barf, J. Vallgarda, L. Abrahmsen, U. Oppermann, Active site variability of type 1 11 β -hydroxysteroid dehydrogenase revealed by selective inhibitors and cross-species comparisons, *Mol. Cell. Endocrinol.* 248 (2006) 26–33.
- [80] S. Hofer, D.V. Kratschmar, B. Scherthanner, A. Vuorinen, D. Schuster, A. Odermatt, J. Easmon, Synthesis and biological analysis of benzazol-2-yl piperazine sulfonamides as 11 β -hydroxysteroid dehydrogenase 1 inhibitors, *Bioorg. Med. Chem. Lett.* 23 (2013) 5397–5400.
- [81] J.M. Rollinger, D.V. Kratschmar, D. Schuster, P.H. Pfisterer, C. Gummy, E.M. Aubry, S. Brandstötter, H. Stuppner, G. Wolber, A. Odermatt, 11 β -hydroxysteroid dehydrogenase 1 inhibiting constituents from *Eriobotrya japonica* revealed by bioactivity-guided isolation and computational approaches, *Bioorg. Med. Chem.* 18 (2010) 1507–1515.
- [82] C. Gummy, C. Thurnbichler, E.M. Aubry, Z. Balazs, P. Pfisterer, L. Baumgartner, H. Stuppner, A. Odermatt, J.M. Rollinger, Inhibition of 11 β -hydroxysteroid dehydrogenase type 1 by plant extracts used as traditional antidiabetic medicines, *Fitoterapia* 80 (2009) 200–205.
- [83] A. Vuorinen, L.G. Nashev, A. Odermatt, J.M. Rollinger, D. Schuster, Pharmacophore model refinement for 11 β -hydroxysteroid dehydrogenase inhibitors: search for modulators of intracellular glucocorticoid concentrations, *Mol. Inf.* 33 (2014) 15–25.
- [84] A. Vuorinen, J. Seibert, V.P. Papageorgiou, J.M. Rollinger, A. Odermatt, D. Schuster, A.N. Assimopoulou, Pistacia lentiscus oleoresin: virtual screening and identification of masticadienonic and isomasticadienonic acids as inhibitors of 11 β -hydroxysteroid dehydrogenase 1, *Planta Med.* 81 (2015) 525–532.
- [85] L. Miguez, Z. Zhang, M. Barbier, M.G. Grigorov, Comparison of a homology model and the crystallographic structure of human 11 β -hydroxysteroid dehydrogenase type 1 (11HSD1) in a structure-based identification of inhibitors, *J. Comput.-Aided Mol. Des.* 20 (2006) 67–81.
- [86] H. Yang, W. Dou, J. Lou, Y. Leng, J. Shen, Discovery of novel inhibitors of 11 β -hydroxysteroid dehydrogenase type 1 by docking and pharmacophore modeling, *Bioorg. Med. Chem. Lett.* 18 (2008) 1340–1345.
- [87] H. Yang, Y. Shen, J. Chen, Q. Jiang, Y. Leng, J. Shen, Structure-based virtual screening for identification of novel 11(-HSD1) inhibitors, *Eur. J. Med. Chem.* 44 (2009) 1167–1171.
- [88] G. Xia, M. Xue, L. Liu, J. Yu, H. Liu, P. Li, J. Wang, Y. Li, B. Xiong, J. Shen, Potent and novel 11(-HSD1) inhibitors identified from shape and docking based virtual screening, *Bioorg. Med. Chem. Lett.* 21 (2011) 5739–5744.
- [89] K. Aertgeerts, N. Brennan, S.X. Cao, E. Chang, A.A. Kiryanov, Y. Liu, Arylsulfonylpiperazines and Related Compounds as Hydroxysteroid Dehydrogenase Inhibitors and Their Preparation and Pharmaceutical Compositions, Takeda San Diego, Inc., USA, 2006.
- [90] J.S. Xiang, E. Saiah, S.Y. Tam, J.C. Mckew, L. Chen, M. Ipek, K. Lee, H.-Q. Li, J. Li, W. Li, T.S. Mansour, V. Suri, R. Vargas, Y. Wu, Z.-K. Wan, J. Lee, E. Binnun, D.P. Wilson, Sulfonlated Piperidine and Piperazine Derivatives as 11 β -HSD1 Inhibitors and Their Preparation, Pharmaceutical Compositions and Use in the Treatment of Diseases, Wyeth, John, and Brother Ltd., USA, 2007.
- [91] P.W.R. Caulkett, W. McCoull, M. Packer, P.R.O. Whittamore, Preparation of 1,4-disubstituted Piperazine or Diazepane Derivatives as 11 β -hydroxysteroid Dehydrogenase 1 Inhibitors, AstraZeneca AB, AstraZeneca UK Limited, Swed, 2007.
- [92] G. Xia, L. Liu, M. Xue, H. Liu, J. Yu, P. Li, Q. Chen, B. Xiong, X. Liu, J. Shen, Discovery of novel sulfonamides as potent and selective inhibitors against human and mouse 11 β -hydroxysteroid dehydrogenase type 1, *Mol. Cell. Endocrinol.* 358 (2012) 46–52.
- [93] C.F. Lagos, A. Vecchiola, F. Allende, C.A. Fuentes, J.E. Tichauer, C. Valdivia, S. Solari, C. Campino, A. Tapia-Castillo, R. Baudrand, P. Villarreal, M. Cifuentes, G. I. Owen, C.A. Carvajal, C.E. Fardella, Identification of novel 11(-HSD1) inhibitors by combined ligand- and structure-based virtual screening, *Mol. Cell. Endocrinol.* 384 (2014) 71–82.
- [94] E.R. Hugo, T.D. Brandebourg, C.E. Comstock, K.S. Gersin, J.J. Sussman, N. Ben-Jonathan, LS14: a novel human adipocyte cell line that produces prolactin, *Endocrinology* 147 (2006) 306–313.
- [95] S. Shave, E.A. Blackburn, J. Adie, D.R. Houston, M. Auer, S.P. Webster, P. Taylor, M.D. Walkinshaw, UFSRAT: ultra-fast Shape Recognition with Atom Types-the discovery of novel bioactive small molecular scaffolds for FKBP12 and 11 β HSD1, *PLoS One* 10 (2015) e0116570.
- [96] C.D. Boyle, T.J. Kowalski, 11 β -hydroxysteroid dehydrogenase type 1 inhibitors: a review of recent patents, *Expert Opin. Ther. Pat.* 19 (2009) 801–825.
- [97] C.M. Tice, W. Zhao, Z. Xu, S.T. Cacatian, R.D. Simpson, Y.J. Ye, S.B. Singh, B.M. McKeever, P. Lindblom, J. Guo, P.M. Krosky, B.A. Kruk, J. Berbaum, R.K. Harrison, J.J. Johnson, Y. Bukhtiyarov, R. Panemangalore, B.B. Scott, Y. Zhao, J. G. Bruno, L. Zhuang, G.M. McGeehan, W. He, D.A. Claremon, Spirocyclic ureas: orally bioavailable 11 β -HSD1 inhibitors identified by computer-aided drug design, *Bioorg. Med. Chem. Lett.* 20 (2010) 881–886.
- [98] Z. Xu, C.M. Tice, W. Zhao, S. Cacatian, Y.J. Ye, S.B. Singh, P. Lindblom, B.M. McKeever, P.M. Krosky, B.A. Kruk, J. Berbaum, R.K. Harrison, J.A. Johnson, Y. Bukhtiyarov, R. Panemangalore, B.B. Scott, Y. Zhao, J.G. Bruno, J. Togias, J. Guo, R. Guo, P.J. Carroll, G.M. McGeehan, L. Zhuang, W. He, D.A. Claremon, Structure-based design and synthesis of 1, 3-oxazinan-2-one inhibitors of 11 β -hydroxysteroid dehydrogenase type 1, *J. Med. Chem.* 54 (2011) 6050–6062.
- [99] B.S. Hamilton, F. Himmelsbach, H. Nar, A. Schuler-Metz, P. Krosky, J. Guo, R. Guo, S. Meng, Y. Zhao, D.S. Lala, L. Zhuang, D.A. Claremon, G.M. McGeehan, Pharmacological characterization of the selective 11 β -hydroxysteroid dehydrogenase 1 inhibitor, BI 135585, a clinical candidate for the treatment of type 2 diabetes, *Eur. J. Pharmacol.* 746 (2015) 50–55.
- [100] F. Lepifre, S. Christmann-Franck, D. Roche, C. Leriche, D. Carniato, C. Charon, S. Bozec, L. Doare, F. Schmidlin, M. Lecomte, E. Valeur, Discovery and structure-guided drug design of inhibitors of 11 β -hydroxysteroid-dehydrogenase type I based on a spiro-carboxamide scaffold, *Bioorg. Med. Chem. Lett.* 19 (2009) 3682–3685.
- [101] E. Valeur, S. Christmann-Franck, F. Lepifre, D. Carniato, D. Cravo, C. Charon, S. Bozec, D. Musil, P. Hillertz, L. Doare, F. Schmidlin, M. Lecomte, M. Schultz, D. Roche, Structure-based design of 7-azaindole-pyrrolidine amides as inhibitors of 11 β -hydroxysteroid dehydrogenase type I, *Bioorg. Med. Chem. Lett.* 22 (2012) 5909–5914.
- [102] G. Xia, X. You, L. Liu, H. Liu, J. Wang, Y. Shi, P. Li, B. Xiong, X. Liu, J. Shen, Design, synthesis and SAR of piperidyl-oxadiazoles as 11 β -hydroxysteroid dehydrogenase 1 inhibitors, *Eur. J. Med. Chem.* 62 (2013) 1–10.
- [103] S.P. Hong, K.Y. Nam, Y.J. Shin, K.W. Kim, S.K. Ahn, Discovery of 11 β -hydroxysteroid dehydrogenase type 1 inhibitor, *Bioorg. Med. Chem. Lett.* 25 (2015) 3501–3506.

- [104] Y. Lee, Y.J. Shin, S.K. Ahn, 3-Amino -N-adamantyl -3-methylbutanamide derivatives as 11 β -hydroxysteroid dehydrogenase 1 inhibitor, *Bioorg. Med. Chem. Lett.* 24 (2014) 1421–1425.
- [105] N. Vicker, X. Su, D. Ganeshapillai, A. Smith, A. Purohit, M.J. Reed, B.V. Potter, Novel non-steroidal inhibitors of human 11 β -hydroxysteroid dehydrogenase type 1, *J. Steroid Biochem. Mol. Biol.* 104 (2007) 123–129.
- [106] X.Y. Ye, D. Yoon, S.Y. Chen, A. Nayeem, R. Golla, R. Seethala, M. Wang, T. Harper, B.G. Slecza, A. Apedo, Y.X. Li, B. He, M. Kirby, D.A. Gordon, J.A. Robl, Synthesis and structure-activity relationship of 2-adamantylmethyl tetrazoles as potent and selective inhibitors of human 11 β -hydroxysteroid dehydrogenase type 1 (11 β -HSD1), *Bioorg. Med. Chem. Lett.* 24 (2014) 654–660.
- [107] A. Blum, A.D. Favia, E. Maser, 11 β -hydroxysteroid dehydrogenase type 1 inhibitors with oleanan and ursan scaffolds, *Mol. Cell. Endocrinol.* 301 (2009) 132–136.
- [108] X. Su, H.A. Halem, M.P. Thomas, C. Moutrille, M.D. Culler, N. Vicker, B.V. Potter, Adamantyl carboxamides and acetamides as potent human 11 β -hydroxysteroid dehydrogenase type 1 inhibitors, *Bioorg. Med. Chem.* 20 (2012) 6394–6402.
- [109] G. Moeller, J. Adamski, Integrated view on 17 β -hydroxysteroid dehydrogenases, *Mol. Cell. Endocrinol.* 301 (2009) 7–19.
- [110] D. Poirier, Inhibitors of 17 β -hydroxysteroid dehydrogenases, *Curr. Med. Chem.* 10 (2003) 453–477.
- [111] P. Lukacik, K.L. Kavanagh, U. Oppermann, Structure and function of human 17 β -hydroxysteroid dehydrogenases, *Mol. Cell. Endocrinol.* 248 (2006) 61–71.
- [112] A. Jansson, 17 β -hydroxysteroid dehydrogenase enzymes and breast cancer, *J. Steroid Biochem. Mol. Biol.* 114 (2009) 64–67.
- [113] O.O. Oduwole, Y. Li, V.V. Isomaa, A. Mantyniemi, A.E. Pulkka, Y. Soini, P.T. Viikko, 17 β -hydroxysteroid dehydrogenase type 1 is an independent prognostic marker in breast cancer, *Cancer Res.* 64 (2004) 7604–7609.
- [114] Y. Miyoshi, A. Ando, E. Shiba, T. Taguchi, Y. Tamaki, S. Noguchi, Involvement of up-regulation of 17 β -hydroxysteroid dehydrogenase type 1 in maintenance of intratumoral high estradiol levels in postmenopausal breast cancers, *Int. J. Cancer* 94 (2001) 685–689.
- [115] B. Husen, K. Huhtinen, M. Poutanen, L. Kangas, J. Messinger, H. Thole, Evaluation of inhibitors for 17 β -hydroxysteroid dehydrogenase type 1 in vivo in immunodeficient mice inoculated with MCF-7 cells stably expressing the recombinant human enzyme, *Mol. Cell. Endocrinol.* 248 (2006) 109–113.
- [116] D. Ayan, R. Maltais, J. Roy, D. Poirier, A new nonestrogenic steroidal inhibitor of 17 β -hydroxysteroid dehydrogenase type 1 blocks the estrogen-dependent breast cancer tumor growth induced by estrone, *Mol. Cancer Ther.* 11 (2012) 2096–2104.
- [117] T. Smuc, M.R. Pucelj, J. Sinkovec, B. Husen, H. Thole, T.L. Rizner, Expression analysis of the genes involved in estradiol and progesterone action in human ovarian endometriosis, *Gynecol. Endocrinol.* 23 (2007) 105–111.
- [118] B. Delvoux, T.D. Hooghe, C. Kyama, P. Koskimies, R.J. Hermans, G.A. Dunselman, A. Romano, Inhibition of type 1 17 β -hydroxysteroid dehydrogenase impairs the synthesis of 17 β -estradiol in endometriosis lesions, *J. Clin. Endocrinol. Metab.* 99 (2014) 276–284.
- [119] K.M. Cornel, R.F. Kruitwagen, B. Delvoux, L. Visconti, K.K. Van de Vijver, J.M. Day, T. Van Gorp, R.J. Hermans, G.A. Dunselman, A. Romano, Overexpression of 17 β -hydroxysteroid dehydrogenase type 1 increases the exposure of endometrial cancer to 17 β -estradiol, *J. Clin. Endocrinol. Metab.* 97 (2012) E591–601.
- [120] T. Kasai, M. Shozu, K. Murakami, T. Segawa, K. Shinohara, K. Nomura, M. Inoue, Increased expression of type 1 17 β -hydroxysteroid dehydrogenase enhances in situ production of estradiol in uterine leiomyoma, *J. Clin. Endocrinol. Metab.* 89 (2004) 5661–5668.
- [121] E. Bey, S. Marchais-Oberwinkler, P. Kruchten, M. Frotscher, R. Werth, A. Oster, O. Algül, A. Neugebauer, R.W. Hartmann, Design, synthesis and biological evaluation of bis(hydroxyphenyl) azoles as potent and selective non-steroidal inhibitors of 17 β -hydroxysteroid dehydrogenase type 1 (17 β -HSD1) for the treatment of estrogen-dependent diseases, *Bioorg. Med. Chem.* 16 (2008) 6423–6435.
- [122] A.M. Hoffren, C.M. Murray, R.D. Hoffmann, Structure-based focusing using pharmacophores derived from the active site of 17 β -hydroxysteroid dehydrogenase, *Curr. Pharm. Des.* 7 (2001) 547–566.
- [123] A. Krazeisen, R. Breitling, G. Moller, J. Adamski, Phytoestrogens inhibit human 17 β -hydroxysteroid dehydrogenase type 5, *Mol. Cell. Endocrinol.* 171 (2001) 151–162.
- [124] N. Chanplakorn, P. Chanplakorn, T. Suzuki, K. Ono, M.S.M. Chan, Y. Miki, S. Saji, T. Ueno, M. Toi, H. Sasano, Increased estrogen sulfatase (STS) and 17 β -hydroxysteroid dehydrogenase type 1 (17 β -HSD1) following neoadjuvant aromatase inhibitor therapy in breast cancer patients, *Breast Cancer Res. Treat.* 120 (2010) 639–648.
- [125] L.W. Woo, O.B. Sutcliffe, C. Bubert, A. Grasso, S.K. Chander, A. Purohit, M.J. Reed, B.V. Potter, First dual aromatase-steroid sulfatase inhibitors, *J. Med. Chem.* 46 (2003) 3193–3196.
- [126] L.W. Woo, C. Bubert, O.B. Sutcliffe, A. Smith, S.K. Chander, M.F. Mahon, A. Purohit, M.J. Reed, B.V. Potter, Dual aromatase-steroid sulfatase inhibitors, *J. Med. Chem.* 50 (2007) 3540–3560.
- [127] M.P. Thomas, B.V. Potter, Discovery and development of the aryl O-Sulfamate pharmacophore for oncology and women's health, *J. Med. Chem.* 58 (2015) 7634–7658.
- [128] L.W. Woo, T. Jackson, A. Putey, G. Cozier, P. Leonard, K.R. Acharya, S.K. Chander, A. Purohit, M.J. Reed, B.V. Potter, Highly potent first examples of dual aromatase-steroid sulfatase inhibitors based on a biphenyl template, *J. Med. Chem.* 53 (2010) 2155–2170.
- [129] M. Berube, D. Poirier, Synthesis of simplified hybrid inhibitors of type 1 17 β -hydroxysteroid dehydrogenase via cross-metathesis and songashira coupling reactions, *Org. Lett.* 6 (2004) 3127–3130.
- [130] D. Fournier, D. Poirier, M. Mazumdar, S.X. Lin, Design and synthesis of bisubstrate inhibitors of type 1 17 β -hydroxysteroid dehydrogenase: overview and perspectives, *Eur. J. Med. Chem.* 43 (2008) 2298–2306.
- [131] D. Schuster, L.G. Nashev, J. Kirchmair, C. Laggner, G. Wolber, T. Langer, A. Odermatt, Discovery of nonsteroidal 17 β -hydroxysteroid dehydrogenase 1 inhibitors by pharmacophore-based screening of virtual compound libraries, *J. Med. Chem.* 51 (2008) 4188–4199.
- [132] W.M. Brown, L.E. Metzger, J.P. Barlow, L.A. Hunsaker, L.M. Deck, R.E. Royer, D.L. Vander Jagt, 17 β -Hydroxysteroid dehydrogenase type 1: Computational design of active site inhibitors targeted to the Rossmann fold, *Chem.-Biol. Interact.* 143–144 (2003) 481–491.
- [133] G.X. Hu, H.Y. Zhou, X.W. Li, B.B. Chen, Y.C. Xiao, Q.Q. Lian, G. Liang, H.H. Kim, Z. Q. Zheng, D.O. Hardy, R.S. Ge, The (+) and (–) gossypols potently inhibit both 3 β -hydroxysteroid dehydrogenase and 17 β -hydroxysteroid dehydrogenase 3 in human and rat testes, *J. Steroid Biochem. Mol. Biol.* 115 (2009) 14–19.
- [134] B.B. Chen, H. Lin, G.X. Hu, Y. Su, H.Y. Zhou, Q.Q. Lian, H. Cai, D.O. Hardy, D.Y. Gu, R.S. Ge, The (+) and (–) gossypols potently inhibit human and rat 11 β -hydroxysteroid dehydrogenase type 2, *J. Steroid Biochem. Mol. Biol.* 113 (2009) 177–181.
- [135] A. Spadaro, M. Negri, S. Marchais-Oberwinkler, E. Bey, M. Frotscher, Hydroxybenzothiazoles as new nonsteroidal inhibitors of 17 β -hydroxysteroid dehydrogenase type 1 (17 β -HSD1), *PLoS One* 7 (2012) e29252.
- [136] A. Spadaro, M. Frotscher, R.W. Hartmann, Optimization of hydroxybenzothiazoles as novel potent and selective inhibitors of 17 β -HSD1, *J. Med. Chem.* 55 (2012) 2469–2473.
- [137] S. Karkola, S. Alho-Richmond, K. Wahala, Pharmacophore modelling of 17 β -HSD1 enzyme based on active inhibitors and enzyme structure, *Mol. Cell. Endocrinol.* 301 (2009) 225–228.
- [138] S. Starcevic, S. Turk, B. Brus, J. Cesar, T. Lanisnik Rizner, S. Gobec, Discovery of highly potent, nonsteroidal 17 β -hydroxysteroid dehydrogenase type 1 inhibitors by virtual high-throughput screening, *J. Steroid Biochem. Mol. Biol.* 127 (2011) 255–261.
- [139] M. Frotscher, E. Ziegler, S. Marchais-Oberwinkler, P. Kruchten, A. Neugebauer, L. Fetzer, C. Scherer, U. Muller-Vieira, J. Messinger, H. Thole, R.W. Hartmann, Design, synthesis, and biological evaluation of (hydroxyphenyl)naphthalene and -quinoline derivatives: potent and selective nonsteroidal inhibitors of 17 β -hydroxysteroid dehydrogenase type 1 (17 β -HSD1) for the treatment of estrogen-dependent diseases, *J. Med. Chem.* 51 (2008) 2158–2169.
- [140] S. Marchais-Oberwinkler, P. Kruchten, M. Frotscher, E. Ziegler, A. Neugebauer, U. Bhoga, E. Bey, U. Muller-Vieira, J. Messinger, H. Thole, R.W. Hartmann, Substituted 6-phenyl-2-naphthols, Potent and selective nonsteroidal inhibitors of 17 β -hydroxysteroid dehydrogenase type 1 (17 β -HSD1): design, synthesis, biological evaluation, and pharmacokinetics, *J. Med. Chem.* 51 (2008) 4685–4698.
- [141] S. Marchais-Oberwinkler, M. Frotscher, E. Ziegler, R. Werth, P. Kruchten, J. Messinger, H. Thole, R.W. Hartmann, Structure-activity study in the class of 6-(3'-hydroxyphenyl)naphthalenes leading to an optimization of a pharmacophore model for 17 β -hydroxysteroid dehydrogenase type 1 (17 β -HSD1) inhibitors, *Mol. Cell. Endocrinol.* 301 (2009) 205–211.
- [142] E. Bey, S. Marchais-Oberwinkler, R. Werth, M. Negri, Y.A. Al-Soud, P. Kruchten, A. Oster, M. Frotscher, B. Birk, R.W. Hartmann, Design, synthesis, biological evaluation and pharmacokinetics of bis(hydroxyphenyl) substituted azoles, thiophenes, benzenes, and aza-benzenes as potent and selective nonsteroidal inhibitors of 17 β -hydroxysteroid dehydrogenase type 1 (17 β -HSD1), *J. Med. Chem.* 51 (2008) 6725–6739.
- [143] G. Moller, D. Deluca, C. Gege, A. Rosinus, D. Kowalik, O. Peters, P. Droscher, W. Elger, J. Adamski, A. Hillisch, Structure-based design, synthesis and in vitro characterization of potent 17 β -hydroxysteroid dehydrogenase type 1 inhibitors based on 2-substitutions of estrone and D-homo-estrone, *Bioorg. Med. Chem. Lett.* 19 (2009) 6740–6744.
- [144] J. Messinger, L. Hirvela, B. Husen, L. Kangas, P. Koskimies, O. Pentikainen, P. Saarenketo, H. Thole, New inhibitors of 17 β -hydroxysteroid dehydrogenase type 1, *Mol. Cell. Endocrinol.* 248 (2006) 192–198.
- [145] D. Schuster, M. Spetea, M. Music, S. Rief, M. Fink, J. Kirchmair, J. Schütz, G. Wolber, T. Langer, H. Stuppner, H. Schmidhammer, J.M. Rollinger, Morphinans and isoquinolines: acetylcholinesterase inhibition, pharmacophore modeling, and interaction with opioid receptors, *Bioorg. Med. Chem.* 18 (2010) 5071–5080.
- [146] L. Wu, M. Einstein, W.M. Geissler, H.K. Chan, K.O. Elliston, S. Andersson, Expression cloning and characterization of human 17 β -hydroxysteroid dehydrogenase type 2, a microsomal enzyme possessing 20 α -hydroxysteroid dehydrogenase activity, *J. Biol. Chem.* 268 (1993) 12964–12969.
- [147] T.J. Puranen, R.M. Kurkela, J.T. Lakkakorpi, M.H. Poutanen, P.V. Itaranta, J.P. Melis, D. Ghosh, R.K. Vihko, P.T. Viikko, Characterization of molecular and catalytic properties of intact and truncated human 17 β -hydroxysteroid dehydrogenase type 2 enzymes: intracellular localization of the wild-type enzyme in the endoplasmic reticulum, *Endocrinology* 140 (1999) 3334–3341.

- [148] Y. Dong, Q.Q. Qiu, J. Debear, W.F. Lathrop, D.R. Bertolini, P.P. Tamburini, 17 β -hydroxysteroid dehydrogenases in human bone cells, *J. Bone Miner. Res.* 13 (1998) 1539–1546.
- [149] P. Vihko, V. Isomaa, D. Ghosh, Structure and function of 17 β -hydroxysteroid dehydrogenase type 1 and type 2, *Mol. Cell. Endocrinol.* 171 (2001) 71–76.
- [150] H. Michael, P.L. Harkonen, H.K. Vaananen, T.A. Hentunen, Estrogen and testosterone use different cellular pathways to inhibit osteoclastogenesis and bone resorption, *J. Bone Miner. Res.* 20 (2005) 2224–2232.
- [151] J.A. Kanis, E.V. McCloskey, H. Johansson, C. Cooper, R. Rizzoli, J.Y. Reginster, European guidance for the diagnosis and management of osteoporosis in postmenopausal women, *Osteoporosis Int.* 24 (2013) 23–57.
- [152] C.M. Bagi, J. Wood, D. Wilkie, B. Dixon, Effect of 17 β -hydroxysteroid dehydrogenase type 2 inhibitor on bone strength in ovariectomized cynomolgus monkeys, *J. Musculoskeletal Neuronal Interact.* 8 (2008) 267–280.
- [153] A. Vuorinen, R. Engeli, A. Meyer, F. Bachmann, U.J. Griesser, D. Schuster, A. Odermatt, Ligand-based pharmacophore modeling and virtual screening for the discovery of novel 17 β -hydroxysteroid dehydrogenase 2 inhibitors, *J. Med. Chem.* 57 (2014) 5995–6007.
- [154] M. Wetzel, E.M. Gargano, S. Hinsberger, S. Marchais-Oberwinkler, R.W. Hartmann, Discovery of a new class of bicyclic substituted hydroxyphenylmethanones as 17 β -hydroxysteroid dehydrogenase type 2 (17 β -HSD2) inhibitors for the treatment of osteoporosis, *Eur. J. Med. Chem.* 47 (2012) 1–17.
- [155] A. Oster, S. Hinsberger, R. Werth, S. Marchais-Oberwinkler, M. Frotscher, R.W. Hartmann, Bicyclic substituted hydroxyphenylmethanones as novel inhibitors of 17 β -hydroxysteroid dehydrogenase type 1 (17 β -HSD1) for the treatment of estrogen-dependent diseases, *J. Med. Chem.* 53 (2010) 8176–8186.
- [156] W.M. Geissler, D.L. Davis, L. Wu, K.D. Bradshaw, S. Patel, B.B. Mendonca, K.O. Elington, J.D. Wilson, D.W. Russell, S. Andersson, Male pseudohermaphroditism caused by mutations of testicular 17 β -hydroxysteroid dehydrogenase 3, *Nat. Genet.* 7 (1994) 34–39.
- [157] A.L. Boehmer, A.O. Brinkmann, L.A. Sandkuijl, D.J. Halley, M.F. Niermeijer, S. Andersson, F.H. de Jong, H. Kayserili, M.A. de Vroede, B.J. Otten, C.W. Rouwe, B.B. Mendonca, C. Rodrigues, H.H. Bode, P.E. de Ruiter, H.A. Delemarre-van de Waal, S.L. Drop, 17 β -hydroxysteroid dehydrogenase-3 deficiency: diagnosis, phenotypic variability, population genetics, and worldwide distribution of ancient and de novo mutations, *J. Clin. Endocrinol. Metab.* 84 (1999) 4713–4721.
- [158] N. Phelan, E.L. Williams, S. Cardamone, M. Lee, S.M. Creighton, G. Rumsby, G.S. Conway, Screening for mutations in 17 β -hydroxysteroid dehydrogenase and androgen receptor in women presenting with partially virilized 46, XY disorders of sex development, *Eur. J. Endocrinol.* 172 (2015) 745–751.
- [159] J. Chuang, A. Vallerie, L. Breech, H.M. Saal, S. Alam, P. Crawford, M.M. Rutter, Complexities of gender assignment in 17 β -hydroxysteroid dehydrogenase type 3 deficiency: is there a role for early orchiectomy? *Int. J. Pediatr. Endocrinol.* 2013 (2013) 15.
- [160] E. Koh, T. Noda, J. Kanaya, M. Namiki, Differential expression of 17 β -hydroxysteroid dehydrogenase isozyme genes in prostate cancer and noncancer tissues, *Prostate* 53 (2002) 154–159.
- [161] J.M. Day, P.A. Foster, H.J. Tutill, F. Schmidlin, C.M. Sharland, J.D. Hargrave, N. Vicker, B.V. Potter, M.J. Reed, A. Purohit, STX2171, a 17 β -hydroxysteroid dehydrogenase type 3 inhibitor, is efficacious in vivo in a novel hormone-dependent prostate cancer model, *Endocr.-Relat. Cancer* 20 (2013) 53–64.
- [162] A.R. Hamid, M.J. Pfeiffer, G.W. Verhaegh, E. Schaafsma, A. Brandt, F.C. Sweep, J.P. Sedelaar, J.A. Schalken, Aldo-keto reductase family 1 member C3 (AKR1C3) is a biomarker and therapeutic target for castration-resistant prostate cancer, *Mol. Med.* 18 (2012) 1449–1455.
- [163] T.M. Penning, M.E. Burczynski, J.M. Jez, H.K. Lin, H. Ma, M. Moore, K. Ratnam, N. Palackal, Structure-function aspects and inhibitor design of type 5 17 β -hydroxysteroid dehydrogenase (AKR1C3), *Mol. Cell. Endocrinol.* 171 (2001) 137–149.
- [164] B. Legeza, Z. Balazs, L.G. Nashev, A. Odermatt, The microsomal enzyme 17 β -hydroxysteroid dehydrogenase 3 faces the cytoplasm and uses NADPH generated by glucose-6-phosphate dehydrogenase, *Endocrinology* 154 (2013) 205–213.
- [165] M. Tsachaki, J. Birk, A. Egert, A. Odermatt, Determination of the topology of endoplasmic reticulum membrane proteins using redox-sensitive green-fluorescence protein fusions, *Biochim. Biophys. Acta* 1853 (2015) 1672–1682.
- [166] N. Vicker, C.M. Sharland, W.B. Heaton, A.M. Gonzalez, H.V. Bailey, A. Smith, J.S. Springall, J.M. Day, H.J. Tutill, M.J. Reed, A. Purohit, B.V. Potter, The design of novel 17 β -hydroxysteroid dehydrogenase type 3 inhibitors, *Mol. Cell. Endocrinol.* 301 (2009) 259–265.
- [167] D. Schuster, D. Kowalik, J. Kirchmair, C. Laggner, P. Markt, C. Aebischer-Gumy, F. Strohle, G. Moller, G. Wolber, T. Wilckens, T. Langer, A. Odermatt, J. Adamski, Identification of chemically diverse, novel inhibitors of 17 β -hydroxysteroid dehydrogenase type 3 and 5 by pharmacophore-based virtual screening, *J. Steroid Biochem. Mol. Biol.* 125 (2011) 148–161.
- [168] X.Y. He, G. Merz, Y.Z. Yang, P. Mehta, H. Schulz, S.Y. Yang, Characterization and localization of human type 10 17 β -hydroxysteroid dehydrogenase, *Eur. J. Biochem.* 268 (2001) 4899–4907.
- [169] X.Y. He, G. Merz, Y.Z. Yang, R. Pullarkat, P. Mehta, H. Schulz, S.Y. Yang, Function of human brain short chain L-3-hydroxyacyl coenzyme A dehydrogenase in androgen metabolism, *Biochim. Biophys. Acta* 1484 (2000) 267–277.
- [170] S.Y. Yang, X.Y. He, D. Miller, Hydroxysteroid (17 β) dehydrogenase X in human health and disease, *Mol. Cell. Endocrinol.* 343 (2011) 1–6.
- [171] J.W. Lustbader, M. Cirilli, C. Lin, H.W. Xu, K. Takuma, N. Wang, C. Caspersen, X. Chen, S. Pollak, M. Chaney, F. Trinchese, S. Liu, F. Gunn-Moore, L.F. Lue, D.G. Walker, P. Kuppasamy, Z.L. Zewier, O. Arancio, D. Stern, S.S. Yan, H. Wu, ABAD directly links Abeta to mitochondrial toxicity in Alzheimer's disease, *Science* 304 (2004) 448–452.
- [172] C.R. Kissinger, P.A. Rejto, L.A. Pelletier, J.A. Thomson, R.E. Showalter, M.A. Abreo, C.S. Agree, S. Margosiak, J.J. Meng, R.M. Aust, D. Vanderpool, B. Li, A. Tempczyk-Russell, J.E. Villafranca, Crystal structure of human ABAD/HSD10 with a bound inhibitor: implications for design of Alzheimer's disease therapeutics, *J. Mol. Biol.* 342 (2004) 943–952.
- [173] V. Jazbutyte, F. Kehl, L. Neyses, T. Pelzer, Estrogen receptor alpha interacts with 17 β -hydroxysteroid dehydrogenase type 10 in mitochondria, *Biochem. Biophys. Res. Commun.* 384 (2009) 450–454.
- [174] X.Y. He, J. Wegiel, Y.Z. Yang, R. Pullarkat, H. Schulz, S.Y. Yang, Type 10 17 β -hydroxysteroid dehydrogenase catalyzing the oxidation of steroid modulators of gamma-aminobutyric acid type A receptors, *Mol. Cell. Endocrinol.* 229 (2005) 111–117.
- [175] E. Nordling, U.C. Oppermann, H. Jornvall, B. Persson, Human type 10 17 β -hydroxysteroid dehydrogenase: molecular modelling and substrate docking, *J. Mol. Graph. Model.* 19 (2001) 514–520 (591–513).
- [176] N. Shafiqat, H.U. Marschall, C. Filling, E. Nordling, X.Q. Wu, L. Bjork, J. Thyberg, E. Martensson, S. Salim, H. Jornvall, U. Oppermann, Expanded substrate screenings of human and *Drosophila* type 10 17 β -hydroxysteroid dehydrogenases (HSDs) reveal multiple specificities in bile acid and steroid hormone metabolism: characterization of multifunctional 3 α /7 α /7 β /17 β /20 β /21-HSD, *Biochem. J.* 376 (2003) 49–60.
- [177] A.J. Powell, J.A. Read, M.J. Banfield, F. Gunn-Moore, S.D. Yan, J. Lustbader, A.R. Stern, D.M. Stern, R.L. Brady, Recognition of structurally diverse substrates by type II 3-hydroxyacyl-CoA dehydrogenase (HADH II)/amyloid-beta binding alcohol dehydrogenase (ABAD), *J. Mol. Biol.* 303 (2000) 311–327.
- [178] N. Tanaka, T. Nonaka, T. Tanabe, T. Yoshimoto, D. Tsuru, Y. Mitsui, Crystal structures of the binary and ternary complexes of 7 β -hydroxysteroid dehydrogenase from *Escherichia coli*, *Biochemistry* 35 (1996) 7715–7730.
- [179] P. Lukacik, B. Keller, G. Bunkoczi, K.L. Kavanagh, W.H. Lee, J. Adamski, U. Oppermann, Structural and biochemical characterization of human orphan DHRS10 reveals a novel cytosolic enzyme with steroid dehydrogenase activity, *Biochem. J.* 402 (2007) 419–427.
- [180] T. Sivik, S. Vikingson, H. Green, A. Jansson, Expression patterns of 17 β -hydroxysteroid dehydrogenase 14 in human tissues, *Horm. Metab. Res.* 44 (2012) 949–956.
- [181] N. Bertoletti, F. Braun, M. Lepage, G. Moller, J. Adamski, A. Heine, G. Klebe, S. Marchais-Oberwinkler, New insights into human 17 β -Hydroxysteroid dehydrogenase type 14: first crystal structures in complex with a steroidal ligand and with a potent nonsteroidal inhibitor, *J. Med. Chem.* 59 (2016) 6961–6967.
- [182] F. Braun, N. Bertoletti, G. Moller, J. Adamski, T. Steinmetzer, M. Salah, A.S. Abdelsamie, C.J. van Koppen, A. Heine, G. Klebe, S. Marchais-Oberwinkler, First structure-Activity relationship of 17 β -Hydroxysteroid dehydrogenase type 14 nonsteroidal inhibitors and crystal structures in complex with the enzyme, *J. Med. Chem.* 59 (2016) 10719–10737.
- [183] A.D. Favia, I. Nobeli, F. Glaser, J.M. Thornton, Molecular docking for substrate identification: the short-chain dehydrogenases/reductases, *J. Mol. Biol.* 375 (2008) 855–874.
- [184] J.C. Hermann, R. Marti-Arbona, A.A. Fedorov, E. Fedorov, S.C. Almo, B.K. Shoichet, F.M. Raushel, Structure-based activity prediction for an enzyme of unknown function, *Nature* 448 (2007) 775–779.
- [185] P.L. Mallipeddi, M. Joshi, J.M. Briggs, Pharmacophore-based virtual screening to aid in the identification of unknown protein function, *Chem. Biol. Drug Des.* 80 (2012) 828–842.
- [186] N. Reinhardt, J. Fischer, R. Coppi, E. Blum, W. Brandt, B. Drager, Substrate flexibility and reaction specificity of tropinone reductase-like short-chain dehydrogenases, *Bioorg. Chem.* 53 (2014) 37–49.
- [187] U. Oppermann, Carbonyl reductases: the complex relationships of mammalian carbonyl- and quinone-reducing enzymes and their role in physiology, *Annu. Rev. Pharmacol. Toxicol.* 47 (2007) 293–322.
- [188] E.S. Pilka, F.H. Niesen, W.H. Lee, Y. El-Hawari, J.E. Dunford, G. Kochan, V. Wsol, H.J. Martin, E. Maser, U. Oppermann, Structural basis for substrate specificity in human monomeric carbonyl reductases, *PLoS One* 4 (2009) e7113.
- [189] Y. El-Hawari, A.D. Favia, E.S. Pilka, M. Kisiela, U. Oppermann, H.J. Martin, E. Maser, Analysis of the substrate-binding site of human carbonyl reductases CBR1 and CBR3 by site-directed mutagenesis, *Chem. Biol. Interact.* 178 (2009) 234–241.
- [190] J.A. Botella, J.K. Ulschmid, C. Gruenewald, C. Moehle, D. Kretzschmar, K. Becker, S. Schneuwly, The *Drosophila* carbonyl reductase sniffer prevents oxidative stress-induced neurodegeneration, *Curr. Biol.* 14 (2004) 782–786.
- [191] T. Sgraja, J. Ulschmid, K. Becker, S. Schneuwly, G. Klebe, K. Reuter, A. Heine, Structural insights into the neuroprotective-acting carbonyl reductase Sniffer of *Drosophila melanogaster*, *J. Mol. Biol.* 342 (2004) 1613–1624.
- [192] H.J. Martin, M. Ziemba, M. Kisiela, J.A. Botella, S. Schneuwly, E. Maser, The *Drosophila* carbonyl reductase sniffer is an efficient 4-oxonon-2-enal (4ONE) reductase, *Chem. Biol. Interact.* 191 (2011) 48–54.
- [193] B. Blumberg, T. Iguchi, A. Odermatt, Endocrine disrupting chemicals, *J. Steroid Biochem. Mol. Biol.* 127 (2011) 1–3.

- [194] T. Mune, F.M. Rogerson, H. Nikkila, A.K. Agarwal, P.C. White, Human hypertension caused by mutations in the kidney isozyme of 11 β -hydroxysteroid dehydrogenase, *Nat. Genet.* 10 (1995) 394–399.
- [195] R.C. Wilson, M.D. Harbison, Z.S. Krozowski, J.W. Funder, C.H.L. Shackleton, H. M. Hanauskeabel, J.Q. Wei, J. Hertecant, A. Moran, R.E. Neiberger, J.W. Balfe, A. Fattah, D. Daneman, T. Licholai, M.I. New, Several homozygous mutations in the gene for 11 β -hydroxysteroid dehydrogenase type-2 in patients with apparent mineralocorticoid excess, *J. Clin. Endocrinol. Metab.* 80 (1995) 3145–3150.
- [196] R.S. Lindsay, R.M. Lindsay, C.R. Edwards, J.R. Seckl, Inhibition of 11 β -hydroxysteroid dehydrogenase in pregnant rats and the programming of blood pressure in the offspring, *Hypertension* 27 (1996) 1200–1204.
- [197] M.J. Nyirenda, R.S. Lindsay, C.J. Kenyon, A. Burchell, J.R. Seckl, Glucocorticoid exposure in late gestation permanently programs rat hepatic phosphoenolpyruvate carboxykinase and glucocorticoid receptor expression and causes glucose intolerance in adult offspring, *J. Clin. Invest.* 101 (1998) 2174–2181.
- [198] E.C. Cottrell, J.R. Seckl, M.C. Holmes, C.S. Wyrwoll, Foetal and placental 11 β -HSD2: a hub for developmental programming, *Acta Physiol. (Oxf.)* 210 (2014) 288–295.
- [199] K.L. Togher, M.M. O'Keefe, A.S. Khashan, H. Gutierrez, L.C. Kenny, G.W. O'Keefe, Epigenetic regulation of the placental HSD11B2 barrier and its role as a critical regulator of fetal development, *Epigenetics* 9 (2014) 816–822.
- [200] L. Wang, K. Kannan, Characteristic profiles of benzophenone-3 and its derivatives in urine of children and adults from the United States and China, *Environ. Sci. Technol.* 47 (2013) 12532–12538.
- [201] D. Fourches, E. Muratov, A. Tropsha, Trust, but verify: on the importance of chemical structure curation in cheminformatics and QSAR modeling research, *J. Chem. Inf. Model.* 50 (2010) 1189–1204.
- [202] V. Temml, C.V. Voss, V.M. Dirsch, D. Schuster, Discovery of new liver X receptor agonists by pharmacophore modeling and shape-based virtual screening, *J. Chem. Inf. Model.* 54 (2014) 367–371.
- [203] J.B. Cross, D.C. Thompson, B.K. Rai, J.C. Baber, K.Y. Fan, Y. Hu, C. Humblet, Comparison of several molecular docking programs: pose prediction and virtual screening accuracy, *J. Chem. Inf. Model.* 49 (2009) 1455–1474.
- [204] T. Kaserer, M. Höferl, K. Müller, S. Elmer, M. Ganzer, W. Jäger, D. Schuster, In silico predictions of drug–drug interactions caused by CYP1A2, 2C9, and 3A4 inhibition – a comparative study of virtual screening performance, *Mol. Inf.* 34 (2015) 431–457.
- [205] A. Gaulton, A. Hersey, M. Nowotka, A.P. Bento, J. Chambers, D. Mendez, P. Mutowo, F. Atkinson, L.J. Bellis, E. Cibrian-Uhalte, M. Davies, N. Dedman, A. Karlsson, M.P. Magarinos, J.P. Overington, G. Papadatos, I. Smit, A.R. Leach, The ChEMBL database in 2017, *Nucleic Acids Res.* (2016).
- [206] D.S. Wishart, T. Jewison, A.C. Guo, M. Wilson, C. Knox, Y. Liu, Y. Djoumbou, R. Mandal, F. Aziat, E. Dong, S. Bouatra, I. Sinelnikov, D. Arndt, J. Xia, P. Liu, F. Yallou, T. Bjorn Dahl, Perez-Pineiro R, R. Eisner, F. Allen, V. Neveu, R. Greiner, A. Scalbert, HMDB 3.0—the human metabolome database in 2013, *Nucleic Acids Res.* 41 (2013) D801–D807.
- [207] M.A. Koch, L.O. Wittenberg, S. Basu, D.A. Jeyaraj, E. Gourzoulidou, K. Reinecke, A. Odermatt, H. Waldmann, Compound library development guided by protein structure similarity clustering and natural product structure, *Proc. Natl. Acad. Sci. U. S. A.* 101 (2004) 16721–16726.
- [208] I. Beets, M. Lindemans, T. Janssen, P. Verleyen, Deorphanizing G protein-coupled receptors by a calcium mobilization assay, *Methods Mol. Biol.* 789 (2011) 377–391.
- [209] G. Moller, B. Husen, D. Kowalik, L. Hirvela, D. Plewczynski, L. Rychlewski, J. Messinger, H. Thole, J. Adamski, Species used for drug testing reveal different inhibition susceptibility for 17 β -hydroxysteroid dehydrogenase type 1, *PLoS One* 5 (2010) e10969.
- [210] A.S. Abdelsamie, E. Bey, E.M. Gargano, C.J. van Koppen, M. Empting, M. Frotscher, Towards the evaluation in an animal disease model: fluorinated 17 β -HSD1 inhibitors showing strong activity towards both the human and the rat enzyme, *Eur. J. Med. Chem.* 103 (2015) 56–68.
- [211] M. Mazumdar, D. Fournier, D.-W. Zhu, C. Cadot, D. Poirier, S.-X. Lin, Binary and ternary crystal structure analyses of a novel inhibitor with 17 β -HSD type 1: a lead compound for breast cancer therapy, *Biochem. J.* 424 (2009) 357–366.

Supplementary info

SDR	Reference	description
11 β -HSD1 inhibitors	[1]	High predictive power and good performance of pharmacophore models are fundamental for reliable in silico tools. This can be achieved by systematic evaluation and refinement of pharmacophore models. The 11 β -HSD pharmacophore models from Schuster et al. [2] and an 11 β -HSD2-selective model reported by Kratschmar et al.[3] were re-evaluated and refined by Vuorinen et al. [1]. Repeated exchanging, removing, or adding of chemical features to the pharmacophore model in order to focus the model to find more active and respectively less inactive compounds which are described in newly available literature data is a key step in this process. However, subsequent prospective VS and biological evaluations are just as important to compare the effective improvement towards the unrefined model. Against the background that no crystal structure for 11 β -HSD2 is available and the few known selective 11 β -HSD2 inhibitors belong to the same chemical scaffold class, the data of the 11 β -HSD2 model are biased. Nevertheless, the authors were able to show improved model performance and discovered novel scaffolds as selective 11 β -HSD2 inhibitors.
11 β -HSD1 inhibitors	[4]	Vuorinen et al. used the refined 11 β -HSD1 model as a query to screen a database for constituents of the traditionally used Greek medical plant <i>Pistacia lenticus</i> . <i>P. lenticus</i> , so-called mastic gum, is used to treat diabetes or control cholesterol levels. The mode of action is currently unknown, but it is hypothesized that inhibition of 11 β -HSD1 by secondary metabolites contributes to the antidiabetic activity of mastic gum. These secondary metabolites are proposed to belong to the class of triterpenes, as they are detected at high concentrations in the neutral and acidic fraction of <i>Pistacia oleoresins</i> . Therefore, the evaluation of the virtual hit list focused on triterpenes and revealed eight hits, which are constituents of <i>P. lenticus</i> . Masticadienonic acid and isomasticadienonic acid were selected for biological assessments, because they displayed the two main constituents of the acidic fraction of the resin. Masticadienonic acid and isomasticadienonic acid selectively inhibited 11 β -HSD1 over 11 β -HSD2 in a cell-lysate based assay with IC ₅₀ of 2.51 μ M and 1.94 μ M, respectively. Analyzing the acidic fraction of the resin for 11 β -HSD1 inhibition showed a comparable IC ₅₀ of 2.1 μ M, whereas the whole resin exhibited somewhat more potent activity against 11 β -HSD1 with an IC ₅₀ of 1.33 μ M, suggesting an additive effect. Binding mode examinations of the two single substances by docking revealed an occupation of the binding site without interactions with the catalytic residues. Thus, masticadienonic acid and isomasticadienonic acid are suggested to competitively prevent cortisol from binding.

Substrate identification of non SDR enzymes	[5]	Mallipeddi and Joshi et al. used five resolved crystal structures for computational prediction of the binding site and mapping of energetically favorable positions of functional groups. Based on these analyses they converted the observed chemical features into a pharmacophore model which was then used for VS of metabolites from the KEGG ligand database. The filter function of the pharmacophore model was fulfilled by eliminating >92% of the database compounds and by ranking the known substrates or products within the top 0.7% and substrate-like compounds in the top 1%.
---	-----	--

References

- [1] A. Vuorinen, L.G. Nashev, A. Odermatt, J.M. Rollinger, D. Schuster, Pharmacophore model refinement for 11 β -xhydroxysteroid dehydrogenase inhibitors: Search for modulators of intracellular glucocorticoid concentrations, *Mol. Inf.*, 33 (2014) 15-25.
- [2] D. Schuster, E.M. Maurer, C. Laggner, L.G. Nashev, T. Wilckens, T. Langer, A. Odermatt, The discovery of new 11beta-hydroxysteroid dehydrogenase type 1 inhibitors by common feature pharmacophore modeling and virtual screening, *J. Med. Chem.*, 49 (2006) 3454-3466.
- [3] D.V. Kratschmar, A. Vuorinen, T. Da Cunha, G. Wolber, D. Classen-Houben, O. Doblhoff, D. Schuster, A. Odermatt, Characterization of activity and binding mode of glycyrrhetic acid derivatives inhibiting 11beta-hydroxysteroid dehydrogenase type 2, *J. Steroid Biochem. Mol. Biol.*, 125 (2011) 129-142.
- [4] A. Vuorinen, J. Seibert, V.P. Papageorgiou, J.M. Rollinger, A. Odermatt, D. Schuster, A.N. Assimopoulou, Pistacia lentiscus oleoresin: Virtual screening and identification of masticadienonic and isomasticadienonic acids as inhibitors of 11beta-hydroxysteroid dehydrogenase 1, *Planta Med.*, 81 (2015) 525-532.
- [5] P.L. Mallipeddi, M. Joshi, J.M. Briggs, Pharmacophore-based virtual screening to aid in the identification of unknown protein function, *Chem Biol Drug Des*, 80 (2012) 828-842.

3. Endocrine disrupting chemicals

Annually, a substantial amount of synthetic chemicals in the form of body care products, cosmetics, dyes, food additives, pharmaceuticals as well as chemicals used for industrial production or agriculture are manufactured and released on the market. This occurs frequently with an inadequate safety assessment. The evaluation and characterization of potential risk factors on the environment and on human health originating from those exogenous chemicals is a topic of high actual interest addressed by several authorities as for instance the Registration, Evaluation, Authorization and Restriction of Chemicals (REACH) regulation of the European Union, the Toxicology in the 21st century (Tox21) inter-agency collaboration program or the Toxicity Forecaster (ToxCast) from the U.S. Environmental Protection Agency/ Food and Drug Administration/ National Toxicology Program [11-14]. These so-called endocrine disrupting chemicals (EDCs) can interfere with the hormone synthesis, metabolism or hormonal signaling and as a result of that, potentially contributing to major diseases. Although nuclear hormone receptors such as estrogen receptors (ER) and androgen receptor (AR) belong to the most extensively studied targets for EDC action, other receptors such as mineralocorticoid receptors (MR) or glucocorticoid receptors (GR) are much less well investigated. In addition, the enzymatic regulation of biosynthetic and metabolic pathways have a considerable impact on the tissue- and cell-specific steroid availability and thereby impact on steroid hormone action [15]. However, only a few steroid metabolizing enzymes are currently covered in the analysis of potential EDCs. The present thesis selected one SDR, 11 β -hydroxysteroid dehydrogenase 2 (11 β -HSD2), as an example to test the use of molecular modeling and biological assessment for the identification and characterization of potential inhibitors.

3.1. 11 β -hydroxysteroid dehydrogenase type 2

Compared to the GR, the MR has a rather broad ligand specificity and binds the glucocorticoids cortisol and corticosterone as well as the mineralocorticoids aldosterone and 11-deoxycorticosterone with similar affinity [16-19]. 11 β -HSD2 catalyzes the oxidation of the potent 11 β -hydroxyglucocorticoids (cortisol, corticosterone) into their inactive 11-oxo forms (cortisone, 11-dehydrocorticosterone), thereby acting as gate-keeper to protect the MR from cortisol that is present in the circulation in excess amounts and rendering specificity for aldosterone and 11-deoxycorticosterone [20, 21]. Patients with genetic loss-of-function mutations in the *HSD11B2* gene suffer from so-called apparent mineralocorticoid excess (AME), characterized by severe hypertension, hypernatremia, hypokalemia, metabolic alkalosis, low aldosterone, low renin, and increased plasma and urinary cortisol to cortisone

ratios, due to the excessive cortisol-dependent MR activation in the kidney and colon [22-24]. Besides the regulation of electrolyte balance and vascular function, the expression of 11 β -HSD2 in the placenta ensures fetal protection from excess maternal glucocorticoids [22, 25]. Deficient placental 11 β -HSD2 activity has been associated with reduced birth weight, albeit in normal ranges, and a higher risk for cardio-metabolic and neuropsychiatric disorders in later life. Importantly, different animal models and human observational data (a more detailed overview is provided in the introduction of the published article 'Inhibition of 11 β -hydroxysteroid dehydrogenase 2 by the fungicides itraconazole and posaconazole' [26], see the section below) supported the hypothesis that reduced placental 11 β -HSD2 activity is responsible for the high glucocorticoid concentrations reaching the fetus and subsequent programming of disease susceptibility [27]. Due to the important physiological roles of 11 β -HSD2, it can be considered as an anti-target during the development of therapeutic SDR inhibitors but it should also be considered for risk assessment of potential EDCs. Currently, 11 β -HSD2 is not part of the common off-target screening approaches. Therefore, possible inhibitory activities of approved drugs toward 11 β -HSD2 were addressed in the following study using pharmacophore-based virtual screening (VS) and subsequent biological evaluation of selected hits.

Furthermore, this study additionally served as proof of concept for the application of pharmacophore-based VS techniques to identify potential inhibitors/substrates of proteins with unresolved structural information. To date, the structural information for many members of the SDR superfamily is either completely lacking, as it is the case for the ER membrane anchored protein 11 β -HSD2, or only partially available. Several available crystal structures of SDRs do not include the transmembrane domain, which is found in about half of all SDRs, and in many structures the cofactor is missing (so-called apoenzymes). The experimental 3D resolution of the membrane bound SDR proteins still remains a major challenge as they require extraction from the membrane using detergents, whilst simultaneously trying to retain proper folding and stability in solution [28]. Homology modeling as an alternative approach is not less demanding because of the low sequence similarity among members of the SDR family. Thus, structure-guided design strategies are limited for several SDRs. Ligand-based methods can display an interesting alternative to target these proteins, provided that at least some information about the mechanistic details of the enzyme activity is known (several examples can be found in the two published review articles described in the section above [9, 10]).

3.1.1. Published article:

Inhibition of 11 β -hydroxysteroid dehydrogenase 2 by the fungicides itraconazole and posaconazole

Katharina R. Beck^a, Murielle Bächler^a, Anna Vuorinen^a, Sandra Wagner^b, Muhammad Akram^b, Ulrich Griesser^c, Veronika Temml^b, Petra Klusonova^a, Hideaki Yamaguchi^d, Daniela Schuster^b, Alex Odermatt^a, *Biochem Pharmacol.* 2017 Apr 15;130:93-103.

^aSwiss Center for Applied Human Toxicology and Division of Molecular and Systems Toxicology, Department of Pharmaceutical Sciences, Pharmazentrum, University of Basel, Klingelbergstrasse 50, 4056 Basel, Switzerland

^bInstitute of Pharmacy/Pharmaceutical Chemistry and Center for Molecular Biosciences Innsbruck (CMBI), Computer Aided Molecular Design Group, University of Innsbruck, Innrain 80/82, 6020 Innsbruck, Austria

^cInstitute of Pharmacy/Pharmaceutical Technology, University of Innsbruck, Innrain 80/82, 6020 Innsbruck, Austria

^dDepartment of Applied Biological Chemistry, Meijo University, Nagoya 468-8502, Japan



Inhibition of 11 β -hydroxysteroid dehydrogenase 2 by the fungicides itraconazole and posaconazole



Katharina R. Beck^a, Murielle Bächler^a, Anna Vuorinen^a, Sandra Wagner^b, Muhammad Akram^b, Ulrich Griesser^c, Veronika Temml^b, Petra Klusonova^a, Hideaki Yamaguchi^d, Daniela Schuster^b, Alex Odermatt^{a,*}

^aSwiss Center for Applied Human Toxicology and Division of Molecular and Systems Toxicology, Department of Pharmaceutical Sciences, Pharmazentrum, University of Basel, Klingelbergstrasse 50, 4056 Basel, Switzerland

^bInstitute of Pharmacy/Pharmaceutical Chemistry and Center for Molecular Biosciences Innsbruck (CMBI), Computer Aided Molecular Design Group, University of Innsbruck, Innrain 80/82, 6020 Innsbruck, Austria

^cInstitute of Pharmacy/Pharmaceutical Technology, University of Innsbruck, Innrain 80/82, 6020 Innsbruck, Austria

^dDepartment of Applied Biological Chemistry, Meijo University, Nagoya 468-8502, Japan

ARTICLE INFO

Article history:

Received 23 December 2016

Accepted 23 January 2017

Available online 25 January 2017

Chemical compounds studied in this article:

Albendazole (PubChem CID: 2082)
 Butoconazole (PubChem CID: 47472)
 Climbazole (PubChem CID: 37907)
 Itraconazole (PubChem CID: 55283)
 Hydroxyitraconazole (PubChem CID: 108222)
 Ketoconazole (PubChem CID: 47576)
 Posaconazole (PubChem CID: 468595)
 Sertaconazole (PubChem CID: 65863)
 Terconazole (PubChem CID: 441383)
 Tioconazole (PubChem CID: 5482)

Keywords:

11 β -Hydroxysteroid dehydrogenase
 Virtual screening
 Reproductive toxicity
 Itraconazole
 Posaconazole
 Glucocorticoid

ABSTRACT

Impaired 11 β -hydroxysteroid dehydrogenase type 2 (11 β -HSD2)-dependent cortisol inactivation can lead to electrolyte dysbalance, hypertension and cardiometabolic disease. Furthermore, placental 11 β -HSD2 essentially protects the fetus from high maternal glucocorticoid levels, and its impaired function has been associated with altered fetal growth and a higher risk for cardio-metabolic diseases in later life. Despite its important role, 11 β -HSD2 is not included in current off-target screening approaches. To identify potential 11 β -HSD inhibitors among approved drugs, a pharmacophore model was used for virtual screening, followed by biological assessment of selected hits. This led to the identification of several azole fungicides as 11 β -HSD inhibitors, showing a significant structure-activity relationship between azole scaffold size, 11 β -HSD enzyme selectivity and inhibitory potency. A hydrophobic linker connecting the azole ring to the other, more polar end of the molecule was observed to be favorable for 11 β -HSD2 inhibition and selectivity over 11 β -HSD1. The most potent 11 β -HSD2 inhibition, using cell lysates expressing recombinant human 11 β -HSD2, was obtained for itraconazole (IC₅₀ 139 \pm 14 nM), its active metabolite hydroxyitraconazole (IC₅₀ 223 \pm 31 nM) and posaconazole (IC₅₀ 460 \pm 98 nM). Interestingly, experiments with mouse and rat kidney homogenates showed considerably lower inhibitory activity of these compounds towards 11 β -HSD2, indicating important species-specific differences. Thus, 11 β -HSD2 inhibition by these compounds is likely to be overlooked in preclinical rodent studies. Inhibition of placental 11 β -HSD2 by these compounds, in addition to the known inhibition of cytochrome P450 enzymes and P-glycoprotein efflux transport, might contribute to elevated local cortisol levels, thereby affecting fetal programming.

© 2017 Elsevier Inc. All rights reserved.

Abbreviations: 11 β -HSD2, 11 β -hydroxysteroid dehydrogenase 2; AME, apparent mineralocorticoid excess; androstenedione, Δ 4-androstene-3,17-dione; CRH, corticotrophin releasing hormone; DHEA, dehydroepiandrosterone; DHT, 5 α -dihydrotestosterone; DMEM, Dulbecco's modified Eagle medium; GR, glucocorticoid receptor; H6PDH, hexose-6-phosphate dehydrogenase; HEK-293, Human Embryonic Kidney-293 cells; HPA, hypothalamic-pituitary-adrenal; MR, mineralocorticoid receptor; OHI, hydroxyitraconazole; P-gp, P-glycoprotein; TLC, thin layer chromatography; VS, virtual screening.

* Corresponding author at: Swiss Center for Applied Human Toxicology and Division of Molecular and Systems Toxicology, Department of Pharmaceutical Sciences, University of Basel, Klingelbergstrasse 50, 4056 Basel, Switzerland.

E-mail addresses: katharina.beck@unibas.ch (K.R. Beck), murielle.baechler@stud.unibas.ch (M. Bächler), anna.vuorinen1@gmail.com (A. Vuorinen), sandra.wagner@student.uibk.ac.at (S. Wagner), muhammad.akram@uibk.ac.at (M. Akram), ulrich.griesser@uibk.ac.at (U. Griesser), veronika.temml@uibk.ac.at (V. Temml), petra.klusonova@unibas.ch (P. Klusonova), hyamagu@meijo-u.ac.jp (H. Yamaguchi), daniela.schuster@uibk.ac.at (D. Schuster), alex.odermatt@unibas.ch (Alex Odermatt).

<http://dx.doi.org/10.1016/j.bcp.2017.01.010>

0006-2952/© 2017 Elsevier Inc. All rights reserved.

1. Introduction

11 β -Hydroxysteroid dehydrogenase 2 (11 β -HSD2) converts potent 11 β -hydroxyglucocorticoids (cortisol, corticosterone) into their inactive 11-keto forms (cortisone, 11-dehydrocorticosterone), thereby controlling tissue-specific activities of mineralocorticoid receptors (MR) and glucocorticoid receptors (GR) [1]. 11 β -HSD2 is essentially involved in the regulation of electrolyte balance, vascular function, and angiogenesis, as well as in the fetal-placental barrier to inactivate cortisol and protect the fetus from high maternal glucocorticoid levels [2,3].

The consequences of impaired 11 β -HSD2 function are manifested in patients with genetic loss-of-function mutations suffering from apparent mineralocorticoid excess (AME) [2,4,5]. In these patients the excessive cortisol-dependent MR activation in the kidney and colon results in hypokalemia, hypernatremia and water retention, leading to severe hypertension characterized by low renin, low aldosterone and increased plasma and urinary cortisol to cortisone ratios. 11 β -HSD2 activity is essential since very early on in life, because birth weights of individuals homozygous/compound heterozygous for *HSD11B2* mutations were found to be significantly lower than those of their unaffected siblings [6]. Milder acquired forms of AME can be caused by inhibition of 11 β -HSD2, for instance upon consumption of considerable amounts of licorice, containing the potent 11 β -HSD inhibitor glycyrrhetic acid (GA) [7].

The exposure to 11 β -HSD2 inhibitors is especially critical during pregnancy. 11 β -HSD2 builds a placental barrier by protecting the fetus from the 5–10 times higher maternal glucocorticoid levels in the course of a normal pregnancy [8–11]. Nevertheless, this barrier is not entirely complete, as a minor proportion of maternal cortisol is able to cross the placenta [11]. Glucocorticoids are important mediators of fetal growth, development and organ maturation. Rising total plasma cortisol levels during pregnancy, peaking in the third trimester at threefold non-pregnant levels [12], are in parallel with progressive maturation of fetal organs, most notably the stimulation of surfactant production by the lung. However, glucocorticoid administration, especially during late gestation, has been associated with reduced birth weight, elevated blood pressure, higher insulin, increased distractibility and attention deficit later in life [13–17]. The correlation between low birth weight, albeit in normal ranges, and subsequent diseases in adulthood was found to be largely independent of confounding life style factors such as smoking or obesity [15]. It has been hypothesized that a reduced placental 11 β -HSD2 activity is responsible for the high glucocorticoid concentrations reaching the fetus and subsequent programming of disease susceptibility [18]. Importantly, low 11 β -HSD2 expression was found to be associated with intrauterine growth restriction pregnancies in humans and in rodent models [19–22]. Determination of osteocalcin concentration in human cord blood samples, which is a sensitive marker of glucocorticoid exposure in adult humans, revealed a direct correlation with placental 11 β -HSD2 activity [23].

Treatment of pregnant rats with dexamethasone, which cannot be inactivated by 11 β -HSD2 [24], led to lower birth weights and caused HPA axis hyperactivity, hypertension, hyperglycemia and increased anxiety behavior [20,25]. Similarly, administration of the unselective 11 β -HSD inhibitor carbenoxolone to pregnant rats resulted in reduced birth weight, and adult offspring showed enhanced HPA activity with increased glucocorticoid and CRH levels as well as elevated blood pressure [26,27]. Evidence for the importance of placental 11 β -HSD2 was contributed by studies with placentas from 11 β -HSD2-deficient mice showing increased amino acid and reduced glucose transport as well as lower expression levels of genes important for angiogenesis [28]. Furthermore, maternal stress and malnutrition in rats were reported to be able

to down regulate placental 11 β -HSD2 and program for diseases in adult life [29–31]. Factors including sex steroids, nitric oxide, prostaglandins, proinflammatory cytokines, infections and environmental pollutants were shown to have the potential to reduce 11 β -HSD2 activity in studies using placental cell lines [32,33].

Observational studies showed that pregnant Finnish women consuming large amounts of licorice (containing the unselective 11 β -HSD inhibitor glycyrrhetic acid) had shorter gestation times [34] and gave birth to children with behavioral disturbances and poorer cognitive functions coupled with increased HPA axis activity, in a dose-dependent manner [35,36]. Compromised 11 β -HSD2 function during pregnancy has also been implicated in preeclampsia, a major cause of maternal and perinatal mortality; however, the etiology is poorly understood [37,38].

Due to its important physiological role and the adverse effects observed upon its inhibition, 11 β -HSD2 can be considered as an anti-target for drug development (with a few specific exceptions where these effects are wanted); however, it is not included in current off-target screening approaches. The present study addressed possible inhibitory effects of approved drugs towards 11 β -HSD2 by performing a virtual screening (VS) of the DrugBank database using an 11 β -HSD pharmacophore model. This was followed by a biological evaluation of selected hits, with a focus on the azole fungicides itraconazole and posaconazole.

2. Materials and methods

2.1. Chemicals and reagents

[1,2,6,7-³H]-cortisol, [2,4,6,7-³H]-estrone and [2,4,6,7-³H]-estradiol were purchased from PerkinElmer (Boston, MA, USA), [1,2-³H]-cortisone from American Radiolabeled Chemicals (St. Louis, MO), hydroxyitraconazole (OHI) from Carbosynth (Berkshire, UK) and all other chemicals from Sigma Aldrich (Buchs, Switzerland) of the highest grade available. Cell culture media were obtained from Sigma Aldrich (Buchs, Switzerland).

2.2. Pharmacophore modeling and virtual screening

The 11 β -HSD inhibitor pharmacophore model used for this study was previously reported and validated [39]. The model was initially based on three potent, structurally diverse 11 β -HSD inhibitors [40] and refined with recent literature and novel screening data (model 4new in reference [39], Fig. 1A).

To discover potential 11 β -HSD inhibitors among FDA-approved drugs and nutraceuticals, the DrugBank version 3.0 was downloaded as sd file (1543 approved drugs and 84 nutraceuticals) and transformed into a 3D-multiconformational database using the “build database” protocol of Discovery Studio 4.0 (Discovery Studio, Version 4.0, Biovia Inc., San Diego, CA, 2014). For each compound, a maximum of 255 conformers was calculated using fast settings. For the VS, the “search 3D database” protocol with BEST flexible search was used. The DrugBank database was screened with the 11 β -HSD inhibitors model using Discovery Studio 4.0.

2.3. Cell culture

Human Embryonic Kidney-293 cells (HEK-293) cells (used at passage number 15–30), human SW-620 colon carcinoma cells (passage number 11–15) and human MCF-7 breast cancer cells (passage number 19–27) were obtained from ATCC (Manassas, VA, USA) and were cultured in Dulbecco's modified Eagle medium (DMEM) supplemented with 10% fetal bovine serum, 4.5 g/L glucose, 100 U/mL penicillin/streptomycin, 2 mM L-glutamine, 10 mM HEPES, pH 7.4, and 10% MEM non-essential amino acid solution.

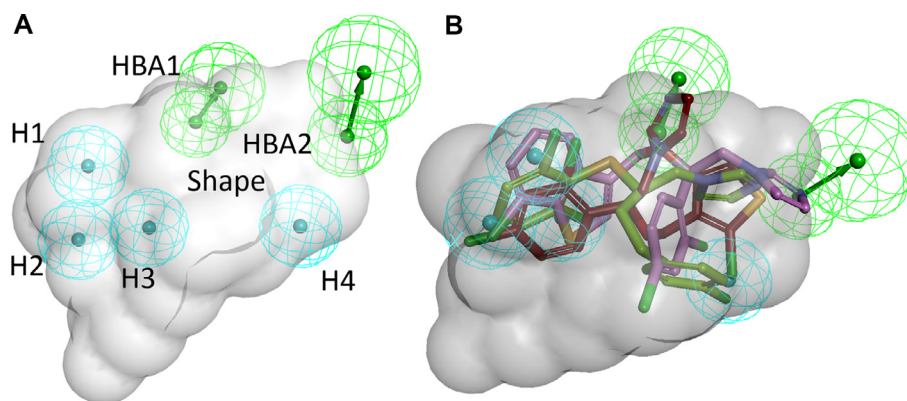


Fig. 1. Pharmacophore model used for virtual screening of the DrugBank database. (A) The model consists of four hydrophobic (H) features (cyan), two hydrogen bond acceptors (HBA, green) and a sterical shape restriction (grey) [39]. (B) Virtual hits from the DrugBank screening fitted into the model. Compounds are color-coded: red – tioconazole; green – butoconazole; violet – sertaconazole.

2.4. Determination of 11 β -HSD activity in cell lysates

Enzyme activities were determined as described earlier using lysates of HEK-293 cells stably expressing human 11 β -HSD1 and hexose-6-phosphate dehydrogenase (H6PDH; HHH7 clone) or 11 β -HSD2 (AT8 clone) [41]. 11 β -HSD1 reductase activity was measured by incubating the lysates for 10 min at 37 °C in a total volume of 22 μ L containing 200 nM radiolabeled cortisone, 500 μ M NADPH and test substance or vehicle (DMSO at a maximal concentration of 0.1%). 11 β -HSD2-dependent oxidation was assessed in the presence of 200 nM radiolabeled cortisol and 500 μ M NAD⁺. The reactions were stopped by adding an excess amount of unlabeled cortisone and cortisol (1:1, 2 mM in methanol). Approximately 20–25% of the substrate were converted to the corresponding product. Steroids were separated by thin layer chromatography (TLC) using chloroform and methanol (9:1). Conversion of radiolabeled substrate was measured by scintillation counting. The substrate conversion was determined and compared to the enzyme activity in the control sample.

To exclude irreversible 11 β -HSD2 inhibition by the investigated compounds, HEK cell lysates were preincubated with the corresponding compounds for 0, 5 and 20 min at 4 °C, followed by determination of enzyme activity. Alternatively, lysate were preincubated with the compounds for 10 min followed by subsequent dilution (1:2 or 1:4) and determination of enzyme activity [42]. Data (mean \pm SD) were normalized to vehicle control (DMSO) and obtained from at least three independent experiments.

2.5. Determination of 11 β -HSD2 activity in intact cells

11 β -HSD2 activity measurement in intact SW-620 and MCF-7 cells was determined as described earlier [43]. Briefly, 100,000 SW-620 and 50,000 MCF-7 cells per well were seeded in 96-well plates. The medium was replaced after 24 h by 40 μ L steroid- and serum-free DMEM (DMEMsf) containing either vehicle or inhibitor and 10 μ L medium containing 10 nCi radiolabeled cortisol and unlabeled cortisol to reach a final concentration of 50 nM. SW-620 cells were incubated for 4 h and MCF-7 cells for 5 h at 37 °C, followed by analysis of steroid conversion by TLC and scintillation counting.

2.6. Determination of 17 β -HSD1 and 17 β -HSD2 activity in cell lysates

Determination of 17 β -HSD1 and 17 β -HSD2 activity was conducted as described earlier [44]. Briefly, lysates of HEK-293 cells transiently expressing human 17 β -HSD1 and 17 β -HSD2 were incu-

bated for 10 min at 37 °C in a total volume of 22 μ L in the presence 200 nM estrone containing 50 nCi of [2,4,6,7-³H]-estrone and 500 μ M NADPH for 17 β -HSD1, and with 200 nM estradiol containing 50 nCi of [2,4,6,7-³H]-estradiol and 500 μ M NAD⁺ for 17 β -HSD2 activity measurements. Steroids were separated using TLC and substrate conversion determined by scintillation counting. Data (mean \pm SD) were normalized to vehicle control (DMSO) and obtained from at least three independent experiments.

2.7. Determination of 11 β -HSD activity in mouse and rat kidney homogenates

Mouse (C57BL6) and rat (Wistar) kidney tissue from adult males were snap frozen in liquid nitrogen and stored at –80 °C until further use. For homogenate preparation, frozen tissue was sonicated in homogenization buffer (250 mM sucrose, 10 mM HEPES, pH 7.4; 900 μ L for 100 mg of kidney) and centrifuged at 2000g, 4 °C for 10 min to remove cell debris. The total protein concentration was determined by BCA assay [45]. The homogenates were prediluted to a protein concentration of 3.75 mg of protein/mL (mouse) or 10 mg of protein/mL (rat) in homogenization buffer. Reactions were performed in a total volume of 22 μ L incubation buffer (300 mM NaCl, 20 mM Tris(hydroxymethyl)aminomethane-hydrochloride, 1 mM EDTA, 10% glycerol, pH 7.7) containing 0.075 mg/mL of mouse and 0.2 mg/mL of rat total kidney protein, respectively, as well as 10 μ M of test compound, 50 nM of corticosterone (containing 50 nCi [1,2,6,7-³H] corticosterone) and 500 μ M NAD⁺ at 37 °C for 20 min. Approximately 20–25% of the substrate were converted. The steroids were separated by TLC and conversion of radiolabeled substrate was measured by scintillation counting.

2.8. Docking

Docking was performed using GOLD 5.2 (The Cambridge Crystallographic Data Centre, Cambridge, UK, [46]) based on a crystal structure of 11 β -HSD1 (co-crystallized with (2R)-4-[4-fluoro-2-(tri fluoromethyl)phenyl]-2-methyl-1-(3-(1H-1,2,4-triazol-1-yl)phenyl)sulfonyl]piperazine, PDB code 3HFG [47]) and a homology model for human 11 β -HSD2 [48] and murine 11 β -HSD2 [49]. The PDB entry 3HFG was chosen for two reasons. First, it was the template for generating the homology model of human and murine 11 β -HSD2. Second, the co-crystallized inhibitor is of similar size as some of the investigated antifungals and contains a triazole moiety. It therefore probably constitutes a binding site conformation suitable for docking this class of 11 β -HSD1 inhibitors.

The ligand binding pocket was defined as a sphere with a 10 Å radius around the coordinates $X = -19.50$ $Y = 4.00$, $Z = 14.25$. ChemPLP was used as scoring function. As workflow validation, redocking of the original ligand was performed using default settings and the best ranked pose deviates from the crystal structure with an RMSD of 0.856 for 11 β -HSD1. As both the homology models for human and murine 11 β -HSD2 were initially based on PDB entry 3HFG, the same coordinates were used to define the binding site for this docking. For human 11 β -HSD2, the docking was additionally repeated setting Arg212 as flexible amino acid. The binding poses were analyzed using LigandScout 4.1 [50] (Inte:Ligand GmbH, Vienna, Austria).

3. Results

3.1. Virtual screening of the DrugBank database using a 11 β -HSD pharmacophore model and virtual hit selection for biological evaluation

Despite its role in the regulation of electrolyte balance and cardiovascular function and its importance during pregnancy to control the *in utero* environment and therefore fetal growth and development, 11 β -HSD2 is not included in current drug off-target screenings. Thus, the present project aimed to evaluate some approved drugs for their ability to interfere with 11 β -HSD2 activity. For this purpose, the FDA-approved small molecule drug entries of the DrugBank database were subjected to VS using a previously developed 11 β -HSD pharmacophore model (Fig. 1A) [39]. This model is not expected to discriminate between 11 β -HSD1 and 11 β -HSD2 inhibitors because no crystal structure is available for 11 β -HSD2 and the model is, at least in part, built based on available 11 β -HSD1 ligands. Of the 1543 DrugBank entries, 101 approved drugs fitted into the model. Not surprisingly, several steroidal compounds (in total 18 hits) including mainly glucocorticoids, were among the hits. Besides, the virtual hit list contained several prostaglandin analogues as well as anti-infective agents, including antifungals, antibiotics and antiparasitic agents. Antifungals were especially represented by the class of azole fungicides, with sertaconazole, butoconazole and tioconazole as virtual hits (Fig. 1B). The majority of antibiotics comprised β -lactam antibiotics and lincosamides, with cloxacillin, flucloxacillin and nafcillin, as well as clindamycin and lincomycin as representative structural classes. Further virtual hits included members of the classes of anti hypertensives/antiarrhythmics, diuretics, lipid lowering drugs, antidiabetics, analgesics and antipsychotics. Several hits from the VS, belonging to the different structural classes mentioned above and available through an in-house chemical repository, were selected for biological assessment.

3.2. Effect of selected virtual hits and further structurally related compounds on 11 β -HSD activity

The selected compounds were first tested for their potential to inhibit cortisol to cortisone conversion in lysates of HEK-293 cells stably expressing human 11 β -HSD2. The selectivity over the closely related 11 β -HSD1 was then determined by measuring the effect of the chemicals on the conversion of cortisone to cortisol. The selected steroids (nandrolone), antiarrhythmics (amiodarone), lipid lowering drugs (atorvastatin, simvastatin), diabetics (rosiglitazone), diuretics (ethacrynic acid), analgesics (indomethacin, nabilone), antipsychotics/sedative (chlorpromazine), the uricosuric probenecid, antiparasitic agents (amodiaquine, chloroquine and pentamidine), β -lactam antibiotics (cloxacillin, flucloxacillin and nafcillin), lincosamides (clindamycin and lincomycin) and the steroid-like antibiotic fusidic acid showed no or weak inhibition (less than 40% inhibition) of 11 β -HSD1 and 11 β -HSD2 enzyme

activity at a concentration of 20 μ M (data not shown). However, the azole fungicides sertaconazole, butoconazole and tioconazole showed moderate activity and inhibited 11 β -HSD2 at a concentration of 20 μ M, resulting in 61%, 44% and 50% residual activity, respectively. These azole fungicides were not selective, and they equally well or preferentially inhibited 11 β -HSD1, showing residual enzyme activities of 35%, 48% and 18%, respectively.

Due to their wide use and partial over-the-counter availability, and their previous association with 11 β -HSDs (triadimefon as a substrate of 11 β -HSD1 and ketoconazole as a weak inhibitor of 11 β -HSD1 and 11 β -HSD2 [39,51]), additional, structurally related azole fungicides were selected for biological testing in order to provide proof of concept in applying pharmacophores as initial filter for the identification of hazardous compound classes [52]. The biological analyses using HEK-293 cell lysates expressing recombinant human enzymes revealed a clear structure-activity relationship between 11 β -HSD selectivity and structural size and shape of the azoles: the larger the structural size the more potent its inhibitory activity against 11 β -HSD2 and the higher the selectivity over 11 β -HSD1 (Fig. 2). One requirement of high activity was a hydrophobic central region of the azole scaffold linked to a more polar end. The compounds with a smaller scaffold preferentially inhibited 11 β -HSD1. In addition, the subdivision of azoles in imidazole and triazole derivatives revealed a further relationship. Imidazoles such as tioconazole, sertaconazole and butoconazole preferably inhibited 11 β -HSD1 over 11 β -HSD2, whereas triazoles such as terconazole, posaconazole and itraconazole more potently inhibited 11 β -HSD2. Albendazole, possessing a small azole scaffold containing a benzimidazole structure, was inactive against both enzymes. The most potent 11 β -HSD2 inhibition was found for itraconazole and posaconazole, with IC_{50} values of 139 ± 14 nM and 460 ± 98 nM (Fig. 3), respectively, and selectivity over 11 β -HSD1 (Fig. 2). Furthermore, as itraconazole is mainly metabolized to the pharmacologically active OHI, this metabolite was also tested, yielding an IC_{50} value of 223 ± 31 nM against 11 β -HSD2. Irreversible 11 β -HSD2 inhibition by itraconazole, OHI and posaconazole was excluded by preincubation experiments; however, preincubation did not alter the inhibitory effect, suggesting a competitive mode of inhibition in line with competition for substrate binding.

3.3. Selectivity assessment of the azole fungicides over 17 β -HSD1 and 17 β -HSD2

Although 11 β -HSD2 and 11 β -HSD1 are responsible for the interconversion of the same substrate, i.e. glucocorticoids, they are distant homologs sharing only about 18% sequence identity [53]. In contrast, human 17 β -HSD2 is more closely related to 11 β -HSD2 with about 45% amino acid sequence identity. 17 β -HSD2 is predominantly involved in the metabolism of sex steroid hormones, inactivating estradiol to estrone, testosterone into Δ 4-androstene-3,17-dione (androstenedione), 5 α -dihydrotestosterone (DHT) into 5 α -androstenedione or 5-androstene-3 β ,17-diol to dehydroepiandrosterone (DHEA). The reverse reaction of activating the weak estrogen estrone to the potent estradiol and to a minor extent DHEA to 5-androstene-3 β ,17-diol is catalyzed by 17 β -HSD1. Due to the high expression of 17 β -HSD1 and 17 β -HSD2 in placenta [54,55], itraconazole, OHI and posaconazole were assessed for their potential to inhibit 17 β -HSD1 and 17 β -HSD2 enzyme activity in lysates of HEK-293 cells transiently expressing human 17 β -HSD1 and 17 β -HSD2. None of the compounds inhibited 17 β -HSD1 or 17 β -HSD2 activity (data not shown).

3.4. Species-specific 11 β -HSD2 inhibition by the selected azole fungicides

Earlier studies emphasized the importance to assess species-specific differences of 11 β -HSD1 and 11 β -HSD2 inhibitors, espe-

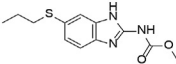
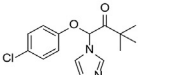
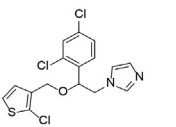
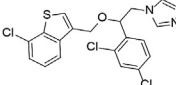
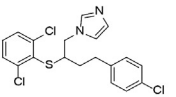
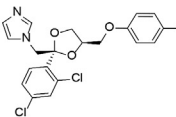
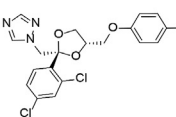
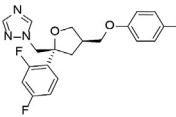
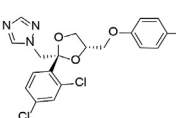
compound	structure	residual enzyme activity [% of control] (20 μ M)		IC ₅₀ values [μ M]	
		11 β -HSD1	11 β -HSD2	11 β -HSD1	11 β -HSD2
Albendazole		105 \pm 5	100 \pm 15	n.d.	n.d.
Climbazole		57 \pm 10	86 \pm 12	n.d.	n.d.
Tioconazole		18 \pm 3	44 \pm 5	4.97 \pm 0.64	n.d.
Sertaconazole		35 \pm 3	61 \pm 5	12.73 \pm 1.69	n.d.
Butoconazole		48 \pm 6	50 \pm 6	n.d.	n.d.
Ketoconazole		67 \pm 4 ^a	26 \pm 2 ^a	n.d.	n.d.
Terconazole		97 \pm 6	62 \pm 5	n.d.	n.d.
Posaconazole		88 \pm 11	8 \pm 5	n.d.	0.460 \pm 0.098
Itraconazole		89 \pm 6	4 \pm 3	n.d.	0.139 \pm 0.014

Fig. 2. Structure-activity relationship of azole fungicides inhibiting 11 β -HSDs. 11 β -HSD1-dependent reduction of cortisone (200 nM) to cortisol and 11 β -HSD2-dependent oxidation of cortisol (200 nM) to cortisone were measured using HEK-293 cell lysates in the presence of 500 μ M NADPH or NAD⁺, respectively. Residual enzyme activity upon exposure to 20 μ M test substance (mean \pm SD) and IC₅₀ values (mean \pm SD) were obtained from three independent experiments. For compounds with residual enzyme activities (% of control) >40%, at a compound concentration of 20 μ M, IC₅₀ values were not determined (n.d.). a, values reported earlier by Vuorinen et al. [39].

cially prior to conducting *in vivo* experiments [43,51,56]. Thus, prior to designing a rodent study to assess the effect of the selected azole fungicides on glucocorticoid inactivation, inhibition of 11 β -HSD2 by itraconazole, OHI and posaconazole was further analyzed in rat and mouse kidney homogenates incubated with 50 nM of the rodent substrate corticosterone in the absence or presence of 10 μ M test compound. In a qualitative comparison to the potent activity against recombinant human 11 β -HSD2, which was expressed in HEK-293 cells and measured upon incubation with 200 nM of the human substrate cortisol, considerably lower inhibitory activity was detected against the rat and mouse enzymes. The different concentrations of corticosterone and cortisol used for rodent and human 11 β -HSD2, respectively, reflect the approximately 5–10-fold affinity difference for these substrates [57,58]. Itraconazole (Fig. 4A) and OHI (Fig. 4B) were at least 10-fold less potent towards rat and mouse 11 β -HSD2 compared to the human enzyme, while posaconazole (Fig. 4C) tended to be 2 times less

active against rat 11 β -HSD2 and was about 4 times less active against mouse 11 β -HSD2. Although the activities of the human and rodent enzymes were measured under different conditions, considering their different physiological substrates, the data suggest a higher inhibitory activity of these azole fungicides towards human 11 β -HSD2 compared to the rodent enzymes.

3.5. Inhibition of 11 β -HSD2 in cell models with endogenous enzyme expression

To determine the inhibitory potential of itraconazole, OHI and posaconazole in intact cell systems, SW-620 and MCF-7 cells expressing relatively high endogenous 11 β -HSD2 levels [43] were applied. Itraconazole inhibited 11 β -HSD2 in a concentration-dependent manner with IC₅₀ values of 1.07 \pm 0.29 μ M in SW-620 and 1.19 \pm 0.24 μ M in MCF-7 cells. In contrast to the inhibitory potency ranking observed in lysates of stably transfected HEK-

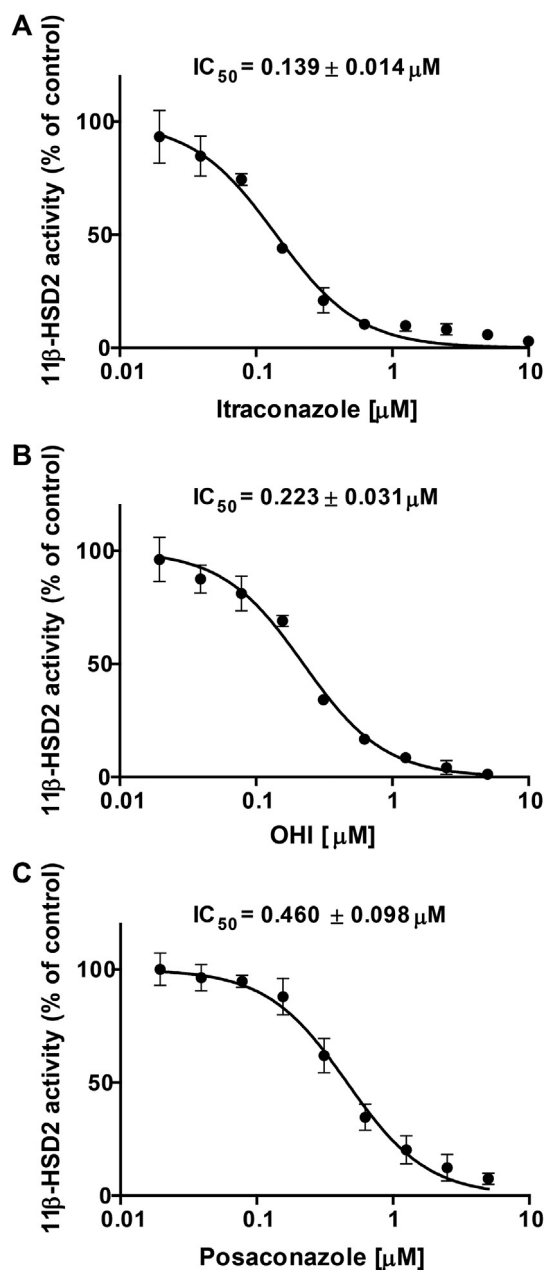


Fig. 3. Inhibition of 11 β -HSD2 enzyme activity determined in HEK-293 cell lysates. Lysates of HEK-293 cells stably expressing recombinant human 11 β -HSD2 were incubated for 10 min at 37 °C with 200 nM radiolabeled cortisol, 500 μ M NAD⁺ and increasing concentrations of itraconazole (A), hydroxyitraconazole (OHI) (B) and posaconazole (C). The substrate conversion was determined and compared to the enzyme activity in the control samples (0.1% DMSO). Data represent mean \pm SD from three independent experiments.

293 cells, OHI was slightly more potent than itraconazole with IC₅₀ values of 0.82 \pm 0.18 μ M in SW-620 and 0.68 \pm 0.20 μ M in MCF-7 cells, respectively. Posaconazole did not substantially inhibit 11 β -HSD2 activity, resulting in approximately 60% and 40% residual 11 β -HSD2 activity in SW-620 and MCF-7 cells at a concentration of 5 μ M.

3.6. Predicted binding of selected fungicides to 11 β -HSD1 and 11 β -HSD2

Docking studies with 11 β -HSD1 showed two important protein-ligand interactions for azole fungicides such as sertaconazole and

itraconazole: a hydrophobic contact with Tyr183 and a hydrogen bond of the azole ring with the backbone nitrogen of Ala172 (Fig. 5A). This hydrogen bond interaction was also the only ligand-coordinating hydrogen bond observed in the 11 β -HSD1 crystal structure co-crystallized with a sulfonyl-piperazine inhibitor and thus, presumably essential for the inhibitory activity. In contrast, terconazole does not form any hydrogen bonds with the binding pocket of 11 β -HSD1. Furthermore, docking of itraconazole and posaconazole revealed steric clashes with Thr124, Thr222 and Ala226 of the 11 β -HSD1 substrate binding pocket, providing an explanation for their inactivity towards 11 β -HSD1. However, a major difference between 11 β -HSD1 and 11 β -HSD2 is the shape of the binding site entry. While Met233 flanks the binding site entry of 11 β -HSD1, Arg212 replaces this amino acid at the analogous position in 11 β -HSD2. The difference in size and electrostatic properties of these amino acids likely influences the inhibitory activity. Indeed, all 11 β -HSD2 active compounds analyzed formed an interaction with Arg212. Furthermore, the extended azole scaffolds were found to form additional interactions in their docking poses with 11 β -HSD2, pointing towards tighter binding to the protein. Interestingly, itraconazole and posaconazole did not fit entirely into the binding site of 11 β -HSD2 but rather lined the surface next to the binding site entry with their azole part (Fig. 5B). Moreover, the additional hydroxyl group of posaconazole was able to form several hydrogen bonds with the phosphate moiety of NADPH.

To rationalize the relative selectivity of the three azole compounds to inhibit human 11 β -HSD2, they were also docked into the murine homology model [49]. The murine 11 β -HSD2 homology model revealed some crucial differences in the amino acid sequence compared to the human 11 β -HSD2. Unlike the equivalent Arg212 on human 11 β -HSD2, Arg279 on mouse 11 β -HSD2 was not flanking the binding pocket entrance but oriented away (Fig. 5C). Furthermore, part of the binding cavity near the cofactor was occupied by Trp276, a residue located outside the binding pocket in human 11 β -HSD2, and this residue caused itraconazole to adopt a different angle within the binding cavity in the docking simulation. Additionally, the docking poses for itraconazole predicted no hydrogen bonds with the protein (Fig. 5D). This missing structural anchoring provides an explanation for the weak activity of this fungicide towards murine 11 β -HSD2. Interestingly, regarding murine 11 β -HSD2, posaconazole and OHI showed greater inhibitory activity than itraconazole. Compared to itraconazole these two fungicides formed interactions with the cofactor via their hydroxyl groups (Fig. 5E).

One important aspect of *in silico*-driven screening studies is the analysis of the predictions and a possible refinement of the model that was used for screening. The screening model performance was very powerful, as all three azole fungicides identified by the model (tioconazole, sertaconazole and butoconazole) inhibited 11 β -HSD1 enzyme activity at a concentration of 20 μ M by at least 50%. However, although itraconazole and posaconazole were represented in the DrugBank, they were not found by the model as virtual hits. A previous refinement study on this model [39], addressed the shape restriction as one major restrictivity aspect. Shape deletion and subsequent VS of all tested compounds, including OHI, with this model retrieved all compounds except for climbazole as hits. For more thorough VS for potential 11 β -HSD inhibitors, the shape-less model version may therefore be more suitable.

4. Discussion

Molecular modeling-based *in silico* approaches are important in drug development for the identification of bioactive molecules. Pharmacophore-based VS is a powerful strategy to enrich poten-

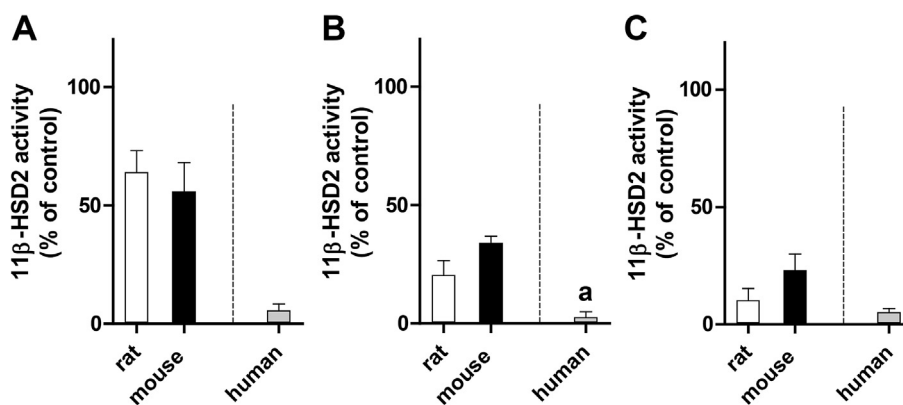


Fig. 4. Inhibition of rat and mouse 11 β -HSD2 activity measured in kidney homogenates, compared to human 11 β -HSD2 in HEK-293 cell lysates. Rat and mouse kidney homogenates were incubated for 20 min at 37 °C with 50 nM radiolabeled corticosterone in the absence or presence of 10 μ M itraconazole (A), 10 μ M hydroxyitraconazole (OHI) (B) or 10 μ M posaconazole (C). Human 11 β -HSD2 activity was measured in HEK-293 cells stably expressing recombinant human 11 β -HSD2 upon incubation for 10 min at 37 °C with 200 nM radiolabeled cortisol, 500 μ M NAD⁺ and the corresponding concentration of azole fungicide (10 μ M itraconazole, 10 μ M posaconazole or 5 μ M OHI). The substrate conversion was calculated (in nmoles/min) and normalized to the enzyme activity in the control sample (0.1% DMSO). Data represent mean \pm SD from at least three independent experiments. a, 5 μ M was used (due to complete inhibition higher concentrations were not analyzed).

tially active compounds among a large number of test compounds, thereby facilitating the identification of drug lead structures [59]. Such *in silico* tools are also applied in anti-target screenings; however, in contrast to lead compound identification this is more challenging since this approach aims to identify all potentially harmful substances. The present study applied a pharmacophore model based on 11 β -HSD1 crystal structures for VS of the DrugBank database to find approved drugs that might inhibit 11 β -HSD2, an enzyme not included in current off-target screenings during drug development. The goal was to identify, as a first step, structural compound classes inhibiting 11 β -HSD2, followed by a more detailed analysis of a selected compound class including an *in vitro* validation of selected virtual hits.

The pharmacophore model used in this study demonstrated already earlier high predictive power [60], and azole fungicides have been previously associated with 11 β -HSDs: The azole fungicide triadimefon was reported to be a substrate of 11 β -HSD1 (K_m 3.5 μ M), thereby acting as a weak competitive inhibitor (IC₅₀ 15 μ M) [51]. Ketoconazole was found to have weak inhibitory effects towards 11 β -HSD1 and 11 β -HSD2 [39,61]. Thus, this compound class was chosen for further investigations. Biological evaluation revealed several azole fungicides as 11 β -HSD inhibitors, showing a significant structure-activity relationship between azole scaffold size and 11 β -HSD enzyme selectivity and potency of inhibition. The large scaffolds of itraconazole and posaconazole, which were not initial VS hits, potently inhibited 11 β -HSD2 enzyme activity. Compared to terconazole, which was considerably less active on 11 β -HSD2, itraconazole and posaconazole contain an extended hydrophobic central region and an additional triazolone side chain, which may form additional stabilizing interactions with the binding pocket, including Arg212, thereby providing an explanation for the potent inhibition. Thus, the VS approach has proven useful to identify azole fungicides as 11 β -HSD2 inhibitors and to prioritize this compound class for further biological analyses, which were necessary to identify the most potent compounds itraconazole and posaconazole.

Itraconazole and posaconazole are clinically used for the prophylaxis and treatment of systemic mycotic infections and exert their mode of action by inhibiting the biosynthesis of ergosterol, an essential component of the fungal cell membrane [62,63]. They can be applied for a prolonged period of time, up to years when used as prophylactic treatment, especially in immunosuppressed patients [64]. After oral exposure, itraconazole is extensively metabolized in the liver by cytochrome P450 3A4 (CYP3A4) to its

main metabolite OHI, which retains potent 11 β -HSD2 inhibitory activity. Thus, cortisol-dependent MR and GR activation due to prolonged 11 β -HSD2 inhibition may contribute to the observed adverse effects of these fungicides. In contrast to itraconazole, hepatic metabolism of posaconazole plays a minor role and mainly involves conjugation by UDP-glucuronyltransferase UGT1A4 [65]. Although posaconazole is not a substrate of CYP3A4, it acts like itraconazole and OHI as a potent CYP3A4 inhibitor and it is therefore prone to considerable pharmacokinetic interactions with CYP3A4 substrates, including glucocorticoids [66,67]. Inhibition of CYP3A4 by a single dose of itraconazole was shown to significantly decrease the formation clearance (CL_f) of the metabolites 6 β -hydroxycortisol and 6 β -hydroxycortisone [68]. Plasma cortisol and cortisone concentrations were not altered, indicating negative feedback regulation by the HPA axis and suggesting that cortisol levels are locally increased in CYP3A4 expressing tissues, particularly in the liver. Itraconazole, OHI and posaconazole might further promote local glucocorticoid effects by inhibiting P-glycoprotein (P-gp) mediated cortisol efflux [69,70]. Besides its important role in the liver, P-gp expression has been detected in the human placenta from the first trimester to full-term [71] and P-gp was shown *in vitro* to support the placental 11 β -HSD2 glucocorticoid barrier [72].

Inhibition of 11 β -HSD2 by itraconazole and posaconazole might impair glucocorticoid inactivation in the kidney, colon, vasculature and placenta. Indeed, Denolle et al. reported a case study of a patient on long-term itraconazole treatment developing hypokalemia, edema, hypertension, low plasma renin and aldosterone concentrations and normal serum cortisol, typical symptoms of AME as a result of cortisol-dependent MR activation [73]. Similar side effects including hypokalemia, edema, hypertension and mildly reduced aldosterone serum levels were described by Sharkey et al. for several patients during long-term itraconazole use [74]. Importantly, the drug safety sheet of Sporanox[®] (itraconazole) reports hypokalemia and edema as occasionally (\geq 1/1000, <1/100 patients) occurring, whereas the safety sheet for the *i.v.* solution of Noxafil[®] (posaconazole) notes hypokalemia as one of the most likely occurring adverse effect (22% of the reports) and a rise in blood pressure as frequent (1/100, <1/10) [75,76].

Due to the high plasma protein binding capacity of itraconazole (99.8%), OHI (99.6%) and posaconazole (\geq 98%), predominately to albumin, the circulating fraction of unbound drug is low [75,76]. However, in specific situations the plasma protein binding capacity can be reduced. Pregnancy leads to several metabolic and physio-

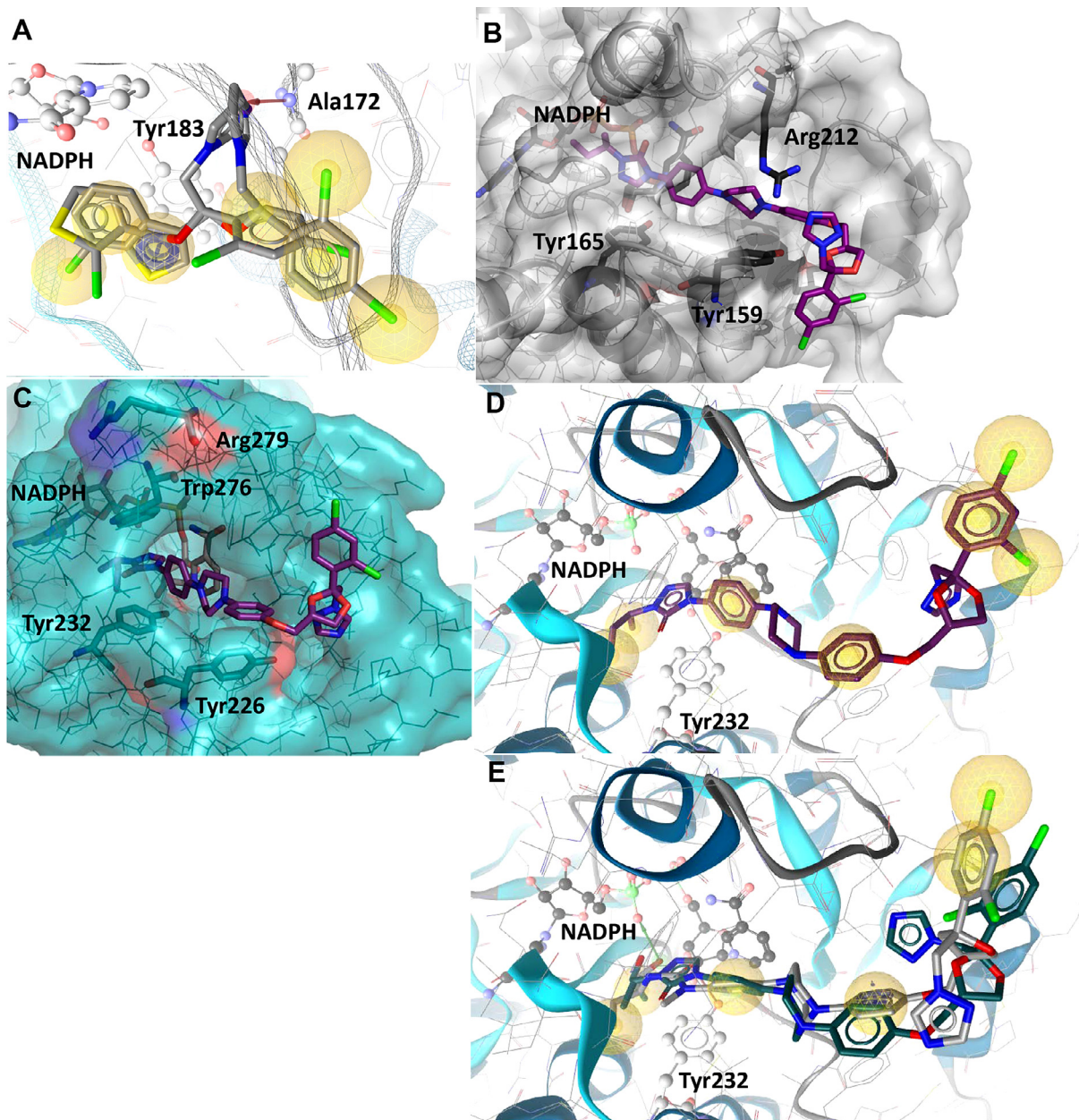


Fig. 5. Predicted binding of selected fungicides to 11 β -HSD1 and 11 β -HSD2. (A) Representative binding poses of inhibitors in human 11 β -HSD1 exemplified by tioconazole and sertaconazole. Important interactions for protein-ligand binding and the cofactor are shown in ball-and-stick style. Hydrophobic contacts between the ligand and the binding site are represented as yellow spheres, the HBA to Ala172 as red arrow and the aromatic stacking with Tyr183 as blue circle. (B) Binding mode of itraconazole docked into the homology model of human 11 β -HSD2. (C) Itraconazole docked into the homology model of murine 11 β -HSD2. Arg279 (equivalent to Arg212 in human 11 β -HSD2) is pointing away from the binding pocket, while Trp276 blocks the binding pocket next to the cofactor NADPH. (D) Itraconazole docked into the homology model of murine 11 β -HSD2. The ligand is not anchored via hydrogen bonds or charged interactions, only hydrophobic contacts (yellow spheres) are formed. (E) Posaconazole (grey) and OHI (green) docked into murine 11 β -HSD2. Their hydroxyl groups form hydrogen bonds (green arrow) with the cofactor, which provides an explanation for their higher activity compared to itraconazole.

logic changes, including a decrease in serum albumin levels to about half of those in non-pregnant women. Considering this change, the unbound fraction of itraconazole/OHI and of posaconazole in plasma at steady state conditions during 200 mg b.d.i. itraconazole or 400 mg b.d.i. posaconazole treatment [75,77] can be roughly estimated to reach IC₂₅ values of itraconazole (78 nM) and posaconazole (237 nM) for 11 β -HSD2 as determined in HEK-293 cell lysates. Despite the high plasma protein binding ability, extensive extravascular distribution and accumulation in tissues are of considerable importance for these lipophilic compounds. Itraconazole was found to exceed plasma concentrations in fat tissue approximately 17-fold and in lung, liver, muscle and kidney

about 2–3-fold [64]. Less data are available for posaconazole, although it was shown that posaconazole concentrations are 31–42-fold higher in pulmonary alveolar cells compared with plasma [78]. Thus, the concentration of these triazole fungicides might also be elevated in placental tissue compared with plasma and therefore may reach relevant concentrations to inhibit 11 β -HSD2 enzyme activity.

Animal studies revealed embryotoxicity and teratogenicity with craniofacial and skeletal anomalies at concentrations exceeding those obtained at the maximum recommended human dose by 5–20-fold during itraconazole treatment but at concentrations lower than those observed at therapeutic doses during posaconazole

zole treatment [75,76]. Therefore, it is recommended to use these drugs in pregnancy only if the benefit outweighs the potential risk. Extrapolation of findings from animal studies to human is often difficult due to species-specific differences. The present study provides evidence for a considerably weaker inhibition of mouse and rat 11 β -HSD2 by itraconazole and OHI, and lower activity of posaconazole towards the rodent enzymes. Thus, 11 β -HSD2-related effects on electrolyte balance, cardiovascular system and placental barrier function would be detected in rodent models only at much higher concentrations than in humans. Furthermore, regarding the latter, animal studies might be unreliable due to the highly variable 11 β -HSD2 expression levels during gestation between different species. Mouse placental 11 β -HSD2 mRNA drops towards late gestation, while rat placental 11 β -HSD2 reduction occurs later and less pronounced. In contrast, human placental 11 β -HSD2 levels are rising during gestation (reviewed by [13]).

In a prospective cohort study, de Santis et al. evaluated first trimester exposure to itraconazole in 206 pregnant women compared with 207 unexposed controls [79]. The mean duration of the therapy was 6.9 ± 6.4 days with a daily dose of 182 ± 63 mg. No statistical difference between the exposed and the control group was found in terms of major congenital anomalies, premature birth or birth weight, but rates of live births and spontaneous abortion were higher in the exposed group. Bar-Oz et al. reported in a retrospective cohort study four times higher congenital malformation rates after first trimester exposure to itraconazole; however, strongly suggesting reporting bias due to retrospective data analysis [80]. The same authors found no difference in the rate of malformations compared to the control in a prospective cohort study with 229 women exposed to 50–800 mg itraconazole daily throughout 8.5 ± 12.4 days during the first trimester of pregnancy [81]. However, the rate live birth and the mean birth weight were lower in the exposed group compared to the control. No human data for prenatal posaconazole exposure have been published so far.

Developmental programming implies that an environmental factor affects fetal development during a sensitive time window to predispose the fetus towards diseases permanently throughout life [15]. A critical parameter includes the duration of the exposure to an environmental factor. The mean prenatal itraconazole exposure reported by de Santis et al. and Bar-Oz et al. was 6.9–8.5 days, thus shorter than the 15 days of treatment needed to reach plasma steady-state levels of itraconazole. This is important regarding 11 β -HSD2 inhibition and thus prenatal programming through glucocorticoids. Several investigations found a reduction in birth weight in infants exposed to multiple courses of antenatal glucocorticoid therapy when adjusting for gestational age [82–84]. In addition, only first trimester itraconazole exposures were examined in the above described studies, but the effects of dexamethasone exposure on birth weight in rats was reported to be more pronounced when administered during later stages of pregnancy [85]. Chronic glucocorticoid treatment in mice was observed to impair the development of the cerebellum through inhibition of Sonic hedgehog (Shh) induced proliferation, a pathway important during embryonic growth and postembryonic tissue homeostasis. By upregulation of 11 β -HSD2 expression Shh signaling partly antagonized the glucocorticoid-dependent effects, thus representing a feedback mechanism [86]. Interestingly, itraconazole, OHI and posaconazole were found to inhibit Shh signaling [87–89], which may result in downregulation of 11 β -HSD2 expression, thereby adding to the direct inhibitory effect of these azole fungicides.

Elevated glucocorticoid levels are known to inhibit angiogenesis, a crucial process during placental development that was shown to be inhibited by itraconazole [88,90,91]. Insufficient placental vascularization has been associated with intrauterine growth

restriction, preeclampsia and fetal death, both in human and animal studies (reviewed by [92]).

In conclusion, itraconazole, OHI and posaconazole were identified as novel potent inhibitors of human 11 β -HSD2 by VS of the DrugBank database using an 11 β -HSD pharmacophore model. Inhibition of placental 11 β -HSD2 by these azole fungicides might contribute to an elevated local increase in cortisol levels, in addition to the known inhibition of cytochrome P450 enzymes and P-gp, thereby affecting fetal programming. Due to the observed species-specific differences, the consequences of placental 11 β -HSD2 inhibition may have been overlooked in preclinical studies using rodents, although similar biological responses might be detected in rodents, albeit at higher concentrations.

Conflicts of interest

The authors declare no conflict of interest.

Acknowledgements

This work was supported by the Swiss National Science Foundation No 31003A-159454, the Austrian Science Fund (P26782), the Swiss Center for Applied Human Toxicology (SCAHT) and the Swiss Federal Office of Public Health (FOPH). A.O. was supported as Chair for Molecular and Systems Toxicology by the Novartis Research Foundation. D.S. is an Ingeborg Hochmair Professor at the University of Innsbruck. We thank Prof. Thierry Langer, University of Vienna, and Inte:Ligand GmbH for providing the LigandScout software.

References

- [1] A. Odermatt, D.V. Kratschmar, Tissue-specific modulation of mineralocorticoid receptor function by 11 β -hydroxysteroid dehydrogenases: an overview, *Mol. Cell. Endocrinol.* 350 (2) (2012) 168–186.
- [2] P. Ferrari, The role of 11 β -hydroxysteroid dehydrogenase type 2 in human hypertension, *Biochim. Biophys. Acta* 2010 (1802) 1178–1187.
- [3] P.C. White, T. Mune, A.K. Agarwal, 11 β -Hydroxysteroid dehydrogenase and the syndrome of apparent mineralocorticoid excess, *Endocr. Rev.* 18 (1) (1997) 135–156.
- [4] M.I. New, L.S. Levine, E.G. Biglieri, J. Pareira, S. Ulick, Evidence for an unidentified steroid in a child with apparent mineralocorticoid hypertension, *J. Clin. Endocrinol. Metab.* 44 (5) (1977) 924–933.
- [5] T. Mune, F.M. Rogerson, H. Nikkila, A.K. Agarwal, P.C. White, Human hypertension caused by mutations in the kidney isozyme of 11 β -hydroxysteroid dehydrogenase, *Nat. Genet.* 10 (4) (1995) 394–399.
- [6] S. Dave-Sharma, R.C. Wilson, M.D. Harbison, R. Newfield, M.R. Azar, Z.S. Krozowski, J.W. Funder, C.H. Shackleton, H.L. Bradlow, J.Q. Wei, J. Hertecant, A. Moran, R.E. Neiberger, J.W. Balfe, A. Fattah, D. Daneman, H.I. Akkurt, C. DeSantis, M.I. New, Examination of genotype and phenotype relationships in 14 patients with apparent mineralocorticoid excess, *J. Clin. Endocrinol. Metab.* 83 (7) (1998) 2244–2254.
- [7] E.P. Gomez-Sanchez, C.E. Gomez-Sanchez, Central hypertensinogenic effects of glycyrrhizic acid and carbenoxolone, *Am. J. Physiol.* 263 (6 Pt 1) (1992). E1125–30.
- [8] I.Z. Beitins, F. Bayard, I.G. Ances, A. Kowarski, C.J. Migeon, The metabolic clearance rate, blood production, interconversion and transplacental passage of cortisol and cortisone in pregnancy near term, *Pediatr. Res.* 7 (5) (1973) 509–519.
- [9] R. Gitau, A. Cameron, N.M. Fisk, V. Glover, Fetal exposure to maternal cortisol, *Lancet* 352 (9129) (1998) 707–708.
- [10] R.W. Brown, K.E. Chapman, Y. Kotelevtsev, J.L. Yau, R.S. Lindsay, L. Brett, C. Leckie, P. Murad, V. Lyons, J.J. Mullins, C.R. Edwards, J.R. Seckl, Cloning and production of antisera to human placental 11 β -hydroxysteroid dehydrogenase type 2, *Biochem. J.* 313 (Pt 3) (1996) 1007–1017.
- [11] R. Benediktsson, A.A. Calder, C.R. Edwards, J.R. Seckl, Placental 11 β -hydroxysteroid dehydrogenase: a key regulator of fetal glucocorticoid exposure, *Clin. Endocrinol. (Oxf)* 46 (2) (1997) 161–166.
- [12] J. Jung, J.T. Ho, D.J. Torpy, A. Rogers, M. Doogue, J.G. Lewis, R.J. Czajko, W.J. Linder, A longitudinal study of plasma and urinary cortisol in pregnancy and postpartum, *J. Clin. Endocrinol. Metab.* 96 (5) (2011) 1533–1540.
- [13] A. Harris, J. Seckl, Glucocorticoids, prenatal stress and the programming of disease, *Horm. Behav.* 59 (3) (2011) 279–289.
- [14] E.C. Cottrell, J.R. Seckl, M.C. Holmes, C.S. Wyrwoll, Foetal and placental 11 β -HSD2: a hub for developmental programming, *Acta Physiol. (Oxf)* 210 (2) (2014) 288–295.

- [15] D.J. Barker, The developmental origins of adult disease, *J. Am. Coll. Nutr.* 23 (Suppl. 6) (2004) 588S–595S.
- [16] D.I. Phillips, D.J. Barker, C.H. Fall, J.R. Seckl, C.B. Whorwood, P.J. Wood, B.R. Walker, Elevated plasma cortisol concentrations: a link between low birth weight and the insulin resistance syndrome? *J. Clin. Endocrinol. Metab.* 83 (3) (1998) 757–760.
- [17] N.P. French, R. Hagan, S.F. Evans, M. Godfrey, J.P. Newnham, Repeated antenatal corticosteroids: size at birth and subsequent development, *Am. J. Obstet. Gynecol.* 180 (1 Pt 1) (1999) 114–121.
- [18] J.R. Seckl, Prenatal glucocorticoids and long-term programming, *Eur. J. Endocrinol.* 151 (Suppl. 3) (2004) U49–U62.
- [19] M. Shams, M.D. Kilby, D.A. Somerset, A.J. Howie, A. Gupta, P.J. Wood, M. Afnan, P.M. Stewart, 11 β -Hydroxysteroid dehydrogenase type 2 in human pregnancy and reduced expression in intrauterine growth restriction, *Hum. Reprod.* 13 (4) (1998) 799–804.
- [20] R. Benediktsson, R.S. Lindsay, J. Noble, J.R. Seckl, C.R. Edwards, Glucocorticoid exposure in utero: new model for adult hypertension, *Lancet* 341 (8841) (1993) 339–341.
- [21] J. Dy, H. Guan, R. Sampath-Kumar, B.S. Richardson, K. Yang, Placental 11 β -hydroxysteroid dehydrogenase type 2 is reduced in pregnancies complicated with idiopathic intrauterine growth restriction: evidence that this is associated with an attenuated ratio of cortisone to cortisol in the umbilical artery, *Placenta* 29 (2) (2008) 193–200.
- [22] C.L. McTernan, N. Draper, H. Nicholson, S.M. Chalder, P. Driver, M. Hewison, M. D. Kilby, P.M. Stewart, Reduced placental 11 β -hydroxysteroid dehydrogenase type 2 mRNA levels in human pregnancies complicated by intrauterine growth restriction: an analysis of possible mechanisms, *J. Clin. Endocrinol. Metab.* 86 (10) (2001) 4979–4983.
- [23] R. Benediktsson, J. Brennan, L. Tibi, A.A. Calder, J.R. Seckl, C.R. Edwards, Fetal osteocalcin levels are related to placental 11 β -hydroxysteroid dehydrogenase activity in humans, *Clin. Endocrinol. (Oxf)* 42 (5) (1995) 551–555.
- [24] A.G. Rebuffat, S. Tam, A.R. Nawrocki, M.E. Baker, B.M. Frey, F.J. Frey, A. Odermatt, The 11-ketosteroid 11-ketodexamethasone is a glucocorticoid receptor agonist, *Mol. Cell. Endocrinol.* 214 (1–2) (2004) 27–37.
- [25] L.A. Welberg, J.R. Seckl, M.C. Holmes, Prenatal glucocorticoid programming of brain corticosteroid receptors and corticotrophin-releasing hormone: possible implications for behaviour, *Neuroscience* 104 (1) (2001) 71–79.
- [26] L.A. Welberg, J.R. Seckl, M.C. Holmes, Inhibition of 11 β -hydroxysteroid dehydrogenase, the foeto-placental barrier to maternal glucocorticoids, permanently programs amygdala GR mRNA expression and anxiety-like behaviour in the offspring, *Eur. J. Neurosci.* 12 (3) (2000) 1047–1054.
- [27] R.S. Lindsay, R.M. Lindsay, C.R. Edwards, J.R. Seckl, Inhibition of 11 β -hydroxysteroid dehydrogenase in pregnant rats and the programming of blood pressure in the offspring, *Hypertension* 27 (6) (1996) 1200–1204.
- [28] C.S. Wyrwoll, J.R. Seckl, M.C. Holmes, Altered placental function of 11 β -hydroxysteroid dehydrogenase 2 knockout mice, *Endocrinology* 150 (3) (2009) 1287–1293.
- [29] J. Mairesse, J. Lesage, C. Breton, B. Breant, T. Hahn, M. Darnaudery, S.L. Dickson, J. Seckl, B. Blondeau, D. Vieau, S. Maccari, O. Viltart, Maternal stress alters endocrine function of the foeto-placental unit in rats, *Am. J. Physiol. Endocrinol. Metab.* 292 (6) (2007) E1526–E1533.
- [30] S.C. Langley-Evans, G.J. Phillips, R. Benediktsson, D.S. Gardner, C.R. Edwards, A. A. Jackson, J.R. Seckl, Protein intake in pregnancy, placental glucocorticoid metabolism and the programming of hypertension in the rat, *Placenta* 17 (2–3) (1996) 169–172.
- [31] D. Vieau, N. Sebaai, M. Leonhardt, I. Dutriez-Casteloot, O. Molendi-Coste, C. Laborie, C. Breton, S. Deloof, J. Lesage, HPA axis programming by maternal undernutrition in the male rat offspring, *Psychoneuroendocrinology* 32 (Suppl. 1) (2007) S16–S20.
- [32] J.R. Seckl, M.C. Holmes, Mechanisms of disease: glucocorticoids, their placental metabolism and fetal 'programming' of adult pathophysiology, *Nat. Clin. Pract. Endocrinol. Metab.* 3 (6) (2007) 479–488.
- [33] A. Odermatt, C. Gury, Glucocorticoid and mineralocorticoid action: why should we consider influences by environmental chemicals? *Biochem. Pharmacol.* 76 (10) (2008) 1184–1193.
- [34] T.E. Strandberg, S. Andersson, A.L. Jarvenpaa, P.M. McKeigue, Preterm birth and licorice consumption during pregnancy, *Am. J. Epidemiol.* 156 (9) (2002) 803–805.
- [35] K. Raikonen, J.R. Seckl, K. Heinonen, R. Pyhala, K. Feldt, A. Jones, A.K. Pesonen, D.I. Phillips, J. Lahti, A.L. Jarvenpaa, J.G. Eriksson, K.A. Matthews, T.E. Strandberg, E. Kajantie, Maternal prenatal licorice consumption alters hypothalamic-pituitary-adrenocortical axis function in children, *Psychoneuroendocrinology* 35 (10) (2010) 1587–1593.
- [36] K. Raikonen, A.K. Pesonen, K. Heinonen, J. Lahti, N. Komi, J.G. Eriksson, J.R. Seckl, A.L. Jarvenpaa, T.E. Strandberg, Maternal licorice consumption and detrimental cognitive and psychiatric outcomes in children, *Am. J. Epidemiol.* 170 (9) (2009) 1137–1146.
- [37] E. Schoof, M. Girstl, W. Frobenius, M. Kirschbaum, H.G. Dorr, W. Rascher, J. Dotsch, Decreased gene expression of 11 β -hydroxysteroid dehydrogenase type 2 and 15-hydroxyprostaglandin dehydrogenase in human placenta of patients with preeclampsia, *J. Clin. Endocrinol. Metab.* 86 (3) (2001) 1313–1317.
- [38] M. Aufdenblatten, M. Baumann, L. Raio, B. Dick, B.M. Frey, H. Schneider, D. Surbek, B. Hochar, M.G. Mohaupt, Prematurity is related to high placental cortisol in preeclampsia, *Pediatr. Res.* 65 (2) (2009) 198–202.
- [39] A. Vuorinen, L.G. Nashev, A. Odermatt, J.M. Rollinger, D. Schuster, Pharmacophore model refinement for 11 β -hydroxysteroid dehydrogenase inhibitors: search for modulators of intracellular glucocorticoid concentrations, *Mol. Inform.* 33 (1) (2014) 15–25.
- [40] D. Schuster, E.M. Maurer, C. Laggner, L.G. Nashev, T. Wilckens, T. Langer, A. Odermatt, The discovery of new 11 β -hydroxysteroid dehydrogenase type 1 inhibitors by common feature pharmacophore modeling and virtual screening, *J. Med. Chem.* 49 (12) (2006) 3454–3466.
- [41] D.V. Kratschmar, A. Vuorinen, T. Da Cunha, G. Wolber, D. Classen-Houben, O. Doblhoff, D. Schuster, A. Odermatt, Characterization of activity and binding mode of glycyrrhetic acid derivatives inhibiting 11 β -hydroxysteroid dehydrogenase type 2, *J. Steroid Biochem. Mol. Biol.* 125 (1–2) (2011) 129–142.
- [42] A.G. Atanasov, S. Tam, J.M. Rocken, M.E. Baker, A. Odermatt, Inhibition of 11 β -hydroxysteroid dehydrogenase type 2 by dithiocarbamates, *Biochem. Biophys. Res. Commun.* 308 (2) (2003) 257–262.
- [43] C. Furstenberger, A. Vuorinen, T. Da Cunha, D.V. Kratschmar, M. Saugy, D. Schuster, A. Odermatt, The anabolic androgenic steroid fluoxymesterone inhibits 11 β -hydroxysteroid dehydrogenase 2-dependent glucocorticoid inactivation, *Toxicol. Sci.* 126 (2) (2012) 353–361.
- [44] A. Vuorinen, R. Engeli, A. Meyer, F. Bachmann, U.J. Gressler, D. Schuster, A. Odermatt, Ligand-based pharmacophore modeling and virtual screening for the discovery of novel 17 β -hydroxysteroid dehydrogenase 2 inhibitors, *J. Med. Chem.* 57 (14) (2014) 5995–6007.
- [45] P.K. Smith, R.I. Krohn, G.T. Hermanson, A.K. Mallia, F.H. Gartner, M.D. Provenzano, E.K. Fujimoto, N.M. Goeke, B.J. Olson, D.C. Klenk, Measurement of protein using bicinchoninic acid, *Anal. Biochem.* 150 (1) (1985) 76–85.
- [46] G. Jones, P. Willett, R.C. Glen, A.R. Leach, R. Taylor, Development and validation of a genetic algorithm for flexible docking, *J. Mol. Biol.* 267 (3) (1997) 727–748.
- [47] Z.K. Wan, E. Chenail, J. Xiang, H.Q. Li, M. Ipek, J. Bard, K. Svenson, T.S. Mansour, X. Xu, X. Tian, V. Suri, S. Hahn, Y. Xing, C.E. Johnson, X. Li, A. Qadri, D. Panza, M. Perreault, J.F. Tobin, E. Saiah, Efficacious 11 β -hydroxysteroid dehydrogenase type I inhibitors in the diet-induced obesity mouse model, *J. Med. Chem.* 52 (17) (2009) 5449–5461.
- [48] H. Yamaguchi, T. Akitaya, T. Yu, Y. Kidachi, K. Kamiie, T. Noshita, H. Umetsu, K. Ryoyama, Homology modeling and structural analysis of 11 β -hydroxysteroid dehydrogenase type 2, *Eur. J. Med. Chem.* 46 (4) (2011) 1325–1330.
- [49] H. Yamaguchi, T. Akitaya, Y. Kidachi, K. Kamiie, T. Noshita, H. Umetsu, K. Ryoyama, Mouse 11 β -hydroxysteroid dehydrogenase type 2 for human application: homology modeling, structural analysis and ligand-receptor interaction, *Cancer Inform.* 10 (2011) 287–295.
- [50] G. Wolber, T. Langer, LigandScout: 3-D pharmacophores derived from protein-bound ligands and their use as virtual screening filters, *J. Chem. Inf. Model.* 45 (1) (2005) 160–169.
- [51] A. Meyer, A. Vuorinen, A.E. Zielinska, T. Da Cunha, P. Strajhar, G.G. Lavery, D. Schuster, A. Odermatt, Carbonyl reduction of triadimefon by human and rodent 11 β -hydroxysteroid dehydrogenase 1, *Biochem. Pharmacol.* 85 (9) (2013) 1370–1378.
- [52] T. Kaserer, K.R. Beck, M. Akram, A. Odermatt, D. Schuster, Pharmacophore models and pharmacophore-based virtual screening: concepts and applications exemplified on hydroxysteroid dehydrogenases, *Molecules* 20 (12) (2015) 22799–22832.
- [53] A.G. Atanasov, L.G. Nashev, S. Tam, M.E. Baker, A. Odermatt, Organotins disrupt the 11 β -hydroxysteroid dehydrogenase type 2-dependent local inactivation of glucocorticoids, *Environ. Health Perspect.* 113 (11) (2005) 1600–1606.
- [54] M.V. Mustonen, V.V. Isomaa, T. Huskivu, J. Tapanainen, M.H. Poutanen, F. Stenback, R.K. Vihko, P.T. Vihko, Human 17 β -hydroxysteroid dehydrogenase type 2 messenger ribonucleic acid expression and localization in term placenta and in endometrium during the menstrual cycle, *J. Clin. Endocrinol. Metab.* 83 (4) (1998) 1319–1324.
- [55] J. Takeyama, H. Sasano, T. Suzuki, K. Inuma, H. Nagura, S. Andersson, 17 β -hydroxysteroid dehydrogenase types 1 and 2 in human placenta: an immunohistochemical study with correlation to placental development, *J. Clin. Endocrinol. Metab.* 83 (10) (1998) 3710–3715.
- [56] S. Arampatzis, B. Kadereit, D. Schuster, Z. Balazs, R.A. Schweizer, F.J. Frey, T. Langer, A. Odermatt, Comparative enzymology of 11 β -hydroxysteroid dehydrogenase type 1 from six species, *J. Mol. Endocrinol.* 35 (1) (2005) 89–101.
- [57] A.G. Atanasov, I.D. Ignatova, L.G. Nashev, B. Dick, P. Ferrari, F.J. Frey, A. Odermatt, Impaired protein stability of 11 β -hydroxysteroid dehydrogenase type 2: a novel mechanism of apparent mineralocorticoid excess, *J. Am. Soc. Nephrol.* 18 (4) (2007) 1262–1270.
- [58] P. Ferrari, R.E. Smith, J.W. Funder, Z.S. Krozowski, Substrate and inhibitor specificity of the cloned human 11 β -hydroxysteroid dehydrogenase type 2 isoform, *Am. J. Physiol.* 270 (5 Pt 1) (1996) E900–E904.
- [59] D. Schuster, 3D pharmacophores as tools for activity profiling, *Drug Discov. Today Technol.* 7 (4) (2010) 205–211.
- [60] L.G. Nashev, A. Vuorinen, L. Praxmarer, B. Chantong, D. Cereghetti, R. Winiger, D. Schuster, A. Odermatt, Virtual screening as a strategy for the identification of xenobiotics disrupting corticosteroid action, *PLoS One* 7 (10) (2012) e46958.
- [61] S. Diederich, C. Grossmann, B. Hanke, M. Quinkler, M. Herrmann, V. Bahr, W. Oelkers, In the search for specific inhibitors of human 11 β -hydroxysteroid-dehydrogenases (11 β -HSDs): chenodeoxycholic acid selectively inhibits 11 β -HSD-I, *Eur. J. Endocrinol.* 142 (2) (2000) 200–207.
- [62] M.I. Morris, Posaconazole: a new oral antifungal agent with an expanded spectrum of activity, *Am. J. Health Syst. Pharm.* 66 (3) (2009) 225–236.
- [63] N.H. Georgopadakou, T.J. Walsh, Antifungal agents: chemotherapeutic targets and immunologic strategies, *Antimicrob. Agents Chemother.* 40 (2) (1996) 279–291.

- [64] L. Willems, R. van der Geest, K. de Beule, Itraconazole oral solution and intravenous formulations: a review of pharmacokinetics and pharmacodynamics, *J. Clin. Pharm. Ther.* 26 (3) (2001) 159–169.
- [65] A. Ghosal, N. Hapangama, Y. Yuan, J. Achanfuo-Yeboah, R. Iannucci, S. Chowdhury, K. Alton, J.E. Patrick, S. Zbaida, Identification of human UDP-glucuronosyltransferase enzyme(s) responsible for the glucuronidation of posaconazole (Noxafil), *Drug Metab. Dispos.* 32 (2) (2004) 267–271.
- [66] N. Isoherranen, K.L. Kunze, K.E. Allen, W.L. Nelson, K.E. Thummel, Role of itraconazole metabolites in CYP3A4 inhibition, *Drug Metab. Dispos.* 32 (10) (2004) 1121–1131.
- [67] D. Wexler, R. Courtney, W. Richards, C. Banfield, J. Lim, M. Laughlin, Effect of posaconazole on cytochrome P450 enzymes: a randomized, open-label, two-way crossover study, *Eur. J. Pharm. Sci.* 21 (5) (2004) 645–653.
- [68] C.C. Peng, I. Templeton, K.E. Thummel, C. Davis, K.L. Kunze, N. Isoherranen, Evaluation of 6 β -hydroxycortisol, 6 β -hydroxycortisone, and a combination of the two as endogenous probes for inhibition of CYP3A4 in vivo, *Clin. Pharmacol. Ther.* 89 (6) (2011) 888–895.
- [69] L.M. Vermeer, C.D. Isringhausen, B.W. Ogilvie, D.B. Buckley, Evaluation of ketoconazole and its alternative clinical CYP3A4/5 inhibitors as inhibitors of drug transporters: the in vitro effects of ketoconazole, ritonavir, clarithromycin, and itraconazole on 13 clinically-relevant drug transporters, *Drug Metab. Dispos.* 44 (3) (2016) 453–459.
- [70] A.H. Saad, D.D. DePestel, P.L. Carver, Factors influencing the magnitude and clinical significance of drug interactions between azole antifungals and select immunosuppressants, *Pharmacotherapy* 26 (12) (2006) 1730–1744.
- [71] M. Ceckova-Novotna, P. Pavek, F. Staud, P-glycoprotein in the placenta: expression, localization, regulation and function, *Reprod. Toxicol.* 22 (3) (2006) 400–410.
- [72] P.J. Mark, B.J. Waddell, P-glycoprotein restricts access of cortisol and dexamethasone to the glucocorticoid receptor in placental BeWo cells, *Endocrinology* 147 (11) (2006) 5147–5152.
- [73] T. Denolle, M. Azizi, C. Massart, M.C. Zennaro, Itraconazole: a new drug-related cause of hypertension, *Ann. Cardiol. Angeiol. (Paris)* 63 (3) (2014) 213–215.
- [74] P.K. Sharkey, M.G. Rinaldi, J.F. Dunn, T.C. Hardin, R.J. Fetchick, J.R. Graybill, High-dose itraconazole in the treatment of severe mycoses, *Antimicrob. Agents Chemother.* 35 (4) (1991) 707–713.
- [75] Janssen-Cilag-AG, *Sporanox drug safety sheet*, (2015).
- [76] MSD-MERCK-SHARP&DOHME-AG, *NOXAFIL Inf Konz 18 mg/ml drug safety sheet*, (2014).
- [77] R. Courtney, S. Pai, M. Laughlin, J. Lim, V. Batra, Pharmacokinetics, safety, and tolerability of oral posaconazole administered in single and multiple doses in healthy adults, *Antimicrob. Agents Chemother.* 47 (9) (2003) 2788–2795.
- [78] J.E. Conte Jr., J.A. Golden, G. Krishna, M. McIver, E. Little, E. Zurlinden, Intrapulmonary pharmacokinetics and pharmacodynamics of posaconazole at steady state in healthy subjects, *Antimicrob. Agents Chemother.* 53 (2) (2009) 703–707.
- [79] M. De Santis, E. Di Gianantonio, E. Cesari, G. Ambrosini, G. Straface, M. Clementi, First-trimester itraconazole exposure and pregnancy outcome: a prospective cohort study of women contacting teratology information services in Italy, *Drug Saf.* 32 (3) (2009) 239–244.
- [80] B. Bar-Oz, M.E. Moretti, G. Mareels, T. Van Tittelboom, G. Koren, Reporting bias in retrospective ascertainment of drug-induced embryopathy, *Lancet* 354 (9191) (1999) 1700–1701.
- [81] B. Bar-Oz, M.E. Moretti, R. Bishai, G. Mareels, T. Van Tittelboom, J. Verspeelt, G. Koren, Pregnancy outcome after in utero exposure to itraconazole: a prospective cohort study, *Am. J. Obstet. Gynecol.* 183 (3) (2000) 617–620.
- [82] K.E. Murphy, M.E. Hannah, A.R. Willan, S.A. Hewson, A. Ohlsson, E.N. Kelly, S.G. Matthews, S. Saigal, E. Asztalos, S. Ross, M.F. Delisle, K. Amankwah, P. Guselle, A. Gafni, S.K. Lee, B.A. Armson, Multiple courses of antenatal corticosteroids for preterm birth (MACS): a randomised controlled trial, *Lancet* 372 (9656) (2008) 2143–2151.
- [83] R.J. Wapner, Y. Sorokin, E.A. Thom, F. Johnson, D.J. Dudley, C.Y. Spong, A.M. Peaceman, K.J. Leveno, M. Harper, S.N. Caritis, M. Miodovnik, B. Mercer, J.M. Thorp, A. Moawad, M.J. O'Sullivan, S. Ramin, M.W. Carpenter, D.J. Rouse, B. Sibai, S.G. Gabbe, Single versus weekly courses of antenatal corticosteroids: evaluation of safety and efficacy, *Am. J. Obstet. Gynecol.* 195 (3) (2006) 633–642.
- [84] E. Bevilacqua, R. Brunelli, M.M. Anceschi, Review and meta-analysis: benefits and risks of multiple courses of antenatal corticosteroids, *J. Matern. Fetal Neonatal* 23 (4) (2010) 244–260.
- [85] M.J. Nyirenda, R.S. Lindsay, C.J. Kenyon, A. Burchell, J.R. Seckl, Glucocorticoid exposure in late gestation permanently programs rat hepatic phosphoenolpyruvate carboxykinase and glucocorticoid receptor expression and causes glucose intolerance in adult offspring, *J. Clin. Invest.* 101 (10) (1998) 2174–2181.
- [86] V.M. Heine, D.H. Rowitch, Hedgehog signaling has a protective effect in glucocorticoid-induced mouse neonatal brain injury through an 11 β -HSD2-dependent mechanism, *J. Clin. Invest.* 119 (2) (2009) 267–277.
- [87] J. Kim, J.Y. Tang, R. Gong, J.J. Lee, K.V. Clemons, C.R. Chong, K.S. Chang, M. Fereshteh, D. Gardner, T. Reya, J.O. Liu, E.H. Epstein, D.A. Stevens, P.A. Beachy, Itraconazole, a commonly used antifungal that inhibits Hedgehog pathway activity and cancer growth, *Cancer Cell* 17 (4) (2010) 388–399.
- [88] J.R. Pace, A.M. DeBerardinis, V. Sail, S.K. Tacheva-Grigorova, K.A. Chan, R. Tran, D.S. Raccuia, R.J. Wechsler-Reya, M.K. Hadden, Repurposing the clinically efficacious antifungal agent itraconazole as an anticancer chemotherapeutic, *J. Med. Chem.* 59 (8) (2016) 3635–3649.
- [89] B. Chen, V. Trang, A. Lee, N.S. Williams, A.N. Wilson, E.H. Epstein Jr., J.Y. Tang, J. Kim, Posaconazole, a second-generation triazole antifungal drug, inhibits the hedgehog signaling pathway and progression of basal cell carcinoma, *Mol. Cancer Ther.* 15 (5) (2016) 866–876.
- [90] C.R. Chong, J. Xu, J. Lu, S. Bhat, D.J. Sullivan Jr., J.O. Liu, Inhibition of angiogenesis by the antifungal drug itraconazole, *ACS Chem. Biol.* 2 (4) (2007) 263–270.
- [91] R. Del Carratore, A. Carpi, P. Befly, V. Lubrano, L. Giorgetti, B.E. Maserti, M.A. Carluccio, M. Simili, G. Iervasi, S. Balzan, Itraconazole inhibits HMEC-1 angiogenesis, *Biomed. Pharmacother.* 66 (4) (2012) 312–317.
- [92] E.V. Khankin, C. Royle, S.A. Karumanchi, Placental vasculature in health and disease, *Semin. Thromb. Hemost.* 36 (3) (2010) 309–320.

3.1.2. Discussion

Pharmacophore-based VS facilitates the identification of lead structures by enriching potentially active virtual hits among an abundant number of possible test compounds. While highly helpful during drug development, the implementation for anti-target screenings remains rather challenging as this application intends to find all conceivably active (and harmful) substances. To address this issue, the identification of compound classes, which can then be further biologically evaluated may be a promising alternative. The virtual hit list of the DrugBank Database screening for the identification of 11 β -HSD2 inhibitors, included among other hits, several antifungal agents, especially represented by the class of azole fungicides. *In vitro* assessment of the virtually retrieved azole fungicides and further structurally related compounds revealed a significant structure-activity relationship (SAR) between azole scaffold size, selectivity and inhibitory potency toward 11 β -HSD2 and the closely related 11 β -HSD1. An extended hydrophobic central region of the azole scaffold connected to a more polar end was observed to be favorable for 11 β -HSD2 inhibition, demonstrated by the most potent 11 β -HSD2 inhibitors itraconazole, its metabolite hydroxyitraconazole (OHI) and posaconazole. Docking calculations predicted major differences between 11 β -HSD1 and 11 β -HSD2 in the shape of their binding site entry, allowing the extended azole scaffolds to interact with Arg212, while a Met is situated at the binding site entry of 11 β -HSD1. Importantly, these compounds were not retrieved as hits by the VS, although available in the screening library. This emphasizes and supports the approach of using VS as an initial filter to identify hazardous compound classes rather than individual compounds.

Clinical evidence for 11 β -HSD2 inhibition by itraconazole comes from case studies including patients on long-term treatment developing typical symptoms of AME [29, 30]. Due to the delayed market launch of posaconazole (Noxafil®), less data is available. However, a recent report described a case of AME secondary to posaconazole therapy and stated a serum posaconazole concentration in the patient that exceeded the IC₅₀ value (460 ± 98 nM) determined in our published article [31]. Nevertheless, due to the high binding capacity of posaconazole (≥98%), as well as itraconazole (99.8%) and OHI (99.6%), to human serum albumin (HSA), the circulating fraction of unbound compound is low [32, 33]. This needs to be taken into account when comparing drug serum concentrations with IC₅₀ values determined *in vitro* as well as the effect on the binding capacity by diverse physiological and pathophysiological conditions such as pregnancy, inflammation, cancer or hemodialysis which can alter HSA levels [34]. Besides, extensive extravascular tissue distribution to liver, lung, kidney, fat tissue and muscles with concentrations exceeding those found in plasma have been reported for these lipophilic compounds [35, 36]. Thus, the concentration of azole fungicides can highly vary between different tissues and should be considered for data evaluation. Unfortunately, the authors did not specify further mechanisms additionally contributing to locally elevated cortisol levels such as the

potent inhibition of cytochrome P450 (CYP) 3A4 and P-glycoprotein (P-gp) efflux transport by posaconazole [37, 38].

The effects mediated by azole-dependent 11 β -HSD2 inhibition may have been overlooked in animal studies using rodents due to the observed species-specific differences. Considerable weaker rat and mouse 11 β -HSD2 inhibition by itraconazole, OHI, and to a lesser extent by posaconazole, measured in kidney homogenates, was detected. Even though similar biological effects in rodents are expected at higher concentrations, these observations could be biased through the extended target promiscuity and/or unspecific binding at higher compound concentrations. Furthermore, the expression of placental 11 β -HSD2 is highly variable during gestation between the different species, making the extrapolations from animals to humans even more difficult (reviewed in [39]). The molecular mechanisms behind the question how altered fetal glucocorticoid exposure may affect fetal growth and predispose the fetus towards diseases later in life are not yet understood. Hence, azole fungicides may exert their potential adverse effects towards the fetus by changing the environment through regulation of the glucocorticoid accessibility and thereby reduce glucose and increased amino acid transport through the placenta, as it was shown for 11 β -HSD2-deficient mice [40]. Alternatively, azole fungicides may lead to an insufficient placental vascularization by inhibiting angiogenesis [41-43]; or may directly affect the fetal development by interfering with fetal target structures such as the Sonic hedgehog (Shh) signaling [41, 44-46]. Clearly further research is needed to address these questions.

Another molecular mechanism potentially underlying the developmental programming effects involve epigenetic alterations in the target gene promoters. Epidemiological studies in humans revealed that early life environmental conditions can lead to epigenetic changes, which are retained throughout life. Individuals prenatally exposed to famine during the Dutch Hunger Winter showed, six decades later, less DNA methylation of the insulin-like growth factor II (IGF2) gene compared with their unexposed, same-sex siblings [47]. Several studies provided evidence suggesting epigenetic regulation of placental 11 β -HSD2 as a mechanistic connection linking maternal environment, infant birth and long-term consequences for an affected offspring [48-52]. This programming may affect the direct offspring as well as the subsequent generations. Rats that had been exposed prenatally to dexamethasone, but were not manipulated during their own pregnancy, had offspring with reduced birth weight and glucose intolerance, effects observed until the third generation [53]. Thus, epigenetic changes may display an important factor for the (intergenerational) appearance of the 'programmed phenotype' and needs further comprehensive investigations. However, to understand how early life exposure controls epigenetic changes and thus potentially the health over a lifetime, requires further epigenetic epidemiologic studies that need to be large and include replication [47]. This challenging suggestion may play a part in the mapping of the exposome, discussed below.

Metabolites can display equal or even higher potency towards certain targets compared to their parent substances. Thus, EDC safety evaluation studies should include in the assessment besides the parental compound also the main metabolites, as it was done in the present study for itraconazole and OHI. Moreover, a parental compound could be assessed *in vitro* as safe, but a metabolite may cause harmful effects. For instance, no inhibitory activity of the UV-filter benzophenone 3 (BP-3) was detected towards 17 β -HSD3, whilst *in vivo* BP-3 is rapidly demethylated to the potent 17 β -HSD3 inhibitor BP-1 [54, 55]. However, these evaluations are often limited, due to incomplete knowledge of the metabolite spectrum or the implementation of cell-free testing systems, as it is typically the case in early screening phases with high throughput screenings (HTS), as for example in the Tox21 project. Intact cells as testing systems can only partially overcome this problem; for example, immortalized hepatocyte-derived cell lines are highly dedifferentiated and show only very limited expression of metabolic enzymes. Although primary hepatocytes sustain the major drug-metabolizing enzymes for a certain time period in cell culture, they have a great variability in genotype, short life span, and limited availability [56, 57]. In addition, also the metabolism by phase II enzymes, which are involved in conjugation reactions, as well as transport proteins should be integrated due to their ability to facilitate and accelerate the excretion of compounds and therefore to reduce exposure levels and the probability to cause toxic effects (example in the section below in the published article: 'Evaluation of tetrabromobisphenol A effects on human glucocorticoid and androgen receptors: a comparison of results from human- with yeast-based *in vitro* assays' [58]). Thus, *in vivo* studies and a careful consideration of epidemiological data are vital and essential for an appropriate EDC safety assessment.

This leads to another limitation of the 'common' way of EDC evaluation – mixtures. The majority of compounds are analyzed as single substances; however, an individual is concurrently exposed to a multitude of different exogenous compounds. Taking this into account, makes the safety assessment of EDCs even more difficult; compound-compound interactions, additive or opposite effects and synergistic action represent only a few and evident examples. Which compounds and at what ratios should they be selected; do they act on different target structures, tissue-specifically - to mention some questions which could arise. Hence, this issue was realized and resulted in the introduction of the exposome, the analysis of the life-course environmental exposures (including lifestyle factors), from the prenatal period onwards [59]. The evolving field of 'omics' approaches was thereby addresses as promising technologies to improve EDC risk assessment and to support the identification of individual susceptibilities by targeted biomarkers, which should reconstruct past exposure [60]. However, mapping the entire exposome might be extremely challenging if not even impossible due to the complexity of a life-time exposure burden [61]. The variety of confounding variables such as stress, genetic polymorphisms, socioeconomic status and general lifestyle including diet is immense, apart from knowing of an exposure to have been occurred (e.g. prenatally) or sensitive methods to detect

them. Another major challenge regarding exposome analysis remains the definition of normal range and distinguishing between deviations due to adaptive responses and adverse health effects. The concept, nevertheless, is a paradigm shift, albeit the feasibility is still questionable and further research is evidently required [62].

Further limitations of *in vitro* testing systems in EDC assessment and evaluation strategies are discussed in the section below.

3.2. *In vitro* testing systems – validation - limitations

Successful application of *in silico* tools requires accurate *in vitro* validation strategies. However, the limitations of each *in vitro* testing system should be carefully taken into account and considered during data interpretation. The analysis of enzymatic activities demands conduction under cell-free conditions such as purified protein or cell lysates expressing the protein of interest at a low background environment. Data acquired in intact cell models lack direct target access and can therefore only be employed for the verification of active hits. Compound-target interactions in intact cell systems highly depend on the prevailing expression of transport proteins, intracellular binding proteins or other metabolizing enzymes, limiting thereby the availability of a compound at the target structure. Whereas parameters such as cell handling, passage number of a cell line or medium composition can influence cell-based assays, similar problems may arise in the preparation of purified proteins or cell lysates, where different handling procedures can lead to different enzyme activities, for example due to altered protein conformation, loss of interacting partner proteins and/or oligomer structure. The application of suitable positive and negative controls allows the detection of alterations in the testing system itself and facilitates the comparison with results obtained by other investigators. Nevertheless, comprehensive biological characterization and the usage of different assay read-outs are crucial for an *in vitro* validation. The published review 'Virtual screening applications in short-chain dehydrogenase/reductase research' provides further insight into the limitations of virtual hit validation in biological systems [9].

The same challenges arise for all applications where *in vitro* testing systems are used. Such testing systems are widely employed during the safety evaluation process of EDCs and gained even more importance since chemicals used in body care products are no longer be allowed to be tested in animals. To study EDC action on hormone receptors, many assays make use of receptor-mediated activation of reporter genes in human cell lines. A cost-effective alternative are yeast reporter cell assays, often applied for HTS in ecotoxicology. However, the Organization for Economic Co-operation and Development (OECD) issued a guidance document for the assessment of EDCs in which they excluded yeast estrogen and yeast androgen screens as a result of transport issues, limited cell membrane permeability, and insufficient capability to distinguish between compounds activating or suppressing the receptor activity [63].

In this regard, the following study addressed the re-evaluation of a potential EDC on GR and AR function. The widely used flame retardant tetrabromobisphenol A (TBBPA) was reported to exert potent antagonistic activity on GR and to a lesser extent on AR in yeast-based reporter gene assays [64]. However, the applied yeast GR assay displayed very low sensitivity towards the potent GR ligand dexamethasone, resulting in a need of high dexamethasone concentrations (60 μ M) used for reporter

gene activation. As already pointed out in the section above, the inclusion of suitable controls can lead to the identification of inconsistencies in the assay performance, for example such as the requirement for exceptionally high positive control concentrations. Unfortunately, the authors from this study did not provide further experiments to confirm their data obtained from the yeast reporter assays. Thus, the re-evaluation aimed to assess the impact of TBBPA on GR and AR function by performing cell-free receptor displacement and human cell-based transactivation assays.

3.2.1. Published article:

Evaluation of tetrabromobisphenol A effects on human glucocorticoid and androgen receptors: a comparison of results from human- with yeast-based in vitro assays

Katharina R. Beck¹, Tanja J. Sommer¹, Daniela Schuster², Alex Odermatt¹, Toxicology. 2016 Aug 31;370:70-77.

¹Swiss Center for Applied Human Toxicology and Division of Molecular and Systems Toxicology, Department of Pharmaceutical Sciences, Pharmazentrum, University of Basel, Klingelbergstrasse 50, 4056 Basel, Switzerland

²Institute of Pharmacy / Pharmaceutical Chemistry and Center for Molecular Biosciences Innsbruck (CMBI), Computer Aided Molecular Design Group, University of Innsbruck, Innrain 80/82, 6020 Innsbruck, Austria

In addition, this research article was published as layman summary on the atlas of science online platform:

Studying potential endocrine disrupting chemicals: comparison of yeast and human cell-based in vitro assays

Katharina R. Beck, Alex Odermatt, June 26, 2017, Atlas of Science



Evaluation of tetrabromobisphenol A effects on human glucocorticoid and androgen receptors: A comparison of results from human- with yeast-based *in vitro* assays



Katharina R. Beck^a, Tanja J. Sommer^a, Daniela Schuster^b, Alex Odermatt^{a,*}

^a Swiss Center for Applied Human Toxicology and Division of Molecular and Systems Toxicology, Department of Pharmaceutical Sciences, Pharmazentrum, University of Basel, Klingelbergstrasse 50, 4056 Basel, Switzerland

^b Institute of Pharmacy/Pharmaceutical Chemistry and Center for Molecular Biosciences Innsbruck (CMBI), Computer Aided Molecular Design Group, University of Innsbruck, Innrain 80/82, 6020 Innsbruck, Austria

ARTICLE INFO

Article history:

Received 24 August 2016

Received in revised form 23 September 2016

Accepted 27 September 2016

Available online 28 September 2016

Keywords:

Glucocorticoid receptor

Androgen receptor

Endocrine disrupting chemical

Tetrabromobisphenol A

In vitro assay

Toxicity

ABSTRACT

The incidence of immune-related diseases increased over the last years in industrialized countries, suggesting a contribution of environmental factors. Impaired glucocorticoid action has been associated with immune disorders. Thus, there is an increasing interest to identify chemicals disrupting glucocorticoid action. The widely used flame retardant tetrabromobisphenol A (TBBPA) was reported earlier to potentially inhibit glucocorticoid receptor (GR) and moderately androgen receptor (AR) activity in yeast-based reporter gene assays. To further characterize possible GR disrupting effects of TBBPA, transactivation experiments using a human HEK-293 cell-based reporter gene assay and cell-free receptor binding experiments were performed in the present study. Both, transactivation and GR binding experiments failed to detect any activity of TBBPA on GR function. Molecular docking calculations supported this observation. Additionally, the current study could confirm the antiandrogenic activity of TBBPA seen in the yeast assay, although the effect was an order of magnitude less pronounced in the HEK-293 cell-based system. In conclusion, TBBPA does not directly affect GR function and, considering its rapid metabolism and low concentrations found in humans, it is unlikely to cause adverse effects by acting through AR. This study emphasizes the use of cell-free assays in combination with cell-based assays for the *in vitro* evaluation of endocrine disrupting chemicals.

© 2016 Elsevier Ireland Ltd. All rights reserved.

1. Introduction

The annual production of chemicals for industry, agriculture, personal care products, or food processing is continuously rising. Programs initiated by the authorities such as the Registration, Evaluation, Authorization and Restriction of Chemicals (REACH) regulation of the European Union or the Endocrine Disruptor Screening Program (EDSP) of the U.S. Environmental Protection

Agency aim to improve the safety assessment of man-made chemicals and thereby protect human health and the environment. In the past, extensive research focused on endocrine disrupting chemicals (EDCs) acting on sex steroid hormone action, with a major focus on estrogen receptor (ER) and androgen receptor (AR) function. In contrast, rather few studies addressed chemicals disrupting glucocorticoid action (Macikova et al., 2014; Nashev et al., 2012; Neel et al., 2013; Odermatt and Gumy 2008; Odermatt et al., 2006; Stavreva et al., 2012).

Glucocorticoids are regulating the immune system, cell proliferation and differentiation, brain function, energy metabolism, blood pressure and electrolyte balance. Due to their immunomodulatory effects, glucocorticoids are still among the most widely prescribed drugs to prevent graft rejection and to treat allergic or chronic inflammatory disease such as asthma, skin infections or rheumatoid arthritis (Baschant and Tuckermann, 2010). Experiments in adult mice with keratinocyte-restricted GR inactivation showed an exacerbated inflammatory response to epidermal challenge, while postnatal mice displayed skin barrier

Abbreviations: AR, androgen receptor; EDCs, endocrine disrupting chemicals; EDSP, Endocrine Disruptor Screening Program; ER, estrogen receptor; GR, glucocorticoid receptor; HSP, heat shock protein; IARC, International Agency for Research on Cancer; LOD, limit of detection; MAPK, mitogen activated protein kinase; NCoR, nuclear receptor corepressor; NK cell, natural killer cell; NTP, U. S. National Toxicology Program; PCBs, polychlorinated biphenyls; PDB, Protein Data Bank; P-gp, P-glycoprotein; PR, progesterone receptor; REACH, registration evaluation authorization and restriction of chemicals; T3, triiodothyronine; T4, thyroxine; TBBPA, tetrabromobisphenol A; TSH, thyroid stimulating hormone.

* Corresponding author.

E-mail address: alex.odermatt@unibas.ch (A. Odermatt).

<http://dx.doi.org/10.1016/j.tox.2016.09.014>

0300-483X/© 2016 Elsevier Ireland Ltd. All rights reserved.

defects and hallmarks of atopic dermatitis (Sevilla et al., 2013). Importantly, the incidence of atopic dermatitis and asthma has increased over the last decades, with significant variations between and within countries (Eder et al., 2006; Nutten 2015). Thus, exposure to EDCs that antagonize glucocorticoid receptor (GR) function may lead to impaired stress responses and immunosuppression and result in an enhanced susceptibility to allergies and aggravated inflammatory reactions. Environmental chemicals associated with disturbed GR function at human relevant concentrations are arsenic and dibutyltin (Gosse et al., 2014; Gummy et al., 2008; Kaltreider et al., 2001). Arsenic has been linked to type 2 diabetes, cardiovascular disease, several forms of cancer, and reproductive and developmental disorders (Abernathy et al., 1999), whereas dibutyltin is considered to be highly neuro- and immunotoxic (Jenkins et al., 2004; Whalen et al., 1999). Part of these effects might be due to interference with glucocorticoid action. Furthermore, exposure to polychlorinated biphenyls (PCBs) was observed to induce severe clinical symptoms including skin lesions, respiratory distress, neurologic disorders, disturbed liver function and suppression of cellular immunity (Nakanishi et al., 1985; Reggiani and Bruppacher 1985). Interestingly, several methyl sulfone metabolites have been shown to act as GR antagonists with IC₅₀ values in the low micromolar range (Johansson et al., 2005; Johansson et al., 1998). Thus, it has been hypothesized that they account at least partially for the respiratory symptoms (Grimm et al., 2015).

In vitro testing systems are widely applied in the safety assessment process, and the importance of such testing systems increased by the decision that chemicals used in body care products can no longer be tested in animals. Cell-based assays are used to investigate potential EDCs. Many assays, including the ER α β -lactamase reporter gene assay in HEK-293 cells, the ER α luciferase reporter gene assay in BG-1 ovarian cells and the multiplexed ER reporter gene assay in HepG2 cells that are also used in the ToxCast21 testing battery (Rotroff et al., 2014), are based on the receptor-mediated activation of a reporter gene in human cell lines. Alternatively, green-fluorescence protein reporter gene assays in yeast cells are used for the detection of potential EDCs due to the low costs and high throughput capacity of these assays (Gaido et al., 1997; Routledge and Sumpter 1996). Yeast strains expressing AR and progesterone receptor (PR) are also available (Baker, 2001). However, the limitations of these assays need to be taken into account for data interpretation. The OECD issued a guidance document for the evaluation of EDCs in which they excluded the yeast estrogen screen and yeast androgen screen due to limited cell membrane permeability, transport issues and insufficient ability to discriminate between agonists and antagonists (OECD, 2012).

In a recent study Roelofs et al. investigated the widely used flame retardant tetrabromobisphenol A (TBBPA) for its potential to interfere with GR function using recombinant yeast cells expressing the human GR and a GR-dependent green fluorescence protein (Roelofs et al., 2015). They reported a highly potent GR antagonistic effect of TBBPA with an IC₅₀ value of 22 nM. However, these authors did not provide additional experiments to support their data from the yeast GR reporter gene assay. Nevertheless, TBBPA was recently shown to decrease the secretion of interferon- γ from immune cells (Almughamsi and Whalen, 2016). As possible mechanism, activation of the ERK1/2 MAPK pathway and of P38 kinase by TBBPA has been suggested. Since there is a functional interaction between GR activity and the MAPK pathway, and glucocorticoids are well-known modulators of inflammatory cytokines and chemokines, a block of GR function by TBBPA may disturb the regulation of the immune system.

TBBPA covers more than half of the global annual production of brominated flame retardants (Law et al., 2006). It is mainly applied

in the laminate coating of printed circuit boards, where it is covalently bound to a polymer matrix and cannot be released into the environment (ECB, 2006). Nevertheless, up to 20% of the manufactured TBBPA is used as an additive flame retardant in electronic equipment, furniture, building and construction materials, packaging, and consumer products (ECB, 2006). Since additive flame retardants do not chemically react with their coated basis, they are prone to leach out of this matrix.

The aim of the current study was to re-evaluate the impact of TBBPA on GR function by performing cell-free receptor binding experiments and transactivation experiments in a human HEK-293 cell-based assay. Additionally, the effects of TBBPA on AR-mediated transactivation and on binding to AR were investigated.

2. Materials and methods

2.1. Chemicals and reagents

[1,2,4,6,7-³H]-dexamethasone and [1,2,6,7-³H]-testosterone were purchased from American Radiolabeled Chemicals (St. Louis, MO). Cell culture medium and other chemicals were obtained from Sigma Aldrich (Buchs, Switzerland).

2.2. Cell culture

Human Embryonic Kidney-293 cells (HEK-293) cells were cultured in Dulbecco's modified Eagle medium (DMEM) supplemented with 10% fetal bovine serum, 4.5 g/l glucose, 100 U/ml penicillin/streptomycin, 2 mM L-glutamine, 10 mM HEPES, pH 7.4, and 10% MEM non-essential amino acid solution. Sf9 cells were cultured at 27 °C in EX-Cell 420 medium supplemented with 10% FBS and 100 U/ml penicillin/streptomycin.

2.3. Competitive cell-free receptor binding assay

Recombinant human glucocorticoid receptor α (GR) baculovirus stock was produced using the Bac-to-Bac expression system and recombinant GR was expressed in Sf9 cells according to the instructions by the manufacturer (Invitrogen, Carlsbad, CA). Human androgen receptor (AR) was transiently expressed in HEK-293 cells upon transfection by the calcium phosphate precipitation method and cultivation for 72 h. Cells transfected with pcDNA3 vector served as control.

For preparation of lysates, cells were collected in ice-cold PBS and centrifuged for 10 min at 3000 \times g and 4 °C, resuspended in binding buffer (50% glycerol, 10 mM EDTA, 50 mM sodium tungstate, 50 mM HEPES, pH 7.4) and homogenized with 50 strokes using a glass puller. The lysates were centrifuged (16'000 \times g, 10 min, 4 °C) and supernatants stored at -80 °C.

Recombinant human GR lysates were incubated in the presence of 10 nM [1,2,4,6,7-³H]-dexamethasone and unlabeled competitor (either 10 μ M or 100 nM cortisol or 10 μ M TBBPA) for 4 h at 16 °C. Human AR lysates were incubated with 10 nM [1,2,6,7-³H]-testosterone and unlabeled competitor (either testosterone or TBBPA at different concentrations). Unbound ligand was separated by adding 5% dextran coated charcoal into the binding buffer, followed by incubation at 4 °C for 10 min and centrifugation for 10 min at 3200 \times g and 4 °C. The receptor bound fraction of radioligand in supernatants was measured by scintillation counting.

2.4. GR- and AR-dependent transactivation assay

HEK-293 cells (100,000 cells/well for GR and 200,000 cell/well for AR transfection) were seeded in poly-L-lysine coated 24-well plates, incubated for 24 h and transiently transfected using calcium

phosphate precipitation. For the GR transactivation assay, cells were transfected with plasmid for human GR (0.3 $\mu\text{g}/\text{well}$), pCMV-lacZ β -galactosidase transfection control (0.05 $\mu\text{g}/\text{well}$) and TAT3-TATA luciferase reporter (0.45 $\mu\text{g}/\text{well}$). For the AR transactivation assay cells were transfected with human AR (0.4 $\mu\text{g}/\text{well}$), pCMV-lacZ β -galactosidase control (0.025 $\mu\text{g}/\text{well}$) and TAT3-TATA luciferase reporter (0.375 $\mu\text{g}/\text{well}$). At 6 h post-transfection cells were washed with DMEM and incubated for another 18 h. The cells were then washed with steroid-free DMEM (cDMEM) and cultivated for 3 h at 37 °C. This culture medium was then replaced with fresh cDMEM containing steroid hormones (10, 25 and 100 nM cortisol for GR, 10 nM testosterone for AR), receptor antagonist (1 μM RU486 for GR and 0.5 μM flutamide for AR) or TBBPA (10 μM or 1 μM), followed by incubation for 24 h. Cells were lysed in 60 μl of tropix lysis solution (Applied Biosystems, Foster City, CA) supplemented with 0.5 μM dithiothreitol and frozen at -80 °C for at least 20 min. Luciferase activity was determined in 20 μl lysate adding 100 μl of D-luciferin-firefly substrate solution at a final concentration of 0.47 mM D-luciferin, 53 mM ATP, 0.27 mM coenzyme A, 0.13 mM EDTA, 33.3 mM dithiothreitol, 8 mM MgSO_4 , 20 mM tricine, pH 7.8. β -galactosidase activity was measured in 20 μl lysate using the Tropix kit. Samples were measured using a SpectraMax-L luminometer (Molecular Devices, Devon, UK).

2.5. Docking of TBBPA into the ligand binding pocket of GR

Docking was performed using the GOLD version 5.2 software (Chambridge Crystallographic Data Centre, Cambridge, UK) (Jones et al., 1997). This program applies a genetic algorithm for the identification of accurate docking poses for small molecules into the binding pocket of a protein. The crystal structure with the Protein Data Bank (PDB) entry 3H52 [DOI: <http://dx.doi.org/10.1016/j.jmb.2009.11.011>] was chosen for the GR protein due to the antagonistic conformation. First, the co-crystallized ligand (RU486, also known as mifepristone) was deleted from the binding

site and re-docked into the GR binding pocket to investigate whether GOLD could restore the original binding orientation and therefore validate the docking settings (RMSD value of 0.057). The binding site was centered on the primary amine nitrogen of Gln570 ($x = -48.19$; $y = 16.58$; $z = -36.62$) surrounded by a 10 Å sphere. GoldScore was selected as scoring function. Interactions found by the docking solutions between the ligand and the GR binding pocket were evaluated using LigandScout 3.12 (inte:ligand GmbH, Vienna, Austria). This program automatically analyzes the observed interaction pattern between the docked ligand and the protein, based on the chemical functionalities, the geometric distances and the angles between neighboring structures (Wolber and Langer, 2005).

2.6. Statistical analysis

Data were analyzed using *t*-test in the GraphPad Prism 5 software. Values represent mean \pm SD.

3. Results

3.1. Assessment of TBBPA effects on GR binding and transcriptional activity

In order to evaluate the potent antagonistic activity of TBBPA on GR (IC_{50} 22 nM) that was observed in a recombinant yeast reporter gene assay by Roelofs et al. (Roelofs et al., 2015), a transactivation assay in HEK-293 cells was employed in the present study. For this purpose, HEK-293 cells were transiently transfected with human GR and a GR-dependent luciferase reporter gene (Fig. 1A). As expected, cortisol at different concentrations induced the GR-dependent expression of the luciferase activity; however, TBBPA did not act as an antagonist and no decrease in the cortisol-dependent GR activation, using 10 nM, 25 nM and 100 nM cortisol, could be observed when cells were co-treated with 10 μM TBBPA. A slight, statistically significant, increase in reporter gene activity

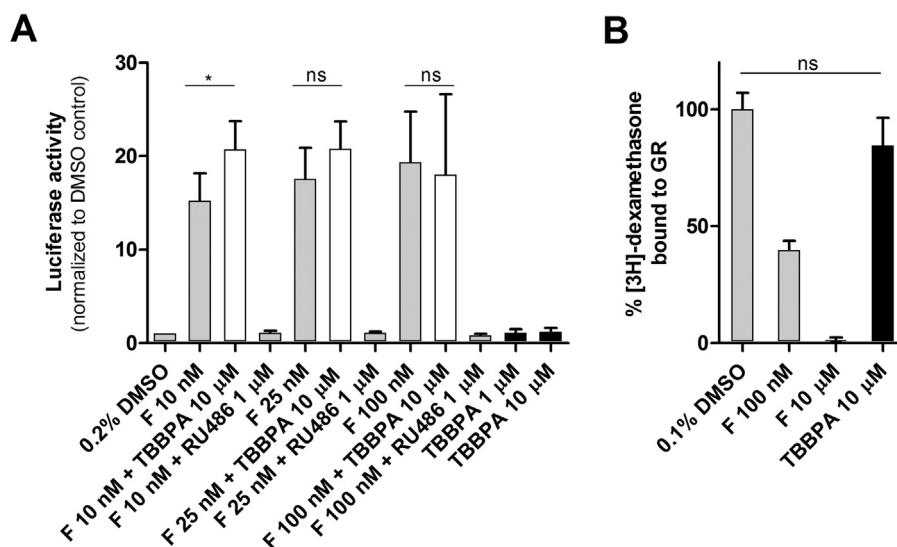


Fig. 1. Effect of TBBPA on GR binding and activity. (A) Impact of TBBPA on GR transactivation in HEK-293 cells transiently transfected with plasmids for human GR, a corticosteroid receptor-sensitive luciferase reporter gene and a galactosidase transfection control. Cells were incubated for 24 h in the presence of 10 nM, 25 nM and 100 nM cortisol (F), 1 μM mifepristone (RU486) or different concentrations of TBBPA. The luciferase reporter activity was normalized to the internal galactosidase control. Data were normalized to vehicle control (0.2% DMSO) and represent mean \pm SD from three independent experiments each performed in triplicates. (B) Displacement of 10 nM radiolabeled [^3H]-dexamethasone from GR by unlabeled competitor (either cortisol (F) or TBBPA). Sf9 lysates expressing recombinant human GR were incubated with 10 nM [^3H]-dexamethasone and either 10 μM or 100 nM unlabeled cortisol (F) or 10 μM TBBPA until the binding equilibrium was reached. Values were normalized to the maximal binding of 10 nM [^3H]-dexamethasone and represent the remaining [^3H]-dexamethasone bound to GR. ns (not significant); * $p < 0.05$.

was observed upon co-treatment with 10 nM cortisol and 10 μ M TBBPA. This may be explained by competition of TBBPA with cortisol for unspecific binding sites. Unlike TBBPA, the antagonist RU486 at 1 μ M completely blocked the cortisol-induced GR activation. Also, TBBPA was not able to induce GR-mediated activation of the luciferase reporter gene, even at the high concentration of 10 μ M. Thus, an interference of TBBPA with GR-mediated transactivation could not be demonstrated in this human cell-based assay.

To exclude limited cellular uptake or potential efflux of TBBPA as a reason for the lack of effect on GR, a competitive receptor binding assay was performed under cell-free conditions. Lysates of cells expressing recombinant human GR were co-incubated with 10 nM [3 H]-dexamethasone and unlabeled competitor (either different concentrations of cortisol (F) or 10 μ M TBBPA), followed by determination of the GR bound fraction of [3 H]-dexamethasone (Fig. 1B). TBBPA at a concentration of 10 μ M did not substantially displace the radiolabeled dexamethasone from the receptor, in contrast to the known ligand cortisol. These results indicate that TBBPA has no direct effect on GR ligand binding and does not affect GR transcriptional activity.

3.2. Structural modeling of ligand binding to GR

To computationally elucidate the results for TBBPA obtained in the transactivation and binding assays, docking calculations were performed to investigate the interactions formed with the GR ligand binding site and therefore the potential to trigger a molecular switch of the helix 12. In the X-ray crystal structure, the GR antagonist RU486 (mifepristone) induces a relocation of the helix 12 position to reshape the coactivator towards a corepressor site with the possibility to bind nuclear receptor corepressor (NCoR) (Schoch et al., 2010) (Fig. 2A and B). TBBPA adopts a position similar to GR agonists without covering the side pocket compared to the dimethyl amino phenyl moiety of RU486 in order to interact with the helix 12 and induce a position change (Fig. 2C and D). RU486 was found to form hydrophobic contacts with Ile756 and Met752 of helix 12 as well as with Leu2263 and Ile2266 of the NCoR motif. The only interaction with the helix 12 and TBBPA found is a hydrophobic interaction with Ile756, but with considerable larger distances compared to RU486. Furthermore, the interactions with the GR binding site observed for TBBPA are mainly of hydrophobic nature with one additional hydrogen bond (H-bond) involving the sulfur atom of Met560. H-bonds including a sulfur center are generally considered as weak H-bonds compared to interactions with oxygen or nitrogen groups. The same

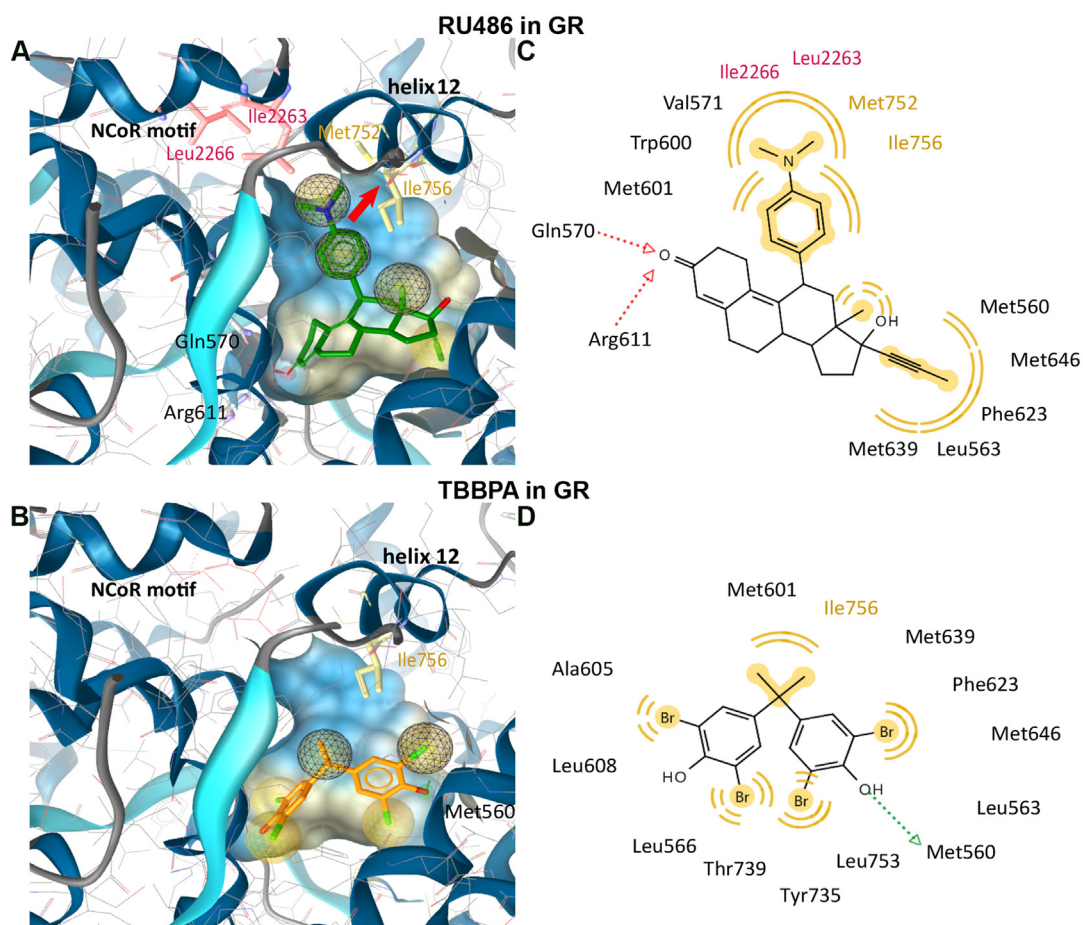


Fig. 2. Docking of TBBPA and mifepristone into the ligand binding site of GR. Co-crystallized mifepristone (RU486) (A) and docked TBBPA (B) in complex with the GR ligand binding domain and a receptor-interacting motif of the nuclear receptor corepressor (NCoR) in an active antagonistic conformation (PDB code 3H52, domain A). The automatically generated pharmacophore maps the important structural details of the ligand for binding (yellow spheres: hydrophobic interactions and red and green arrows with spheres are H-bond interactions). Amino acid residues involved in ligand binding are depicted as sticks. Whereas the interactions formed by RU486 (marked yellow spheres) trigger a molecular switch of the helix 12 to reshape the corepressor site (red arrow), TBBPA is not able to cover this side pocket and form the required interactions to modulate helix 12. Two-dimensional representation of the binding interactions of RU486 (B) and TBBPA (D). The color code corresponds with part A and C.

interaction pattern was also found when docking TBBPA into a GR crystal structure with an agonistic conformation (data not shown).

3.3. Effect of TBBPA on human androgen receptor

The earlier study by Roelofs et al. reported an antiandrogenic activity of TBBPA with an IC_{50} value of 982 nM in the yeast AR-dependent reporter gene assay (Roelofs et al., 2015). In order to compare these earlier observations from the yeast GR and AR reporter gene assays with our human cell-based systems, an AR transactivation assay in HEK-293 cells was conducted (Fig. 3A). Treatment of the cells with 10 nM testosterone resulted in an approximately eight fold increase in luciferase activity. Co-treatment with the antagonist flutamide partially reduced the testosterone-mediated reporter gene activation. TBBPA did not exert an antiandrogenic effect at a concentration of 1 μ M; however, at 10 μ M it reduced the testosterone-dependent AR activation by 37%. Moreover, at 10 μ M TBBPA showed weak agonist properties and resulted in the activation of the AR-dependent luciferase reporter gene. Furthermore, a cell-free competitive binding assay was conducted with cell lysates expressing recombinant AR (Fig. 3B). TBBPA exhibited a concentration-dependent displacement of the radiolabeled testosterone, whereby 10 μ M TBBPA displaced 62% of the AR-bound [3 H]-testosterone. At 1 μ M TBBPA, which is close to the IC_{50} value reported by Roelofs et al. (Roelofs et al., 2015), 31% of [3 H]-testosterone were displaced from the AR. Thus, these results could confirm the antiandrogenic activity of TBBPA, although the effect was less pronounced in the human cell-based system compared with the yeast assay.

4. Discussion

The results of the present study suggest that TBBPA does not affect GR function. TBBPA showed neither agonistic nor antagonistic effects in the GR transactivation assay in HEK-293 cells, and

TBBPA was not able to displace the radiolabeled ligand dexamethasone from the GR binding site in a cell-free assay. In addition, molecular modeling was applied to study possible interactions of TBBPA with residues of the GR ligand binding pocket. Although TBBPA was not excluded from the GR ligand binding pocket due to steric hindrance, key stabilizing interactions that are formed with the agonist dexamethasone (not shown) or the antagonist RU486 (Fig. 2) are absent in the case of TBBPA. The antagonistic effect of TBBPA observed by Roelofs et al. on AR in the yeast assay with an IC_{50} of 982 nM (Roelofs et al., 2015) could also be detected in the HEK-293 cell-based assay in the present study, although the effect was much weaker with an estimated $IC_{50} > 10 \mu$ M. TBBPA was found to displace the bound radiolabeled ligand testosterone from AR with an estimated IC_{50} between 5 and 10 μ M. Thus, at least ten fold weaker activity of TBBPA towards AR was found in the human cell-based assay compared with the yeast assay.

The discrepancy of the current study with the potent antagonistic activity of TBBPA on GR (IC_{50} 22 nM) measured in the yeast GR assay by Roelofs et al. (Roelofs et al., 2015) may be due to limitations of the yeast assay. The applied yeast GR assay showed a very low sensitivity to the potent ligand dexamethasone and a very high concentration of 60 μ M was used to activate the reporter gene, an issue that has been observed before in yeast (Garabedian and Yamamoto 1992; Picard et al., 1990). The low sensitivity of the yeast GR assay is probably a result of limited access of dexamethasone to the cytosolic compartment. The yeast ATP-binding cassette transporter PDR5 was found to modulate the intracellular amount of dexamethasone (Kralli et al., 1995). Lack of PDR5 activity in a mutant yeast strain led to increased intracellular dexamethasone concentration and an increased response to glucocorticoids. Interestingly, PDR5 represents a functional homologue of the human P-glycoprotein (P-gp), and TBBPA was shown to inhibit P-gp, although at very high concentrations with an IC_{50} value of 25 μ M (Dankers et al., 2013). Considering the supposed anti-glucocorticoid effect of TBBPA, it is unlikely that TBBPA at

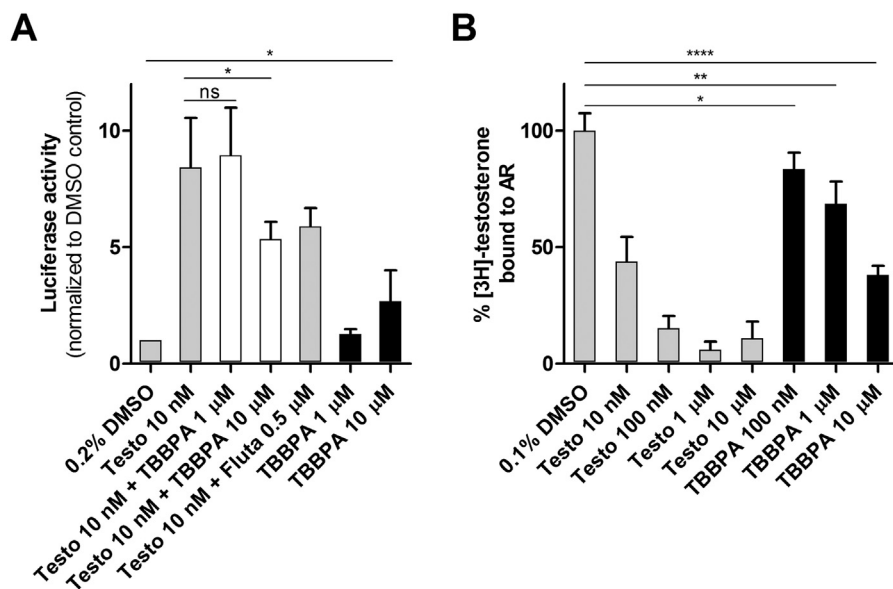


Fig. 3. Effect of TBBPA on AR binding and activity. (A) Impact of TBBPA on AR transactivation in HEK-293 cells transiently transfected with plasmids for human AR, an AR-sensitive luciferase reporter gene and a galactosidase transfection control. Cells were incubated for 24 h in the presence of 10 nM testosterone (Testo), 0.5 μ M flutamide (Fluta) or different concentrations of TBBPA. The luciferase reporter activity was normalized to the internal galactosidase control. Data were normalized to vehicle control (0.2% DMSO) and represent mean \pm SD from four independent experiments each performed in triplicates. (B) Displacement of radiolabeled [3 H]-testosterone from the AR by unlabeled competitor (either testosterone or TBBPA). HEK-293 lysates expressing AR were incubated with 10 nM [3 H]-testosterone and various concentrations of unlabeled testosterone or TBBPA until the binding equilibrium was reached. Values were normalized to the maximal binding at 10 nM [3 H]-testosterone and represent the AR bound fraction of [3 H]-testosterone. ns (not significant), * $p < 0.05$, ** $p < 0.01$, **** $p < 0.0001$.

concentrations below 1 μM inhibits PDR5, and a hypothesis to be tested in future experiments includes the induction of the expression of PDR5 or another transport protein that catalyzes the efflux of glucocorticoids from the yeast cytosolic compartment. Transport was found to be at least partly responsible for the distinct GR-ligand response in yeast (Kralli et al., 1995). Another important factor impacting on steroid hormone receptor activity is the availability of chaperones and co-activator/co-repressor proteins. Although yeast does not have steroid receptors, it expresses two heat shock proteins (HSP82 and HSC82) that might fulfill at least in part the function of HSP90 in controlling the folding of human steroid hormone receptors (Chang and Lindquist, 1994). Nevertheless, the limitations of the low sensitivity of the yeast receptor assays have been addressed by introducing the co-chaperones FKBP52 and HIP, resulting in enhanced GR reporter gene activation (Nelson et al., 2004; Riggs et al., 2003).

Rather than directly modulating GR function it is more likely that TBBPA might act on pathways downstream of GR. Several studies suggested that TBBPA interacts with mitogen-activated protein kinase (MAPK) pathways. Exposure of natural killer (NK) cells to TBBPA led to the activation of the MAPKs ERK1/2 and P38 as well as their upstream activator MAPK kinases (Cato et al., 2014). This appeared to be involved in the TBBPA-mediated reduction of the lytic function of NK cells (Kibakaya et al., 2009). Additionally, a study in murine RAW 264.7 macrophage showed that TBBPA induced COX2, TNF α , IL-1 β and IL-6 expression through enhanced phosphorylation of Akt, the MAPKs p38, ERK1/2 and JNK, as well as transcriptional activation of NF- κ B and AP-1 (Han et al., 2009). Furthermore, TBBPA was reported to induce reactive oxygen species formation by an ERK1/2-dependent pathway (Reistad et al., 2005; Reistad et al., 2007).

A majority of *in vitro* studies on TBBPA-mediated effects used concentrations in the lower micromolar range. Thus, evaluation of relevant concentrations observed in the human body is crucial for its risk assessment. TBBPA blood serum concentrations in the general population were assessed in different studies worldwide including two large Canadian biomonitoring surveys (Canada, 2012). One study evaluated 50,599 serum samples of which all analyzed samples displayed TBBPA concentrations below the limit of detection (LOD) of 0.03 ng/l serum. The second study determined TBBPA concentrations in plasma samples of 771 Inuit participants. In 5% of the measured subjects, TBBPA was found at concentrations ranging from 10 to 480 ng/l (0.08–3.5 nM). A Belgian study involving 515 participants detected maximal TBBPA serum levels of 0.186 ng/l (Kicinski et al., 2012). Measurements in human milk displayed average TBBPA levels of 0.06–4.11 ng/g fat (EFSA, 2011). Limited data are available for personnel with occupational exposure to TBBPA. Two studies examining the TBBPA serum levels of computer technicians and workers at electronic dismantling plants revealed serum concentrations up to 7.4 pmol/g fat (EFSA 2011; Jakobsson et al., 2002). The low systemic bioavailability of TBBPA after oral exposure can be explained by the extensive first-pass metabolism by conjugation with glucuronic acid or sulfate (Kuester et al., 2007; Schauer et al., 2006). The TBBPA conjugates are preferentially translocated into the bile and excreted by the feces (Colnot et al., 2014). Therefore, TBBPA does not bioaccumulate and the concentrations measured in the general population are several orders of magnitude lower than the concentrations causing the reported biochemical effects in the *in vitro* experiments.

However, the International Agency for Research on Cancer (IARC) recently classified TBBPA as probably carcinogenic to humans (group 2A) (Grosse et al., 2016), based on rodent carcinogenicity studies by the U.S. National Toxicology Program (NTP). A significantly increased incidence of uterine adenocarcinomas, adenomas and malignant mixed Müllerian tumors was

found in female Wistar Han rats receiving 500 or 1000 mg TBBPA/kg body weight (bw)/day in a two-year gavage study (Dunnick et al., 2015; NTP 2013). At such high concentrations, the enzymes for sulfation and glucuronidation may become saturated and conjugation of TBBPA likely competes with that of endogenous mediators such as estrogens, resulting in a higher concentration of free estrogens which stimulate cell proliferation and promote tumor growth (Lai et al., 2015; Wikoff et al., 2016). In support of this, several *in vitro* and computational studies provided evidence that TBBPA inhibits estrogen sulfotransferases (Gosavi et al., 2013; Hamers et al., 2006; Kester et al., 2002). However, the TBBPA serum concentrations measured in humans differ by several orders of magnitude from the plasma concentrations that compromised sulfation of TBBPA in rats. Thus, at the exposure levels seen in humans TBBPA is expected to be conjugated and excreted before it can cause adverse effects. Moreover, TBBPA toxicity studies in rats addressing non-cancer endpoints indicated no considerable effects on histopathology, organ and body weights, reproductive and developmental parameters, behavior and neuropathology, clinical signs, serum chemistry or mortality rate (reviewed by (Colnot et al., 2014; Lai et al., 2015; EPA, 2015)). The only treatment-related alteration in rats was limited to decreased circulating thyroxine (T_4) serum levels, the inactive form of thyroid hormones. However, no concomitant changes of active triiodothyronine (T_3) and compensatory increase of thyroid stimulating hormone (TSH) were noted, as well as any evidence of histopathological changes of the thyroid tissue. As this observation was only found in rats, it is suggested to be species-specific and related to hepatic induction of T_4 -uridine diphosphate glucuronyl transferase (UDP-GT) enzymes which increase T_4 metabolism in the liver. Due the non-biologically relevant doses of TBBPA applied in these studies and the absence of other thyroid-related effects, this effect is not considered to be of relevance for human health (Canada, 2012; ECB, 2006). Therefore, to our knowledge, so far no effects of concern for human health have been reported for TBBPA.

5. Conclusion

In vitro and *in vivo* risk assessment studies of potential EDCs should include a careful consideration of human exposure and toxicokinetic parameters for the determination of systemically relevant compound concentrations. To avoid biased results in mode-of-action studies, the limitations and applicability of the *in vitro* testing systems need to be considered. Yeast GR screens are highly limited because of their low sensitivity towards glucocorticoids, probably due to efflux transport proteins. This may lead to false negative or false positive results, as exemplified in the current study for TBBPA. Using cell-free receptor binding and human cell-based transactivation assays, the results of the current study show no direct effect of TBBPA on GR function and very weak antagonistic effects on AR. Considering its rapid metabolism and low concentrations found in humans, TBBPA is unlikely to cause adverse effects by acting through GR or AR. The current study emphasizes the combined use of cell-based and cell-free assays for the assessment of chemical effects on steroid hormone receptors.

Conflicts of interest

The authors declare no conflict of interest.

Acknowledgements

This study was supported by the Swiss Center for Applied Human Toxicology (SCAHT) and the Swiss Federal Office of Public Health (FOPH). A.O. was supported as Chair for Molecular and Systems Toxicology by the Novartis Research Foundation. We

thank Dr. Martine Bourqui-Pittet and Dr. Orlando Mani from the FOPH for their input to this study. We thank Prof. Thierry Langer and Inte:Ligand GmbH for providing the LigandScout software.

References

- Abernathy, C.O., Liu, Y.P., Longfellow, D., Aposhian, H.V., Beck, B., Fowler, B., Goyer, R., Menzer, R., Rossman, T., Thompson, C., Waalkes, M., 1999. Arsenic: health effects, mechanisms of actions, and research issues. *Environ. Health Perspect.* 107, 593–597.
- Almughamsi, H., Whalen, M.M., 2016. Hexabromocyclododecane and tetrabromobisphenol A alter secretion of interferon gamma (IFN-gamma) from human immune cells. *Arch. Toxicol.* 90, 1695–1707.
- Baker, V.A., 2001. Endocrine disruptors—testing strategies to assess human hazard. *Toxicol. In Vitro* 15, 413–419.
- Baschant, U., Tuckermann, J., 2010. The role of the glucocorticoid receptor in inflammation and immunity. *J. Steroid Biochem. Mol. Biol.* 120, 69–75.
- Canada, 2012. Screening Assessment Report of Phenol, 4,4'-(1-methylethylidene)bis[2,6-dibromo (Tetrabromobisphenol A, TBBPA; CAS 79-94-7), Ethanol, 2,2'-[(1-methylethylidene)bis[(2,6-dibromo-4,1-phenylene)oxy]]bis, CAS 4162-45-2 and Benzene, 1,1'-(1-methylethylidene)bis[3,5-dibromo-4-(2-propenyloxy)-CAS 25327-89-3. Ministry of Environment and Health, Canada 2013.
- Cato, A., Celada, L., Kibakaya, E.C., Simmons, N., Whalen, M.M., 2014. Brominated flame retardants, tetrabromobisphenol A and hexabromocyclododecane, activate mitogen-activated protein kinases (MAPKs) in human natural killer cells. *Cell Biol. Toxicol.* 30, 345–360.
- Chang, H.C., Lindquist, S., 1994. Conservation of Hsp90 macromolecular complexes in *Saccharomyces cerevisiae*. *J. Biol. Chem.* 269, 24983–24988.
- Colnot, T., Kacew, S., Dekant, W., 2014. Mammalian toxicology and human exposures to the flame retardant 2,2',6,6'-tetrabromo-4,4'-isopropylidenediphenol (TBBPA): implications for risk assessment. *Arch. Toxicol.* 88, 553–573.
- Dankers, A.C., Roelofs, M.J., Piersma, A.H., Sweep, F.C., Russel, F.G., van den Berg, M., van Duursen, M.B., Masereeuw, R., 2013. Endocrine disruptors differentially target ATP-binding cassette transporters in the blood-testis barrier and affect Leydig cell testosterone secretion in vitro. *Toxicol. Sci.* 136, 382–391.
- Dunnick, J.K., Sanders, J.M., Kissling, G.E., Johnson, C.L., Boyle, M.H., Elmore, S.A., 2015. Environmental chemical exposure may contribute to uterine cancer development: studies with tetrabromobisphenol A. *Toxicol. Pathol.* 43, 464–473.
- ECB, 2006. European Union Risk Assessment Report – 2,2',6,6'-tetrabromo-4,4'-isopropylidenediphenol (tetrabromobisphenol A or TBBP-A) (CAS:79-94-7) Part II-human Health, Vol 63, EUR 22161 EN. Institute for Health and Consumer Protection, European Chemicals Bureau, European Commission Joint Research Centre, 4th Priority List, Luxembourg. Office for Official Publications of the European Communities.
- EFSA, 2011. EFSA panel on contaminants in the food chain (CONTAM): scientific opinion on tetrabromobisphenol A (TBBPA) and its derivatives in food. EFSA panel on contaminants in the food chain. *EFSA J.* 9 (12), 2477.
- EPA, 2015. U.S. Environmental Protection Agency, TSCA Work Plan Chemical Problem Formulation and Initial Assessment: Tetrabromobisphenol A and Related Chemicals Cluster Flame Retardants. EPA Document #740-R1-4004 (2015).
- Eder, W., Ege, M.J., von Mutius, E., 2006. The asthma epidemic. *N. Engl. J. Med.* 355, 2226–2235.
- Gaido, K.W., Leonard, L.S., Lovell, S., Gould, J.C., Babai, D., Portier, C.J., McDonnell, D. P., 1997. Evaluation of chemicals with endocrine modulating activity in a yeast-based steroid hormone receptor gene transcription assay. *Toxicol. Appl. Pharmacol.* 143, 205–212.
- Garabedian, M.J., Yamamoto, K.R., 1992. Genetic dissection of the signaling domain of a mammalian steroid receptor in yeast. *Mol. Biol. Cell* 3, 1245–1257.
- Gosavi, R.A., Knudsen, G.A., Birnbaum, L.S., Pedersen, L.C., 2013. Mimicking of estradiol binding by flame retardants and their metabolites: a crystallographic analysis. *Environ. Health Perspect.* 121, 1194–1199.
- Gosse, J.A., Taylor, V.F., Jackson, B.P., Hamilton, J.W., Bodwell, J.E., 2014. Monomethylated trivalent arsenic species disrupt steroid receptor interactions with their DNA response elements at non-cytotoxic cellular concentrations. *J. Appl. Toxicol.* 34, 498–505.
- Grimm, F.A., Hu, D., Kania-Korwel, I., Lehmler, H.J., Ludewig, G., Hornbuckle, K.C., Duffel, M.W., Bergman, A., Robertson, L.W., 2015. Metabolism and metabolites of polychlorinated biphenyls. *Crit. Rev. Toxicol.* 45, 245–272.
- Grosse, Y., Loomis, D., Guyton, K.Z., El Ghissassi, F., Bouvard, V., Benbrahim-Tallaa, L., Mattock, H., Straif, K., 2016. Carcinogenicity of some industrial chemicals. *Lancet Oncol.* 17, 419–420.
- Gumy, C., Chandsawangbhuwana, C., Dzyakanchuk, A.A., Kratschmar, D.V., Baker, M. E., Odermatt, A., 2008. Dibutyltin disrupts glucocorticoid receptor function and impairs glucocorticoid-induced suppression of cytokine production. *PLoS One* 3, e3545.
- Hamers, T., Kamstra, J.H., Sonneveld, E., Murk, A.J., Kester, M.H., Andersson, P.L., Legler, J., Brouwer, A., 2006. In vitro profiling of the endocrine-disrupting potency of brominated flame retardants. *Toxicol. Sci.* 92, 157–173.
- Han, E.H., Park, J.H., Kang, K.W., Jeong, T.C., Kim, H.S., Jeong, H.G., 2009. Risk assessment of tetrabromobisphenol A on cyclooxygenase-2 expression via MAP kinase/NF-kappaB/AP-1 signaling pathways in murine macrophages. *J. Toxicol. Environ. Health A* 72, 1431–1438.
- Jakobsson, K., Thuresson, K., Rylander, L., Sjodin, A., Hagmar, L., Bergman, A., 2002. Exposure to polybrominated diphenyl ethers and tetrabromobisphenol A among computer technicians. *Chemosphere* 46, 709–716.
- Jenkins, S.M., Ehman, K., Barone Jr., S., 2004. Structure-activity comparison of organotin species: dibutyltin is a developmental neurotoxicant in vitro and in vivo. *Brain Res. Dev. Brain Res.* 151, 1–12.
- Johansson, M., Nilsson, S., Lund, B.O., 1998. Interactions between methylsulfonyl PCBs and the glucocorticoid receptor. *Environ. Health Perspect.* 106, 769–772.
- Johansson, M., Johansson, N., Lund, B.O., 2005. Xenobiotics and the glucocorticoid receptor: additive antagonistic effects on tyrosine aminotransferase activity in rat hepatoma cells. *Basic Clin. Pharmacol. Toxicol.* 96, 309–315.
- Jones, G., Willett, P., Glen, R.C., Leach, A.R., Taylor, R., 1997. Development and validation of a genetic algorithm for flexible docking. *J. Mol. Biol.* 267, 727–748.
- Kaltreider, R.C., Davis, A.M., Lariviere, J.P., Hamilton, J.W., 2001. Arsenic alters the function of the glucocorticoid receptor as a transcription factor. *Environ. Health Perspect.* 109, 245–251.
- Kester, M.H., Bulduk, S., van Toor, H., Tibboel, D., Meinel, W., Glatt, H., Falany, C.N., Coughtrie, M.W., Schuur, A.G., Brouwer, A., Visser, T.J., 2002. Potent inhibition of estrogen sulfotransferase by hydroxylated metabolites of polyhalogenated aromatic hydrocarbons reveals alternative mechanism for estrogenic activity of endocrine disruptors. *J. Clin. Endocrinol. Metab.* 87, 1142–1150.
- Kibakaya, E.C., Stephen, K., Whalen, M.M., 2009. Tetrabromobisphenol A has immunosuppressive effects on human natural killer cells. *J. Immunotoxicol.* 6, 285–292.
- Kicinski, M., Vienne, M.K., Den Hond, E., Schoeters, G., Covaci, A., Dirtu, A.C., Nelen, V., Bruckers, L., Croes, K., Sioen, I., Baeyens, W., Van Larebeke, N., Nawrot, T.S., 2012. Neurobehavioral function and low-level exposure to brominated flame retardants in adolescents: a cross-sectional study. *Environ. Health* 11, 86.
- Kralli, A., Bohlen, S.P., Yamamoto, K.R., 1995. LEM1, an ATP-binding-cassette transporter, selectively modulates the biological potency of steroid hormones. *Proc. Natl. Acad. Sci. U. S. A.* 92, 4701–4705.
- Kuester, R.K., Solyom, A.M., Rodriguez, V.P., Sipes, I.G., 2007. The effects of dose, route, and repeated dosing on the disposition and kinetics of tetrabromobisphenol A in male F-344 rats. *Toxicol. Sci.* 96, 237–245.
- Lai, D.Y., Kacew, S., Dekant, W., 2015. Tetrabromobisphenol A (TBBPA): Possible modes of action of toxicity and carcinogenicity in rodents. *Food Chem. Toxicol.* 80, 206–214.
- Law, R.J., Allchin, C.R., de Boer, J., Covaci, A., Herzke, D., Lepom, P., Morris, S., Tronczynski, J., de Wit, C.A., 2006. Levels and trends of brominated flame retardants in the European environment. *Chemosphere* 64, 187–208.
- Macikova, P., Groh, K.J., Ammann, A.A., Schirmer, K., Suter, M.J., 2014. Endocrine disrupting compounds affecting corticosteroid signaling pathways in Czech and Swiss waters: potential impact on fish. *Environ. Sci. Technol.* 48, 12902–12911.
- NTP, 2013. Technical Report on the toxicology studies of tetrabromobisphenol A (CAS NO. 79-94-7) in F344/NTac rats and B6C3F1/N mice and toxicology and carcinogenesis study of tetrabromobisphenol A in Wistar Han [Cr:WI(Han)] rats and B6C3F1/N mice (gavage studies). NTP TR 587. National Toxicology Program, Research Triangle Park, NC.
- Nakanishi, Y., Shigematsu, N., Kurita, Y., Matsuba, K., Kanegae, H., Ishimaru, S., Kawazoe, Y., 1985. Respiratory involvement and immune status in yusho patients. *Environ. Health Perspect.* 59, 31–36.
- Nashev, L.G., Vuorinen, A., Praxmarer, L., Chantong, B., Cereghetti, D., Winiger, R., Schuster, D., Odermatt, A., 2012. Virtual screening as a strategy for the identification of xenobiotics disrupting corticosteroid action. *PLoS One* 7, e46958.
- Neel, B.A., Brady, M.J., Sargis, R.M., 2013. The endocrine disrupting chemical tolyfluanid alters adipocyte metabolism via glucocorticoid receptor activation. *Mol. Endocrinol.* 27, 394–406.
- Nelson, G.M., Prapapanich, V., Carrigan, P.E., Roberts, P.J., Riggs, D.L., Smith, D.F., 2004. The heat shock protein 70 cochaperone hsp enhances functional maturation of glucocorticoid receptor. *Mol. Endocrinol.* 18, 1620–1630.
- Nutten, S., 2015. Atopic dermatitis: global epidemiology and risk factors. *Ann. Nutr. Metab.* 66 (Suppl. 1), 8–16.
- OECD, 2012. Guidance Document on Standardised Test Guidelines for Evaluating Chemicals for Endocrine Disruption – Series on Testing and Assessment No. 150, ENV/JM/MONO(2012)22. Environment Directorate Joint Meeting of the Chemicals Committee and the Working Party on Chemicals, Pesticides and Biotechnology.
- Odermatt, A., Gumy, C., 2008. Glucocorticoid and mineralocorticoid action: why should we consider influences by environmental chemicals? *Biochem. Pharmacol.* 76, 1184–1193.
- Odermatt, A., Gumy, C., Atanasov, A.G., Dzyakanchuk, A.A., 2006. Disruption of glucocorticoid action by environmental chemicals: potential mechanisms and relevance. *J. Steroid Biochem. Mol. Biol.* 102, 222–231.
- Picard, D., Schena, M., Yamamoto, K.R., 1990. An inducible expression vector for both fission and budding yeast. *Gene* 86, 257–261.
- Reggiani, G., Bruppacher, R., 1985. Symptoms, signs and findings in humans exposed to PCBs and their derivatives. *Environ. Health Perspect.* 60, 225–232.
- Reistad, T., Mariussen, E., Fonnum, F., 2005. The effect of a brominated flame retardant, tetrabromobisphenol-A, on free radical formation in human neutrophil granulocytes: the involvement of the MAP kinase pathway and protein kinase C. *Toxicol. Sci.* 83, 89–100.
- Reistad, T., Mariussen, E., Ring, A., Fonnum, F., 2007. In vitro toxicity of tetrabromobisphenol-A on cerebellar granule cells: cell death, free radical formation, calcium influx and extracellular glutamate. *Toxicol. Sci.* 96, 268–278.

- Riggs, D.L., Roberts, P.J., Chirillo, S.C., Cheung-Flynn, J., Prapapanich, V., Ratajczak, T., Gaber, R., Picard, D., Smith, D.F., 2003. The Hsp90-binding peptidylprolyl isomerase FKBP52 potentiates glucocorticoid signaling in vivo. *EMBO J.* 22, 1158–1167.
- Roelofs, M.J., van den Berg, M., Bovee, T.F., Piersma, A.H., van Duursen, M.B., 2015. Structural bisphenol analogues differentially target steroidogenesis in murine MA-10 Leydig cells as well as the glucocorticoid receptor. *Toxicology* 329, 10–20.
- Rotroff, D.M., Martin, M.T., Dix, D.J., Filer, D.L., Houck, K.A., Knudsen, T.B., Sipes, N.S., Reif, D.M., Xia, M., Huang, R., Judson, R.S., 2014. Predictive endocrine testing in the 21st century using in vitro assays of estrogen receptor signaling responses. *Environ. Sci. Technol.* 48, 8706–8716.
- Routledge, E.J., Sumpter, J.P., 1996. Estrogenic activity of surfactants and some of their degradation products assessed using a recombinant yeast screen. *Environ. Toxicol. Chem.* 15, 241–248.
- Schauer, U.M., Volkel, W., Dekant, W., 2006. Toxicokinetics of tetrabromobisphenol a in humans and rats after oral administration. *Toxicol. Sci.* 91, 49–58.
- Schoch, G.A., D'Arcy, B., Stihle, M., Burger, D., Bar, D., Benz, J., Thoma, R., Ruf, A., 2010. Molecular switch in the glucocorticoid receptor: active and passive antagonist conformations. *J. Mol. Biol.* 395, 568–577.
- Sevilla, L.M., Latorre, V., Sanchis, A., Perez, P., 2013. Epidermal inactivation of the glucocorticoid receptor triggers skin barrier defects and cutaneous inflammation. *J. Invest. Dermatol.* 133, 361–370.
- Stavreva, D.A., George, A.A., Klausmeyer, P., Varticovski, L., Sack, D., Voss, T.C., Schiltz, R.L., Blazer, V.S., Iwanowicz, L.R., Hager, G.L., 2012. Prevalent glucocorticoid and androgen activity in US water sources. *Sci. Rep.* 2, 937.
- Whalen, M.M., Loganathan, B.G., Kannan, K., 1999. Immunotoxicity of environmentally relevant concentrations of butyltins on human natural killer cells in vitro. *Environ. Res.* 81, 108–116.
- Wikoff, D.S., Rager, J.E., Haws, L.C., Borghoff, S.J., 2016. A high dose mode of action for tetrabromobisphenol A-induced uterine adenocarcinomas in Wistar Han rats: a critical evaluation of key events in an adverse outcome pathway framework. *Regul. Toxicol. Pharmacol.* 77, 143–159.
- Wolber, G., Langer, T., 2005. LigandScout: 3-D pharmacophores derived from protein-bound ligands and their use as virtual screening filters. *J. Chem. Inf. Model.* 45, 160–169.

Studying potential endocrine disrupting chemicals: comparison of yeast and human cell-based *in vitro* assays

The production of chemicals for agricultural and industrial use, cosmetics or food additives is steadily increasing. To protect the environment and human health against the potential risks arising from these man-made chemicals, the authorities introduced several programs to promote adequate substance-based hazard and risk characterizations. Such chemicals may cause harmful effects by disturbing the hormonal system. These so-called endocrine disrupting chemicals (EDCs) can mimic or block the action of endogenous hormones on their corresponding receptors, disrupt their synthesis, metabolism, transport or underlying signaling pathways. Sex steroid hormones (androgens, estrogens) orchestrate in particular developmental and reproductive functions, whereas glucocorticoids (especially cortisol) essentially regulate the immune system, blood pressure, energy metabolism and developmental aspects. Disruption of the endocrine system has been associated with developmental and reproductive malfunctions, allergies, diabetes, cardiovascular diseases, and cancer.

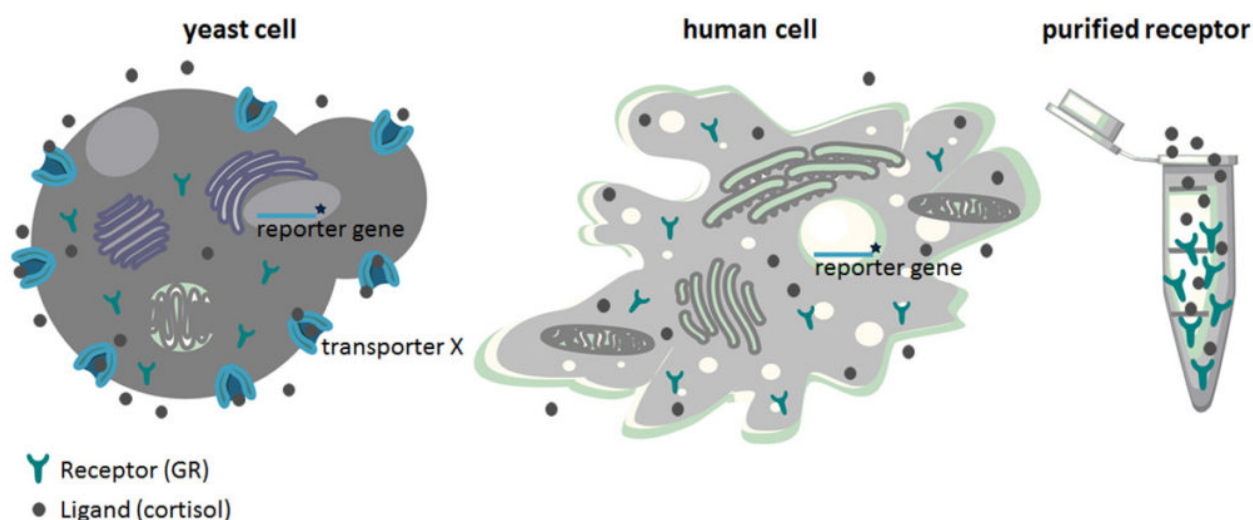


Fig. 1. Schematic representation of a yeast and a human reporter gene cell and the purified receptor in a test tube. Due to a transporter X on the yeast cell membrane, the yeast cell is able to export glucocorticoids, thereby limiting the ligand accessibility to the GR. This alters the assay sensitivity and could lead to false positive or false negative results. In comparison, the human cell is lacking this transporter X. However, the only test system with free ligand accessibility represents the purified receptor in a test tube. Therefore, an adequate evaluation of chemicals acting on steroid hormone receptors should include a combination of cell-based and cell-free assays.

In vitro testing systems play a crucial role during the safety assessment of EDCs and gained even more importance since chemicals used in body care products can no longer be tested in animals.

These *in vitro* studies are conducted with microorganisms or cellular components in an artificial system separated from their natural environment. Human cell-based assays are widely used to study EDC action on hormone receptors, whereby receptor-mediated reporter genes are used as receptor activation read-out. A cost-effective alternative are yeast reporter cell assays. However, each *in vitro* testing system has its limitations, which needs to be considered for data analysis. Yeast androgen (YAS) and estrogen screen (YES) show limited uptake of certain compounds through the yeast cell membrane and may not sufficiently allow discriminating between compounds activating or suppressing the receptor activity.

The extensively applied flame retardant tetrabromobisphenol A (TBBPA) was previously reported to strongly inhibit the activity of the glucocorticoid receptor (GR) and to a lesser extent the androgen receptor (AR) in yeast reporter gene assays. Regarding the limitations of these systems, the current study evaluated this observation in a human cell-based assay. TBBPA did not stimulate nor suppress GR activity. To exclude limitations due to different cellular uptake of TBBPA by yeast and human cells, receptor binding assays were conducted under cell-free conditions with direct access of the compound to the receptor. Nevertheless, this experiment allows only conclusions on the affinity of a substance to bind to a receptor but not its ability to activate or inhibit. In this regard, TBBPA did not affect the ligand binding to the GR. Computer simulations with TBBPA and GR supported this finding. Thus, TBBPA does not directly disturb GR function. However, inhibition of the AR could be confirmed in the human cell-based and cell-free systems, although the effect was much less pronounced.

The discrepancy to the earlier report may be due to limitations of the yeast assay. GR yeast assays are known for their low sensitivity, probably due to a yeast specific transporter exporting glucocorticoids from the cell. By upregulating the expression of this transporter TBBPA might indirectly affect the glucocorticoid concentration in the yeast cell and therefore lead to false positive results. Thus, it is highly important to be aware of the limitations of each *in vitro* testing system to avoid false positive or false negative results. Many studies applied TBBPA concentrations far above those found in the human body. However, appropriate risk assessment should always include the evaluation of the substance at the concentration found in human. TBBPA is rapidly degraded and only detected at very low concentrations in human. Thus, TBBPA unlikely causes adverse effects by disrupting GR or AR action. The current study highlights the use of a combination of cell-based and cell-free assays for the evaluation of chemicals on steroid hormone receptors.

Katharina R. Beck, Alex Odermatt

*Swiss Center of Applied Human Toxicology and Division of Molecular and Systems Toxicology,
Department of Pharmaceutical Sciences, University of Basel, Switzerland*

Publication

[Evaluation of tetrabromobisphenol A effects on human glucocorticoid and androgen receptors: A comparison of results from human- with yeast-based in vitro assays.](#)

Beck KR, Sommer TJ, Schuster D, Odermatt A

Toxicology. 2016 Aug 31

3.2.2. Discussion

The re-evaluation of TBBPA on GR function revealed neither agonistic nor antagonistic effects in the GR transactivation assay in HEK-293 cells. To exclude limitations due to different cellular uptake of TBBPA by yeast and human cells, receptor binding assays were performed under a cell-free environment in order to achieve direct access of the compound to the receptor. Nevertheless, this experiment allows only conclusions on the affinity of a substance to bind to a receptor, respectively its ability to displace an already bound ligand from the binding site but does not allow conclusions about its potential to activate or suppress a receptor's function. In the cell-free GR binding assay TBBPA was not able to displace the radiolabeled ligand dexamethasone from the GR ligand binding pocket. Docking calculations were performed to computationally elucidate the obtained results and to assess the interactions formed between the GR ligand binding pocket and TBBPA. Particular attention was paid on potential interactions with the helix 12, as a relocation of this helix can reshape the coactivator binding site into the corepressor binding site and thereby lead to repression of GR gene transcription mediated by the binding of nuclear receptor corepressors [65]. Although no exclusion of TBBPA from the GR binding pocket was found due to steric hindrance, key stabilizing interactions detected with dexamethasone or the GR antagonist RU486 (mifepristone) were absent in the case of TBBPA. Especially the side pocket important for helix 12 interactions was not covered by TBBPA as compared to RU486. Thus, no direct interactions of TBBPA with GR could be identified.

Nevertheless, the antiandrogenic activity of TBBPA could be confirmed in HEK-293 cells, although an order of magnitude less pronounced than that observed in the yeast screen. The discrepancy between these observations and the earlier report seem to be due to the limitations of the yeast assay. The low sensitivity of GR yeast assays has already been observed earlier and is probably a result of limited intracellular concentrations of dexamethasone modulated by the yeast-specific ATP-binding cassette transporter PDR5 [66-68]. Mutant yeast strains lacking PDR5 showed increased glucocorticoid sensitivity and higher intracellular dexamethasone concentrations. PDR5, a functional homolog of the human P-gp, was further reported to be inhibited by TBBPA, albeit only at high concentrations of TBBPA ($IC_{50} \sim 25 \mu M$) [69]. However, taking the potent antiglucocorticoid effect of TBBPA in the yeast screen into consideration, inhibition of PDR5 at TBBPA concentration below $1 \mu M$ is unlikely. Moreover, reduced PDR5 activity would rather lead to increased dexamethasone concentrations in the cytosolic compartment and thereby counteract the antagonistic activity. Instead, a hypothesis to be tested would include the transcriptional induction of PDR5 or genes encoding for other transport proteins inducing the efflux of glucocorticoids from the yeast cytosol. Interestingly, a study involving a P-gp homologue from scallop showed around 1.5 fold upregulation of the corresponding mRNA compared to control levels upon exposure to 9 nM TBBPA [70]. Nevertheless, an altered transport

mechanism may not be the only factor contributing to distinct GR-ligand response in yeast [68]. Introduction of co-chaperons for example was able to enhance GR reporter activity in yeast cells [71, 72]. To sum up, GR yeast screens display considerable limitations due to their low sensitivity towards glucocorticoids, being highly susceptible to biased results in mode-of-action studies.

EDC safety evaluations present a major challenge concerning assay sensitivity. Highly sophisticated analytical techniques such as Liquid or Gas Chromatography–Tandem Mass Spectrometry Measurements (LC-MS/GC-MS) allow the detection and quantification of almost all analytes of interest. However, an important aspect of hormone action is that it occurs at extremely low concentrations. Alternatively, effect-based methods quantifying the activation of a receptor, including reporter-gene assays, often achieve higher sensitivity in substance screenings. The limit of quantification (LOQ) for the active estrogen estradiol in chemical analytical methods is ~100 pg/L whereas the effect-based ER-Calux assay shows a LOQ of ~17 pg/L [73]. In contrast, the inactive estrone can be analytically quantified with a LOQ of ~10 pg/L, but in the effect-based system only with a LOQ of ~850 pg/L [73]. Regarding estrone, a modified ER-Calux expressing the estrone to estradiol converting enzyme 17 β -HSD1 would be an interesting option to achieve also high sensitivity to detect estrone. Furthermore, effect-based methods are currently the only available methods to detect specific endocrine effects of environmental samples with an unknown composition of different substances. On the other hand, these *in vitro* tests already assume knowledge or hypotheses of the mode of action of an EDC.

An EDC might exert its mode of action not exclusively through one but through multiple mechanisms, and as a part of compound mixtures occurring in the environment a certain compound may react even different. The absence of one mechanism is not automatically the evidence that this compound may not act through another mechanism. Regarding TBBPA, several studies suggested an interference with a pathway further downstream of GR, the mitogen-activated protein kinase (MAPK) pathways (described in our published article [58]). However, the majority of these *in vitro* studies used TBBPA concentrations in the lower micromolar range. Against this background, Knudsen et al stated that ‘the relative specificity of assays/targets/chemicals have revealed the general concept of an ‘assay burst’ of promiscuity at high chemical concentrations [...]’ [74]. Therefore, the relevant concentrations observed in the human body are crucial to elucidate for an appropriate risk assessment. TBBPA was only found at extremely low concentrations in the human body and the concentrations reported to cause biochemical effects in *in vitro* experiments were several orders of magnitude higher. Its rapid first pass metabolism by conjugation with glucuronic acid or sulfate may explain the low bioavailability after oral exposure. A more comprehensive report is found in the published article ‘Evaluation of tetrabromobisphenol A effects on human glucocorticoid and androgen receptors: a comparison of results from human- with yeast-based *in vitro* assays’ in the section above [58]. Hence, at the exposure

levels observed in humans, TBBPA can be considered to be metabolized and excreted before it causes harmful effects.

Concerns about the environmental risk of such industrial chemicals led to the development of a market for novel replacement alternatives. Several TBBPA derivatives belong to this group such as tetrabromobisphenol A-bis(2,3-dibromopropylether) (TBBPA-DBPE), Tetrabromobisphenol A dihydroxyethyl ether (TBBPA-DHEE) or Tetrabromobisphenol A bis(allyl) ether (TBBPA-BAE) [75]. Still, the introduction of new or modified chemicals always implies a lack of sufficient information on environmental and human exposure as well as possible health aspects, a gap that may be filled years after the market launch and with an uncertain outcome. Thus, might there be a solution to avoid the design of hazardous chemicals as early as possible? As already discussed in the published review article 'Virtual screening applications in short-chain dehydrogenase/reductase research', *in silico* applications display valuable tools to evaluate potential EDCs at an early stage and thereby may aid to prioritize the chemicals for further *in vitro* assessments [9]. Computational analysis can include the assessment of potential biologically actives respectively anti-target screenings (by molecular docking, quantitative structure activity relationships (QSAR) models or computational systems biology applications) or the prediction of physico-chemical properties [76-78]. However, computational tools should always be considered as complementary techniques to *in vitro* testing systems. The prioritizing of chemicals can facilitate the selection of effect-based methods as, discussed in the section above, this requires previous knowledge of a potential mode of action. On the other hand, high-throughput *in vitro* screens offer a solution for this issue as well, albeit the selection of the most predictive assays seems to be a major challenge. Unfortunately, receptor activities are often determined with partial constructs including only the ligand binding domain, which can lead to biased results. To meet the requirements of the complex biology behind the endocrine system, further intact as well as secondary mechanistic assays and finally *in vivo* studies would be crucial to fully elucidate the safety of a chemical. Figure 2 displays a potential strategy for the evaluation of potential EDCs, adapted from the screening strategy for biological validation published in our review article and with reference to the Tiered Protocol for Endocrine Disruptors [9, 76]. Nevertheless, it is essential to always consider the limitations of each testing system including the distinct sensitivities and specificities as well as observational human data if available.

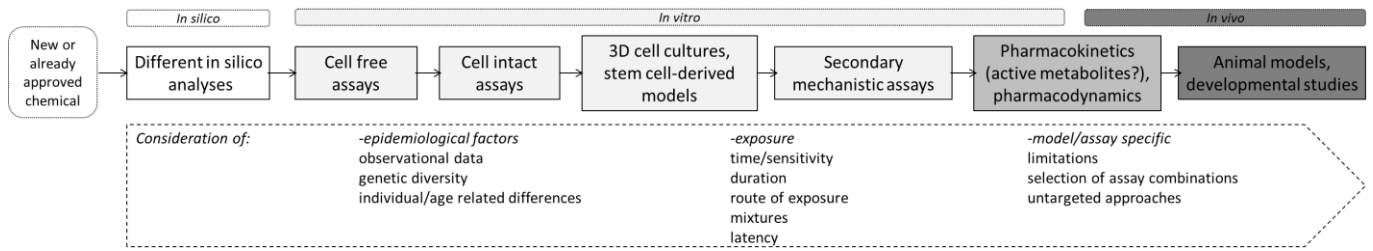


Figure 2. Potential EDC screening strategy.

4. Substrate identification

SDRs metabolize a remarkably broad range of substrates including steroid hormones, oxysterols, bile acids, fatty acids, prostaglandins, retinoids and various xenobiotics [4, 79]. Despite the considerable structural similarity between the different members of the SDR superfamily, their primary sequence similarities are rather low and the substrate specificities and the physiological functions of a large percentage of the SDRs remain poorly investigated. Therefore, to improve the understanding of the physiological roles of so-called orphan SDRs and by that potentially identifying novel drug or anti-drug targets, SDR deorphanization strategies are of great importance.

However, SDRs do not have a common activity element that could be used as suitable assay read-out to assess potential substrates, compared to other protein families. This impedes the effort and the progression of SDR deorphanization. G protein-coupled receptors (GPCR), for instance, exert specific changes upon activation that can be detected by monitoring well-described steps including the accumulation of second messengers [80]. Furthermore, the wide spectrum of metabolic reactions catalyzed by SDRs and the lack of structural information for many SDR, additionally hamper the attempt to deorphanize SDRs. In this regard, only a small number of studies applied structural modeling approaches for SDR substrate identification. Examples for members of the SDR family, but also for non-SDR enzymes, can be found in the published review 'Virtual screening applications in short-chain dehydrogenase/reductase research', therein under chapter 2.2.3. 'Application of structural modeling for substrate identification' [9].

The application of the VS approach used for the identification of enzyme inhibitors, as it was described in the sections above, is extended in following parts including investigations of novel substrate specificities for three different SDR members: the two multi-functional enzymes, 11 β -HSD1 and carbonyl reductase (CBR) 1 as well as the orphan enzyme DHRS7.

4.1. 11 β -hydroxysteroid dehydrogenase type 1

By catalyzing the local conversion of inactive to active glucocorticoids, 11 β -HSD1 plays an important role in the regulation of metabolic functions. In most tissues it is co-expressed with the enzyme hexose-6-phosphate-dehydrogenase (H6PDH) [81], both facing the endoplasmic reticulum (ER) lumen [82-84]. H6PDH functions as supplier of the cofactor NADPH for 11 β -HSD1 and determines thereby the reaction direction towards an oxoreductase, representing the predominant activity *in vivo* [85]. Additionally, a

physical interaction between 11 β -HSD1 and H6PDH as well as the need of a high NADPH/NADP⁺ ratio for maintaining the 11 β -HSD1 oxoreductase activity was reported [86, 87].

Elevated 11 β -HSD1 activity has been associated with insulin-resistant diabetes, hyperlipidemia, hypertension, and visceral obesity [88, 89]. Several studies addressed drug development efforts and pharmacological inhibition of 11 β -HSD1 as a therapeutic option to treat metabolic diseases as described in more detail in the sections '11 β -hydroxysteroid dehydrogenase type 1' in both published review articles [9, 10].

Several of the steroid metabolizing enzymes are highly promiscuous in their ligand binding specificity due to the fact that the steroid backbone has several symmetry planes [90]. The position 11 of the steroid molecule is rotationally symmetric to position 7 and position 3 is symmetric to positions 17 and 20 (see Figure 6) [90-92]. This property is nicely reflected by the substrate specificity of 11 β -HSD1, metabolizing in addition to glucocorticoids also other 11- and 7-oxygenated steroids and cholesterol derivatives such as 11-oxoandrogens, 11-oxogestagens, 7-oxo bile acids or 7-ketocholesterol (reviewed in [93]). The physiological impact of several of these metabolites is mostly unexplored. The multi-functionality of 11 β -HSD1 is further emphasized by its function as a carbonyl reductase towards a variety of non-steroidal xenobiotics in phase I biotransformation reactions (reviewed in [93, 94]). The reduction of reactive carbonyl compounds displays an important detoxification reaction involving different enzymes, mainly from the SDR family (including CBR1, which is discussed in more detail in the following chapter) and AKRs, which show conserved Tyr and Lys residues in similar positions as described in the introduction of this thesis.

Evidence for glucocorticoid-independent effects and therefore the presence of so far unexplored endogenous substrates of 11 β -HSD1 is provided by earlier studies; 11 β -HSD1 is known to catalyze the conversion of the secondary bile acid 7-oxolithocholic acid (7oxoLCA) mainly into chenodeoxycholic acid (CDCA) [95]. Whereas 11 β -HSD1 deficiency increased the circulating levels of unconjugated bile acids, probably due to a reduced expression of FATP5, an enzyme involved in bile acid conjugation, the expression of glucocorticoid target genes was unaltered [96]. However, liver-specific GR knockdown, although affecting glucocorticoid target gene expression, did not alter FATP5 expression.

Additionally, depending on the duration of an inflammatory condition, 11 β -HSD1 deficiency/inhibition can either lead to a more severe outcome, as found during acute inflammation, or it may be beneficial, as seen in chronic inflammatory situations such as in atherosclerosis (reviewed in [97]). This may also indicate a yet unknown contribution of 11 β -HSD1 to other, glucocorticoid-independent metabolic pathways.

The following sections cover investigations into involvement of 11 β -HSD1 in the generation of dihydroxylated oxysterols and an attempt to apply a VS strategy for the characterization and deorphanization of SDRs, using 11 β -HSD1 as a model enzyme.

4.1.1. Oxysterol metabolism

Manuscript in preparation (data not yet complete):

The Oxysterols 7 β ,25-dihydroxycholesterol and 7 β ,27-dihydroxycholesterol are Enzymatically Formed by 11 β -Hydroxysteroid Dehydrogenase Type 1

Katharina R. Beck¹, Denise V. Kratschmar¹, Carlos A. Penno², Klaus Seuwen², Alex Odermatt^{1*}

¹Division of Molecular and Systems Toxicology, Department of Pharmaceutical Sciences, Pharmazentrum, University of Basel, Klingelbergstrasse 50, 4056 Basel, Switzerland.

²Developmental and Molecular Pathways, Novartis Institutes for BioMedical Research, Basel, Switzerland.

*Address of correspondence: Prof. Dr. Alex Odermatt, Division of Molecular and Systems Toxicology, Department of Pharmaceutical Sciences, Pharmazentrum University of Basel, Klingelbergstrasse 50, 4056 Basel, Switzerland

Alex.Odermatt@unibas.ch; Phone: + 41 61 207 1530; Fax: + 41 61 207 1515

Abstract

Oxysterols are metabolites from cholesterol derived either through autoxidation or enzymatic processes. They consist of a large family of bioactive lipids involved in lipid and carbohydrate homeostasis, neuronal development and immune system regulation, and they have been associated with the progression of multiple pathologies. A role for 11 β -hydroxysteroid dehydrogenase type 1 (11 β -HSD1) in oxysterol metabolism by metabolizing 7ketocholesterol (7kC) has been demonstrated. However, no endogenous receptor has been identified so far for 7kC or its metabolite 7 β -hydroxycholesterol, in contrast to the known receptors for 7 α ,25-dihydroxycholesterol (7 α 25OHC), i.e. Epstein-Barr virus-induced gene 2 (EBI2), or 7 β ,27-dihydroxycholesterol (7 β 27OHC), i.e. retinoic acid related orphan receptor (ROR) γ . In order to unravel the underlying biosynthetic pathways of such dihydroxylated oxysterols, this work investigated the role of 11 β -HSD1 in the generation of dihydroxylated oxysterols. For the first time, the stereospecific and seemingly irreversible oxoreduction of 7-keto,25-hydroxycholesterol (7k25OHC) and 7-keto,27-hydroxycholesterol (7k27OHC) to their corresponding 7 β -hydroxylated metabolites 7 β 25OHC and 7 β 27OHC by recombinant human 11 β -HSD1 could be demonstrated in vitro in intact transfected HEK-293 cells. Furthermore, 7k25OHC and 7k27OHC potently inhibited the 11 β -HSD1-dependent oxoreduction of cortisone to cortisol. Binding of 7k25OHC and 7k27OHC to 11 β -HSD1 was investigated by molecular modeling calculations, suggesting competition with cortisone at the substrate binding pocket. A contribution of the 11 β -HSD1-dependent metabolism of these oxysterols to the pathogenesis of hepatic steatosis by regulation of ROR or to the migration of immune cells by EBI2 activation might be potential target mechanisms that need to be explored.

Keywords

Oxysterol; 11beta-hydroxysteroid dehydrogenase; metabolism; 7-ketocholesterol; reductase

Abbreviations

11 β -HSD1, 11 β -hydroxysteroid dehydrogenase type 1; 25OHC, 25-hydroxycholesterol; 27OHC, 27-hydroxycholesterol; CYP27A1, 27-hydroxylase; 7 α 25OHC, 7 α ,25-dihydroxycholesterol; 7 β 27OHC, 7 β ,27-dihydroxycholesterol; 7 β OHC, 7 β -hydroxycholesterol; 7oxoLCA, 7-oxolithocholic acid; 7kC, 7-ketocholesterol; 7k27OHC, 7-keto,27-hydroxycholesterol; CDCA, chenodeoxycholic acid; Ch25H, cholesterol 25-hydroxylase; EBI2, Epstein-Barr virus-induced gene 2; GPCR, G-protein-coupled

receptor; GR, glucocorticoid receptor; LXR, Liver X receptor; NAFLD, nonalcoholic fatty liver disease; NASH, non-alcoholic steatohepatitis; ROR γ , retinoid-related orphan receptor gamma; UHPLC-MS/MS, ultra-high pressure liquid chromatography tandem mass spectrometry; UDCA, ursodeoxycholic acid

1. Introduction

Oxysterols are oxidized metabolites derived from cholesterol or cholesterol precursors either through radical processes or enzymatic reactions, bearing additional oxygen functionalities at the side chains and/or in the ring system of cholesterol [1]. In the past, oxysterols have been mainly considered as intermediates of bile acid and steroid hormone biosynthetic pathways; however, research in the last years emphasized their role as bioactive lipids involved in cholesterol, lipid and carbohydrate homeostasis, neuronal development and immune system regulation but also implicated a contribution to the progression of multiple pathologies such as atherosclerosis, multiple sclerosis, Alzheimer's disease, retinopathies and nonalcoholic fatty liver disease (NAFLD) (reviewed in [2-5]). In order to unravel (patho-)physiological mechanisms involving oxysterols, it is crucial to elucidate the underlying formation and degradation of oxysterols and to uncover their intracellular and tissue-specific site of generation/metabolism.

7-ketocholesterol (7kC) is one of the most extensively studied oxysterols and particularly known for its pro-inflammatory and cytotoxic properties (reviewed in [1, 6, 7]). It still remains unclear, however, whether the biological effects are caused by 7kC or by its metabolites. In situ, 7kC is mainly generated by autoxidation of cholesterol during conditions of oxidative stress. In contrast to the low abundance of oxysterols in the circulation, compared to cholesterol, 7kC levels of up to 10 μ M have been measured in macrophage-derived foam cells in atherosclerotic lesions and in lenses of patients with cataract [8-10]. In macrophages as well as in the retinal pigment epithelium, conversion of 7kC into 7-keto,27-hydroxycholesterol (7k27OHC) by sterol 27-hydroxylase (CYP27A1) was reported [11, 12]. This metabolic step is ablated in macrophages derived from patients suffering from cerebrotendinous xanthomatosis, bearing a defect in the gene encoding for CYP27A1 [11]. These patients have normal circulating cholesterol, but increased 7kC levels and are prone for the development of premature atherosclerosis [13].

As the mitochondrial CYP27A1 is the first enzyme involved in the alternative biosynthesis pathway of bile acids in the liver, hepatic conversion of dietary 7kC to 7k27OHC is evident [14, 15]. However, a study with mice having a homozygous null mutation in the Cyp27 gene showed rapid and extensive metabolism of 7kC in the liver, indicating the involvement of another enzyme for the hepatic 7kC metabolism [16]. This enzyme was proposed to be 11 β -hydroxysteroid dehydrogenase type 1 (11 β -HSD1), stereo-specifically converting 7kC into 7 β -hydroxycholesterol (7 β OHC) in humans, rats and mice [17-19]. These results were further supported by data from transgenic 11 β -Hsd1-deficient mice exhibiting an increased 7kC to 7 β OHC ratio in liver tissue samples [20].

The role of 11 β -HSD1, well-known for the local conversion of inactive into active glucocorticoids, in oxysterol metabolism and atherosclerotic plaque progression has been addressed in several studies

(reviewed in [21]). Interestingly, no direct accumulation of 7kC could be detected in the arterial wall of Hsd11b1^{-/-} mice [22], and a disturbed 11 β -HSD1 function was rather associated with an atheroprotective and beneficial metabolic profile [23-25]. Whether the observed favorable effects upon 11 β -HSD1 inhibition were due to decreased intracellular levels of active glucocorticoids or whether these effects were glucocorticoid-independent remains unclear and requires further research.

Evidence for metabolic effects of 11 β -HSD1 modulation that are independent of glucocorticoid metabolism was provided by an analysis of its impact on bile acid homeostasis [26]. 11 β -HSD1 catalyzes the conversion of the secondary bile acid 7-oxolithocholic acid (7oxoLCA) mainly into chenodeoxycholic acid (CDCA) and to a lesser extent into ursodeoxycholic acid (UDCA) [27]. Disruption of the 11 β -HSD1 function was found to increase circulating levels of unconjugated bile acids, possibly due to a decreased expression of an enzyme involved in bile acid conjugation, FATP5 [26]. Interestingly, no change in FATP5 expression was detected in liver-specific glucocorticoid receptor (GR) knockdown mice, suggesting that the altered FATP5 expression was glucocorticoid-independent.

Despite the extensive research focusing on the effects of 7kC and 7 β OHC, no cognate endogenous receptors have been identified for them so far, whereas a variety of targets are known for side-chain oxidized oxysterols (e.g. 25-hydroxycholesterol (25OHC) or 27-hydroxycholesterol (27OHC)), dihydroxylated oxysterols such as 7 β ,27-dihydroxycholesterol (7 β 27OHC) or 7 α ,25-dihydroxycholesterol (7 α 25OHC) or the related bile acids (as reviewed in [2, 28, 29]). Members of the nuclear hormone receptor family belong to most extensively studied targets of oxysterol function, with a primary focus on the Liver X receptors (LXR), playing an important role in lipid homeostasis. Another nuclear hormone receptor, the retinoic acid related orphan receptor gamma (ROR γ) and its splice variant ROR γ t, which is required for the generation of IL-17-producing Th17 T cells in immune host defense, was recently discovered to be activated by 7 β 27OHC [30]. Whilst formation of 7 α ,25OHC and 7 α ,27OHC from 25OHC and 27OHC is controlled by CYP7B1 [28, 31], the origin of the 7 β -hydroxy forms remained unknown. However, since the conversion of 7kC into 7k27OHC by CYP27A1 has been detected in different tissues, it remained to be investigated whether 7 β 27OHC can be formed enzymatically from 7k27OHC by 11 β -HSD1 and whether 11 β -HSD1 could control the regulation of nuclear receptors other than GR. A further receptor involved in immune response mechanisms targeted by dihydroxylated oxysterols is the G-protein-coupled receptor (GPCR) Epstein-Barr virus-induced gene 2 (EBI2) [32, 33]. 7 α 25OHC, 7 α 27OHC and to a lesser extent their corresponding β -isomers were found to act as endogenous chemoattractants for immune cells expressing EBI2, thereby regulating immune cell migration. The hydroxylation of 7kC through cholesterol 25-hydroxylase (Ch25H) to 7k25OHC, although, not yet experimentally determined, has been proposed [34]. Considering the stereo-specific conversion of 7kC to 7 β OHC by human 11 β -HSD1, a careful assessment

whether 11 β -HSD1 can metabolize 7k25OHC and 7k27OHC and whether it exclusively forms the 7 β -hydroxy forms or also the 7 α -hydroxy metabolites is necessary.

Thus, the present study aimed to investigate whether 11 β -HSD1 is involved in the generation of dihydroxylated oxysterols. Recombinant human and mouse 11 β -HSD1 were expressed in HEK-293 cells, followed by incubation with the respective oxysterol and assessment of enzyme activity using ultra-high pressure liquid chromatography tandem mass spectrometry (UHPLC-MS/MS). Additionally, the oxysterol-dependent inhibition of cortisone oxoreduction by human and murine 11 β -HSD1 was assessed, and binding to 11 β -HSD1 was investigated by molecular modeling.

2. Materials and Methods

2.1. Chemicals and reagents

[1,2-³H]-cortisone was purchased from American Radiolabeled Chemicals (St.Louis, MO), 7k,25OHC, 7 β ,25OHC, 7 α ,25OHC, 7k,27OHC, 7 β ,27OHC, 7 α ,27OHC, 7 α ,25OHC-d6 and 7 β ,27OHC-d6 from Avanti Polar Lipids, Inc. (Alabaster, AL) and all other chemicals from Sigma Aldrich (Buchs, Switzerland) of the highest grade available. Cell culture media were obtained from Sigma Aldrich. UHPLC-grade purity methanol, acetonitrile and formic acid were obtained from Biosolve (Dieuze, France). T0504 (5H-1,2,4-triazolo(4,3-a)azepine,6,7,8,9-tetrahydro-3-tricyclo(3-3-1-13-7)dec-1-yl) was purchased from Enamine (Kiev, Ukraine).

2.2. Cell culture

Human Embryonic Kidney-293 cells (HEK-293) cells were obtained from ATCC (Manassas, VA, USA) and were cultured in Dulbecco's modified Eagle medium (DMEM) supplemented with 10% fetal bovine serum, 4.5 g/L glucose, 100 U/mL penicillin/streptomycin, 2 mM L-glutamine, 10 mM HEPES, pH 7.4, and 10% MEM non-essential amino acid solution.

2.3. Inhibition of human and mouse 11 β -HSD1 cortisone oxoreduction activity by oxysterols determined in cell lysates

Enzyme activities were determined as described earlier using lysates of HEK-293 cells stably expressing human 11 β -HSD1 and hexose-6-phosphate dehydrogenase (H6PDH; HHH7 clone) [35] or HEK-293 cells transiently expressing mouse 11 β -Hsd1. 11 β -HSD1 reductase activity was measured by incubating the lysates for 10 min at 37°C with 200 nM radiolabeled cortisone, 500 μ M NADPH and test substance or

vehicle. The reaction was stopped by adding an excess amount of unlabeled cortisone and cortisol (1:1, 2 mM each, in methanol). Steroids were separated by thin layer chromatography (TLC) using chloroform and methanol (9:1). Conversion of radiolabeled substrate was measured by scintillation counting. The substrate conversion was determined and compared to the enzyme activity in the control sample. Data (mean \pm SD) were normalized to vehicle control (DMSO) and obtained from at least three independent experiments.

2.4. Determination of the 11 β -HSD1-dependent metabolism of oxysterols in intact cells

HEK-293 cells stably expressing human 11 β -HSD1 and H6PDH (50'000 per well) were seeded in poly-L-lysine coated 96-well plates and cultivated for 24 h. The cells were washed with steroid-free DMEM (cDMEM) and incubated for 2 h at 37°C. The medium was then replaced by 50 μ L cDMEM containing either 1 μ M of the respective oxysterol (7k25OHC, 7k27OHC, 7 β 25OHC, 7 β 27OHC, 7 α 25OHC or 7 α 27OHC) or 1 μ M cortisone in the presence or absence of 1 μ M 11 β -HSD1 inhibitor (T0504), followed by incubation for 1 h. For quantification of oxysterol and cortisone/cortisol levels by UHPLC-MS/MS, liquid-liquid extraction of cell culture supernatants was performed. Cell supernatants (45 μ L) were mixed with 100 μ L ice-cold acetonitrile:isopropanol (7:3) containing 100 nM deuterium-labeled 7 α 25OHC, 7 β 27OHC or corticosterone as internal standards and 1 μ L/20 μ L sample of a standard solution of the antioxidants butylhydroxytoluol (BHT) and triphenylphosphine (TPP) (standard solution of 10 mg BHT and 25 mg TPP in 10 mL ethanol) to avoid autoxidation. After incubating the samples in a shaker for 30 min at 4°C and 300 rotations/min, the samples were evaporated to dryness under nitrogen to minimize oxidation from atmospheric oxygen and reconstituted in 25 μ L methanol:ultra pure water (1:1). The samples were then centrifuged at 4°C, 3220 \times g for 10 min and the supernatant stored at -20°C until further analysis.

2.5. Ultra-high pressure liquid chromatography–tandem mass spectrometry measurements

Oxysterols were simultaneously analyzed by UPLC-MS/MS using an Agilent 1290 Infinity UPLC binary solvent delivery system equipped with a column oven and a temperature controlled auto sampler (maintained at 4°C), coupled to an Agilent 6490 triple quadrupole mass spectrometer with a jet stream electrospray ionization interface (AJS-ESI) (Agilent Technologies, California, USA). Fragmentation for multiple reaction monitoring (MRM) and source conditions within the positive ion mode were automated defined by use of the integrated compound- and source- optimizer software modules (Agilent Technologies, B.07.01). Measured MRM transitions for analytes were automated defined as following: 7k25OHC (m/z 417.34 \rightarrow m/z 399.3 and m/z 191.4; RT = 3.68 min), 7k27OHC (m/z 417.34

→ m/z 417.3; RT = 3.55 min), 7β25OHC (m/z 383.3 → m/z 365.3 and m/z 95; RT = 3.45 min), 7β27OHC (m/z 383.3 → m/z 159.0; RT = 3.38 min), 7α25OHC (m/z 383.3 → m/z 365.3 and m/z 147.3; RT = 3.63 min), 7α27OHC (m/z 383.3 → m/z 383.3 and m/z 159.0; RT = 3.51 min), 7α25OHC-d6 (m/z 389.38 → m/z 371.5 and m/z 95.1; RT = 3.33 min), 7β27OHC-d6 (m/z 407.38 → m/z 389.1 and m/z 159.1; RT = 3.32 min), cortisol (m/z 363.22 → m/z 121.1 and m/z 90.9; RT = 1.01 min), cortisone (m/z 361.2 → m/z 163.0 and m/z 121.1; RT = 1.09 min) or corticosterone-d8 (m/z 355.2 → m/z 337.0 and m/z 125.1; RT = 1.43 min). The general source parameters were set as following: Gas temperature 290°C, gas flow 14 L/min, sheath gas temperature 300°C, sheath gas flow 11 L/min, nozzle voltage 1500 V, Capillary voltage 3000 V, cell accelerator voltage 4 V, fragmentation voltage 380 V and Nebulizer 20 psi. Analyte separation was achieved using a reversed-phase column (ACQUITY UPLC BEH C18, 1.7 μm, 2.1 × 150 mm, Waters, Wexford, Ireland), heated to 65 ± 0.8°C. The mobile phase consisted of water acetonitrile formic acid (A) (95/5/0.1; v/v/v) and (B) (5/95/0.1; v/v/v). The eluent gradient was set from 45 - 97% of B within 0- 4 min using a constant flow-rate from 0.5 mL/min, followed by a washout (80% of B, 4.5- 7 min) and column re-equilibration (45% B, 2 min). The injection volume was 2 μL per sample. Methanol in water (75/25 v/v) was used as needle and needle-seat flushing solvent for 10 s after sample aspiration. Samples were stored until analysis in the auto sampler (maintained at 4°C). Data acquisition and analysis was performed using Mass Hunter Workstation Acquisition Software Version 07.01 SP1 and MassHunter Workstation Software Quantitative Analysis Version B.07.00 /Build 7.0457.0, respectively (Agilent Technologies).

2.6. Docking of oxysterols into the ligand binding pocket of 11β-HSD1

Docking was performed using the GOLD version 5.2 software (Cambridge Crystallographic Data Centre, Cambridge, UK) [36]. This program applies a genetic algorithm for the identification of accurate docking poses for small molecules into the binding pocket of a protein. The crystal structure with the Protein Data Bank (PDB) entry 2BEL [DOI: <http://dx.doi.org/10.2210/pdb2bel/pdb>] was chosen for the human 11β-HSD1 protein and PDB entry 1Y5R [DOI: <http://10.2210/pdb1y5r/pdb>] for the mouse enzyme. First, the co-crystallized ligands (carbenoxolone for 2BEL and corticosterone for 1Y5R) were deleted from the binding site and re-docked into the ligand binding site to investigate whether GOLD could restore the original binding orientation and therefore validate the docking settings (RMSD value of 0.563 for carbenoxolone and 0.683 for corticosterone). The binding site was centered on the hydroxyl group of Tyr183 in 2BEL (x 3.08; y 19.19; z 13.65) as well as in 1Y5R (x 76.88; y 49.68; z 38.08) and surrounded by a 9 Å and a 10 Å sphere, respectively. CHEMPLP was selected as scoring function in both docking settings. Interactions found by the docking solutions between the ligand and the 11β-HSD1 binding pockets were evaluated using LigandScout 3.12 (inte:ligand GmbH, Vienna, Austria). This

program automatically analyzes the observed interaction pattern between the docked ligand and the protein, based on the chemical functionalities, the geometric distances and the angles between neighboring structures [37].

3. Results

3.1. Oxoreduction of 7k25OHC and 7k27OHC by 11 β -HSD1 in intact cells

In a first step, the oxoreduction of 7k25OHC and 7k27OHC in intact HEK293 cells stably expressing human 11 β -HSD1 and H6PDH was investigated. Both 7k25OHC and 7k27OHC were stereo-specifically metabolized by 11 β -HSD1 to 7 β 25OHC and 7 β 27OHC. No formation of 7 α 25OHC and 7 α 27OHC could be detected. Incubation of stably transfected HEK293 cells with 1 μ M 7k25OHC, 7k27OHC or cortisone revealed apparent enzyme velocity values of 0.37 ± 0.12 nmol/h/mg total protein for 7k25OHC, 0.52 ± 0.10 nmol/h/mg total protein for 7k27OHC and 1.59 ± 0.25 nmol/h/mg total protein for cortisone. No dehydrogenase activity could be detected when incubating the stably transfected cells with 7 α 25OHC or 7 β 25OHC or the respective 27-hydroxylated oxysterols. Also, no isomerase activity could be observed between the 7 α - and 7 β -hydroxylated oxysterols. In order to evaluate the mouse as potential animal model for further studies, the metabolism of 7k25OHC and 7k27OHC by the murine 11 β -Hsd1 was determined. Preliminary results for the mouse orthologue indicated, similar to the human enzyme, the exclusive conversion of 7k25OHC and 7k27OHC to 7 β 25OHC and 7 β 27OHC, without the formation of 7 α -hydroxy metabolites, as well as absence of the reverse reaction or isomerization (data not shown).

3.2. Inhibition of 11 β -HSD1-dependent oxoreduction of cortisone by oxysterols

To assess the potential of 7-oxygenated 25OHC and 27OHC oxysterols to interfere with the conversion of inactive to active glucocorticoids, the oxysterol-dependent inhibition of 11 β -Hsd1 enzyme activity was measured in HEK293 cell lysates expressing the human and mouse enzyme, respectively. 7k25OHC and 7k27OHC inhibited the oxoreduction of cortisone to cortisol by the recombinant human 11 β -HSD1 with IC₅₀ values of 400 ± 150 nM and 359 ± 44 nM, respectively (Figure 1A and B), and that by the mouse orthologue with IC₅₀ values of 53 ± 16 nM and 36 ± 7 nM, respectively (Figure 1C and D).

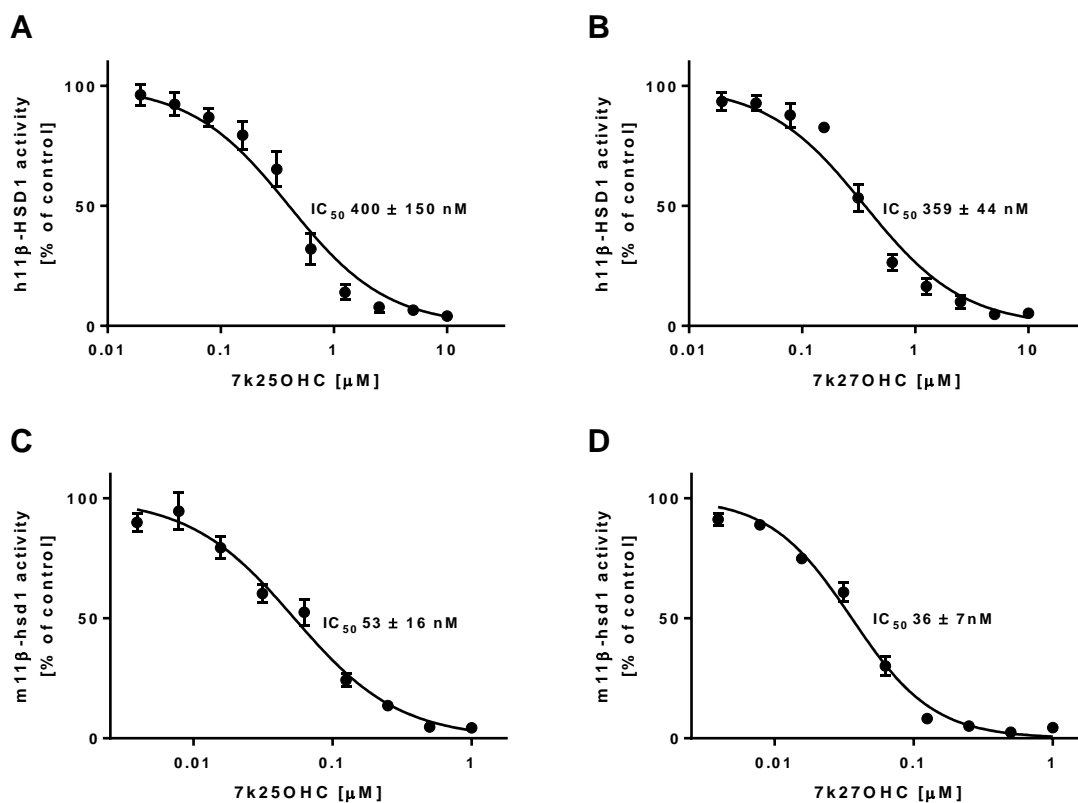


Figure 1. Inhibition of cortisone oxoreduction by human 11β-HSD1 (A and B) and murine 11β-Hsd1 (C and D) by 7k25OHC and 7k27OHC determined in HEK-293 cell lysates. Lysates of HEK-293 cells expressing recombinant human 11β-HSD1 and H6PDH or murine 11β-hsd1 were incubated for 10 min at 37°C with 200 nM radiolabeled cortisone, 500 μM NADPH and increasing concentrations of 7k25OHC (A and C), and 7k27OHC (B and D). The substrate conversion was determined and compared to the enzyme activity in the control samples (0.1% DMSO). Data represent mean ± SD from three independent experiments.

For their corresponding 7β-reduced forms IC₅₀ values of >3μM were obtained for the human enzyme with 7β25OHC and 7β27OHC (not shown) and of 119 ± 24 nM and 66 ± 30 nM, respectively (Figure 2A and B), for the mouse enzyme. The 7α-hydroxy metabolites inhibited human and mouse 11β-HSD1 cortisone oxoreduction to a much lesser extent than the 7β-hydroxy metabolites, albeit the 7α-hydroxy metabolites inhibited the murine enzyme more potently than the human orthologue (data not shown).

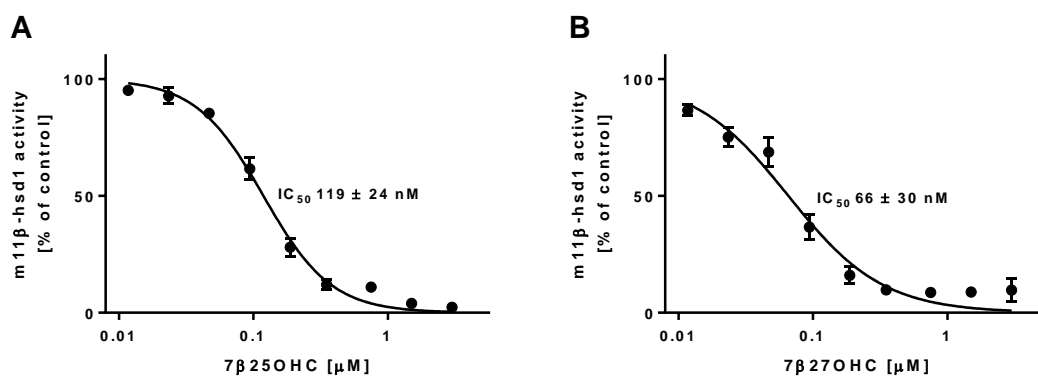


Figure 2. Inhibition of cortisone oxoreduction by murine 11β-Hsd1 by 7β25OHC (A) and 7β27OHC (B) determined in HEK-293 cell lysates. Lysates of HEK-293 cells expressing murine 11β-hsd1 were incubated for 10 min at 37°C with 200 nM radiolabeled cortisone, 500 μM NADPH and increasing concentrations of 7β25OHC and 7β27OHC. The substrate conversion was determined and compared to the enzyme activity in the control samples (0.1% DMSO). Data represent mean ± SD from three independent experiments.

3.3. *In silico* analysis of oxysterol binding to the ligand binding pocket of 11β-HSD1

In order to predict the binding orientation of 7-oxygenated 25OHC and 27OHC oxysterols in the substrate binding pocket of human and mouse 11β-Hsd1 and attempting to provide an explanation for the results obtained from the enzyme activity measurements, molecular docking calculations were performed. 7k25OHC and 7k27OHC fitted into the human 11β-HSD1 binding pocket within a comparable distance to the two key residues of the catalytic site, Ser170 and Tyr183, as observed for the substrate cortisone. Whereas both 7β25OHC and 7β27OHC are orientated to the catalytic site and the nicotinamide ring of the cofactor at a distance similar to that of cortisone, 7k25OHC and 7k27OHC (Figure 3A and 4A), the 7α-reduced oxysterols displayed a slightly turned upwards position and an enlarged distance to Ser170, Tyr183 and especially to the cofactor of 3-5Å (Figure 3B and 4B).

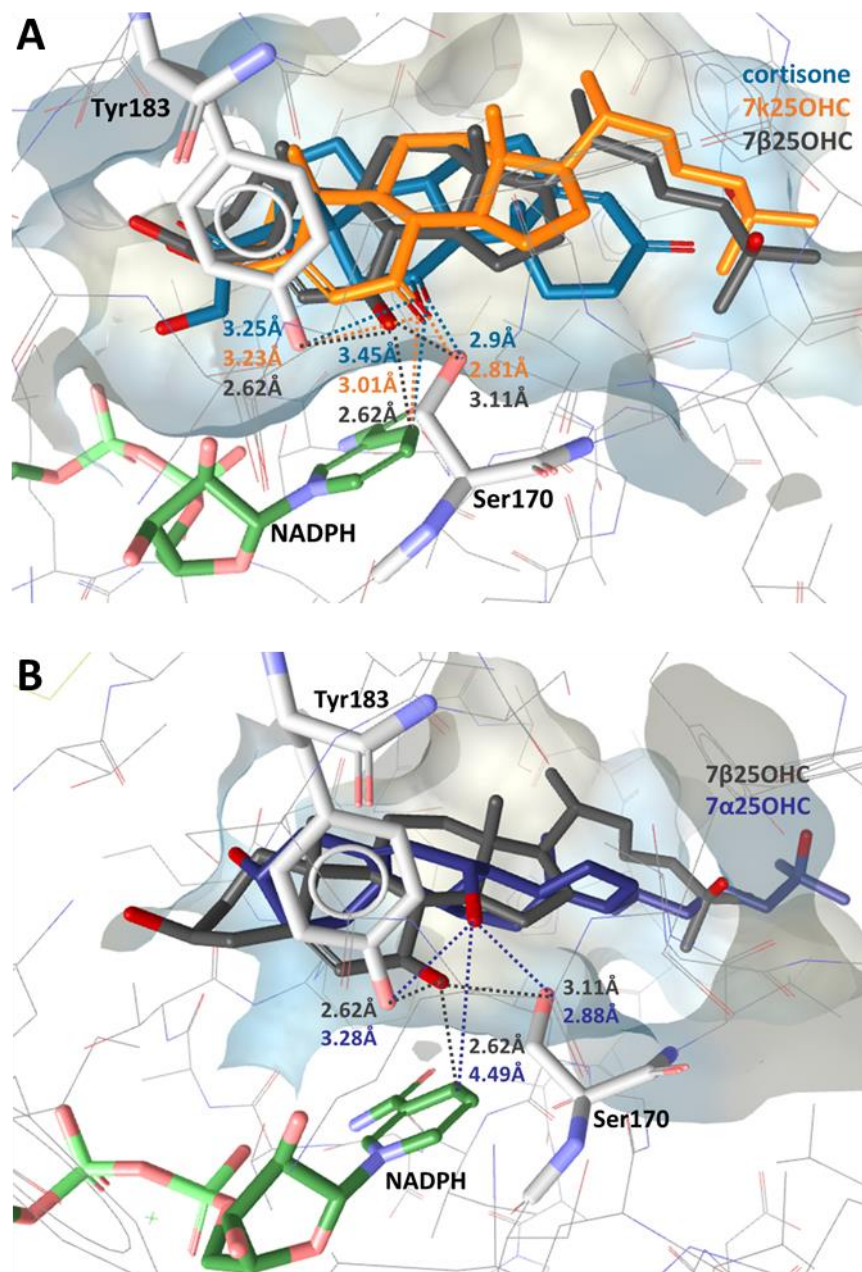


Figure 3. Predicted binding of cortisone and 25-hydroxylated oxysterols to human 11 β -HSD1. (A) Representative binding poses of cortisone (turquoise), 7 α 25OHC (orange) and 7 β 25OHC (grey). Important interactions for protein-ligand binding and the cofactor are shown in stick style and corresponding distances in Å are indicated as dashed lines (same color code as docked ligands). (B) Binding mode of 7 β 25OHC (grey) and 7 α 25OHC (blue).

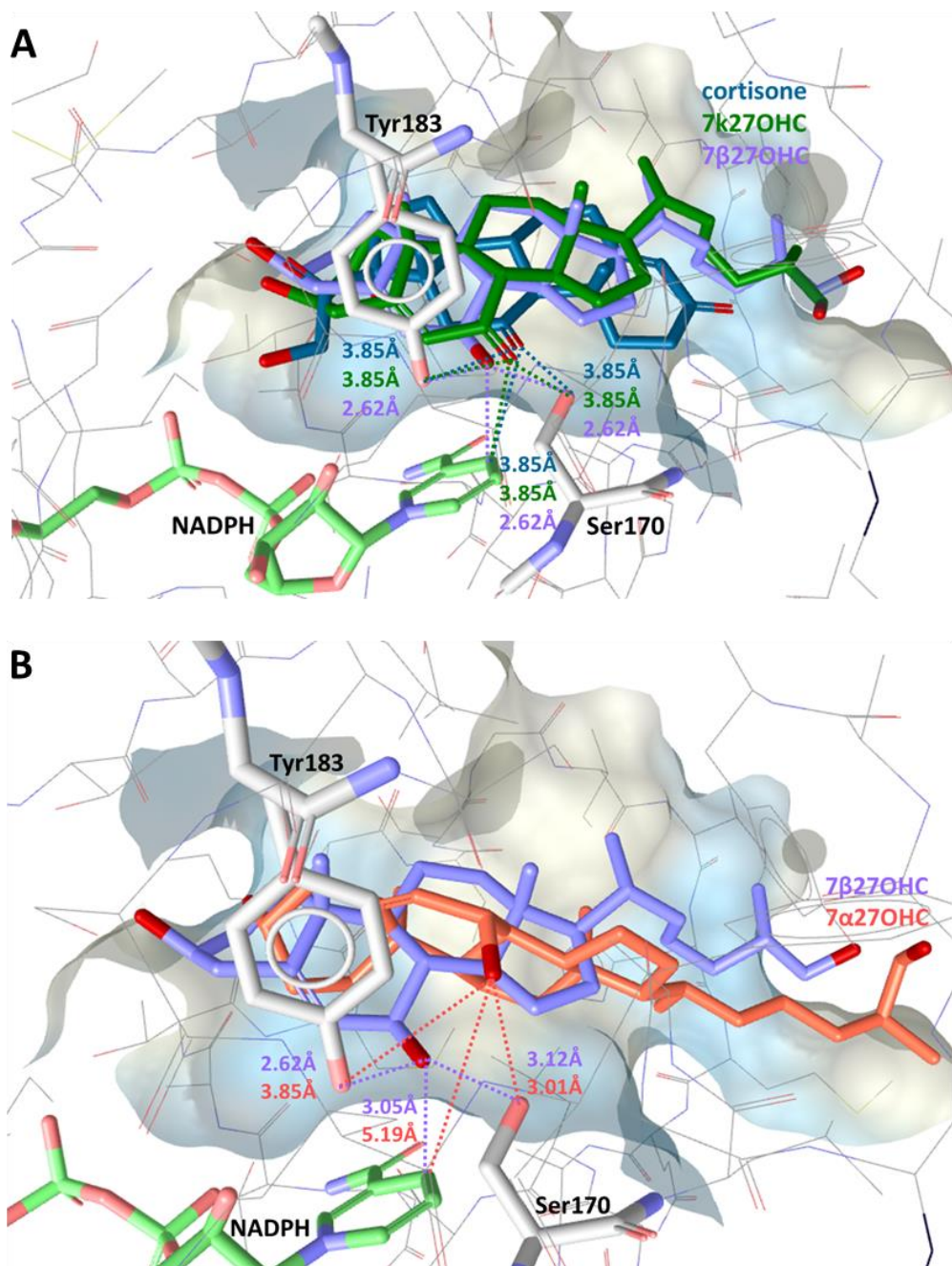


Figure 4. Predicted binding of cortisone and 27-hydroxylated oxysterols to human 11β-HSD1. (A) Representative binding poses of cortisone (turquoise), 7k27OHC (green) and 7β27OHC (purple). Important interactions for protein-ligand binding and the cofactor are shown in stick style and corresponding distances in Å are indicated as dashed lines (same color code as docked ligands). (B) Binding mode of 7β27OHC (green) and 7α27OHC (salmon pink).

An analogous binding mode of 7k25OHC, 7k27OHC, their reduced 7β-hydroxy metabolites and 11-dehydrocorticosterone was also observed in the *in silico* analyses of the murine 11β-Hsd1 (Figure 5A). However, compared to the position of 7α25OHC and 7α27OHC adopted in the human enzyme, these molecules align well in the murine 11β-Hsd1 binding pocket with the known substrates and within a distance of ~3.5Å (Figure 5B and C).

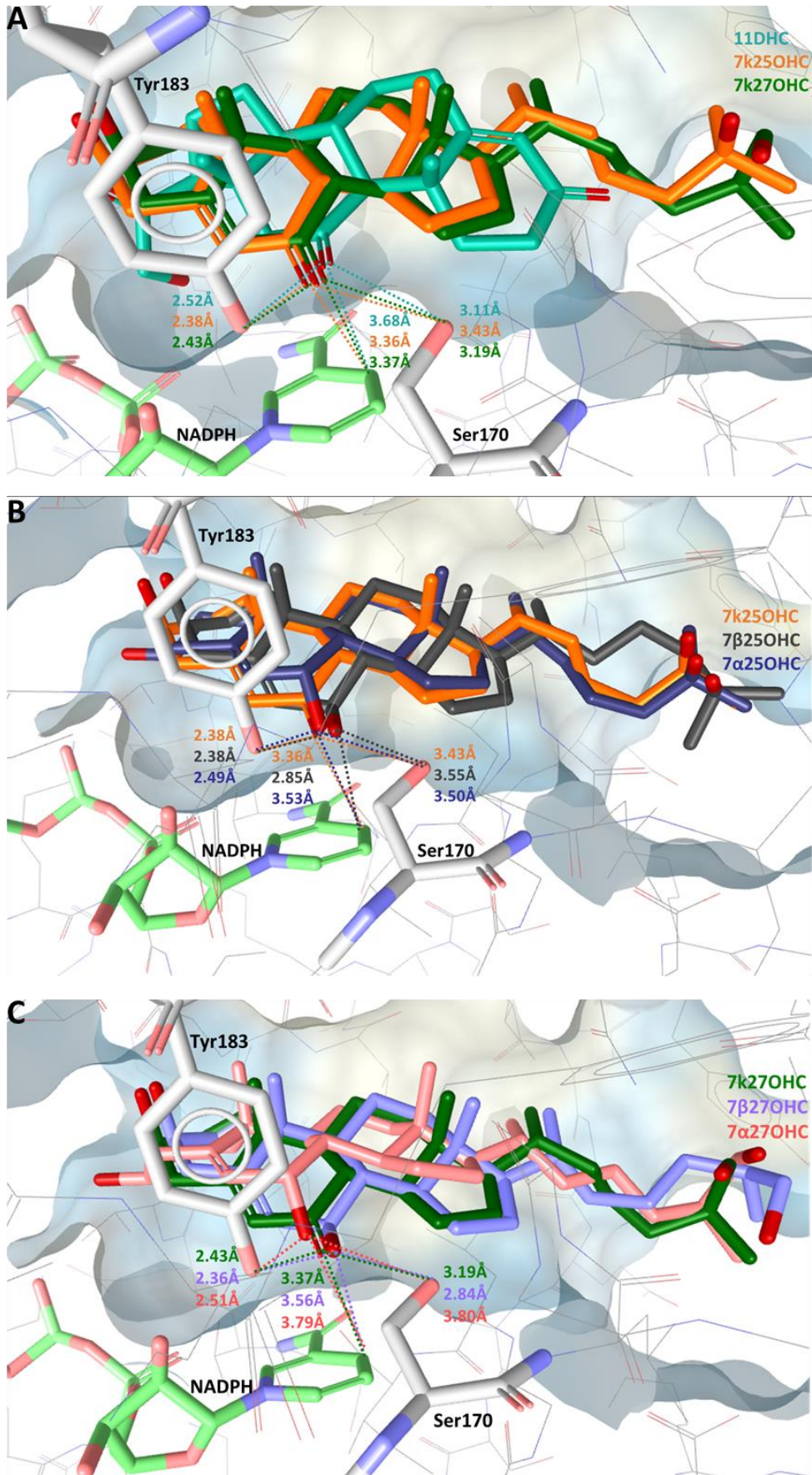


Figure 5. Predicted binding of 11-dehydrocorticosterone (11DHC), 25-hydroxylated and 27-hydroxylated oxysterols to murine 11 β -HSD1. (A) Representative binding poses of 11DHC (bright

turquoise), 7k25OHC (orange) and 7k27OHC (green). Important interactions for protein-ligand binding and the cofactor are shown in stick style and corresponding distances in Å are indicated as dashed lines (same color code as docked ligands). (B) Binding mode of 7k25OHC (orange), 7β25OHC (grey) and 7α25OHC (blue). (C) Binding mode of 7k27OHC (green), 7β27OHC (purple) and 7α27OHC (salmon pink).

4. Discussion

The investigation of oxysterols is highly complex and challenging, arising not only from the large number of molecules in this family, but also due to their low abundance in biological systems compared to cholesterol and their susceptibility for autoxidation, forming the same metabolites *ex vivo* as present *in vivo* [1]. Moreover, a given oxysterol can be derived from different substrates or may be formed non-enzymatically by autoxidation. Additionally, different enzymes can catalyze the conversion of one particular oxysterol. For example, 7β27OHC may be formed either by oxoreduction of 7kC through 11β-HSD1 to 7βOHC and then further by hydroxylation to 7β27OHC through CYP27A1 or via direct hydroxylation of autoxidation-derived 7βOHC by CYP27A1.

The current study proposes a new alternative biosynthetic pathway for the generation of 7β27OHC by 11β-HSD1-dependent oxoreduction of 7k27OHC. Furthermore, for the first time the enzymatic formation of 7β25OHC could be demonstrated *in vitro*. So far, the metabolic pathway leading to 7β25OHC has only been postulated as oxoreduction of 7kC through 11β-HSD1 to 7βOHC and then further by hydroxylation to 7β25OHC by CH25H or CYP27A1 [28], although experimental evidence is still lacking. Similarly, experimental evidence is missing for the hypothesized hydroxylation of 7kC to 7k25OHC by CH25H. Thus, further investigations are required to uncover the biosynthetic pathways of oxysterol metabolism.

Due to the stereospecific and seemingly irreversible action of the human 11β-HSD1, forming exclusively 7β-hydroxylated oxysterols, the potent EBI2 ligand 7α25OHC could neither be formed nor degraded by 11β-HSD1. Nevertheless, although the 7α-hydroxy group was shown to be preferred over the 7β-hydroxy group for EBI2 activation, 7β25OHC was still able to trigger an EBI2 response, with EC50 values in the lower nanomolar range [32]. Therefore, in situations of oxidative stress, with excessive accumulation of 7kC and in the presence of CH25H expression, substantial amounts of 7k25OHC may be generated, followed by 11β-HSD1-dependent formation of 7β25OHC, which in turn could then act as a danger signal to initiate EBI2 response. 7kC serving as a first line danger signal might be supported by mRNA expression studies showing a very dynamic regulation of the enzymes necessary for oxysterol synthesis [38]. Primary human monocytes and macrophages were reported to express high levels of CYP27A1, lower levels of CH25H and even more limited CYP7B1, which is required for 7α-hydroxylation of 25OHC. Upon an immune challenge, immediate strong up-regulation of CH25H and CYP27A1 mRNA levels were observed compared to a delayed rise of CYP7B1 in M0 macrophage. Hence, 7β25OHC may

control EBI2-mediated immune cell migration under oxidative stress in a first step, followed by an adaptive response through signaling via the more potent 7 α 25OHC.

Interestingly, bone marrow-derived macrophage from mice carrying a natural occurring mutation in the gene of Ror α 1, so called staggerer (sg/sg) mice, showed decreased mRNA expression levels of Ch25h before and after an immune challenge with lipopolysaccharide (LPS) and are characterized by impaired innate immunity and a higher susceptibility to atherosclerosis [39]. Against this background, 7 α OHC was reported in vitro as an inverse agonist for ROR α , although submicromolar concentrations were needed to affect receptor activity [40]. Whether 7-hydroxylated 25OHC or 27OHC oxysterols interfere with ROR α activity or its role in CH25H regulation and immune cell migration has not been elucidated so far. However, the closely related nuclear receptors ROR γ and ROR γ t are known to be activated by 7 β 27OHC and 7 α 27OHC, but not by 7 α 25OHC and most importantly not by 7k27OHC when full length receptor constructs were used [30]. The reduction of 7k27OHC to 7 β 27OHC by 11 β -HSD1 observed in the current study may therefore represent a mechanism of pre-receptor control of receptors other than GR such as ROR and/or EBI2. RORs as well as 11 β -HSD1 have both been implicated in different aspects of the metabolic syndrome. 11 β -Hsd1 knockout mice displayed improved insulin sensitivity and plasma lipid profile, whereas transgenic mice overexpressing 11 β -Hsd1 in the adipose tissue developed pronounced visceral obesity [41-43]. Ror α -deficient mice are protected against insulin resistance, hepatosteatosis or diet-induced obesity and also Ror γ -/- mice showed an improved insulin sensitivity (reviewed in [44]). All these characteristics of the metabolic syndrome are strongly associated with NAFLD [45]. As the liver is a major site of oxysterol metabolism and oxidative stress represents a central contributor to non-alcoholic steatohepatitis (NASH), the involvement of oxysterols in NASH progression seems to be evident. However, to date the role of oxysterols in NASH is only poorly explored [46]. Supporting data for an implication of ROR γ and ROR γ t in the pathogenesis of NASH come from preclinical and clinical studies. Liver tissue samples of patients and mouse models with NASH displayed an increased infiltration of Th17 cells and elevated expression levels of ROR γ and IL-17 mRNA [47, 48]. ROR γ protein levels were further upregulated in patients with liver cirrhosis and suggested to regulate epithelial-mesenchymal transition in hepatocytes during fibrosis [49]. Moreover, IL17 was reported to induce liver fibrosis in mice by different pathways [50]. Whether 11 β -HSD1-dependent oxysterol metabolism, in particular of 7k27OHC and thereby regulating ROR γ (t), plays a role in the pathogenesis of NASH warrants further investigations.

The present study showed for the first time the stereospecific oxoreduction of 7k25OHC and 7k27OHC to their corresponding 7 β -hydroxylated metabolites by 11 β -HSD1. A contribution of these oxysterols to the pathogenesis of NASH by regulation of ROR γ or to the migration of immune cells by EBI2 activation represent potential target mechanisms; however, thorough analysis of the involved pathways is needed.

Conflicts of Interest

The authors declare no conflict of interest.

Acknowledgements

This work was supported by the Swiss National Science Foundation No 31003A_159454 to AO.

References

- [1] G.J. Schroepfer, Jr., Oxysterols: modulators of cholesterol metabolism and other processes, *Physiol Rev*, 80 (2000) 361-554.
- [2] O. Guillemot-Legris, V. Mutemberezi, G.G. Muccioli, Oxysterols in Metabolic Syndrome: From Bystander Molecules to Bioactive Lipids, *Trends Mol Med*, 22 (2016) 594-614.
- [3] A. Zarrouk, A. Vejux, J. Mackrill, Y. O'Callaghan, M. Hammami, N. O'Brien, G. Lizard, Involvement of oxysterols in age-related diseases and ageing processes, *Ageing Res Rev*, 18 (2014) 148-162.
- [4] T.M. Jeitner, I. Voloshyna, A.B. Reiss, Oxysterol derivatives of cholesterol in neurodegenerative disorders, *Curr Med Chem*, 18 (2011) 1515-1525.
- [5] G. Poli, F. Biasi, G. Leonarduzzi, Oxysterols in the pathogenesis of major chronic diseases, *Redox Biol*, 1 (2013) 125-130.
- [6] A. Vejux, G. Lizard, Cytotoxic effects of oxysterols associated with human diseases: Induction of cell death (apoptosis and/or oncosis), oxidative and inflammatory activities, and phospholipidosis, *Mol Aspects Med*, 30 (2009) 153-170.
- [7] A.J. Brown, W. Jessup, Oxysterols and atherosclerosis, *Atherosclerosis*, 142 (1999) 1-28.
- [8] H. Girao, M.C. Mota, J. Ramalho, P. Pereira, Cholesterol oxides accumulate in human cataracts, *Exp Eye Res*, 66 (1998) 645-652.
- [9] I. Bjorkhem, O. Andersson, U. Diczfalusy, B. Sevastik, R.J. Xiu, C. Duan, E. Lund, Atherosclerosis and sterol 27-hydroxylase: evidence for a role of this enzyme in elimination of cholesterol from human macrophages, *Proc Natl Acad Sci U S A*, 91 (1994) 8592-8596.
- [10] A.J. Brown, S.L. Leong, R.T. Dean, W. Jessup, 7-Hydroperoxycholesterol and its products in oxidized low density lipoprotein and human atherosclerotic plaque, *J Lipid Res*, 38 (1997) 1730-1745.
- [11] A.J. Brown, G.F. Watts, J.R. Burnett, R.T. Dean, W. Jessup, Sterol 27-hydroxylase acts on 7-ketocholesterol in human atherosclerotic lesions and macrophages in culture, *J Biol Chem*, 275 (2000) 27627-27633.
- [12] G.Y. Heo, I. Bederman, N. Mast, W.L. Liao, I.V. Turko, I.A. Pikuleva, Conversion of 7-ketocholesterol to oxysterol metabolites by recombinant CYP27A1 and retinal pigment epithelial cells, *J Lipid Res*, 52 (2011) 1117-1127.
- [13] J. Fujiyama, M. Kuriyama, S. Arima, Y. Shibata, K. Nagata, S. Takenaga, H. Tanaka, M. Osame, Atherogenic risk factors in cerebrotendinous xanthomatosis, *Clin Chim Acta*, 200 (1991) 1-11.
- [14] N.B. Javitt, Bile acid synthesis from cholesterol: regulatory and auxiliary pathways, *FASEB J*, 8 (1994) 1308-1311.
- [15] M.A. Lyons, A.J. Brown, Metabolism of an oxysterol, 7-ketocholesterol, by sterol 27-hydroxylase in HepG2 cells, *Lipids*, 36 (2001) 701-711.
- [16] M.A. Lyons, N. Maeda, A.J. Brown, Paradoxical enhancement of hepatic metabolism of 7-ketocholesterol in sterol 27-hydroxylase-deficient mice, *Biochim Biophys Acta*, 1581 (2002) 119-126.

- [17] R.A. Schweizer, M. Zurcher, Z. Balazs, B. Dick, A. Odermatt, Rapid hepatic metabolism of 7-ketocholesterol by 11 β -hydroxysteroid dehydrogenase type 1: species-specific differences between the rat, human, and hamster enzyme, *J Biol Chem*, 279 (2004) 18415-18424.
- [18] M. Hult, B. Elleby, N. Shafqat, S. Svensson, A. Rane, H. Jornvall, L. Abrahmsen, U. Oppermann, Human and rodent type 1 11 β -hydroxysteroid dehydrogenases are 7 β -hydroxycholesterol dehydrogenases involved in oxysterol metabolism, *Cell Mol Life Sci*, 61 (2004) 992-999.
- [19] S. Arampatzis, B. Kadereit, D. Schuster, Z. Balazs, R.A. Schweizer, F.J. Frey, T. Langer, A. Odermatt, Comparative enzymology of 11 β -hydroxysteroid dehydrogenase type 1 from six species, *J Mol Endocrinol*, 35 (2005) 89-101.
- [20] T. Mitic, S. Shave, N. Semjonous, I. McNae, D.F. Cobice, G.G. Lavery, S.P. Webster, P.W. Hadoke, B.R. Walker, R. Andrew, 11 β -Hydroxysteroid dehydrogenase type 1 contributes to the balance between 7-keto- and 7-hydroxy-oxysterols in vivo, *Biochem Pharmacol*, 86 (2013) 146-153.
- [21] A. Odermatt, P. Klusonova, 11 β -Hydroxysteroid dehydrogenase 1: Regeneration of active glucocorticoids is only part of the story, *J Steroid Biochem Mol Biol*, 151 (2015) 85-92.
- [22] T. Mitic, R. Andrew, B.R. Walker, P.W. Hadoke, 11 β -Hydroxysteroid dehydrogenase type 1 contributes to the regulation of 7-oxysterol levels in the arterial wall through the inter-conversion of 7-ketocholesterol and 7 β -hydroxycholesterol, *Biochimie*, 95 (2013) 548-555.
- [23] A. Hermanowski-Vosatka, J.M. Balkovec, K. Cheng, H.Y. Chen, M. Hernandez, G.C. Koo, C.B. Le Grand, Z. Li, J.M. Metzger, S.S. Mundt, H. Noonan, C.N. Nunes, S.H. Olson, B. Pikounis, N. Ren, N. Robertson, J.M. Schaeffer, K. Shah, M.S. Springer, A.M. Strack, M. Strowski, K. Wu, T. Wu, J. Xiao, B.B. Zhang, S.D. Wright, R. Thieringer, 11 β -HSD1 inhibition ameliorates metabolic syndrome and prevents progression of atherosclerosis in mice, *J Exp Med*, 202 (2005) 517-527.
- [24] M.J. Luo, R. Thieringer, M.S. Springer, S.D. Wright, A. Hermanowski-Vosatka, A. Plump, J.M. Balkovec, K. Cheng, G.J. Ding, D.W. Kawka, G.C. Koo, C.B. Grand, Q. Luo, M.M. Maletic, L. Malkowitz, K. Shah, I. Singer, S.T. Waddell, K.K. Wu, J. Yuan, J. Zhu, S. Stepaniants, X. Yang, P.Y. Lum, I.M. Wang, 11 β -HSD1 inhibition reduces atherosclerosis in mice by altering proinflammatory gene expression in the vasculature, *Physiol Genomics*, 45 (2013) 47-57.
- [25] T. Kipari, P.W. Hadoke, J. Iqbal, T.Y. Man, E. Miller, A.E. Coutinho, Z. Zhang, K.M. Sullivan, T. Mitic, D.E. Livingstone, C. Schrecker, K. Samuel, C.I. White, M.A. Bouhrel, G. Chinetti-Gbaguidi, B. Staels, R. Andrew, B.R. Walker, J.S. Savill, K.E. Chapman, J.R. Seckl, 11 β -hydroxysteroid dehydrogenase type 1 deficiency in bone marrow-derived cells reduces atherosclerosis, *FASEB J*, 27 (2013) 1519-1531.
- [26] C.A. Penno, S.A. Morgan, A.J. Rose, S. Herzig, G.G. Lavery, A. Odermatt, 11 β -Hydroxysteroid dehydrogenase-1 is involved in bile acid homeostasis by modulating fatty acid transport protein-5 in the liver of mice, *Mol Metab*, 3 (2014) 554-564.
- [27] A. Odermatt, T. Da Cunha, C.A. Penno, C. Chandsawangbhuwana, C. Reichert, A. Wolf, M. Dong, M.E. Baker, Hepatic reduction of the secondary bile acid 7-oxolithocholic acid is mediated by 11 β -hydroxysteroid dehydrogenase 1, *Biochem J*, 436 (2011) 621-629.
- [28] W.J. Griffiths, J. Abdel-Khalik, E. Yutuc, A.H. Morgan, I. Gilmore, T. Hearn, Y. Wang, Cholesterolomics: An update, *Anal Biochem*, 524 (2017) 56-67.
- [29] V. Mutemberezi, O. Guillemot-Legris, G.G. Muccioli, Oxysterols: From cholesterol metabolites to key mediators, *Prog Lipid Res*, 64 (2016) 152-169.

- [30] P. Soroosh, J. Wu, X. Xue, J. Song, S.W. Sutton, M. Sablad, J. Yu, M.I. Nelen, X. Liu, G. Castro, R. Luna, S. Crawford, H. Banie, R.A. Dandridge, X. Deng, A. Bittner, C. Kuei, M. Tootoonchi, N. Rozenkrants, K. Herman, J. Gao, X.V. Yang, K. Sachen, K. Ngo, W.P. Fung-Leung, S. Nguyen, A. de Leon-Tabaldo, J. Blevitt, Y. Zhang, M.D. Cummings, T. Rao, N.S. Mani, C. Liu, M. McKinnon, M.E. Milla, A.M. Fourie, S. Sun, Oxysterols are agonist ligands of ROR gamma t and drive Th17 cell differentiation, *Proc Natl Acad Sci U S A*, 111 (2014) 12163-12168.
- [31] W.J. Griffiths, J. Abdel-Khalik, P.J. Crick, E. Yutuc, Y. Wang, New methods for analysis of oxysterols and related compounds by LC-MS, *J Steroid Biochem Mol Biol*, 162 (2016) 4-26.
- [32] S. Hannedouche, J. Zhang, T. Yi, W. Shen, D. Nguyen, J.P. Pereira, D. Guerini, B.U. Baumgarten, S. Roggo, B. Wen, R. Knochenmuss, S. Noel, F. Gessier, L.M. Kelly, M. Vanek, S. Laurent, I. Preuss, C. Miault, I. Christen, R. Karuna, W. Li, D.I. Koo, T. Suply, C. Schmedt, E.C. Peters, R. Falchetto, A. Katopodis, C. Spanka, M.O. Roy, M. Detheux, Y.A. Chen, P.G. Schultz, C.Y. Cho, K. Seuwen, J.G. Cyster, A.W. Sailer, Oxysterols direct immune cell migration via EBI2, *Nature*, 475 (2011) 524-527.
- [33] C. Liu, X.V. Yang, J. Wu, C. Kuei, N.S. Mani, L. Zhang, J. Yu, S.W. Sutton, N. Qin, H. Banie, L. Karlsson, S. Sun, T.W. Lovenberg, Oxysterols direct B-cell migration through EBI2, *Nature*, 475 (2011) 519-523.
- [34] B.R. Myers, N. Sever, Y.C. Chong, J. Kim, J.D. Belani, S. Rychnovsky, J.F. Bazan, P.A. Beachy, Hedgehog pathway modulation by multiple lipid binding sites on the smoothed effector of signal response, *Dev Cell*, 26 (2013) 346-357.
- [35] D.V. Kratschmar, A. Vuorinen, T. Da Cunha, G. Wolber, D. Classen-Houben, O. Doblhoff, D. Schuster, A. Odermatt, Characterization of activity and binding mode of glycyrrhetic acid derivatives inhibiting 11 β -hydroxysteroid dehydrogenase type 2, *J Steroid Biochem Mol Biol*, 125 (2011) 129-142.
- [36] G. Jones, P. Willett, R.C. Glen, A.R. Leach, R. Taylor, Development and validation of a genetic algorithm for flexible docking, *J Mol Biol*, 267 (1997) 727-748.
- [37] G. Wolber, T. Langer, LigandScout: 3-D pharmacophores derived from protein-bound ligands and their use as virtual screening filters, *J Chem Inf Model*, 45 (2005) 160-169.
- [38] I. Preuss, M.G. Ludwig, B. Baumgarten, F. Bassilana, F. Gessier, K. Seuwen, A.W. Sailer, Transcriptional regulation and functional characterization of the oxysterol/EBI2 system in primary human macrophages, *Biochem Biophys Res Commun*, 446 (2014) 663-668.
- [39] Z.K. Tuong, P. Lau, J.C. Yeo, M.A. Pearen, A.A. Wall, A.C. Stanley, J.L. Stow, G.E. Muscat, Disruption of Roralpha1 and cholesterol 25-hydroxylase expression attenuates phagocytosis in male Rora sg/sg mice, *Endocrinology*, 154 (2013) 140-149.
- [40] Y. Wang, N. Kumar, L.A. Solt, T.I. Richardson, L.M. Helvering, C. Crumbley, R.D. Garcia-Ordonez, K.R. Stayrook, X. Zhang, S. Novick, M.J. Chalmers, P.R. Griffin, T.P. Burris, Modulation of retinoic acid receptor-related orphan receptor alpha and gamma activity by 7-oxygenated sterol ligands, *J Biol Chem*, 285 (2010) 5013-5025.
- [41] Y. Kotelevtsev, M.C. Holmes, A. Burchell, P.M. Houston, D. Schmoll, P. Jamieson, R. Best, R. Brown, C.R. Edwards, J.R. Seckl, J.J. Mullins, 11 β -hydroxysteroid dehydrogenase type 1 knockout mice show attenuated glucocorticoid-inducible responses and resist hyperglycemia on obesity or stress, *Proc Natl Acad Sci U S A*, 94 (1997) 14924-14929.

- [42] H. Masuzaki, J. Paterson, H. Shinyama, N.M. Morton, J.J. Mullins, J.R. Seckl, J.S. Flier, A transgenic model of visceral obesity and the metabolic syndrome, *Science*, 294 (2001) 2166-2170.
- [43] H. Masuzaki, H. Yamamoto, C.J. Kenyon, J.K. Elmquist, N.M. Morton, J.M. Paterson, H. Shinyama, M.G. Sharp, S. Fleming, J.J. Mullins, J.R. Seckl, J.S. Flier, Transgenic amplification of glucocorticoid action in adipose tissue causes high blood pressure in mice, *J Clin Invest*, 112 (2003) 83-90.
- [44] A.M. Jetten, H.S. Kang, Y. Takeda, Retinoic acid-related orphan receptors alpha and gamma: key regulators of lipid/glucose metabolism, inflammation, and insulin sensitivity, *Front Endocrinol (Lausanne)*, 4 (2013) 1.
- [45] V. Ratziu, S. Bellentani, H. Cortez-Pinto, C. Day, G. Marchesini, A position statement on NAFLD/NASH based on the EASL 2009 special conference, *J Hepatol*, 53 (2010) 372-384.
- [46] F. Bellanti, R. Villani, A. Facciorusso, G. Vendemiale, G. Serviddio, Lipid oxidation products in the pathogenesis of non-alcoholic steatohepatitis, *Free Radic Biol Med*, 111 (2017) 173-185.
- [47] Y. Tang, Z. Bian, L. Zhao, Y. Liu, S. Liang, Q. Wang, X. Han, Y. Peng, X. Chen, L. Shen, D. Qiu, Z. Li, X. Ma, Interleukin-17 exacerbates hepatic steatosis and inflammation in non-alcoholic fatty liver disease, *Clin Exp Immunol*, 166 (2011) 281-290.
- [48] L. Vonghia, N. Ruyssers, D. Schrijvers, P. Pelckmans, P. Michielsen, L. De Clerck, A. Ramon, E. Jirillo, D. Ebo, B. De Winter, C. Bridts, S. Francque, CD4+ROR gamma t++ and Tregs in a Mouse Model of Diet-Induced Nonalcoholic Steatohepatitis, *Mediators Inflamm*, 2015 (2015) 239623.
- [49] S.M. Kim, J.E. Choi, W. Hur, J.H. Kim, S.W. Hong, E.B. Lee, J.H. Lee, T.Z. Li, P.S. Sung, S.K. Yoon, RAR-Related Orphan Receptor Gamma (ROR-gamma) Mediates Epithelial-Mesenchymal Transition Of Hepatocytes During Hepatic Fibrosis, *J Cell Biochem*, 118 (2017) 2026-2036.
- [50] F. Meng, K. Wang, T. Aoyama, S.I. Grivennikov, Y. Paik, D. Scholten, M. Cong, K. Iwaisako, X. Liu, M. Zhang, C.H. Osterreicher, F. Stickel, K. Ley, D.A. Brenner, T. Kisseleva, Interleukin-17 signaling in inflammatory, Kupffer cells, and hepatic stellate cells exacerbates liver fibrosis in mice, *Gastroenterology*, 143 (2012) 765-776 e763.

4.1.2. Human metabolome and lipid maps structure database screening

The present project is an attempt towards applying pharmacophore-based modeling and compound library screening for the characterization and deorphanization of SDRs in order to explore novel physiological functions and to identify potential drug targets. To test this strategy, the extensively studied 11 β -HSD1 was selected as a 'model enzyme' and structure-based pharmacophore models were generated and employed for filtering of the human metabolome database (HMDB) and the lipid maps structure database (LMSD) to identify potential novel substrates of this multifunctional enzyme. A similar approach was recently reported by Zemanová et al. for the closely related orphan SDR family member DHRS7 based on homology modeling and structure-based VS of the HMDB (described in more detail in the following section) [98].

Methods

Data sets

A test set of 18 structurally diverse and experimentally confirmed 11 β -HSD1 substrates [93, 99] as well as a set of 20 inactive compounds [100] was collected and used for structure-based pharmacophore modeling (see Appendix Figure A1 and A2). The 2D-structures of these molecules were drawn with ChemBioDraw Ultra 12.0 and for each compound a maximum of 500 different conformations was created using OMEGA-best settings [101-103] implemented in LigandScout 3.12 (inte:ligand GmbH, Vienna, Austria) [104]. For the VS, the HMDB [105-107] version 2.5 and the LMSD [108, 109] (version November 2014), containing 41182 and 35624 structures, respectively, were downloaded as sdf files from their corresponding websites (<http://www.hmdb.ca/downloads>; <http://www.lipidmaps.org/resources/downloads/index.html>) and transformed into 3D-multiconformational databases by creating 500 conformations with OMEGA-best settings using LigandScout 3.12.

Pharmacophore modeling and virtual screening

Structure-based pharmacophore modeling can be implemented if an X-ray crystal structure of the required molecular target containing a bound ligand is available. The interactions found between the protein and the ligand can then directly be integrated into a pharmacophore model. In the current project structure-based pharmacophore models were generated using the LigandScout 3.12 software. Due to the lack of a human 11 β -HSD1 crystal structure in complex with a substrate, cortisone and 7kC were docked into the binding pocket of human 11 β -HSD1 (PDB entry 2BEL [DOI:

<http://dx.doi.org/10.2210/pdb2bel/pdb>) using GOLD software version 5.2 (Cambridge Crystallographic Data Centre, Cambridge, UK) [110] and according to the method described in the manuscript 'The Oxysterols 7 β ,25-dihydroxycholesterol and 7 β ,27-dihydroxycholesterol are Enzymatically Formed by 11 β -Hydroxysteroid Dehydrogenase Type 1' - chapter 3.3. 'In silico analysis of oxysterol binding to the ligand binding pocket of 11 β -HSD1'. Interactions detected by the docking calculations between the ligand and the 11 β -HSD1 binding pocket were evaluated and translated into common pharmacophore features by using LigandScout. In addition, a structure-based pharmacophore was generated of the interactions observed in the crystal structure of the murine 11 β -HSD1 complexed with corticosterone (PDB entry 1Y5R [DOI: <http://10.2210/pdb1y5r/pdb>]). Both models were manually refined and then merged by using the alignment tool of the LigandScout software. The generated model (model_1) was further evaluated and refined (setting features optional, removing features, adding exclusion volumes; for a general model refinement workflow consider the following reference [100]) in order to train the model to retrieve as many active compounds (substrates) as possible and to omit the inactive compounds from the fitting with the data set described above. In addition, further pharmacophore models were constructed to cover all the structurally different active training compounds (11 β -HSD1 substrates). Therefore, model_1 was merged with newly two generated ligand-based pharmacophore models either on the basis of all active compounds containing a steroid backbone (model_2 and model_3) or on metyrapone and triadimefone (model_4). The ligand-based pharmacophore models were constructed according to an earlier described workflow [111]. The quality of the pharmacophore models was quantitatively assessed by calculation of the selectivity and the specificity of a model (see Appendix Table A1). The VS of the HMDB and the LMSD with the generated pharmacophore models representing 11 β -HSD1 substrates was conducted by using LigandScout 3.12. In addition, pharmacophore models for 11 β -HSD1 inhibitors described earlier were also implemented for VS and subsequent comparison of the virtual hits list for consensus hits [100].

Results and Discussion

The VS yielded several hundred virtual hits among which known substrates were successfully found such as endogenous 11-ketoglucocorticoids, synthetic glucocorticoids (such as prednisone), 7kC, and several bile acids known to inhibit the enzyme. The hit list comprised also different constituents of the root of licorice (*Glycyrrhiza spp*) and (processed) coffee, both products with known 11 β -HSD1 inhibitory activity [112, 113]. Furthermore, the hit list contained several different eicosanoids including prostaglandins, leukotrienes, cyclopentenone isoprostanes, levuglandins or hydroxyeicosatetraenoic acids (HETEs). A selection thereof can be found in the appendix (Figure A3). Regarding the pivotal roles

of 11 β -HSD1 and eicosanoids during inflammation, potential 11 β -HSD1 substrates may be found among those compounds. However, their highly flexible molecule structures can easily adopt plausible binding poses in the pharmacophore model and then can then be filtered as hits during the VS. Evidently, this is further supported by the hydrophobic nature of the binding pocket of 11 β -HSD1. Docking of a few hits (Prostaglandin E₃, 12-Keto-leukotriene B₄, 15-oxo-EETE and 12-oxo-EETE), selected on the basis of consensually retrieved hits between the different models respectively their closest related carbonyl-forms (leukotriene B₄ \rightarrow 12-Keto-leukotriene B₄, 15(S)-HETE \rightarrow 15-oxo-EETE and 12-HETE \rightarrow 12-oxo-EETE), into the binding pocket of 11 β -HSD1 predicted different binding conformations for all the selected hits compared to the known substrates cortisone and 7kC, which are found in one major pose (data not shown). Whether this observation is due to the great flexibility of the selected compounds, the rigid docking settings applied, or because they are inert towards the catalytic activity of 11 β -HSD1, needs to be determined in biological assays. Interestingly, a similar observation was reported in molecular modeling experiments of 4-oxonon-2-enal (4ONE) into the active site of CBR1 [114]. The highly reactive and genotoxic lipid aldehyde 4ONE was described in the same study to be converted by CBR1 into less reactive metabolites; however, 4ONE was also found to have a high degree of freedom in the active site of CBR1 and to adopt several active conformations. Moreover, the authors reported no specific contacts (*e.g.* hydrogen bonds) between the substrate and the enzyme in their calculated models.

Due to the evidence for CBR1 to be involved in oxidative stress response (described in more detail in our published review article 'Virtual screening applications in SDR research, chapter 2.2.3. 'Application of structural modeling for substrate identification'), Oppermann et al. suggested the compound class of reactive isoprostanes, which was also retrieved by our 11 β -HSD1 screening, as particularly interesting for further investigations into this research field [115]. As already mentioned, CBR1 and 11 β -HSD1 are both involved in detoxification reactions of xenobiotics and even share a certain substrate specificity (*e. g.* the tobacco-derived carcinogen 4-(methylnitrosoamino)-1-(3-pyridyl)-1-butanone (NKK)). A superimposition of 11 β -HSD1 and CBR1 illustrates the essential SDR-folding pattern for both enzymes; however, CBR1 displays a rather wide pocket opening, whereas the binding pocket of 11 β -HSD1 is more elongated (Figure 3).

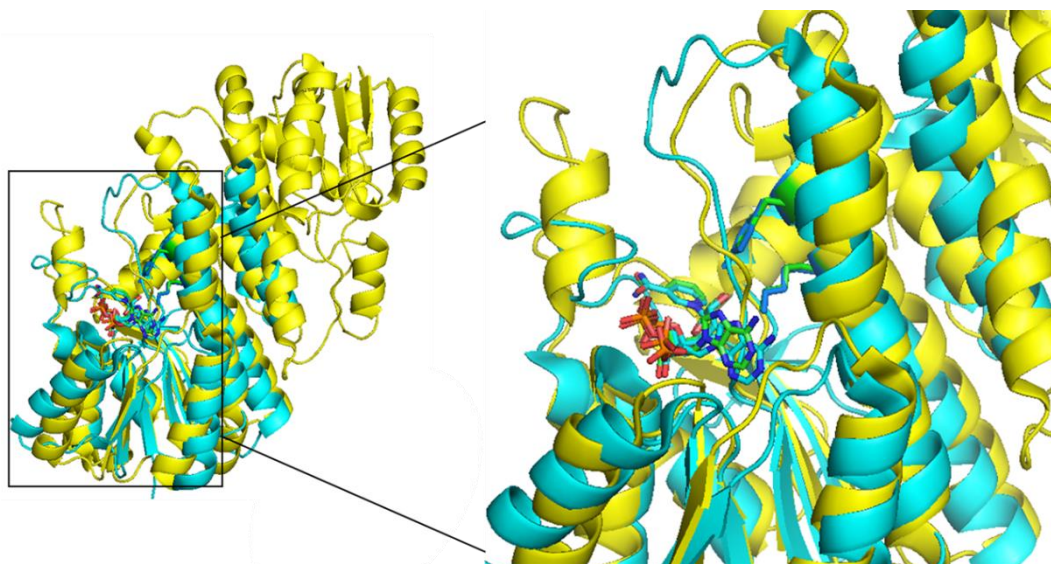


Figure 3. Superimposition of 11 β -HSD1 (yellow; PDB entry 2BEL) and CBR1 (blue; PDB entry 2PFG). NADPH and catalytic residues are depicted as sticks. 11 β -HSD1 shows a more elongated binding pocket compared to the rather wide binding pocket entry of CBR1.

In contrast to the cytoplasmic orientation of CBR1, the active site of 11 β -HSD1 faces the ER lumen. Regarding the metabolism of xenobiotics, the relevance of the luminal orientation of 11 β -HSD1 is not fully understood. Hydroxylation might facilitate conjugation reactions and thereby protect the cytoplasm from reactive ER luminal metabolites [93, 116]. Therefore, whether the suggestion to investigate isoprostanes as substrates for CBR1 should be extended to 11 β -HSD1 requires further *in vitro* mechanistic analyses exploring the role of 11 β -HSD1 in the metabolism of the different eicosanoids.

Another interesting class of compounds filtered by the pharmacophore models belong to the kynurenine pathway (Figure 4).

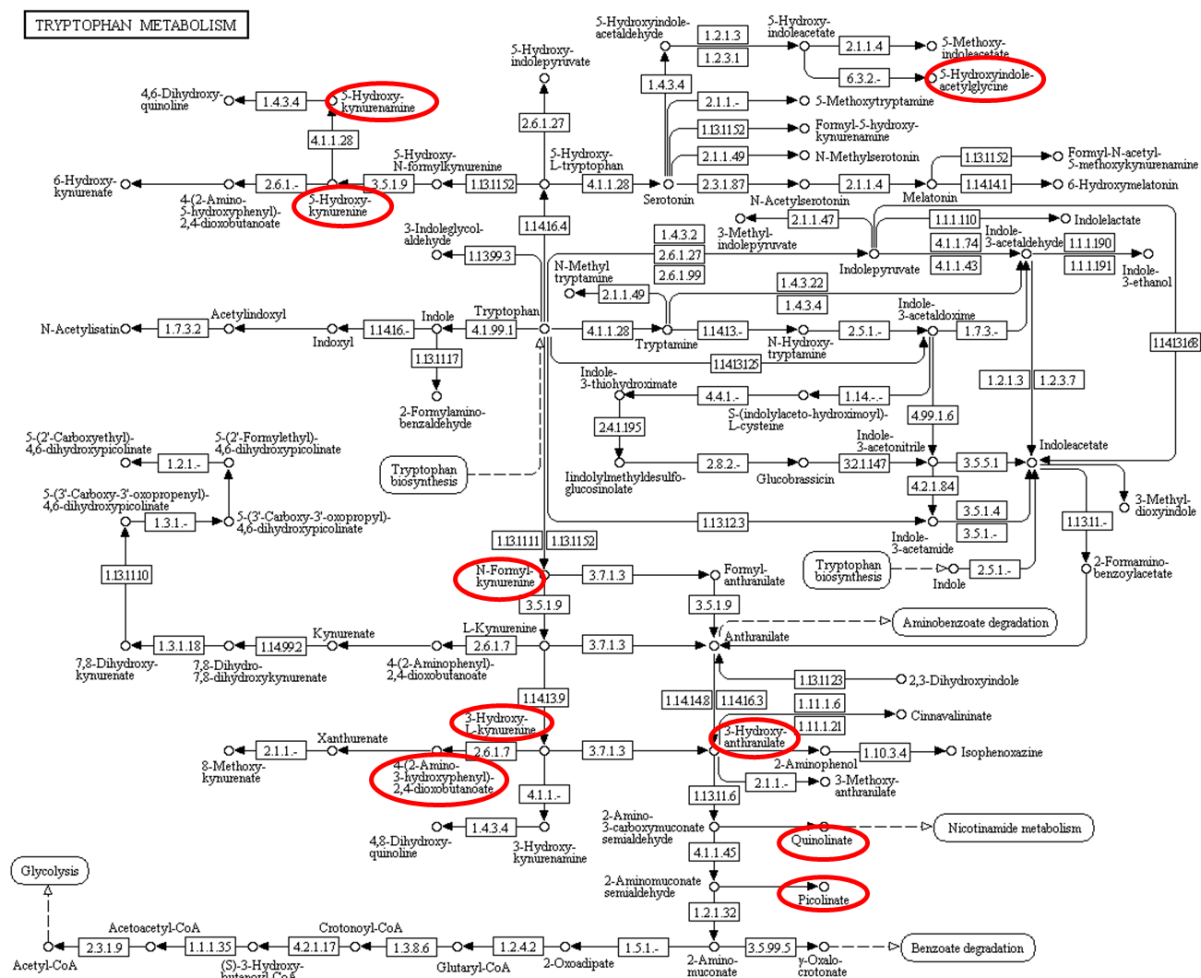


Figure 4. Tryptophan metabolism including the kynurenine pathway with virtual hits circled in red. (Adapted from the Kyoto Encyclopedia of Genes and Genomes (KEGG) database [117-120].)

Kynurenine derivatives are the main products from the enzymatic catabolism of tryptophan, besides serotonin and melatonin, and have been implicated in distinct inflammatory diseases, the regulation of the immune response and the de novo synthesis of nicotinamide adenine dinucleotide (NAD⁺) (reviewed in [121, 122]). The virtual hit list primarily included products downstream of the first rate-limiting steps of the kynurenine pathway: N-Formyl-kynurenine, 3-Hydroxy-L-kynurenine (3-HK), 3-Hydroxy-anthranilate (3-HAA), 4-(2-Amino-3-hydroxyphenyl)-2,4-dioxobutanoate, quinolinic and picolinic acid (Figure 5). Importantly, the latter compounds do not have a reactive carbonyl group required for metabolism by 11β-HSD1.

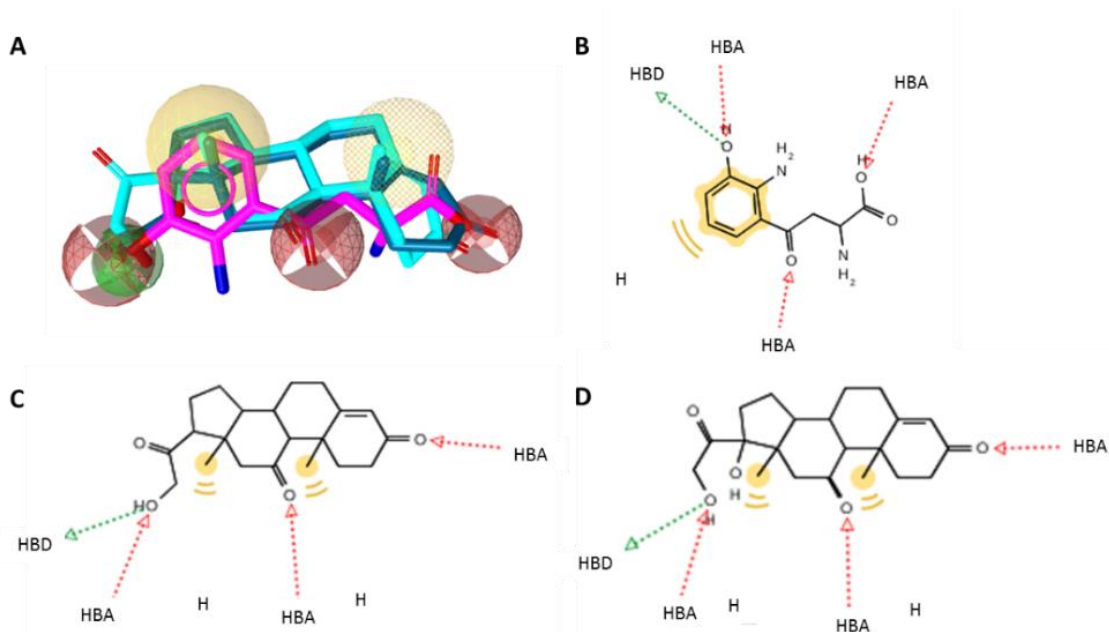


Figure 5. 2D and 3D representation of virtual hits in the 11 β -HSD1 pharmacophore model. (A) Cortisone (bright blue), 11-dehydrocorticosterone (11-DHC) (turquoise) and 3-HK (magenta) in an 11 β -HSD1 pharmacophore model. Yellow spheres display hydrophobic features (H), red hydrogen bond acceptors (HBA) and green hydrogen bond donors (HBD). Dotted spheres are optional features. The 2D representations show the matched pharmacophore features of 3-HK (B), 11-DHC (C) and cortisone (D). The color code corresponds to part A.

Nevertheless, docking into the binding pocket of 11 β -HSD1 revealed one major binding conformation for picolinic acid, 3-HAA and 3-HK (data not shown). 3-HK acts as a substrate concurrently for two metabolic routes, the conversion via 3-HAA and quinolinic acid to the nicotinamide metabolic pathway or to the formation of xanthurenic acid (XA). Vitamin B₆ deficiency was shown to shift the metabolism of 3-HK from the formation of NAD⁺ towards increased levels of XA and kynurenine, due to its function as cofactor for the enzymatic step from 3-HK to 3-HAA [123]. However, elevated levels of XA, 3-HK or kynurenine have been associated with a rather proatherogenic phenotype, showing increased occurrence in patients suffering from type 2 diabetes, induced experimental diabetes in rats and correlated with triglyceride or low-density lipoprotein (LDL) levels (reviewed in [124-126]). On the other hand, administration of 3-HAA to LDL receptor deficient mice led to significantly decreased total plasma cholesterol and triglyceride levels, reduced atherosclerotic lesion size and modulated local and systemic inflammatory responses [127]. In this regard, it becomes evident that the fine tuning of this systems is highly complex and may also involve other yet unexplored interaction partners. Therefore, it can be hypothesized that 11 β -HSD1 potentially stabilizes 3-HK and thus may support the proatherogenic profile, and that inhibition of the enzyme may have glucocorticoid- and oxysterol-independent beneficial effects in atherosclerosis by interfering with the kynurenine pathway. This is highly speculative at the moment, and further biological validation is of utmost necessity to test this

hypothesis based on *in silico* data and also to confirm the substrate identification strategy in order to extend it to orphan SDRs to uncover their physiological roles. A first attempt to implement this approach for an orphan member of the SDR enzyme family, DHRS7, is described in the following section.

4.2. DHRS7

The closest relative of the orphan SDR family member DHRS7 (SDR34C1) is 11 β -HSD1 [128]. Although the physiological role of DHRS7 has not yet been elucidated, DHRS7 knock-down experiments in human LNCaP prostate cancer cells showed increased cell proliferation, migration and reduced cell adhesion [129]. Moreover, reduced DHRS7 expression has been detected with increased prostate cancer progression, suggesting a function as tumor suppressor [129, 130]. The close evolutionary proximity between 11 β -HSD1 and DHRS7, may represent a valuable starting point for the identification of novel substrates for this orphan enzyme. In this regard, Wsol and coworkers proposed several endogenous and exogenous compounds known as 11 β -HSD1 substrates, such as cortisone, NKK or metyrapone, as potential substrates of DHRS7 and they provided evidence that purified recombinant human DHRS7 indeed catalyzes the carbonyl reduction of several compounds [131-133]; however, the physiological relevance of their metabolism by DHRS7 was not further assessed. Regarding cancer progression, cortisone to cortisol conversion would support the decreased anti-proliferative and pro-apoptotic effects found with enhance prostate cancer progression and reduced DHRS7 expression. Araya et al. investigated the role of DHRS7 in the interconversion of cortisone/cortisol and the modulation of AR activity by interconversion of androstenedione/testosterone and 5 α -dihydrotestosterone (5 α DHT)/3 α -androstenediol (3 α Adiol) [92]. Cortisone was found to be reduced by DHRS7, however not at 11 position of the steroid backbone, but at position 20 to 20 β -dihydrocortisone. Androstenedione was excluded as relevant substrate; nevertheless, 5 α DHT was converted by DHRS7 to the inactive metabolite 3 α Adiol thereby showing a suppressive effect on AR activity, although at high concentrations that may not be of physiological relevance. In this regard, DHRS7 nicely exhibits catalytic activity on rotational symmetric sites of the steroid backbone, at positions 3 and 20, compared to positions 7 and 11 as seen with 11 β -HSD1 (Figure 6). Nevertheless, the physiological roles remain uncertain and further investigations are needed.

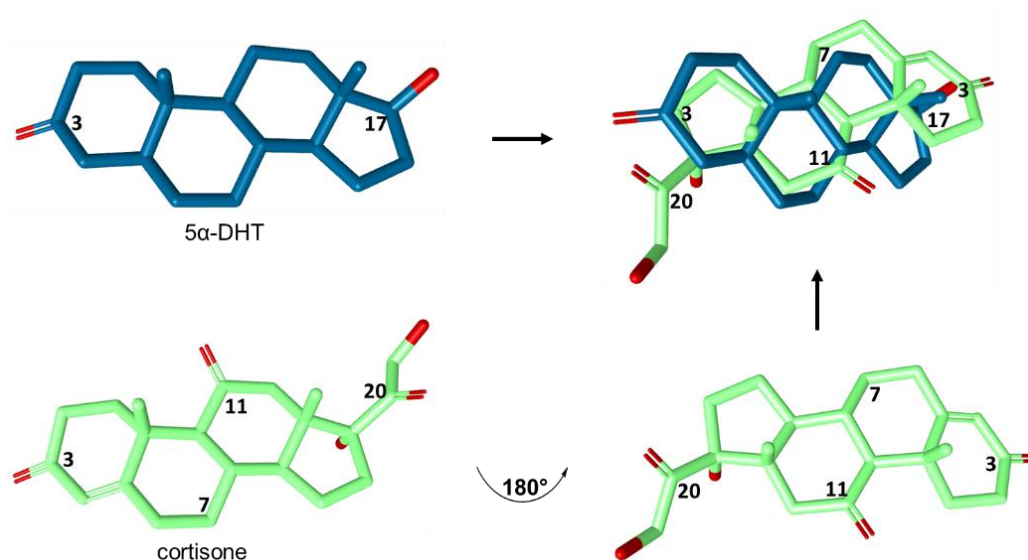


Figure 6. Rotational symmetry of the steroid backbone exemplified on the two DHRS7 substrates 5 α DHT (blue) and cortisone (green). (Figure adapted from Araya et al. [92]) Cortisone 180° rotated and overlaid with 5 α DHT shows the close proximity of the 3-oxo and the 20-oxo groups.

Thus, the existence of other yet unexplored substrates of DHRS7 can be assumed and we intended to employ homology modeling including a structure-based VS approach to identify potential novel substrates. Since DHRS7 has an ER transmembrane anchor, the three-dimensional protein structure resolution has not been accomplished so far. Therefore, 11 β -HSD1 was utilized as structural template due to the highest structural sequence identity. Three DHRS7 homology models were generated using Swiss-Model (<https://swissmodel.expasy.org/interactive>) [134-137] based on the 11 β -HSD1 X-ray structures with the PDB entry 2BEL [DOI: <http://dx.doi.org/10.2210/pdb2bel/pdb>], 1XSE [DOI: <http://dx.doi.org/10.2210/pdb1xse/pdb>] and 1XU9 [DOI: <http://dx.doi.org/10.2210/pdb1xu9/pdb>]. Subsequently, the cofactor NADPH from the template was fitted into the models and subjected to energy minimization within a sphere of 9 Å implemented in the program package Molecular Operating Environment (MOE, Chemical Computing Group, (<http://www.chemcomp.com>)) [138]. 3D structural alignment of all three homology models revealed a highly variable region comprising a part of the ligand binding site but especially the entry of the binding pocket (Figure 7A). This limits the predictivity of the models if applied for further structure-based VS approaches. Nevertheless, the models generally displayed a cone-shaped binding site (Figure 7B) with a rather hydrophobic core. The flexible loops surrounding the binding pocket suggest the induction of an induced fit upon ligand binding. Although rigid docking calculations of cortisone into the homology model of DHRS7 showed the major conformation of cortisone pointing with its carbonyl group at the position 20 towards the catalytic center, the distances to the catalytic residues were >5Å (Figure 7C).

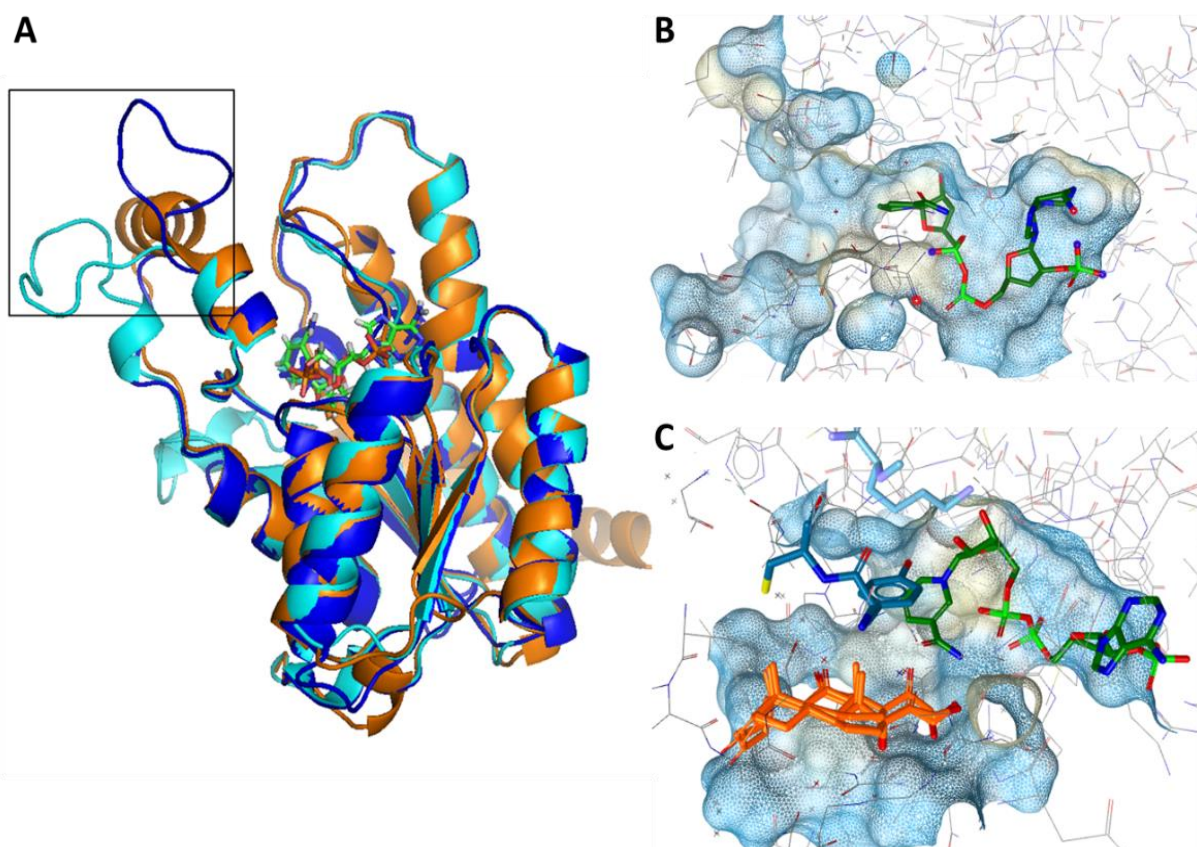


Figure 7. DHR57 homology models. (A) Structural alignment of the three DHR57 homology models (dark blue: PDB: 2BEL as template; bright blue: PDB: 1XU9 and orange: PDB 1XSE). The highly variable regions comprising a part the entry of the binding pockets is depicted in the frame. (B) Cone-shaped binding pocket of the DHR57 homology model (based on 2BEL) with NAPDH. (C) Rigid docking calculation of cortisone (orange) into the binding pocket of DHR57 (model based on 2BEL) with the carbonyl group at position 20 pointing towards the catalytic center.

Thus, structural optimization of the homology models and especially of the poorer resolved binding entry site is required before considering VS for potential substrates.

However, Zemanová et al. recently described a substrate identification approach for DHR57 based on a combination of homology modeling, structure-based docking calculations and experimental evaluations [98] – the initial intention of the current project. By screening of an in-house database and a part of the HMDB, they confirmed 5 α DHT as substrate for DHR57 and reported two novel substrates benzil and 4,4'-dimethylbenzil, albeit the observed kinetic activity was very low. This supports further investigations regarding the identification of other physiologically relevant substrates for DHR57. The elongated cone-shaped binding pocket of DHR57 may suggest larger metabolites to be converted as for instance different eicosanoids or other lipid mediators that represent interesting compound classes for following analyses.

4.3. Carbonyl reductase 1

The cytosolic enzyme CBR1 is particularly known for its role in phase I metabolism of a variety of carbonyl containing xenobiotic compounds including the detoxification of polycyclic aromatic hydrocarbons, p-quinons, but also the conversion of the anthracycline cytostatic agent doxorubicin into a cardiotoxic anthracycline alcohol metabolite, which further contributes to the development of a chemotherapy resistance [139, 140]. Endogenous substrates of CBR1 have been reported and comprise steroids, prostaglandins, S-nitrosoglutathione and lipid aldehydes (see also chapter 4.1.2 HMDB and LMSD screening) [94, 114, 115, 140-143]. However, the physiological relevance of the endogenous substrates proposed to be metabolized by CBR1 remains unclear, since the kinetic properties for the majority of them, are much lower than for several xenobiotic compounds.

Substantial interindividual differences in the expression and activity of CBR1 have been reported, which could lead to unpredictable pharmacokinetics and pharmacodynamics of drugs metabolized by CBR1 (reviewed in [140, 144]). Genetic polymorphisms may contribute to the observed variable CBR1 activities. Their functional impact, however, has not been fully understood yet. Furthermore, CBR1 homozygous null mice showed an embryonic lethal phenotype, indicating an essential role during fetal development [139].

To further explore the physiological roles of CBR1, the following section describes the identification of a novel function for CBR1 in the metabolism glucocorticoids.

4.3.1. Published article:

Carbonyl reductase 1 catalyses 20 β -reduction of glucocorticoids, modulating corticosteroid receptor activation and metabolic complications of obesity

Ruth A Morgan^{1,2}, [Katharina R Beck](#)³, Mark Nixon¹, Natalie ZM Homer⁴, Andrew A Crawford^{1,5}, Diana Melchers⁶, René Houtman⁶, Onno C Meijer⁷, Andreas Stomby⁸, Anna J Anderson¹, Rita Upreti¹, Roland H Stimson¹, Tommy Olsson⁸, Tom Michoel⁹, Ariella Cohain¹⁰, Arno Ruusalepp^{11,12,13}, Eric E. Schadt¹⁰, Johan LM Björkegren^{10,11,12,13,14}, Ruth Andrew^{1,4}, Christopher J Kenyon¹, Patrick WF Hadoke¹, Alex Odermatt³, John A Keen², and Brian R Walker^{1,4}, Scientific Reports 7, Article number: 10633 (2017)

¹ University/BHF Centre for Cardiovascular Science, The Queen's Medical Research Institute, University of Edinburgh, UK

² Royal (Dick) School of Veterinary Studies, University of Edinburgh, UK

³ Division of Molecular and Systems Toxicology, Department of Pharmaceutical Sciences, University of Basel, Switzerland

⁴ Mass Spectrometry Core Laboratory, Wellcome Trust Clinical Research Facility, The Queen's Medical Research Institute, University of Edinburgh, UK

⁵ School of Social and Community Medicine, University of Bristol, UK

⁶ PamGene International, Den Bosch, The Netherlands

⁷ Department of Internal Medicine, Division Endocrinology, Leiden University Medical Center, Leiden, The Netherlands

⁸ Department of Public Health and Clinical Medicine, Umeå University 901 87 Umeå, Sweden

⁹ The Roslin Institute, University of Edinburgh, Easter Bush Campus, UK

¹⁰ Department of Genetics and Genomic Sciences, Icahn Institute for Genomics and Multiscale Biology, Icahn School of Medicine at Mount Sinai, New York, USA

¹¹ Department of Physiology, Institute of Biomedicine and Translation Medicine, University of Tartu, Estonia

¹² Clinical Gene Networks AB, Stockholm, Sweden

¹³ Department of Cardiac Surgery, Tartu University Hospital, Tartu, Estonia

¹⁴ Integrated Cardio Metabolic Centre, Department of Medicine, Karolinska Institute, Sweden

Contribution:

Provided transactivation and binding assay data, as well as molecular modeling investigations.

SCIENTIFIC REPORTS

OPEN

Carbonyl reductase 1 catalyzes 20 β -reduction of glucocorticoids, modulating receptor activation and metabolic complications of obesity

Ruth A. Morgan^{1,2}, Katharina R. Beck³, Mark Nixon¹, Natalie Z. M. Homer⁴, Andrew A. Crawford^{1,5}, Diana Melchers⁶, René Houtman⁶, Onno C. Meijer⁷, Andreas Stomby⁸, Anna J. Anderson¹, Rita Upreti¹, Roland H. Stimson¹, Tommy Olsson⁸, Tom Michael⁹, Ariella Cohain¹⁰, Arno Ruusalepp^{11,12,13}, Eric E. Schadt¹⁰, Johan L. M. Björkegren^{10,11,12,13,14}, Ruth Andrew^{1,4}, Christopher J. Kenyon¹, Patrick W. F. Hadoke¹, Alex Odermatt³, John A. Keen² & Brian R. Walker^{1,4}

Carbonyl Reductase 1 (CBR1) is a ubiquitously expressed cytosolic enzyme important in exogenous drug metabolism but the physiological function of which is unknown. Here, we describe a role for CBR1 in metabolism of glucocorticoids. CBR1 catalyzes the NADPH- dependent production of 20 β -dihydrocortisol (20 β -DHF) from cortisol. CBR1 provides the major route of cortisol metabolism in horses and is up-regulated in adipose tissue in obesity in horses, humans and mice. We demonstrate that 20 β -DHF is a weak endogenous agonist of the human glucocorticoid receptor (GR). Pharmacological inhibition of CBR1 in diet-induced obesity in mice results in more marked glucose intolerance with evidence for enhanced hepatic GR signaling. These findings suggest that CBR1 generating 20 β -dihydrocortisol is a novel pathway modulating GR activation and providing enzymatic protection against excessive GR activation in obesity.

Carbonyl reductase 1 is a member of the short chain dehydrogenase/reductase family and is most commonly studied for its role in exogenous drug metabolism, particularly the conversion of chemotherapeutic drug doxorubicin to cardiotoxic danorubicin^{1,2}. Significant effort has gone into developing inhibitors of this enzyme which could be administered as an adjunct to doxorubicin therapy and thus reduce cardiac side effects³⁻⁵. There is also marked biological variation in expression of the CBR1 protein between ethnicities⁶ and following exposure to environmental agents such as cigarette smoke⁷ and flavonoids⁸. However the physiological role of this enzyme is unknown. Here we describe a novel role for CBR1 in glucocorticoid metabolism.

Glucocorticoids act through ubiquitous glucocorticoid receptors (GR) and cell-specific mineralocorticoid receptors (MR) to modulate, for example, fuel metabolism, inflammation and salt and water balance. Plasma

¹University/BHF Centre for Cardiovascular Science, The Queen's Medical Research Institute, University of Edinburgh, Edinburgh, UK. ²Royal (Dick) School of Veterinary Studies, University of Edinburgh, Edinburgh, UK. ³Division of Molecular and Systems Toxicology, Department of Pharmaceutical Sciences, University of Basel, Basel, Switzerland. ⁴Mass Spectrometry Core Laboratory, Wellcome Trust Clinical Research Facility, The Queen's Medical Research Institute, University of Edinburgh, Edinburgh, UK. ⁵School of Social and Community Medicine, University of Bristol, Bristol, UK. ⁶PamGene International, Den Bosch, The Netherlands. ⁷Department of Internal Medicine, Division Endocrinology, Leiden University Medical Center, Leiden, The Netherlands. ⁸Department of Public Health and Clinical Medicine, Umeå University, 901 87, Umeå, Sweden. ⁹The Roslin Institute, University of Edinburgh, Easter Bush Campus, Edinburgh, UK. ¹⁰Department of Genetics and Genomic Sciences, Icahn Institute for Genomics and Multiscale Biology, Icahn School of Medicine at Mount Sinai, New York, USA. ¹¹Department of Physiology, Institute of Biomedicine and Translation Medicine, University of Tartu, Tartu, Estonia. ¹²Clinical Gene Networks AB, Stockholm, Sweden. ¹³Department of Cardiac Surgery, Tartu University Hospital, Tartu, Estonia. ¹⁴Integrated Cardio Metabolic Centre, Department of Medicine, Karolinska Institute, Stockholm, Sweden. Correspondence and requests for materials should be addressed to R.A.M. (email: ruth.morgan@ed.ac.uk)

Received: 10 May 2017

Accepted: 8 August 2017

Published online: 06 September 2017

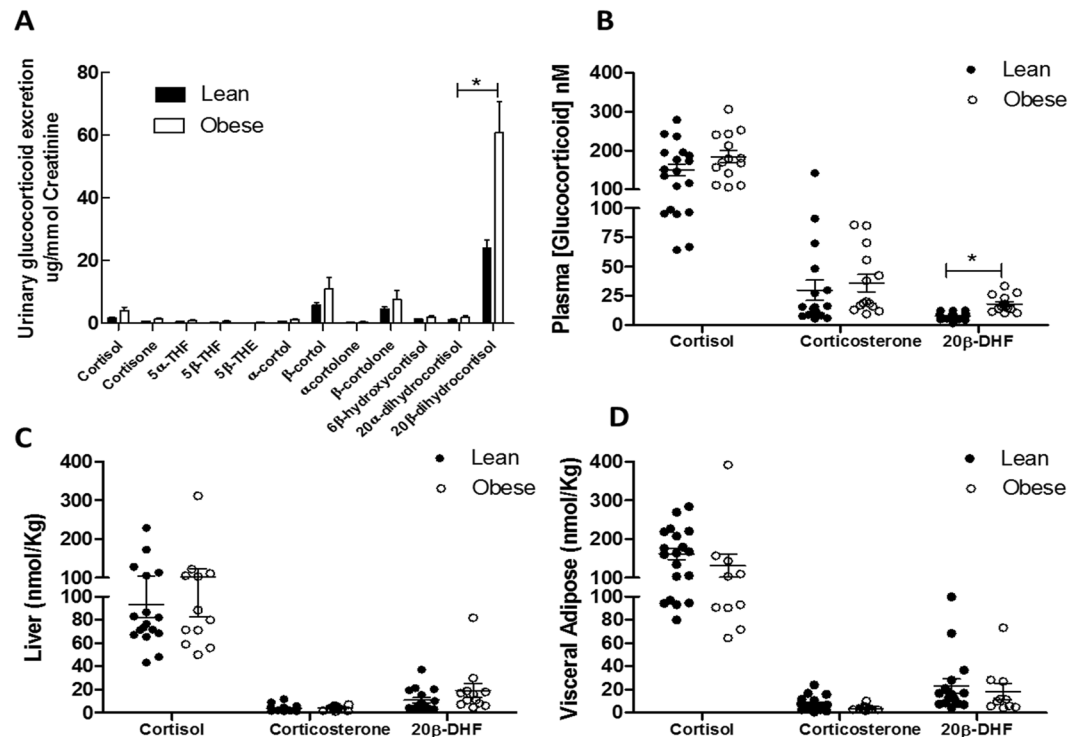


Figure 1. 20 β -Dihydrocortisol (20 β -DHF) is an abundant cortisol metabolite which is increased in plasma and urine of obese horses. **(A)** Obese horses excreted significantly more urinary β -cortol, β -cortolone and 20 β -DHF than lean horses as measured by GC-MS/MS. **(B)** Plasma 20 β -DHF concentrations were significantly higher in obese horses compared to lean horses. **(C)** Hepatic 20 β -DHF concentrations did not differ between lean and obese horses. **(D)** Visceral adipose 20 β -DHF concentrations did not differ between lean and obese horses. Data are mean \pm SEM, $n = 14/\text{group}$, * $P < 0/05$.

glucocorticoid concentrations are controlled by the hypothalamic-pituitary-adrenal axis, which balances adrenal secretion of glucocorticoids against their clearance from the circulation by intracellular enzymes, predominantly active in the liver and kidney. These enzymes also modulate intracellular glucocorticoid concentrations independently of plasma concentrations, thereby conferring tissue-specific control of GR and MR activation. For example, in mineralocorticoid-responsive tissues such as the kidney and colon, MR are protected from exposure to the high-affinity ligand cortisol by 11 β -hydroxysteroid dehydrogenase type 2 (11 β -HSD2)⁹, which converts cortisol to inert cortisone; inhibition of 11 β -HSD2 results in cortisol-dependent excessive MR activation and hypertension. In contrast, in glucocorticoid-responsive tissues such as liver and adipose, cortisol is regenerated from cortisone by 11 β -HSD type 1 (11 β -HSD1) thereby amplifying GR activation¹⁰; inhibition of 11 β -HSD1 improves glucose tolerance in patients with type 2 diabetes¹¹. Further modulation of receptor activation may be conferred by generation of glucocorticoid metabolites which retain activity at corticosteroid receptors. For example, hepatic 5 α -reduction is the predominant clearance pathway for cortisol in humans but the product of this pathway, 5 α -tetrahydrocortisol (5 α -THF), is a selective GR modulator which may contribute to anti-inflammatory signaling¹²; inhibition of 5 α -reductase type 1 results in glucose intolerance and liver fat accumulation, likely due to increased cortisol action in liver or skeletal muscle¹³. In humans and in rodent models, obesity is associated with tissue-specific dysregulation of cortisol metabolism, for example increased 5 α -reductase activity and altered 11 β -HSD1 activity¹⁴.

We embarked on an investigation of cortisol metabolism in domesticated horses, for whom obesity is a growing problem¹⁵ and discovered that the predominant metabolite of cortisol (F) in this species is 20 β -dihydrocortisol (20 β -DHF), which is increased in obesity. 20 β -DHF has previously been identified in equine¹⁶ and human¹⁷ urine. Increased urinary excretion of 20 β -DHF has been associated with Cushing's disease¹⁸ and hypertension¹⁹ in humans. In this study we: dissected pathway producing 20 β -DHF in horses, humans and mice; documented the enzyme responsible as carbonyl reductase 1 (CBR1); discovered that 20 β -DHF modulates GR; and demonstrated the metabolic consequences of inhibiting CBR1.

Results

20 β -Dihydrocortisol is a metabolite of cortisol in horses and humans and its urinary excretion is increased in obesity. Urine, blood and tissue were collected from healthy ($n = 14$) and obese ($n = 14$) horses at post-mortem (see Supplementary Table S1 for clinical characteristics). Glucocorticoids were extracted and quantified using GC-MS/MS (urine) or LC-MS/MS (tissue and plasma). 20 β -DHF accounted for approximately 60% of total glucocorticoid metabolite urinary excretion in healthy horses, and was increased in obese horses (Fig. 1A). Plasma 20 β -DHF, but not cortisol, concentrations were also increased in obese horses (Fig. 1B). In

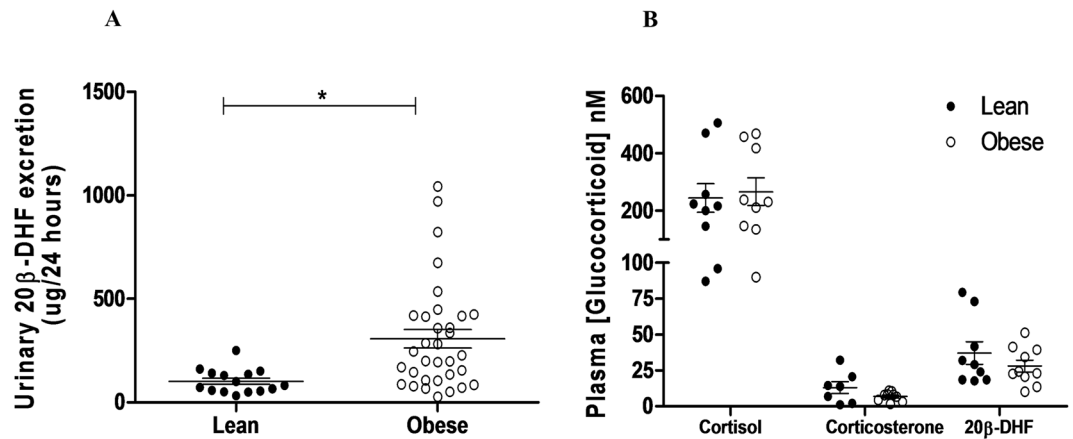


Figure 2. Urinary 20 β -DHF is detectable in human urine and increased in obesity. (A) Obese (BMI >25, n = 37) humans excrete 20 β -DHF at higher levels than lean (BMI <25, n = 15) humans. (B) 20 β -DHF is readily detectable in human plasma but concentrations are not altered in obesity (n = 10/group). Plasma cortisol and corticosterone were not different between the groups. Data are mean \pm SEM, *P < 0/05.

visceral adipose tissue and liver, cortisol and 20 β -DHF concentrations were measurable but not different between lean and obese horses (Fig. 1C–D).

Twenty-four hour urine samples were collected from healthy lean men (mean age 37.7 ± 15.9 years), and from obese men with and without type 2 diabetes (mean age 51.1 ± 14.9 years). As previously reported, the human urinary cortisol metabolite profile was dominated by products of 5 α - and 5 β -reduction, β -cortisol in particular¹⁷, and total metabolite excretion was increased in obesity²⁰ (Supplementary Fig. S1). 20 β -DHF was observed in human urine, accounting for approximately 3% of total urinary cortisol metabolites (Supplementary Fig. S1), and 20 β -DHF excretion was increased in obesity (Fig. 2A), independently of the presence of diabetes, but was not disproportionately increased compared with other measured cortisol metabolites (see Supplementary Fig. S1 for metabolite pathways). 20 β -DHF was also readily detected in plasma from healthy lean men at similar levels to corticosterone (Fig. 2B), but was not altered in obesity.

Carbonyl reductase 1 converts cortisol to 20 β -dihydrocortisol and is increased in equine, murine and human obesity.

The enzyme responsible for 20 β -DHF production was previously unknown. Carbonyl reductase 1 (CBR1) is a ubiquitously expressed short-chain dehydrogenase known for its role in xenobiotic metabolism²¹. Cortisol is reported as a substrate of CBR1 but its product has not been identified²¹. We found that recombinant human CBR1 converted cortisol to 20 β -DHF in the presence of NADPH at a rate of 1.2 ± 0.4 ng/mg CBR1 protein per minute ($1 \mu\text{M}$ cortisol substrate). Moreover, CBR1 accounts for equine production of 20 β -DHF, which was the predominant metabolite in equine liver homogenate incubated with cortisol (Supplementary Fig. S2A), since this reaction was blocked by co-incubation with the CBR1 inhibitor quercetin in equine liver cytosol (Supplementary Fig. S2B). 20 β -DHF was not produced by incubation of equine liver microsomes with cortisol.

CBR1 is highly expressed in gut, liver, adipose and renal tissue of mice and humans (<http://www.proteinatlas.org/ENSG00000159228-CBR1/tissue>), the expression profile of horses has not been reported. We chose to examine the effect of obesity on expression of CBR1 in liver and adipose tissue. Hepatic CBR1 mRNA was not altered in obesity in horses or mice but CBR1 mRNA was increased in adipose tissue of obese horses (Fig. 3A). CBR1 mRNA was also higher in high-fat fed mice (Fig. 3B) and in visceral adipose tissue from obese compared with lean men (n = 8/group, Fig. 3C).

Common functional genetic variants in the CBR1 locus predict metabolic disturbances in obesity.

We used an expression quantitative trait loci (eQTL) approach in the STARNET dataset²² to test whether any SNPs in the CBR1 locus had a functional effect on hepatic or visceral adipose CBR1 expression, and then tested their association with phenotypic traits in publicly accessible datasets using MR-Base²³. There were no eQTLs which influenced visceral adipose expression of CBR1 but eQTLs were identified in liver. Further analyses suggested that SNPs associated with higher CBR1 expression in the liver were causally associated with higher fasting glucose (beta 0.01, se <0.01, p = 0.02), higher glycated haemoglobin (beta 0.01, se <0.01, p = 0.01) (Supplementary Table S5). There was no evidence that CBR1 expression was causally associated with fasting insulin, HOMA-B or HOMA-IR (p > 0.2), although there was suggestive evidence that higher CBR1 expression causes lower body fat (beta -0.01, se 0.01, p = 0.06). In addition to these observations in population based cohorts, eQTLs of CBR1 in liver were associated with BMI in the STARNET study participants (rs2835288, p = 5.7E-4). The eQTL rs2835288 had a negative effect on BMI (r = -0.13) but a positive effect on CBR1 liver expression (r = 0.43); accordingly CBR1 liver expression and BMI were negatively correlated (r = -0.093, p = 0.03). Using a conservative causal inference test²⁴ there was suggestive evidence (p = 0.07) that expression of CBR1 in liver was causal for variation in BMI.

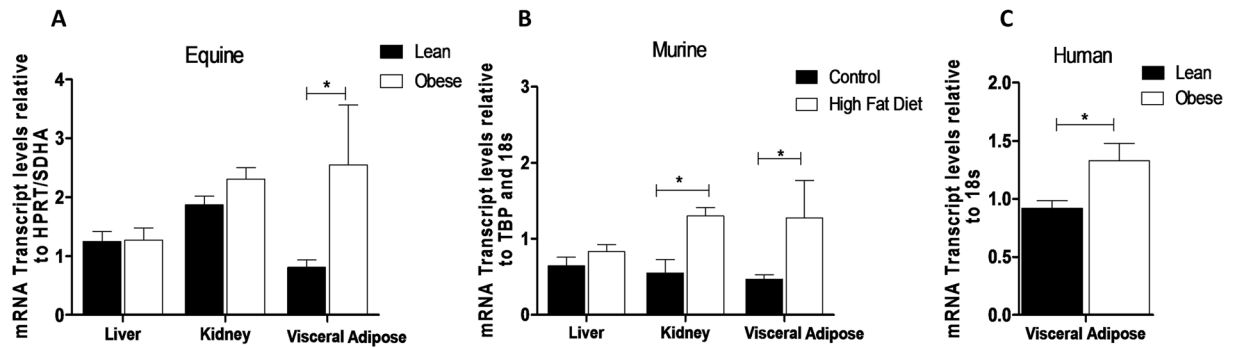


Figure 3. Carbonyl reductase 1 expression is increased in adipose tissue in obese horses, humans and mice. (A) *CBR1* mRNA transcript levels are increased in visceral adipose of obese horses ($n = 14/\text{group}$), (B) Visceral adipose *Cbr1* transcript levels were increased in mice on a high-fat diet for 6 weeks ($n = 6/\text{group}$). (C) Visceral adipose *CBR1* transcript levels were increased in obese humans ($n = 8/\text{group}$). Data are mean \pm SEM, * $P < 0.05$.

20 β -DHF activates glucocorticoid receptors. Given apparently contradictory associations of genetically high *CBR1* activity with metabolic dysfunction but not obesity in humans, and the association of *CBR1* expression and activity with obesity in multiple species, we investigated the interaction of 20 β -DHF with GR in order to predict consequences of elevated *CBR1* for GR activation.

Computational evaluation of the interactions formed by 20 β -DHF with the GR ligand binding site using docking calculations revealed a similar binding pose compared to cortisol (Fig. 4A). Both ligands formed hydrogen-bonds (H-bonds) similar in length with the same amino acid residues (Arg611, Gln570, Asn564 and Thr739). The only difference observed was the hydroxyl group of 20 β -DHF at position 20 representing a hydrogen bond donor instead of the carbonyl group of cortisol at the same position serving as hydrogen bond acceptor. Human epithelial A549 cells expressing endogenous GR and SF9 and HEK293 cells transfected with human GR were used to investigate 20 β -DHF as an endogenous ligand of GR. In binding studies, unlabeled 20 β -DHF displaced dexamethasone from GR in SF9 cell lysate preparations but only at 1000-fold higher concentration than cortisol (Fig. 4B). Nonetheless, transfection of HEK293 cells with GFP-GR showed that 20 β -DHF induced nuclear translocation of GR within 30 minutes (Fig. 4C).

In functional studies, 20 β -DHF was a weak agonist of GR. In A549 cells MMTV promoter-induced luciferase activity, indicative of GR activation, was only partially induced by 20 β -DHF at high concentration (2.5 μM ; Fig. 4D). However, endogenous GR-responsive genes glucocorticoid-induced leucine zipper (*GILZ*), insulin-like growth factor binding protein 1 (*IGFBP1*), dual specificity phosphatase 1 (*DUSP1*) and FK506-binding protein 51 (*FKBP51*) were all up-regulated by 20 β -DHF in a concentration-dependent manner (Fig. 4E) and to a similar maximum as cortisol, albeit at substantially higher concentrations than cortisol. Similar dose-response relationships were seen comparing the effects of cortisol and 20 β -DHF in preventing IL-1 β induction by TNF α in A549 cells (Fig. 4F).

Co-regulator recruitment by GR on binding 20 β -DHF was assessed by microarray assay for real-time co-regulator-nuclear receptor interaction (MARCoNI) with the GR agonist dexamethasone used as a positive control²⁵. Under these conditions, 20 β -DHF-activated GR recruited approximately 36% of the co-regulators recruited by dexamethasone (Fig. 5 and supplementary Excel file).

Pharmacological inhibition of *Cbr1* in mice results in increased hepatic GR activation and worsens the metabolic effects of high-fat feeding.

Knowing that both cortisol and 20 β -DHF might amplify GR activation, we sought to test the effects of *Cbr1* inhibition in mice to determine whether increasing the substrate/product balance would increase or decrease GR activation. Unlike horses and humans, mice produce corticosterone (B) rather than cortisol as their major glucocorticoid. To validate the use of murine models to study the *CBR1*/20 β -dihydroglucocorticoid pathway, preparatory work included demonstration that 20 β -dihydrocorticosterone (20 β -DHB), the murine equivalent of 20 β -DHF, induced MMTV-luciferase activity in HEK293 cells transfected with murine GR (Supplementary Fig. S3) and is present in murine plasma and tissue (Supplementary Fig. S4), and that *Cbr1* mRNA was higher in adipose of C57BL/6J adult male mice fed on a high fat diet for 6 weeks than controls on a normal chow diet ($n = 6/\text{group}$) (Fig. 3B). Murine diet-induced obesity was therefore used as a model in which to investigate the functional role of *CBR1* and 20 β -dihydro metabolites. Groups of adult male C57BL/6J mice ($n = 12/\text{group}$) maintained on a high fat diet were randomly assigned to groups receiving vehicle (ethanol) or *Cbr1* inhibitor (quercetin, 50 $\mu\text{g}/\text{mouse}/\text{day}$, administered in drinking water for 6 weeks).

Quercetin lowered hepatic 20 β -DHB (Fig. 6A) and increased the ratio of *Cbr1* substrate (corticosterone) to product (20 β -DHB) in liver (vehicle B: 20 β -DHB ratio 0.5 ± 0.2 versus quercetin B: 20 β -DHB ratio 1.6 ± 0.4 , $P = 0.01$). Quercetin did not alter 20 β -DHB levels in subcutaneous adipose tissue (Fig. 6B) or plasma (Fig. 6C). Quercetin also raised peak plasma corticosterone concentrations (Fig. 6D) but did not affect food or water intake or bodyweight over the course of the experiment (Fig. 6E). However, quercetin raised fasting plasma insulin concentrations and blood glucose during glucose tolerance tests (Fig. 6F,G). Quercetin also increased hepatic expression of the GR-responsive gene *Period 1* (*Per1*), but did not alter the mineralocorticoid-responsive gene serum glucocorticoid kinase 1 (*Sgk1*) or key gluconeogenic enzyme phosphoenolpyruvate carboxykinase (*Pepck*)

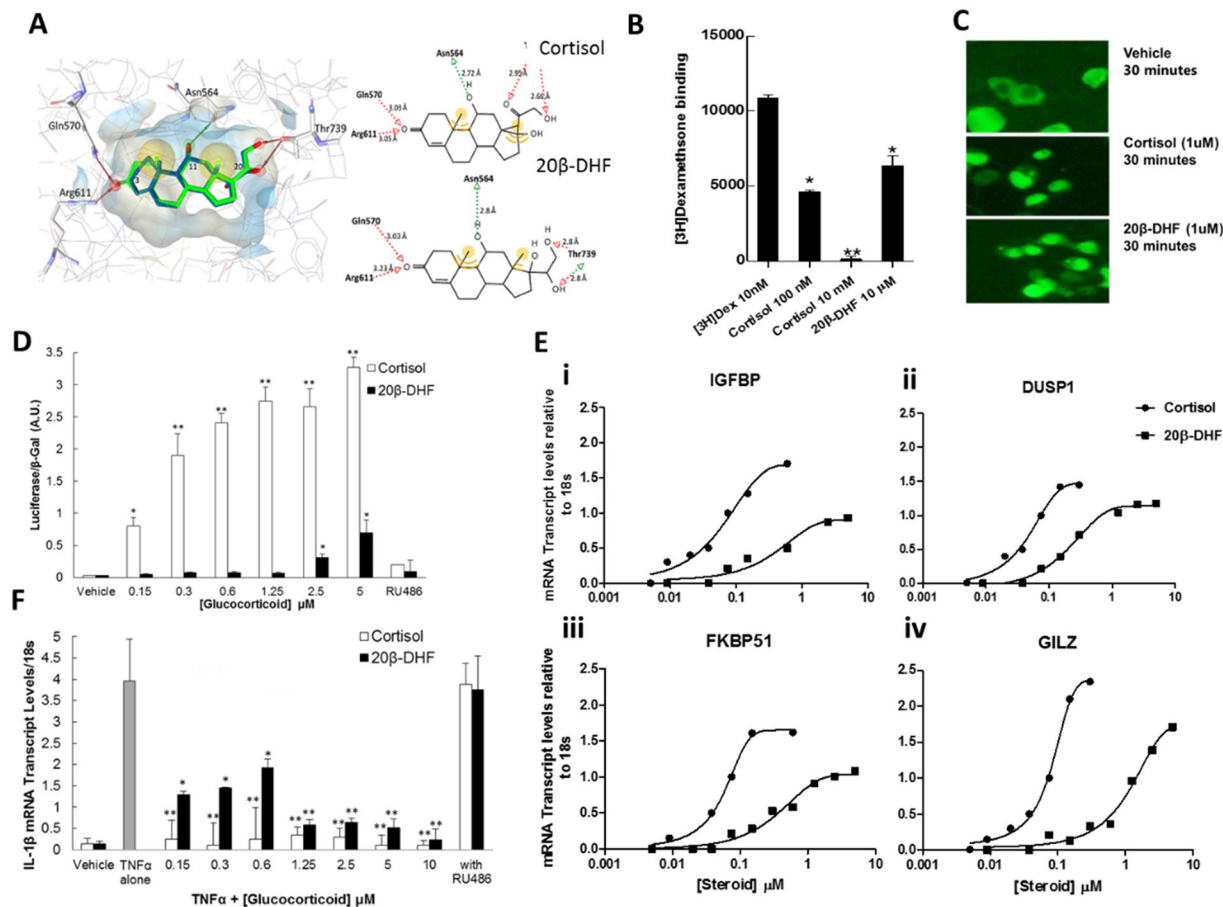


Figure 4. 20 β -Dihydrocortisol binds, translocates and activates glucocorticoid receptor inducing gene transcription and suppressing inflammatory gene transcription. (A) Docking of cortisol and 20 β -DHF into the ligand binding site of GR. The automatically created pharmacophore indicates the essential structural features for ligand binding (red and green arrows with spheres display hydrogen-bond (H-bond) interactions and yellow spheres hydrophobic interactions). Amino acid residues crucial for ligand binding are shown as sticks. Compared to the binding interactions of cortisol 20 β -DHF differs only in the hydroxyl group of cortisol serving as H-bond acceptor. (B) Unlabelled 20 β -DHF displaced 3 [H]-dexamethasone from GR in the lysate of SF9 cells expressing GR. (C) 1 μ M 20 β -DHF induced translocation of cytoplasmic GR to the nucleus of HEK293 cells within 30 minutes visualised by fluorescence imaging at 20x magnification. (D) 2.5 μ M 20 β -DHF induced luciferase activation in A549 cells transfected with glucocorticoid responsive plasmid MMTV-luc. (E) 20 β -DHF induced transcription of GR-responsive genes IGFBP1 (EC₅₀ 0.51 μ M), DUSP1 (EC₅₀ 0.32 μ M), FKBP51 (EC₅₀ 0.44 μ M) and GILZ (EC₅₀ 1.25 μ M) in A549 cells. (F) TNF α induced transcription of IL-1 β in A549 cells, this was inhibited by cortisol and by 20 β -DHF at 0.15 μ M. Transcription was not reduced by co-incubation of cortisol or 20 β -DHF with the GR antagonist RU486. Experiments were performed in triplicate on three occasions. Data are mean \pm SEM (N = 3). Data were compared by two-way ANOVA and Bonferroni correction test: *P < 0.05, **P < 0.01 compared to vehicle.

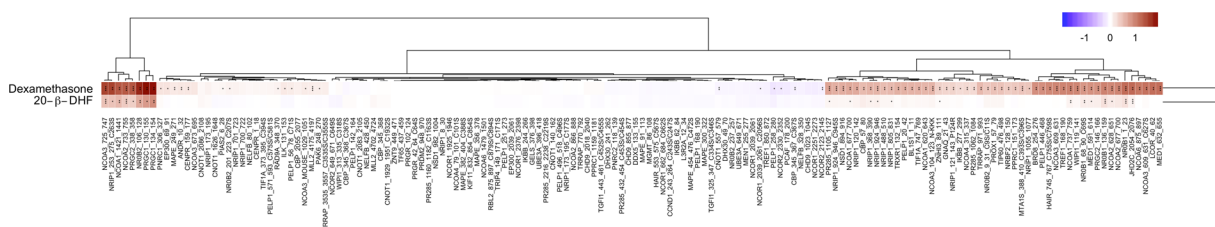


Figure 5. 20 β -Dihydrocortisol induces similar co-regulator interactions with GR as dexamethasone. MARCoNI analysis of co-activator recruitment showed that on binding 20 β -DHF, GR recruited 36% of the co-regulators recruited by dexamethasone. The colour of the bar represents the modulation index i.e. compound induced log-fold change of binding, red a positive fold change and blue a negative fold change. *P < 0.05, **P < 0.01, ***P < 0.001 compared to the unbound receptor.

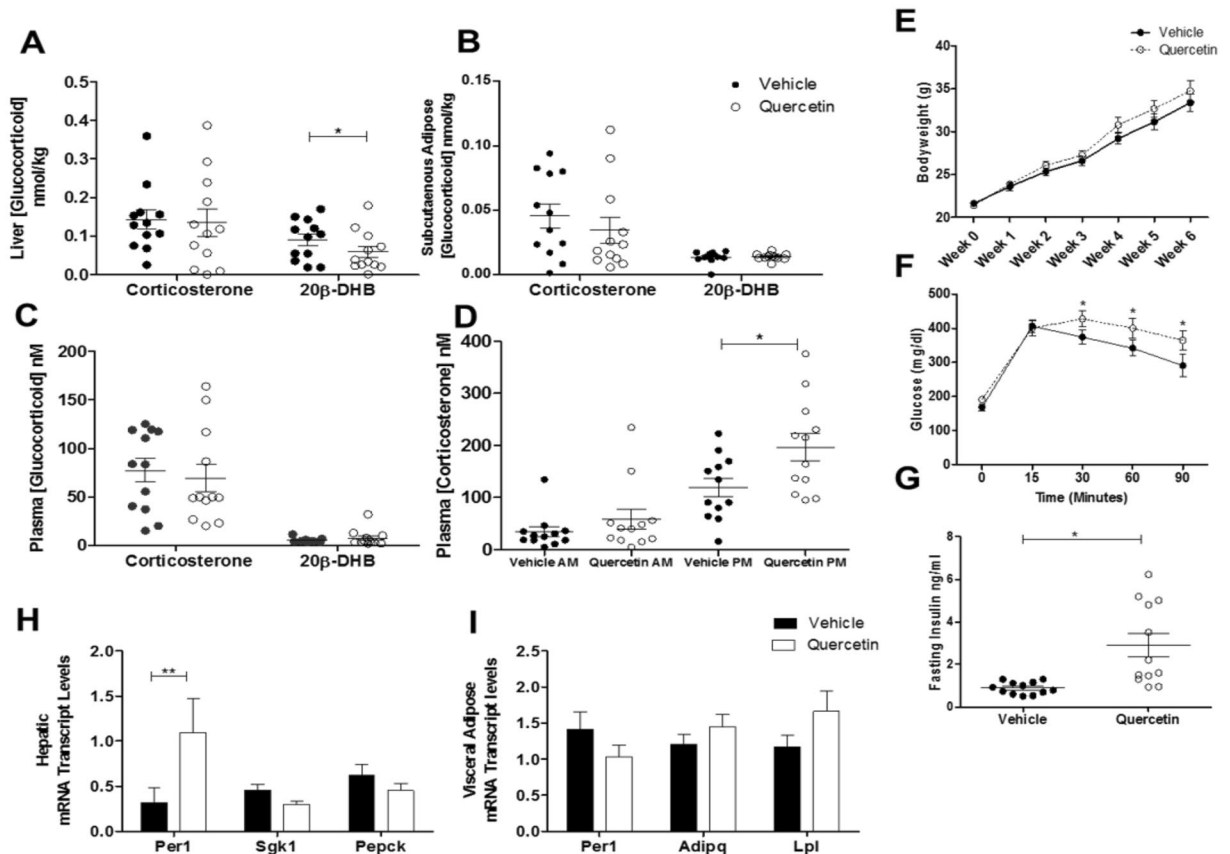


Figure 6. Inhibition of CBR1 in a murine model of diet-induced obesity results in increased GR activation and metabolic dysfunction. (A) Hepatic 20 β -DHB levels were significantly lower in quercetin treated mice, (B) 20 β -DHF levels were not altered in subcutaneous adipose tissue, (C) plasma 20 β -DHB levels were not altered by quercetin treatment (D) quercetin treatment resulted in increased peak plasma corticosterone levels. (E) Bodyweight was not different between mice in the vehicle treated group and mice treated with quercetin. (F,G) Quercetin-treated mice were significantly more insulin resistant and had higher fasted plasma insulin concentrations. (H) mRNA transcript levels of hepatic *Per1* were increased in quercetin treated mice, (I) Adipose mRNA expression of *Per1*, Adiponectin (*Adipq*) and lipoprotein lipase (*Lpl*) were not altered by quercetin treatment. Data are mean \pm SEM, $n = 12$ /group, * $P < 0.05$.

in the liver (Fig. 6H). Transcript levels of *Per1*, adiponectin and lipoprotein lipase were not altered by quercetin in subcutaneous adipose tissue (Fig. 6I).

Discussion

We describe a novel pathway of glucocorticoid metabolism, whereby cortisol is converted to 20 β -dihydrocortisol by the cytosolic enzyme CBR1, producing a metabolite which is a weak activator of GR. This pathway is up-regulated in adipose-tissue of obese horses, humans and mice; genetic variation in the liver predicts glucose dysregulation and its pharmacological inhibition alters the hypothalamic-pituitary-adrenal axis and tissue steroid levels in mice, with associated changes in GR-dependent gene expression and in metabolic homeostasis. This provides important new insights into the control of tissue glucocorticoid action and its contribution to cardio-metabolic disease.

The glucocorticoid metabolite profile of horses, a cortisol-dominant species²⁶, has not previously been described, although inter-species variation in hepatic cortisol metabolism has been reported²⁷. 20 β -DHF has been measured in horse urine¹⁶ and purported to be a sensitive indicator of cortisol administration, but ours are the first data showing 20 β -DHF relative to other metabolites, and the first demonstrating 20 β -DHF in plasma, adipose tissue and liver of horses. Predominance of 20 β -DHF production occurs in other large herbivores, including sheep^{28,29}. The human cortisol metabolome is more thoroughly described^{17,30}, and is dominated by products of 5 α - and 5 β -reduction. However, 20 β -DHF has previously been identified in human urine^{17,18} at levels similar to that of 5 α -tetrahydrocortisol (5 α -THF). Occasional case reports indicate urinary excretion of 20 β -DHF is increased in human Cushing's syndrome¹⁸, collagen disease³¹, rheumatoid arthritis³², hypertension¹⁹ and liver cirrhosis^{33,34}. In our study 20 β -DHF was readily detectable in the plasma of healthy humans at levels equal or higher to that of corticosterone, but 20 β -DHF represented a much smaller proportion of cortisol metabolism than in horses.

There are reports of reduction of cortisol to 20 β -DHF in various human cell/tissue types including kidney and prostate³⁵, gingiva³⁶, fibroblasts³⁷ and thrombocytes³⁸. We found that CBR1, a ubiquitously expressed member of the short-chain dehydrogenase/reductase (SDR) superfamily¹ catalyzes the conversion of cortisol to 20 β -DHF. *CBR1* expression is highest in tissues involved in detoxification or clearance, e.g. liver, colon, renal tubules and placenta³⁹ and has been studied for its role in drug metabolism³ and as an antioxidant⁴⁰. Its expression is associated with cancer, particularly lung cancer⁷, and reported to protect against pancreatic islet cell death⁴¹. Inhibitors of CBR1 have been proposed for use with chemotherapeutic agents to reduce the cardiotoxic side-effects of drugs such as doxorubicin⁴. Although glucocorticoids are known to be substrates of CBR1, the products have not been identified previously⁴⁰. We attribute 20 β -dihydro glucocorticoid generation to CBR1 since isolated CBR1 converts cortisol to 20 β -DHF and not to other metabolites, hepatic microsomal preparations are devoid of such activity, and inhibition of CBR1 is sufficient to prevent 20 β -DHF generation in equine liver cytosol and to lower tissue 20 β -DHB in mouse liver *in vivo*.

The majority of cortisol metabolites are thought to be inert and are produced to facilitate steroid excretion. Some metabolites, however, such as 5 α -tetrahydrocorticosterone (5 α -THB) bind and activate GR¹². Given that 20 β -DHF was found in plasma and tissues of humans at similar levels to the endogenous glucocorticoid corticosterone, and is thus potentially of physiological significance, we investigated the action 20 β -DHF on GR. We found that 20 β -DHF bound GR with a lower affinity than that of cortisol but induced nuclear translocation of the receptor within 30 minutes, a time period comparable with cortisol. 20 β -DHF induced transrepressive and trans-activation effects after binding to GR albeit at higher concentrations than cortisol. The consequences of variation in CBR1 activity for GR activation are therefore hard to predict.

In human obesity, increased total cortisol production⁴² without consistently elevated plasma cortisol concentrations has been attributed to enhanced clearance of cortisol²⁰, and in turn to increased 5 α - and 5 β -reductase and reduced 11 β -HSD1 activities²⁰. In humans, horses and mice obesity was associated with increased *CBR1/Cbr1* expression in adipose tissue, in horses with increased 20 β -DHF in plasma, and in humans and horses with increased 20 β -DHF in urine. Although 20 β -DHF was not disproportionately raised in urine, total cortisol metabolite excretion was increased so these data are consistent with the CBR1/20 β -DHF pathway contributing to increased cortisol clearance in obesity. Up-regulation of the CBR1 pathway in obesity was evident in adipose but not liver in horses and mice. In addition we did not identify any eQTL for *CBR1* expression in adipose suggesting that this up-regulation is a functional response to obesity. This is consistent with intra-adipose inflammation and hypoxia in obesity, since *CBR1* expression is up-regulated in response to hypoxia and inflammation via transcription factors including Nrf2, AhR and HIF-1 α ^{43,44}. In contrast our data suggest that there are genetic influences on hepatic *CBR1* expression in humans and that higher expression is associated with higher leptin, higher fasting glucose and higher HbA1c. Tissue-specific regulation of *CBR1* is reported^{43,45,46} so the eQTLs we identified may, for example, exert their influence through liver-specific promoter(s).

To further explore the contribution of CBR1 dysregulation in obesity, we administered the *Cbr1* inhibitor quercetin to mice with diet-induced obesity. Pharmacodynamic data suggest that quercetin inhibited corticosterone conversion to 20 β -DHB in liver, but not in adipose tissue; this may indicate that adipose 20 β -DHB is mainly derived from plasma rather than from local generation, or that the drug was unable to penetrate adequately into adipose tissue. Although an eQTL predicting higher hepatic CBR1 was associated with adverse metabolic indices, a paradoxical deterioration in glucose metabolism was observed when we inhibited the enzyme. This was accompanied by altered GR-regulated genes in liver which may be explained by the effect of substrate (corticosterone) accumulation or by secondary activation of the HPA axis with elevated peak plasma corticosterone resulting from impaired clearance. A similar phenotype and liver transcript profile occurs in mice with genetic deletion of the glucocorticoid-inactivating enzyme 5 α -reductase type 1⁴⁷. Alternatively we could infer that there is a non-linear relationship between *Cbr1* expression and effect and that an optimal cortisol/20 β -DHF balance may be required for normal liver GR activation, such that dysregulation of *Cbr1* in either direction leads to GR excess.

These findings are important since there are wide variations in CBR1 activity between individuals, in disease and after consumption of a number of naturally occurring CBR1 inhibitors: human tissue CBR1 expression and activity varies significantly between ethnic groups⁶; CBR1 expression and activity is increased in Down's syndrome due to the location of the CBR1 gene on chromosome 21⁴⁸; CBR1 inhibitors such as flavonoids and polyphenols are present in many foods and supplements⁴⁹ and reported enhancers of CBR1 activity include components of cigarette smoke⁷. Our data suggest the resulting variation of CBR1/20 β -DHF has important consequences for glucocorticoid metabolism and GR activation in health and disease.

Materials and Methods

Study design. We conducted case-control, cross-sectional or intervention studies in horses, humans, cells and mice. Sample sizes were chosen for 80% power to detect magnitudes of difference inferred from pilot data with the number of subjects and outcomes defined below or in figure legends. *In vitro* experiments were performed in triplicate with the number of experiments and outcomes defined below and in figure legends. Details on inclusion and exclusion criteria for horse and human subjects are detailed below. There were no dropouts and no outliers were excluded.

Cortisol metabolism in horses. The first aim of the study was to characterize cortisol metabolism in lean and obese horses. We addressed this aim using an observational case-control study recruiting lean horses and obese horses that were destined for euthanasia at the Royal (Dick) School of Veterinary Studies, University of Edinburgh. Studies in horses were approved by the Royal (Dick) School of Veterinary Studies Ethics and Research committee (VERC 7014). The study was performed according to the approved ethical guidelines. The sample size ($n = 14/\text{group}$) was determined by interim analysis using total glucocorticoid metabolite excretion as the end-point (80% power to detect a 20% difference in groups, $p < 0.05$). Lean (body condition score, measure of

obesity $\leq 3/5^{50}$) and obese (body condition score $\geq 4/5$) castrated male and female horses destined for euthanasia, were recruited from clinics at the Royal (Dick) School of Veterinary Studies. Horses were excluded if they were less than 1 year old, suffering from any concurrent systemic illness or had received glucocorticoid treatment in the 3 months prior to commencement of the study. Blood was obtained after overnight fasting, between 0900 h and 1100 h, via an intravenous cannula inserted in the jugular vein for the purpose of euthanasia.

Horses were humanely euthanased (0900 h to 1100 h) with quinalbarbitone sodium and cinchocaine hydrochloride (1 mL/10Kg bodyweight; Somulose, Dechra Veterinary Products, Shrewsbury, UK). Samples of peri-renal adipose, liver and urine were snap frozen and stored at -80°C .

Glucocorticoids were extracted from plasma, adipose and liver and quantified by LC-MS/MS (see supplementary methods). Urinary glucocorticoids were derivatized and quantified by GC-MS/MS (supplementary methods). Urinary creatinine was measured by the modified Jaffe's reaction (IL650 analyzer, Instrumentation Laboratories). Glucocorticoid concentrations were expressed as $\mu\text{g}/\text{mmol}$ creatinine. RNA was extracted from adipose and liver samples for quantification of *CBR1* mRNA relative to housekeeping genes SDHA and 18s (see supplementary methods and supplementary Table S7).

20 β -DHF in humans. In order to determine the relevance of 20 β -DHF to human health and disease samples were collected from male participants at the University of Edinburgh with approval from the University of Edinburgh Research Ethics Committee, National Health Service Lothian Research and Development Office, and at Umea University with approval from the Umea Regional Ethical Review Board. The study was performed according to the approved ethical guidelines. Participants were required to give written informed consent prior to recruitment to the study. Lean individuals were defined as having a BMI $<25\text{ kg}/\text{m}^2$ and obese individuals as having a BMI $>25\text{ kg}/\text{m}^2$. Clinical details are given in supplementary Tables 2–4.

Twenty-four hour urine samples were obtained from healthy lean ($n = 15$) and obese ($n = 18$) men recruited as part of a separate study¹³. In addition, urine was collected from obese men ($n = 19$) with Type 2 diabetes (with no insulin treatment) (Supplementary Table S2). Morning fasted plasma samples were collected from healthy lean ($n = 10$) and obese ($n = 10$) men (Supplementary Table S3). Adipose biopsy samples for RNA extraction were collected from lean ($n = 8$) and obese ($n = 8$) individuals undergoing surgery (Supplementary Table S4). Glucocorticoids were extracted and quantified from plasma and urine as detailed in supplementary methods.

CBR1 activity *in vitro*. In order to determine if CBR1 could convert cortisol to 20 β -DHF recombinant human CBR1 (Source Bioscience, Nottingham, UK) was incubated with cortisol (1 mM) and NADPH (2 mM) for a time course (5, 10, 20, 30, 60 and 120 minutes) at 37°C . The reaction was stopped with the addition of acetonitrile (500 μL). Deuterated cortisol (9, 11, 12, 12- ^2H]-cortisol) was added as an internal standard for quantification of cortisol and 20 β -DHF. Following centrifugation (5 minutes) the supernatant was removed, dried down and re-suspended in mobile phase (60 μL 50:50 Methanol: water) for analysis by LC-MS/MS (Supplementary methods).

Interrogation of genetic data for CBR1 expression and phenotypic associations. No genetic variants have been robustly associated with CBR1 enzyme activity. Therefore, genetic variants that are associated with CBR1 transcript levels in liver were used as a surrogate for CBR1 enzymatic activity. Expression quantitative trait loci (eQTLs) located near to the CBR1 gene and associated with CBR1 expression in the liver were identified from the Stockholm-Tartu Atherosclerosis Network Engineering Task (STARNET) study. STARNET comprises data on 600 cases of cardiovascular disease undergoing surgical intervention with collection of multiple tissue types including the liver. Genome wide genotyping and tissue expression analyses including RNAseq have been performed²².

A two-sample Mendelian randomization approach was used to estimate the effect of CBR1 expression in the liver on outcomes of body mass index (BMI), body fat, and glucose and insulin sensitivity. The outcome data were extracted from publicly available datasets, including from GIANT and MAGIC consortia, using MR-Base²³. In cases where outcome data were available from more than one study, the study containing all the relevant information with the largest sample size was selected. The causal effect of CBR1 expression on the relevant outcomes was estimated using the Wald (or ratio) method. This method divides the coefficient from regression of the outcome on the genetic variant by the coefficient from regression of the exposure on the variant⁵¹; the former was derived from publicly available data and the latter from STARNET. This approach makes the assumption that all instrumental variables are valid and not subject to horizontal pleiotropy where a genetic variant affects the outcome via more than one biological pathway. Study overlap is a concern when undertaking two sample Mendelian randomization analyses. The STARNET study has not provided data to the GIANT or MAGIC consortia.

20 β -DHF interaction with glucocorticoid receptor. *Docking of 20 β -DHF with GR.* Docking studies were performed using the GOLD software version 5.2 (Cambridge Crystallographic Data Centre, Cambridge, UK)⁵². This software allows the identification of precise docking poses for small molecules in the binding pocket of a protein applying a genetic algorithm. The crystal structures with the Protein Data Bank (PDB) entry 4P6X [DOI:10.2210/pdb4p6x/pdb] was selected for GR. First the respective co-crystallized ligand, cortisol for GR, was removed from the binding pocket and re-docked into the binding site to examine whether GOLD could restore the original binding pose and therefore to validate the docking settings (RMSD value of 0.409 for GR). The GR binding sites were defined by the ligand surrounded by a 6 Å region lining the active site. GoldScore was used as scoring function.

Protein ligand interactions determined by the docking software were further assessed using LigandScout 3.12 (intel:ligand GmbH, Vienna, Austria). Based on chemical functionalities, geometric distances and angles between

adjacent structures, this software automatically evaluates the observed binding pattern between the protein and the docked ligand⁵³.

Glucocorticoid binding in SF9 cell lysates. Competitive GR binding experiments were conducted as described previously⁵⁴. Briefly, recombinant human GR α baculovirus stock was produced using the Bac-to-Bac expression system and subsequently expressed in Sf9 cells according to the instructions by the manufacturer (Invitrogen, Carlsbad, CA). Sf9 cell lysates expressing recombinant human GR were then incubated in the presence of 10 nM [1,2,4,6,7-³H]-dexamethasone and unlabelled competitor (either 10 μ M or 100 nM cortisol or 10 μ M 20 β -DHF) for 4 h at 16 °C. Unbound ligand was separated by adding 5% dextran coated charcoal, followed by incubation at 4 °C for 10 min and centrifugation for 10 min at 3200 \times g and 4 °C. The GR bound fraction of [1,2,4,6,7-³H]-dexamethasone in supernatants was measured by scintillation counting.

Experiments in cell culture. Human alveolar carcinoma cell line, A549, the human embryonic kidney cell line, HEK293 and the clonal line of *Spodoptera frugiperda*, SF9 were obtained from the European Collection of Cell cultures (ECACC; distributor Sigma-Aldrich Co.). Cells were grown and maintained in Dulbecco's modified Eagle's medium (DMEM, Lonza Group Ltd., Basel, Switzerland) supplemented with glucose (4.5 g/L), heat-inactivated fetal bovine serum (HI-FBS) (10% v/v), penicillin (100 IU/mL), streptomycin (100 μ g/mL) and L-glutamine (2 mM). Cells were maintained and grown in a humidified atmosphere (95% air, 5% CO₂, 37 °C). Unless otherwise stated cells were seeded at 2×10^5 per 35-mm well. Cells were cultured in steroid-free medium for 24 h prior to experimentation. Plasmids were a kind gift from K.E. Chapman, Centre for Cardiovascular Science, University of Edinburgh.

To study GR translocation, HEK293 cells were transfected with GR labelled with Green Fluorescent Protein (GFP-GR). After seeding and overnight incubation in steroid free medium, the medium was replaced with phenol red free Opti-MEM (Lonza Group Ltd., Basel, Switzerland), and cells transfected using Lipofectamine 2000 (Invitrogen, Thermo Fisher Scientific Co., Waltham, MA, USA) with 1 μ g of GFP-GR plasmid. Cells were then treated with vehicle, cortisol (1 μ M) or 20 β -DHF (1 μ M) and imaged using fluorescence microscopy (Nikon Eclipse TS100) prior to treatment and at 30, 60, 120 minutes and 4 hours.

GR activation by 20 β -DHF was tested in A549 cells transiently transfected with MMTV-luciferase plasmid. Cells were transfected with 1 μ g of pMMTV LTR-luciferase¹² and 1 μ g of pKC275 (encoding β -galactosidase as internal control) and treated with vehicle, cortisol (0.3 μ M–5 μ M) or 20 β -DHF (0.3 μ M–5 μ M) for 4 hours. Cells were lysed and luciferase and β -galactosidase activities measured as described previously⁵⁵. Galactosidase activity was assayed using a Tropix Kit (Applied Biosystems, Foster City, CA, USA). The mean ratio of luciferase/ β -galactosidase activities was calculated.

To determine effects of 20 β -DHF on endogenous glucocorticoid-induced transcripts, A549 cells were incubated in the presence of increasing concentrations of either cortisol, 20 β -DHF (0.15 μ M–5 μ M) or vehicle (ethanol) for 4 hours. RNA was extracted and RT-qPCR used to quantify *DUSP1* (dual specificity phosphatase 1), *GILZ* (glucocorticoid-induced leucine zipper), *IGFBP1* (insulin-like growth factor binding protein 1) and of *FKBP51* (FK506-binding protein 51) relative to 18S (see supplementary Table S6 for primer design and supplementary methods). To determine the effects of 20 β -DHF on inflammatory transcripts cells were pre-incubated with vehicle or TNF α (10 ng/mL) for 1 hour before a further 4 hours in the presence of vehicle, cortisol or 20 β -DHF (0.15 μ M–5 μ M). RNA was extracted and IL-1 β (interleukin 1 β) mRNA quantified relative to 18S.

MARCoNI analysis of 20 β -DHF binding to GR. A microarray Assay for Real-time Co-regulator-Nuclear Receptor Interaction (MARCoNI) was used to compare the quantitative and qualitative co-regulator recruitment induced when 20 β -DHF (1 μ M) binds with GR with that of recruitment in response to dexamethasone (1 μ M) using a previously described method^{22,56}.

Pharmacological inhibition of CBR1 in vivo. For *in vivo* studies in mice, experiments were approved by the University of Edinburgh ethical committee and performed under the Provisions of the Animals Scientific Procedures Act (1986) of the UK Home Office, in accordance with EU Directive 2010/63. Male C57BL/6J mice aged 8 weeks were purchased from Harlan laboratories and used to conduct a randomized vehicle controlled experiment. Mice were randomly assigned to the vehicle (n = 12) or quercetin-treatment group (n = 12). All the mice were fed ad-lib high-fat diet (D12331, Research Diets inc., New Jersey, USA) for 6 weeks. Quercetin treatment was administered in drinking water (50 μ g/mouse/day⁵⁷). Bodyweight, food and water intake were monitored weekly. At week 6 blood collected from tail nick at 0800 h and at 2000h for analysis of plasma basal corticosterone by Enzo Corticosterone EIA Kit (Enzo Life Sciences, Exeter, UK). Mice were fasted for 6 h (0800–1400 h) in clean cages before undergoing a glucose tolerance test (GTT). Glucose (2 mg/g body weight, 40% w/v in saline) was administered via intraperitoneal injection. Blood was collected from tail nick immediately prior to injection, 15, 30, 60, and 90 minutes after injection. Glucose was measured immediately using a point-of-care glucometer. Plasma insulin was measured using the Ultra-Sensitive Mouse Insulin ELISA kit (Crystal Chem, Inc., IL, USA). Seven days after the GTT animals were culled by decapitation. Plasma was extracted from trunk blood and stored at –20 °C. Tissue was extracted and stored at –80 °C. mRNA and glucocorticoid extraction and quantification are described in supplementary methods (see Supplementary Table S8 for murine primer sequences).

Statistical analysis. For horse, human and mouse studies data were tested for normality by Kolmogorov-Smirnov test and subsequent comparisons (lean v obese) performed using unpaired Student's t-tests or Mann-Whitney U test. For cell-based studies with changing steroid concentrations comparisons (20 β -DHF v cortisol) were performed using two-way ANOVA with Bonferroni post-hoc tests. Statistical significance was set at P < 0.05.

References

- Malátková, P., Maser, E. & Wsól, V. Human carbonyl reductases. *Curr. Drug Metab.* **11**, 639–658, doi:10.2174/138920010794233530 (2010).
- Oppermann, U. In *Annual Review of Pharmacology and Toxicology* Vol. 47 (ed A. K. Cho) 293–322 (2007).
- Olson, L. E. *et al.* Protection from Doxorubicin-Induced Cardiac Toxicity in Mice with a Null Allele of Carbonyl Reductase. *Cancer Research* **63**, 6602–6606 (2003).
- Tanaka, M. *et al.* An unbiased cell morphology-based screen for new, biologically active small molecules. *PLoS Biol.* **3**, 0764–0776, doi:10.1371/journal.pbio.0030128 (2005).
- Jo, A. *et al.* Inhibition of Carbonyl Reductase 1 Safely Improves the Efficacy of Doxorubicin in Breast Cancer Treatment. *Antioxidants and Redox Signaling* **26**, 70–83, doi:10.1089/ars.2015.6457 (2017).
- Covarrubias, V. G., Lakhman, S. S., Forrest, A., Relling, M. V. & Blanco, J. G. Higher activity of polymorphic NAD(P)H:quinone oxidoreductase in liver cytosols from blacks compared to whites. *Toxicol. Lett.* **164**, 249–258, doi:10.1016/j.toxlet.2006.01.004 (2006).
- Kalabus, J. L., Cheng, Q., Jamil, R. G., Schuetz, E. G. & Blanco, J. G. Induction of carbonyl reductase 1 (CBR1) expression in human lung tissues and lung cancer cells by the cigarette smoke constituent benzo[a]pyrene. *Toxicology Letters* **211**, 266–273, doi:10.1016/j.toxlet.2012.04.006 (2012).
- Carlquist, M., Frejd, T. & Gorwa-Grauslund, M. F. Flavonoids as inhibitors of human carbonyl reductase 1. *Chemico-Biological Interactions* **174**, 98–108, doi:10.1016/j.cbi.2008.05.021 (2008).
- Edwards, C. R. W. *et al.* Localisation of 11 β -hydroxysteroid dehydrogenase-tissue specific protector of the mineralocorticoid receptor. *The Lancet* **332**, 986–989, doi:10.1016/S0140-6736(88)90742-8 (1988).
- Seckl, J. R. & Walker, B. R. Minireview: 11 beta-hydroxysteroid dehydrogenase type 1 - A tissue-specific amplifier of glucocorticoid action. *Endocrinology* **142**, 1371–1376 (2001).
- Hughes, K. A., Webster, S. P. & Walker, B. R. 11-Beta-hydroxysteroid dehydrogenase type 1 (11 beta-HSD1) inhibitors in Type 2 diabetes mellitus and obesity. *Expert Opinion on Investigational Drugs* **17**, 481–496, doi:10.1517/13543784.17.4.481 (2008).
- McInnes, K. J. *et al.* 5 α -reduced glucocorticoids, novel endogenous activators of the glucocorticoid receptor. *Journal of Biological Chemistry* **279**, 22908–22912, doi:Export Date 9 July 2014 (2004).
- Upreti, R. *et al.* 5 α -Reductase Type I Modulates Insulin Sensitivity in Men. *Journal of Clinical Endocrinology and Metabolism* **99**, E1397–E1406, doi:10.1210/jc.2014-1395 (2014).
- Wake, D. J. & Walker, B. R. 11 beta-Hydroxysteroid dehydrogenase type 1 in obesity and the metabolic syndrome. *Molecular and Cellular Endocrinology* **215**, 45–54, doi:10.1016/j.mce.2003.11.015 (2004).
- Wyse, C. A., McNie, K. A., Tannahil, V. J., Murray, J. K. & Love, S. Prevalence of obesity in riding horses in Scotland. *Veterinary Record* **162**, 590–591 (2008).
- Popot, M. A. *et al.* New approaches to detect cortisol administration in the horse. *Equine Veterinary Journal* **31**, 278–284 (1999).
- Shackleton, C. H. L. Profiling steroid hormones and urinary steroids. *J. Chromatogr. B Biomed. Sci. Appl.* **379**, 91–156, doi:10.1016/S0378-4347(00)80683-0 (1986).
- Schoneshofer, M., Weber, B. & Nigam, S. Increased urinary excretion of free 20 α - and 20 β -dihydrocortisol in a hypercortisolemic but hypocortisolemic patient with Cushing's disease. *CLIN. CHEM.* **29**, 385–389 (1983).
- Kornel, L., Miyabo, S., Saito, Z., Cha, R. W. & Wu, F. T. Corticosteroids in human blood. VIII. Cortisol metabolites in plasma of normotensive subjects and patients with essential hypertension. *Journal of Clinical Endocrinology and Metabolism* **40**, 949–958 (1975).
- Andrew, R., Phillips, D. I. W. & Walker, B. R. Obesity and gender influence cortisol secretion and metabolism in man. *Journal of Clinical Endocrinology and Metabolism* **83**, 1806–1809 (1998).
- Wermuth, B. Purification and properties of an NADPH-dependent carbonyl reductase from human brain. Relationship to prostaglandin 9-ketoreductase and xenobiotic ketone reductase. *Journal of Biological Chemistry* **256**, 1206–1213 (1981).
- Franzén, O. *et al.* Cardiometabolic risk loci share downstream cis- and trans-gene regulation across tissues and diseases. *Science* **353**, 827–830, doi:10.1126/science.aad6970 (2016).
- Hemani, G. *et al.* MR-Base: a platform for systematic causal inference across the phenome using billions of genetic associations. *bioRxiv*. doi:10.1101/078972 (2016).
- Millstein, J., Zhang, B., Zhu, J. & Schadt, E. E. Disentangling molecular relationships with a causal inference test. *BMC Genet.* **10**, doi:10.1186/1471-2156-10-23 (2009).
- Desmet, S. J. *et al.* Cofactor profiling of the glucocorticoid receptor from a cellular environment. *Methods Mol. Biol.* **1204**, 83–94, doi:10.1007/978-1-4939-1346-6_8 (2014).
- Irvine, C. H. G. & Alexander, S. L. Factors affecting the circadian rhythm in plasma cortisol concentrations in the horse. *Domestic Animal Endocrinology* **11**, 227–238 (1994).
- Abel, S. M., Back, D. J., Maggs, J. L. & Park, B. K. Cortisol metabolism *in vitro* - II. Species difference. *Journal of Steroid Biochemistry and Molecular Biology* **45**, 445–453 (1993).
- Picard-Hagen, N. *et al.* Discriminant value of blood and urinary corticoids for the diagnosis of scrapie in live sheep. *Veterinary Record* **150**, 680–684 (2002).
- Schelcher, F. *et al.* Corticoid concentrations are increased in the plasma and urine of ewes with naturally occurring scrapie. *Endocrinology* **140**, 2422–2425 (1999).
- Abel, S. M., Maggs, J. L., Back, D. J. & Park, B. K. Cortisol metabolism by human liver *in vitro*. I. Metabolite identification and inter-individual variability. *Journal of Steroid Biochemistry and Molecular Biology* **43**, 713–719 (1992).
- Ichikawa, Y. Metabolism of cortisol-4-C14 in patients with infectious and collagen diseases. *Metabolism* **15**, 613–625 (1966).
- Kemény, V., Farkas, K. & Gömör, B. Production of unconjugated 20-DHF (11 beta, 17 alpha, 20 beta, 21-tetrahydroxy-pregn-4-en-3-one) in active rheumatoid arthritis. *Acta Med Acad Sci Hung* **27**, 381–387 (1970).
- Bradlow, H. L., Fukushima, D. K., Zumoff, B., Hellman, L. & Gallagher, T. F. Metabolism of Reichstein's substance E in man. *The Journal of clinical endocrinology and metabolism* **22**, 748–753 (1962).
- Bradlow, H. L., Zumoff, B., Fukushima, D. K., Hellman, L. & Gallagher, T. F. Biotransformations of the C-20-dihydro metabolites of cortisol in man. *Journal of Clinical Endocrinology and Metabolism* **34**, 997–1002, doi:10.1210/jcem-34-6-997 (1972).
- Jenkins, J. S. The metabolism of cortisol by human extra-hepatic tissues. *Journal of Endocrinology* **34**, 51–56 (1966).
- El Attar, T. M. A. *In vitro* metabolism studies of [1,2,6,7-³H]-cortisol in human gingiva in health and disease. *Steroids* **25**, 355–364, doi:10.1016/0039-128X(75)90092-6 (1975).
- Sweat, M. L. *et al.* The metabolism of cortisol and progesterone by cultured uterine fibroblasts, strain U12-705. *BBA - Biochimica et Biophysica Acta* **28**, 591–596 (1958).
- Arie, R., Hoogervorst-Spalter, H., Kaufmann, H., Joshua, H. & Klein, A. Metabolism of cortisol by human thrombocytes. *Metabolism* **28**, 67–69, doi:10.1016/0026-0495(79)90170-7 (1979).
- Wirth, H. & Wermuth, B. Immunohistochemical localization of carbonyl reductase in human tissues. *J. HISTOCHEM. CYTOCHEM.* **40**, 1857–1863 (1992).
- Forrest, G. L. & Gonzalez, B. Carbonyl reductase. *Chemico-Biological Interactions* **129**, 21–40, doi:10.1016/S0009-2797(00)00196-4 (2000).
- Rashid, M. A. *et al.* Carbonyl reductase 1 protects pancreatic β -cells against oxidative stress-induced apoptosis in glucotoxicity and lipotoxicity. *Free Radic. Biol. Med.* **49**, 1522–1533, doi:10.1016/j.freeradbiomed.2010.08.015 (2010).

42. Strain, G. W. *et al.* Sex difference in the influence of obesity on the 24 hr mean plasma concentration of cortisol. *Metabolism* **31**, 209–212, doi:10.1016/0026-0495(82)90054-3 (1982).
43. Ebert, B., Kisiela, M. & Maser, E. Transcriptional regulation of human and murine short-chain dehydrogenase/reductases (SDRs) – an in silico approach. *Drug Metab. Rev.* **48**, 183–217, doi:10.3109/03602532.2016.1167902 (2016).
44. Miura, T., Taketomi, A., Nishinaka, T. & Terada, T. Regulation of human carbonyl reductase 1 (CBR1, SDR21C1) gene by transcription factor Nrf2. *Chemico-Biological Interactions* **202**, 126–135, doi:10.1016/j.cbi.2012.11.023 (2013).
45. Guo, C., Wang, W., Liu, C., Myatt, L. & Sun, K. Induction of PGF2 α synthesis by cortisol through GR dependent induction of CBR1 in human amnion fibroblasts. *Endocrinology* **155**, 3017–3024, doi:10.1210/en.2013-1848 (2014).
46. Lakhman, S. S., Chen, X., Gonzalez-Covarrubias, V., Schuetz, E. G. & Blanco, J. G. Functional characterization of the promoter of human carbonyl reductase 1 (CBR1). Role of XRE elements in mediating the induction of CBR1 by ligands of the aryl hydrocarbon receptor. *Mol. Pharmacol.* **72**, 734–743, doi:10.1124/mol.107.035550 (2007).
47. Dowman, J. K. *et al.* Loss of 5 α -Reductase Type 1 accelerates the development of hepatic steatosis but protects against hepatocellular carcinoma in male mice. *Endocrinology* **154**, 4536–4547, doi:10.1210/en.2013-1592 (2013).
48. Quiñones-Lombraña, A. *et al.* Interindividual variability in the cardiac expression of anthracycline reductases in donors with and without Down syndrome. *Pharmaceutical Research* **31**, 1644–1655, doi:10.1007/s11095-013-1267-1 (2014).
49. Boušová, I., Skálová, L., Souček, P. & Matoušková, P. The modulation of carbonyl reductase 1 by polyphenols. *Drug Metab. Rev.* **47**, 520–533, doi:10.3109/03602532.2015.1089885 (2015).
50. Carroll, C. L. & Huntington, P. J. Body condition scoring and weight estimation of horses. *Equine Veterinary Journal* **20**, 41–45 (1988).
51. Didelez, V. & Sheehan, N. Mendelian randomization as an instrumental variable approach to causal inference. *Stat. Methods Med. Res.* **16**, 309–330, doi:10.1177/0962280206077743 (2007).
52. Jones, G., Willett, P., Glen, R. C., Leach, A. R. & Taylor, R. Development and validation of a genetic algorithm for flexible docking. *J. MOL. BIOL.* **267**, 727–748, doi:10.1006/jmbi.1996.0897 (1997).
53. Wolber, G. & Langer, T. LigandScout: 3-D pharmacophores derived from protein-bound ligands and their use as virtual screening filters. *J. Chem. Inf. Model.* **45**, 160–169, doi:10.1021/ci049885e (2005).
54. Beck, K. R., Sommer, T. J., Schuster, D. & Odermatt, A. Evaluation of tetrabromobisphenol A effects on human glucocorticoid and androgen receptors: A comparison of results from human- with yeast-based *in vitro* assays. *Toxicology* **370**, 70–77, doi:10.1016/j.tox.2016.09.014 (2016).
55. Voice, M. W., Seckl, J. R. & Chapman, K. E. The sequence of 5' flanking DNA from the mouse 11 β -hydroxysteroid dehydrogenase type 1 gene and analysis of putative transcription factor binding sites. *GENE* **181**, 233–235, doi:10.1016/S0378-1119(96)00490-8 (1996).
56. Atucha, E. *et al.* A mixed glucocorticoid/mineralocorticoid selective modulator with dominant antagonism in the male rat brain. *Endocrinology* **156**, 4105–4114, doi:10.1210/en.2015-1390 (2015).
57. Hayek, T. *et al.* Reduced progression of atherosclerosis in apolipoprotein E-deficient mice following consumption of red wine, or its polyphenols quercetin or catechin, is associated with reduced susceptibility of LDL to oxidation and aggregation. *Arteriosclerosis, Thrombosis, and Vascular Biology* **17**, 2744–2752 (1997).

Acknowledgements

We are grateful to S. Kothiya, L. Ramage and A. Rutter for analytical support, the staff of the Edinburgh Clinical Research Facility and its Mass Spectrometry Core Laboratory, K Chapman for the gift of the plasmids, Prof Thierry Langer, University of Vienna and Inte:Ligand GmbH for providing LigandScout software and Pro, Daniela Schuster, University of Innsbruck for support with docking, and the staff of the Royal (Dick) School of Veterinary Studies Equine Hospital for their help with sample collection. We would like to thank the owners whose horses were included in the study. The laboratory is supported by a British Heart Foundation Centre of Excellence Award. RM was supported by the Biological and Biotechnological Sciences Research Council and Zoetis Animal Health (Grant No R42126 and R82976) with additional funding from the University of Edinburgh Wellcome Trust Institutional Strategic Support Fund. AO was supported by the Swiss National Science Foundation (Grant No. 31001-159454). BW was supported by a British Heart Foundation Programme Grant and Wellcome Trust Investigator Award.

Author Contributions

R.M., K.B., M.N., A.C., D.M., R.H., A.S., A.A., R.U., P.H., T.M., C.K., J.K. and A.O. designed and/or conducted the experiments and/or analysed the data. N.H. and R.A. developed and supervised the mass spectrometry measurements. R.S., T.O., O.M., and R.A. contributed to the design and execution of the clinical studies. A.C., A.R., E.S. and J.B. contributed data for GWAS analysis. R.M. and B.W. conceived the studies and supervised the experimental design, execution, and analysis. R.M. and B.W. wrote the manuscript, which was reviewed by all authors.

Additional Information

Supplementary information accompanies this paper at doi:10.1038/s41598-017-10410-1

Competing Interests: The authors declare that they have no competing interests.

Publisher's note: Springer Nature remains neutral with regard to jurisdictional claims in published maps and institutional affiliations.



Open Access This article is licensed under a Creative Commons Attribution 4.0 International License, which permits use, sharing, adaptation, distribution and reproduction in any medium or format, as long as you give appropriate credit to the original author(s) and the source, provide a link to the Creative Commons license, and indicate if changes were made. The images or other third party material in this article are included in the article's Creative Commons license, unless indicated otherwise in a credit line to the material. If material is not included in the article's Creative Commons license and your intended use is not permitted by statutory regulation or exceeds the permitted use, you will need to obtain permission directly from the copyright holder. To view a copy of this license, visit <http://creativecommons.org/licenses/by/4.0/>.

© The Author(s) 2017

1 **Carbonyl reductase 1 catalyzes 20 β -reduction of glucocorticoids,**
2 **modulating receptor activation and metabolic complications of obesity**

3
4 ***Authors:*** Ruth A Morgan^{1,2}, Katharina R Beck³, Mark Nixon¹, Natalie ZM Homer⁴, Andrew
5 A Crawford^{1,5}, Diana Melchers⁶, René Houtman⁶, Onno C Meijer⁷, Andreas Stomby⁸, Anna J
6 Anderson¹, Rita Upreti¹, Roland H Stimson¹, Tommy Olsson⁸, Tom Michael⁹, Ariella
7 Cohain¹⁰, Arno Ruusalepp^{11,12,13}, Eric E. Schadt¹⁰, Johan L. M. Björkegren^{10,11,12,13,14}, Ruth
8 Andrew^{1,4}, Christopher J Kenyon¹, Patrick WF Hadoke¹, Alex Odermatt³, John A Keen², and
9 Brian R Walker^{1,4,*}

10
11 ***Affiliations:***

12 ¹ University/BHF Centre for Cardiovascular Science, The Queen's Medical Research
13 Institute, University of Edinburgh, UK

14 ² Royal (Dick) School of Veterinary Studies, University of Edinburgh, UK

15 ³ Division of Molecular and Systems Toxicology, Department of Pharmaceutical Sciences,
16 University of Basel, Switzerland

17 ⁴ Mass Spectrometry Core Laboratory, Wellcome Trust Clinical Research Facility, The
18 Queen's Medical Research Institute, University of Edinburgh, UK

19 ⁵ School of Social and Community Medicine, University of Bristol, UK

20 ⁶ PamGene International, Den Bosch, The Netherlands

21 ⁷ Department of Internal Medicine, Division Endocrinology, Leiden University Medical
22 Center, Leiden, The Netherlands

23 ⁸ Department of Public Health and Clinical Medicine, Umeå University 901 87 Umeå,
24 Sweden

25 ⁹ The Roslin Institute, University of Edinburgh, Easter Bush Campus, UK

26 ¹⁰Department of Genetics and Genomic Sciences, Icahn Institute for Genomics and Multiscale
27 Biology, Icahn School of Medicine at Mount Sinai, New York, USA

28 ¹¹Department of Physiology, Institute of Biomedicine and Translation Medicine, University of
29 Tartu, Estonia

30 ¹²Clinical Gene Networks AB, Stockholm, Sweden

31 ¹³Department of Cardiac Surgery, Tartu University Hospital, Tartu, Estonia

32 ¹⁴Integrated Cardio Metabolic Centre, Department of Medicine, Karolinska Institute, Sweden

33

34 ***Author to whom correspondence should be addressed:**

35 Professor Brian Walker, Email: b.walker@ed.ac.uk, University/BHF Centre for

36 Cardiovascular Science, The Queen's Medical Research Institute, University of Edinburgh,

37 47 Little France Crescent, Edinburgh EH16 4TJ

38

39 **Supplementary Materials:**

40 **SM1 Quantification of urinary glucocorticoid metabolites**

41 Glucocorticoids were extracted from equine urine (20mL) by solid phase extraction on Bond
42 Elut Nexus mixed mode Large Reservoir Capacity, 60 mg columns (Agilent Technologies,
43 Santa Clara, CA, USA). Glucocorticoids were extracted from human urine (10mL) by solid
44 phase extraction on Sep-Pak columns (Waters, Milford, MA, USA).

45 Steroid conjugates were hydrolysed using β -glucuronidase followed by re-extraction. The
46 steroids obtained were derivatized to form methoxime-trimethylsilyl (MO-TMS) derivatives.
47 Steroidal derivatives were separated by gas chromatography using the TRACE GC Ultra Gas
48 Chromatograph (Thermo Fisher Scientific). Analysis was performed on a TSQ Quantum Triple
49 Quadrupole GC-tandem mass spectrometer (Thermo Fisher Scientific) using a 35HT
50 Phenomenex column (30m, 0.25mm, 0.25 μ m, Agilent Technologies) as previously described
51 (45, 46). Epi-cortisol and epi-tetrahydrocortisol were used as internal standards (Steraloids,
52 Newport, RI, USA). The steroids analyzed were cortisol (F), cortisone (E), 5 β -
53 tetrahydrocortisol (5 β -THF), 5 β -tetrahydrocortisone (5 β -THE), 5 α -tetrahydrocortisol (5 α -
54 THF) (45, 46) with the inclusion of the following transitions (collision energy) α -cortol
55 (535 \rightarrow 355, 20V) and β -cortol (535 \rightarrow 455, 10V), α - and β -cortolone (449 \rightarrow 269, 10V), 6 β -
56 hydroxycortisol (693 \rightarrow 513, 10V), 20 α - dihydrocortisol (578 \rightarrow 488, 10V) and 20 β -
57 dihydrocortisol (681 \rightarrow 578, 10V).

58

59 Steroid quantities in equine urine were expressed as a ratio to creatinine, which was measured
60 using a colorimetric method based on the modified Jaffe's reaction (IL650 analyser,
61 Instrumentation Laboratories, Barcelona, Spain).

62 **SM2 Quantification of glucocorticoids in plasma**

63 Plasma samples (1 mL Equine, 200 μ L Human) enriched with internal standard (D4-F, D4-E
64 and D8-B; 250 ng of each) were extracted by liquid-liquid extraction. Chloroform (10 volumes)
65 was added to each sample, mixed and the organic layer was dried under nitrogen (60 $^{\circ}$ C). The
66 extracts were re-suspended in mobile phase (60 μ L, water: methanol 70:30 v/v) for
67 quantification of steroids by LC-MS/MS. The injection volume was 30 μ L.

68 **SM3 Quantification of glucocorticoids in adipose tissue**

69 Adipose samples (100mg) were homogenized in ethyl acetate (1 mL) and enriched with internal
70 standard (D4-F, D8-E, D8-B; 250ng of each). The homogenate was slowly dripped onto chilled
71 ethanol: glacial acetic acid: water (95:3:2 v/v, 10 mL) and frozen at -80 $^{\circ}$ C overnight. Samples
72 were thawed (4 $^{\circ}$ C) prior to sonication (8 x 15 second bursts) and centrifugation (3000 x g, 30
73 mins, 4 $^{\circ}$ C). The supernatant was dried under nitrogen (60 $^{\circ}$ C), re-suspended in methanol (10
74 mL) and frozen at -80 $^{\circ}$ C overnight. Samples were thawed (RT) and hexane (10 mL) added
75 and mixed. The hexane layer was removed, the remaining methanol dried down under nitrogen
76 (60 $^{\circ}$ C) and re-suspended in water (400 μ L) and ethyl acetate (4 mL). The organic layer was
77 removed, dried under nitrogen (60 $^{\circ}$ C) and re-suspended in 30 % methanol (5 mL). C18 Bond
78 Elut columns (Agilent Technologies, Santa Clara, CA, USA) were conditioned (methanol 5
79 mL) and equilibrated (water 5 mL), samples were loaded and steroids eluted with methanol (2
80 mL). Eluates were dried down under nitrogen (60 $^{\circ}$ C) and re-suspended in 60 μ L mobile phase
81 (water: methanol, 70:30 v/v) for quantification of steroids by LC-MS/MS. Injection volume
82 was 30 μ L.

83 **SM4 Quantification of mRNA by RT-qPCR**

84 Total RNA was extracted from adipose and liver using the RNAeasy Mini Kit (Qiagen Inc,
85 Valencia, CA, USA). The tissue was mechanically disrupted in either QIAzol (Qiagen) for

86 adipose tissue or RLT buffer (Qiagen) for liver tissue. Total RNA was extracted from cells in
87 QIAzol lysis reagent using an RNeasy Mini Kit according to the manufacturer's instructions.
88 Quantitative real-time polymerase chain reaction was performed using a Light-cycler 480
89 (Roche Applied Science, Indianapolis, IN, USA). Primers were designed using sequences from
90 the National Centre of Biotechnological Information and the Roche Universal Probe Library
91 (see Table S7-9) for details of primers for genes of interest and housekeeping genes). Samples
92 were analysed in triplicate and amplification curves plotted (y axis fluorescence, x axis cycle
93 number). Triplicates were deemed acceptable if the standard deviation of the crossing point
94 was < 0.5 cycles. A standard curve (y axis crossing point, x axis log concentration) for each
95 gene was generated by serial dilution of cDNA pooled from different samples and fitted with
96 a straight line and deemed acceptable if reaction efficiency was between 1.7 and 2.1.

Supplementary Tables and Figures

Table S 1 Characteristics of equine study subjects

	Lean (n=14)	Obese (n=14)
Age (years)	15.6 ± 5.6	13.8 ± 7.8
Sex	4 Females 10 Castrated males	8 Female 5 Castrated males
Breeds	11 Thoroughbred 2 Native pony 1 Percheron	2 Thoroughbred 3 Cob 7 Native ponies 1 Arab pony 1 Clydesdale
Body condition score (5)	2.3 ± 0.3	3.8 ± 0.7*

Data are expressed as mean ± SEM. Student's t-test or Mann-Whitney U test: *p<0.05

Table S 2 Characteristics of obese human participants with type 2 diabetes providing 24 hour urine samples

n	19
Age (years)	58.9 ± 1.5
Body Mass Index (kg/m²)	32.60 ± 1.2
Concurrent medications	4 no medication 15 metformin

All participants were male and diagnosed with diabetes. Participants provided 24 hour urine samples. The additional lean and obese participants providing urine were recruited as part of a different study (Upreti et al 2014). Data are expressed as mean ± SEM.

Table S 3 Characteristics of lean and obese study participants providing plasma samples

	Lean (n=10)	Obese (n=10)
Age (years)	50.5 ± 10.4	50.0 ± 11.8
Body Mass Index (kg/m²)	23.8 ± 1.2	32.9 ± 2.7
Concurrent medications	<ul style="list-style-type: none"> • 6 No medication • 1 perindopril, nifedipine, • 1 citalopram, simvastatin, clopidogrel, ranitidine • 1 clomipramine • 1 ranitidine 	<ul style="list-style-type: none"> • 8 No medication • 1 tamsulosin, lansoprazole • 1 pantoprazole

Plasma was collected (between 8 and 9am) from lean and obese but otherwise healthy men. Participants with diabetes or prior corticosteroid treatment were excluded prior to recruitment. Data are expressed as mean ± SEM.

Table S 4 Characteristics of lean and obese men providing adipose biopsy samples during surgery.

	Lean (n=8)	Obese (n=8)
Age (years)	55.7 ± 12.7	52.8 ± 13.7
Body Mass Index (kg/m²)	23.0 ± 1.7	38.8 ± 6.7
Surgery	<ul style="list-style-type: none"> • Cholecystectomy • Laparoscopic cholecystectomy • Removal of gastric band • Hernia repair • Open cholecystectomy • 3 Abdominal hernia repairs 	<ul style="list-style-type: none"> • Gastric bypass • Laparoscopic sleeve gastrectomy • Laparoscopic cholecystectomy • Cholecystectomy • 2 Laparoscopic funduplications • Laparoscopic cholecystectomy • Laparoscopic removal of gastric band and gastric bypass

All the participants were male. Samples were obtained at the time of surgery. Data are expressed as mean ± SEM.

Table S 5 Estimates of the phenotypic associations with CBR1 expression in the liver based on Mendelian Randomisation

Outcome	Beta	Se	P value	N	Sample
BMI	-0.01	0.01	0.25	339224	(55)
Body Fat	-0.01	0.01	0.06	100716	(56)
2hr glucose adjusted for BMI	<0.01	0.03	0.89	15234	(57)
Fasting glucose	0.01	<0.01	0.02	58074	(58)
Fasting insulin	<0.01	<0.01	0.45	51750	(58)
HOMA-B	<0.01	<0.01	0.59	46186	(59)
HOMA-IR	0.01	0.01	0.27	46186	(59)
HbA1c	0.01	<0.01	0.01	46368	(60)

These analyses used rs1005696 as the instrument for CBR1 expression in liver and associations were analysed using MR-base. See supplementary references for further details of studies used.

Table S 6 Human primer sequences for PCR

Gene Symbol, full name	Forward Primer (3'→ 5')	Reverse Primer (5'→ 3')
<i>RNA18s</i> (ribosomal RNA 18s)	CTTCCACAGGAGGCCTACA C	CGCAAAATATGCTGGAAC TT
<i>DUSP1</i> (dual specificity phosphatase 1)	TTCAAGAGGCCATTGACTT	CCTGGCAGTGGACAAACA C
<i>GILZ</i> (glucocorticoid- induced leucine zipper)	CCGTTAAGCTGGACAACAG TG	ATGGCCTGTTTCGATCTTGT T
<i>FKBP51</i> (FK506-binding protein 51)	GGATATACGCCAACATGTT CAA	CCATTGCTTTATTGGCCTCT
<i>IGFBP1</i> (insulin-like growth factor binding protein 1)	GCCTTGGCTAAACTCTCTA CGA	CCATGTCACCAACATCAAA AA
<i>IL-1β</i> (Interleukin 1β)	TGTAATGAAAGACGGCACA CC	TCTTCTTTGGGTATTGCTTG G
<i>CBR1</i> (Carbonyl Reductase 1)	TCCCTCTAATAAAACCCCA AGG	GGTCTCACTGCGGAACTTC T

Table S 7 Equine primer sequences for PCR

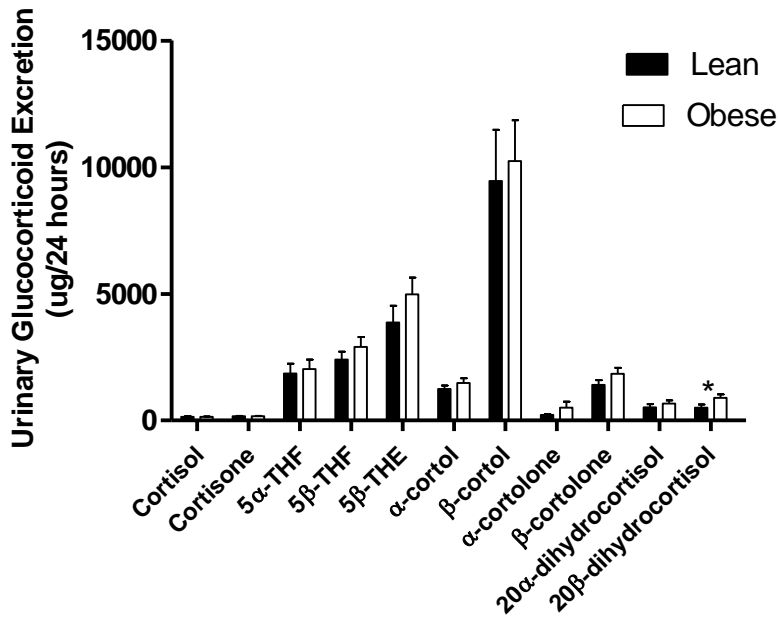
Gene Symbol, full name	Forward Primer (3'→ 5')	Reverse Primer (5'→ 3')
<i>RNA18s</i> (ribosomal RNA 18s)	TGACCCAAGGCTAGTAGCT GA	TTCAACACATCACCCACCA T
<i>SDHA</i> (Succinate)	CTACGGAGACCTTAAGCAT CTGA	GGGTCTCCACCAGGTCAGT A

dehydrogenase complex)		
<i>Equine CBRI</i> (Carbonyl Reductase 1)	ACCCAGCCATGTCTTACAC C	CAGGATAGTGAAGCCGAT GC

Table S 8 Murine primer sequences for PCR

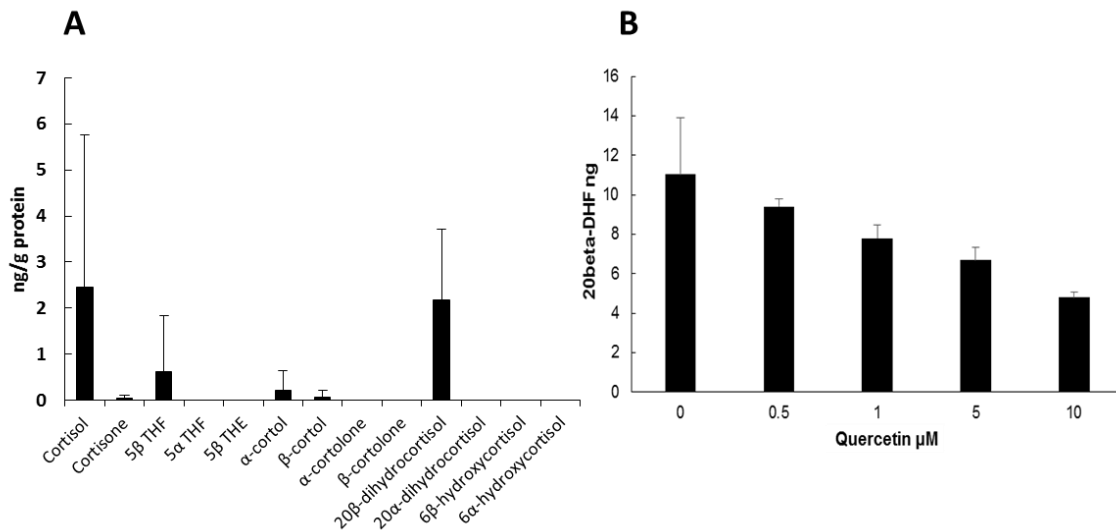
Gene Symbol, full name	Forward Primer (3'→ 5')	Reverse Primer (5'→ 3')
<i>RNA18s</i> (<i>ribosomal RNA 18s</i>)	CTCAACACGGGAAACCT CAC	CGCTCCACCAACTAAGA ACG
<i>Tbp</i> (<i>TATA-binding protein</i>)	GGGAGAATCATGGACCA GAA	GATGGGAATTCCAGGAG TCA
<i>Per1</i> (<i>Period 1</i>)	GCTTCGTGGACTTGACAC CT	TGCTTTAGATCGGCAGT GGT
<i>Pepck</i> (phosphoenolpyruvate carboxykinase)	GAGGCACAGGTCCTTTTC AG	GTTCTGGGCCTTTGTG AC
<i>Adipq</i> (<i>Adiponectin</i>)	GGTGAGAAGGGTGAGAA AGGA	TTTCACCGATGTCTCCCT TAG
<i>Lpl</i> (<i>Lipoprotein lipase</i>)	CTCGCTCTCAGATGCCCT AC	GGTTGTGTTGCTTGCCAT T
<i>Sgk1</i> (<i>serum glucocorticoid kinase 1</i>)	TTTCCAAAGGGGGATGC T	TGTTGGCATGATTACAT TGTTCT
<i>ENaC1</i> (<i>Epithelial sodium channel 1</i>)	AGCACAGAGAACACCCC TGT	TGGCTCTTCCTACCCTCT CTC
<i>Cbr1</i> (Carbonyl Reductase 1)	AGGTGACAATGAAAACG AACTTT	GGACACATTCACCACTC TGC

Figure S 1 The human urinary glucocorticoid metabolite profile in lean and obese individuals



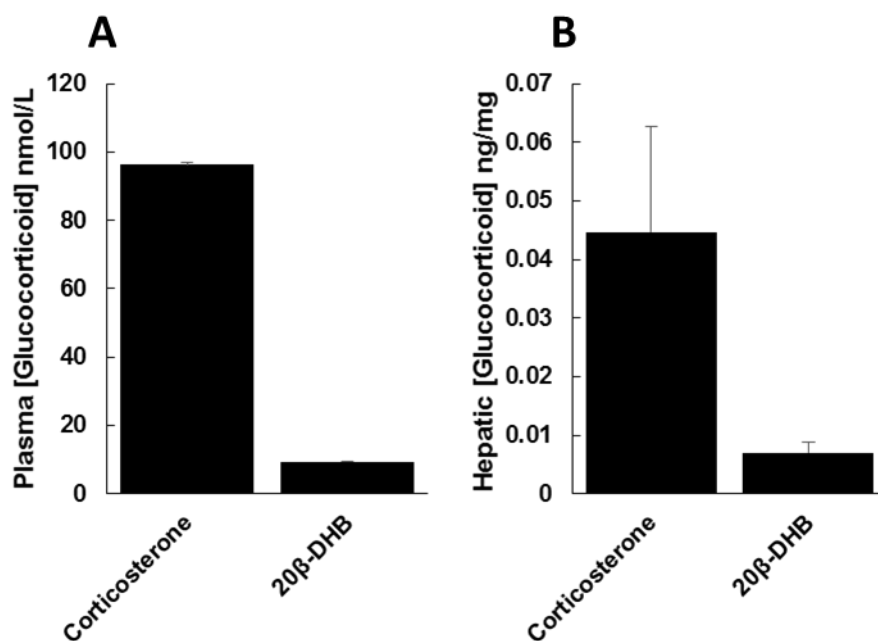
Urinary glucocorticoids of lean and obese participants were extracted, derivitized and quantified by GC-MS/MS. Urinary excretion of 20β-dihydrocortisol was higher in the obese group.

Figure S 2 Equine liver cytosol metabolises cortisol to 20β-dihydrocortisol and this production is inhibited by quercetin



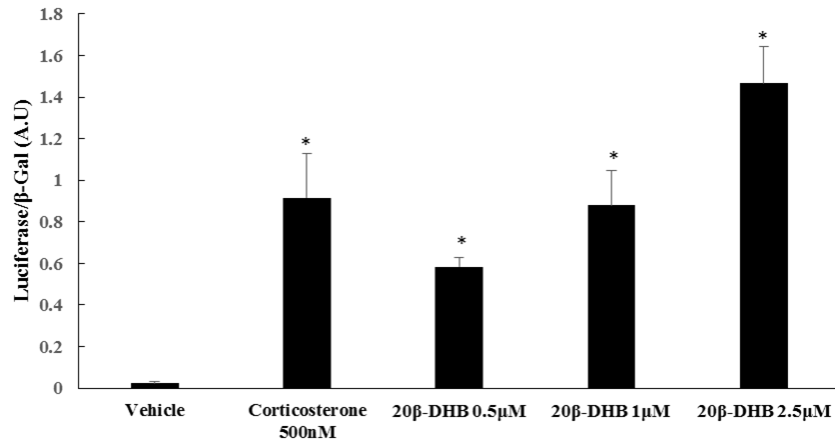
[A] In the presence of NADPH equine liver cytosol produced 20 β -DHF as the predominant metabolite. (THF = tetrahydrocortisol, THE = tetrahydrocortisone). [B] CBR1 inhibitor quercetin prevented production of 20 β -DHF by equine liver cytosol. Data are mean \pm SEM.

Figure S 3 20 β -Dihydrocorticosterone is present in murine tissues



20 β -Dihydrocortisone (the murine equivalent of 20 β -dihydrocortisol) was measured by LC-MS/MS in murine [A] plasma and [B] liver. Data are mean \pm SEM.

Figure S 4 20 β -Dihydrocorticosterone induces murine glucocorticoid receptor activation



HEK293 cells transfected with murine GR-MMTV-Luc were incubated with increasing concentrations of 20 β -dihydrocorticosterone (20 β -DHB) the murine equivalent of 20 β -dihydrocortisol. Data are mean \pm SEM, *P<0.05 compared to vehicle.

Supplementary References

- Locke AE, Kahali B, Berndt SI, Justice AE, Pers TH, Day FR, Powell C, Vedantam S, Buchkovich ML, Yang J, et al. Genetic studies of body mass index yield new insights for obesity biology. *Nature*. 2015;518(7538):197-206.
- Lu Y, Day FR, Gustafsson S, Buchkovich ML, Na J, Bataille V, Cousminer DL, Dastani Z, Drong AW, Esko T, et al. New loci for body fat percentage reveal link between adiposity and cardiometabolic disease risk. *Nat Commun*. 2016;7(
- Saxena R, Hivert MF, Langenberg C, Tanaka T, Pankow JS, Vollenweider P, Lyssenko V, Bouatia-Naji N, Dupuis J, Jackson AU, et al. Genetic variation in GIPR influences the glucose and insulin responses to an oral glucose challenge. *Nat Genet*. 2010;42(2):142-8.
- Manning AK, Hivert MF, Scott RA, Grimsby JL, Bouatia-Naji N, Chen H, Rybin D, Liu CT, Bielak LF, Prokopenko I, et al. A genome-wide approach accounting for body mass index identifies genetic variants influencing fasting glycemic traits and insulin resistance. *Nat Genet*. 2012;44(6):659-69.
- Dupuis J, Langenberg C, Prokopenko I, Saxena R, Soranzo N, Jackson AU, Wheeler E, Glazer NL, Bouatia-Naji N, Gloyn AL, et al. New genetic loci implicated in fasting glucose homeostasis and their impact on type 2 diabetes risk. *Nat Genet*. 2010;42(2):105-16.
- Soranzo N, Sanna S, Wheeler E, Gieger C, Radke D, Dupuis J, Bouatia-Naji N, Langenberg C, Prokopenko I, Stolerman E, et al. Common variants at 10 genomic loci influence hemoglobin A1C levels via glycemic and nonglycemic pathways. *Diabetes*. 2010;59(12):3229-39.

4.4. Discussion

In silico approaches represent valuable tools for the identification of drug-like compounds to a cognate protein. The present thesis extended this concept to toxicologically relevant compounds and further to aid the prediction of potentially novel substrates for already characterized enzymes; however with the ultimate goal to support enzyme deorphanization. Three different members of the SDR superfamily were investigated for novel substrate specificities during this thesis: the two multi-functional enzymes 11 β -HSD1 and CBR1 as well as the orphan enzyme DHRS7.

The dihydroxylated oxysterols 7 β ,25OHC and 7 β ,27OHC were found to be generated by 11 β -HSD1 from their corresponding 7-keto oxidized forms. Their close structural relationship to the known 11 β -HSD1 substrate 7kC, led to the analysis of 7k25OHC and 7k27OHC. The subsequently performed VS of the HMDB with the 11 β -HSD1 substrate pharmacophore models, implemented to further explore 11 β -HSD1 function, did not retrieve these oxysterols as hits. However, this could be especially attributed to the fact that neither the 7keto- nor the 7 β -dihydroxylated forms were contained in the screening library. This represents a major limitation of the VS assessment. Obviously, only compounds present in the chemical database can be potentially filtered during the screening process. Thus, one needs to be aware that these databases used for VS are not fully representative. Moreover, particularly enzyme-substrate recognition purposes are influenced by this factor, since many databases contain small-drug like compounds. In this regard, the HMDB is a highly useful database even though many metabolites that are difficult to detect or that exist at very low concentrations are not contained in the library.

On the other hand, pharmacophore-based VS only retrieves molecules that exactly match the individual features of the model; an advantage during the drug development process, but not necessarily for the identification of endogenous substrates of a certain enzyme, as for example a ligand-induced fit cannot be simulated with this method. Therefore, the 11 β -HSD1 substrates models, generated in this thesis, allowed some degree of freedom for instance with the use of optional features or by employing considerably different pharmacophore models to cover all the structurally distinct training compounds.

Additionally, it becomes evident that also the predictive power of a model is determined by the underlying data. In this regard, the limitations of the DHRS7 homology models have already been addressed in the corresponding part in this thesis. The quality of a homology model varies depending on the sequence alignment with the template used for model construction. A sequence identity of >40% is regarded as ideal and <25% as a poor basis [145]. The template results for the DHRS7 homology model construction, however, showed for all templates a sequence identity of \leq 32%. The generally found low sequence identity among SDRs certainly represents another key challenge in the

deorphanization process of SDR members. To improve the poorly resolved regions at the binding site entry, detected in the DHRS7 homology models, a potential solution might be the identification of homologous protein sequences particularly for this region, which could then be used to complete the model. Although the physiological value of the recently detected DHRS7 substrates remains unclear, they can be used in further studies for the generation of a ligand-based pharmacophore model. Importantly, the compounds with no observed catalytic activity are as well highly useful as inactive training compounds to improve the model quality. Nevertheless, to receive a more complete recovery of active hits, a combination of different computational programs may be suitable, since they can generate distinct virtual hit lists, even when the same protein structure and the same screening library was used [146-148].

Importantly, to verify the results obtained from the *in silico* screenings, appropriate *in vitro* assays are essential. As already described, SDRs do not have a common activity element that could be used as suitable assay read-out, to assess potential substrates. Individual solutions for each enzyme need to be established. Therefore, large *in vitro* HTS applications for SDR deorphanization are practically not feasible, but pharmacophore-based VS approaches represent promising alternatives to enable a preselection of potential novel substrate candidates based on structural features of the substrate binding pocket and/or on already known ligands, which then can be tested *in vitro* with, for instance, LC-MS based bioassays.

Catalytic *in vitro* activity does not automatically imply an *in vivo* function. Especially for orphan enzymes, when their physiological role is completely unexplored, the prediction and the assessment of potential substrates is highly challenging. An interesting approach addressing this issue, includes expanded metabolite docking to entire pathways (reviewed in [145]). Docking or filtering of a metabolite against multiple models for proteins participating or hypothesized to participate in a given pathway may enhance the predictive *in silico* reliability. With this in mind, the assessment of a potential involvement of 11 β -HSD1 in the kynurenine pathway becomes particularly interesting, because several consecutively generated metabolites were filtered through the VS.

Instead of directly studying an orphan enzyme, one could also assess metabolites of 'orphan enzymatic reactions', for instance by docking or fitting them into the substrate binding site of proteins with unknown and/or known functions. 20 β -DHF was discovered in the accepted research article 'Carbonyl reductase 1 catalyses 20 β -reduction of glucocorticoids, modulating corticosteroid receptor activation and metabolic complications of obesity' as the predominant metabolite of cortisol in domestic horses, which is increased in obesity. However, the responsible enzyme for its generation was previously unexplored. Docking calculations confirmed cortisol in a single position fitting into the binding pocket of CBR1 (unpublished data, see Appendix Figure A4) and additionally revealed similar binding poses in

the binding pocket of GR for 20 β -DHF and cortisol. 20 β -DHF was further demonstrated as weak endogenous agonist of the GR, suggesting a novel pathway to modulate GR activation by CBR1-dependent protection against excessive GR activation in obesity. Nevertheless, further research is required to explore the contribution of CBR1 dysregulation in obesity and the consequence of the wide interindividual variability of CBR1 expression. Unfortunately, to date no specific CBR1 inhibitors are available [144]. In order to study enzyme functions and to avoid biased results due to unspecific inhibitor activity, specific enzyme inhibitors represent valuable and important tools, also with regard to the deorphanization of enzymes. Although knockdown by siRNA can solve part of the specificity problem, this technique has the disadvantage of the long time needed until a given enzyme is silenced, and therefore cannot replace the use of specific inhibitors but rather should be used in combination.

An example of remarkably high sequence identity (72%) among SDR members can be found for CBR1 and CBR3 [149]. However, a comparison of the substrate profiles of CBR1 and CBR3 showed a much narrower substrate spectrum for CBR3 and most of the known CBR1 substrates were either inactive or had lower catalytic activity compared to CBR1 [150]. Moreover, to date no validated endogenous substrate for CBR3 is known. Although CBR1 and CBR3 share a considerable sequence similarity, the resolution of the CBR3 crystal structure showed differences in their active sites considering size, shape, critical residues for substrate recognition and surface properties (Appendix Figure A5 and described in more detail in our published review [9]). Hence, the orphan CBR3 shows most probably a distinct substrate spectrum from that of CBR1 and represents an interesting target to be further explored by the proposed *in silico* approach, particularly since the protein structure has already been solved. In this regard, solely sequence similarities do not guarantee a simplified identification of (endogenous) substrates for orphan enzymes, an important point to take into account during substrate identification. In contrast, Koch et al. proposed structural organization of the binding sites rather than sequence similarity as criterion whether a certain substance may affect the activity of enzymes [151]. To identify drug-like proteins, they proposed structure similarity clustering of the ligand-sensing cores of protein domains in combination with a compound library development guided by natural products. This may as well represent a strategy that could be employed for the identification of substrates for orphan enzymes; however, a reliable resolution of the binding sites of all enzymes would be crucial for this approach. Nevertheless, by screening of known substrates from structurally related enzymes and scaffold hopping to related derivatives, novel substrate specificities might be identified.

To sum up, successful applications of pharmacophore-based *in silico* tools for the identification of inhibitors for a broad spectrum of SDR members led us to the implementation of these tools for substrate identification purposes in the domain of multifunctional SDRs, and particularly with the intent to extend this approach as deorphanization strategy for unexplored SDR members. First

attempts revealed promising results, however, careful consideration of the individual limitations is crucial.

5. Appendix

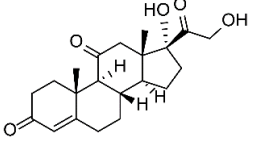
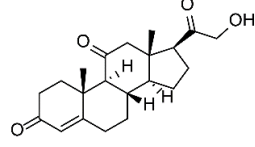
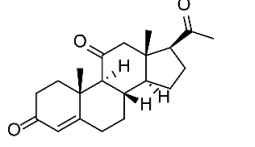
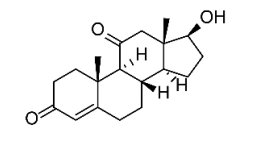
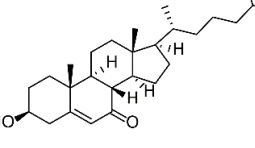
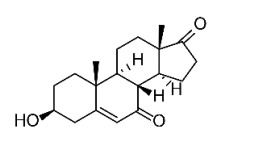
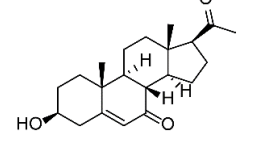
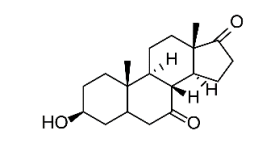
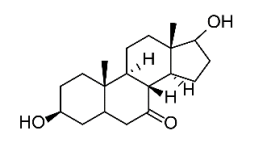
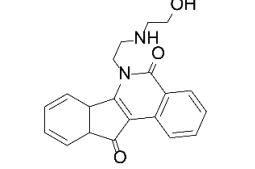
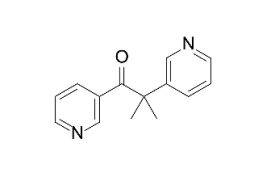
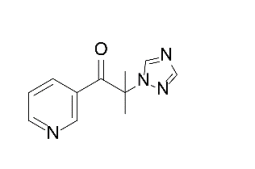
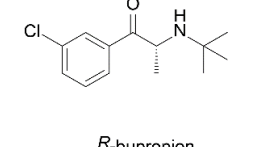
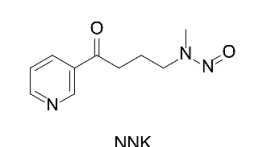
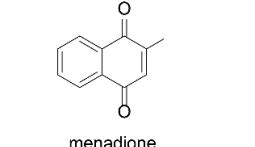
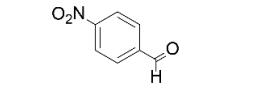
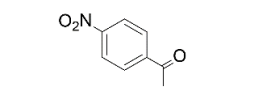
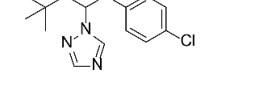
 cortisol	 11-dehydrocorticosterone	 11-ketoprogesterone
 11-ketotestosterone	 7-ketocholesterol	 7-keto-DHEA
 7-keto-pregnenolone	 5 α -androstane-3 β -ol-7,17-dione	 5 α -androstane-3 β ,17 β -diol-7-one
 oracin	 metyrapone	 metyrapone analogue
 <i>R</i> -bupropion	 NNK	 menadione
 p-nitrobenzaldehyde	 p-nitroacetophenone	 triadimefon

Figure A1. 2D-structures of the active test set compounds [93, 116].

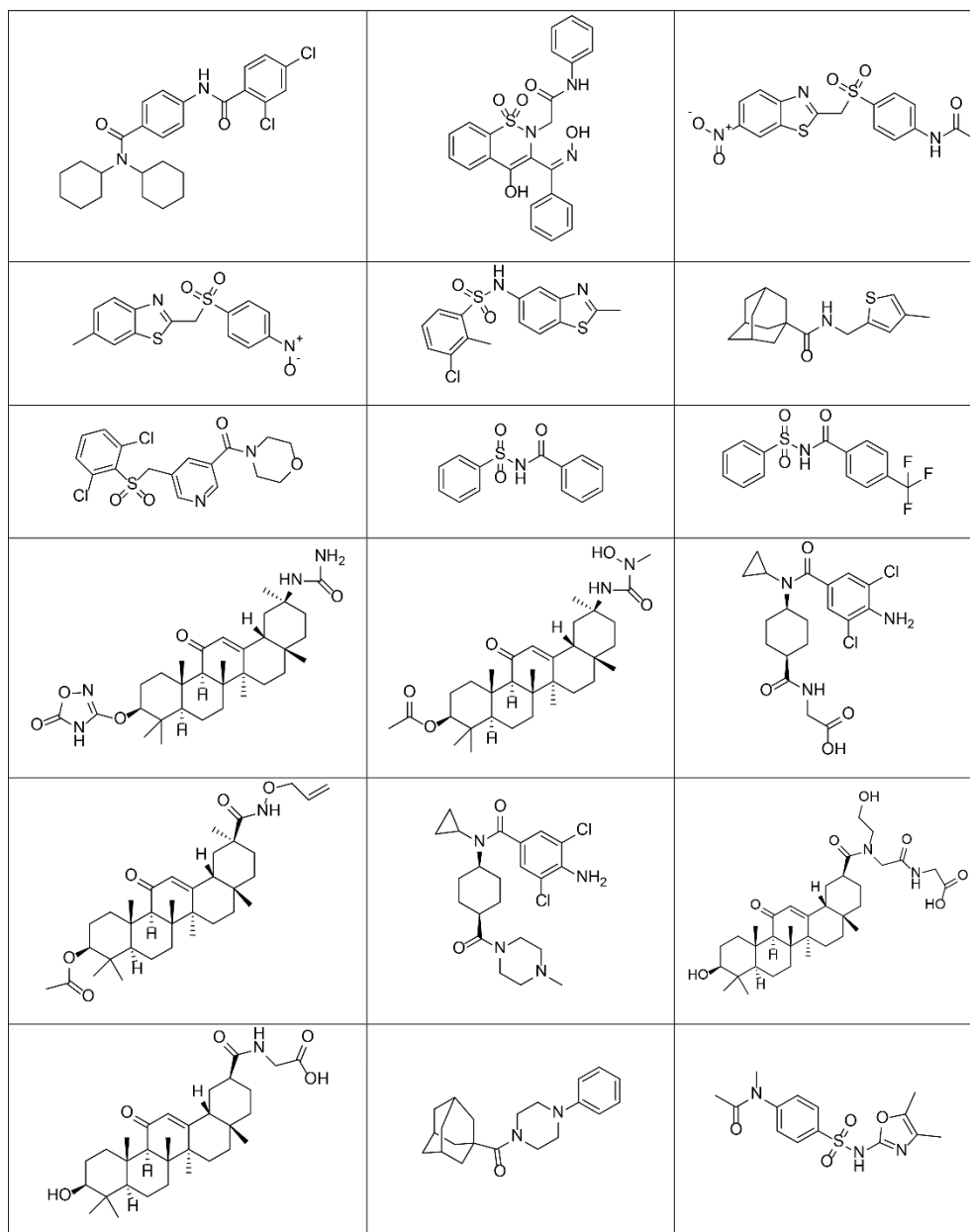


Figure A2. 2D-structures of the inactive test set compounds [100].

Table A1. Calculation of descriptive model parameters. The model performance was analyzed by counting the number of fitting active test compounds (true positives), fitting inactive test compounds (false positives), discarded actives (false negatives) and discarded inactives (true negatives). These numbers were further used to calculate the following parameters: yield of actives (YA) (Equation 1), enrichment factor (EF) (Equation 2), sensitivity (Equation 3) and specificity (Equation 4).

Model	YA (1)	EF (2)	Sensitivity (3)	Specificity (4)
model_1	1.0	2.11	0.22	1.0
model_2	1.0	2.11	0.39	1.0
model_3	1.0	2.11	0.50	1.0
model_4	1.0	2.11	0.22	1.0

$$(1) YA = \frac{\text{true positives}}{\text{number of hits}}$$

$$(2) EF = \frac{YA}{(\text{true positives in the database})/(\text{database size})}$$

$$(3) \text{sensitivity} = \frac{\text{true positives}}{\text{true positives in the database}}$$

$$(4) \text{specificity} = \frac{\text{true negatives}}{\text{true negatives in the database}}$$

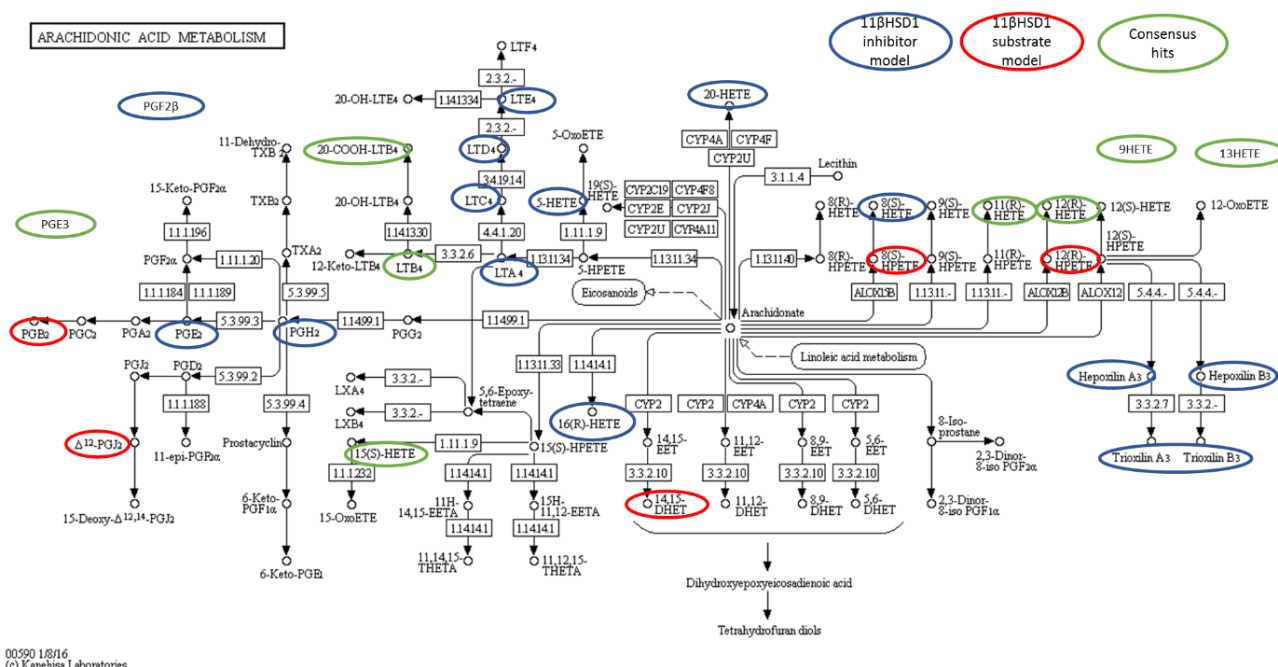


Figure A3. Arachidonic acid metabolism with virtual hits retrieved from the VS with the 11β-HSD1 substrate models (circled in red), the 11β-HSD1 inhibitor models (blue) and consensus hits (green). (Adapted from the Kyoto Encyclopedia of Genes and Genomes (KEGG) database [117-119, 152].)

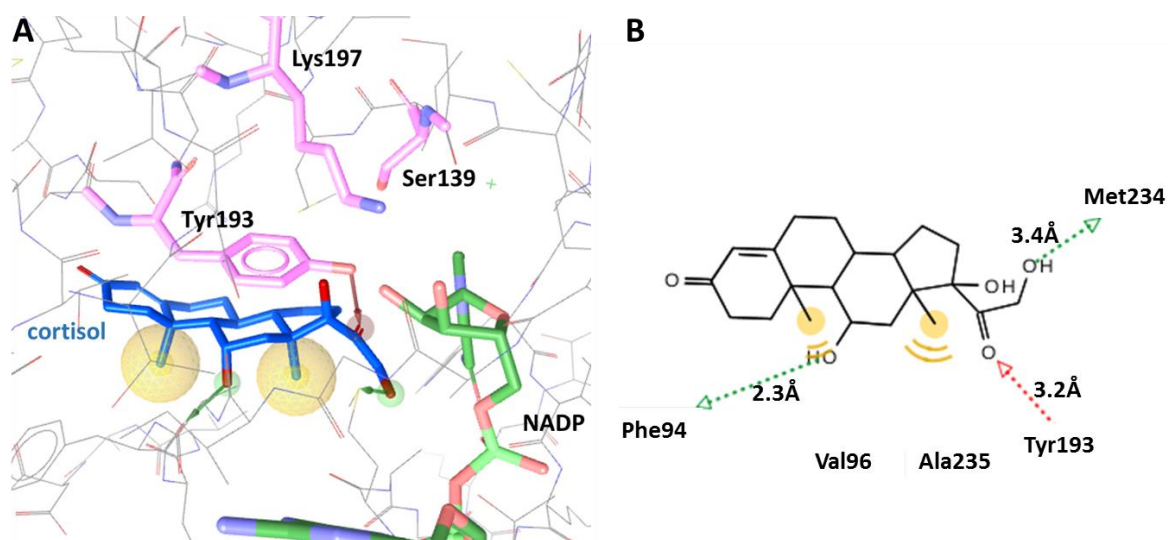


Figure A4. Docking of cortisol into the binding pocket of CBR1 (PDB code 2PFG). (A) The automatically generated pharmacophore maps important structural details of the ligand for binding (yellow spheres illustrate hydrophobic interactions, red/green arrows are hydrogen bond interactions; amino acid residues of the catalytic center and the cofactor are depicted as sticks). (B) Two-dimensional representation of the binding interactions of cortisol. Distance of hydrogen bonds are shown in angstrom (\AA).

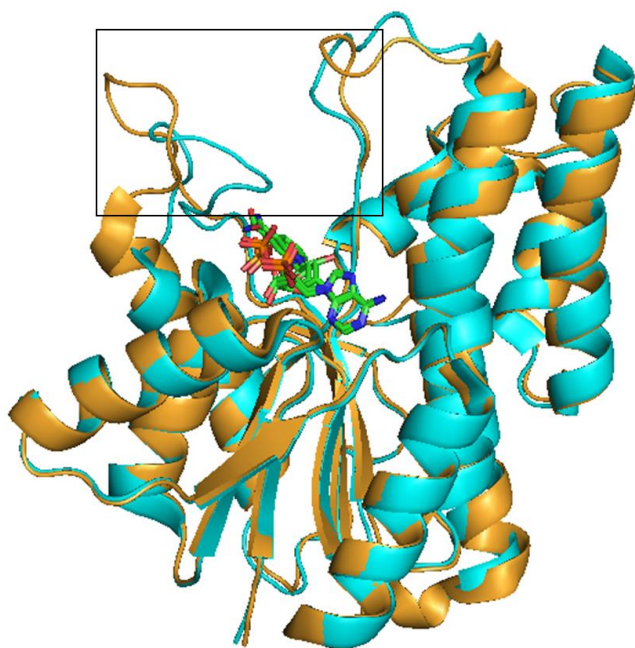


Figure A5. Superimposition of CBR1 (blue; PDB entry 2PFG) and CBR3 (orange; PDB entry 2HRB). CBR1 forms a barrier with a short segment of the substrate binding loop whereas CBR3 shows a rather open binding pocket. NADPH is depicted as sticks.

6. Acknowledgement

I would like to thank Prof. Alex Odermatt for his continuous support, valuable recommendations, stimulating discussions and for giving me the opportunity to perform this thesis in his laboratory. I thank Prof. Michael Arand for being the co-advisor within my thesis committee. Furthermore, I want to thank Prof. Daniela Schuster, her group members and particularly Dr. Anna Vuorinen, for giving me the opportunity to work as a trainee in her group, without them this whole thesis would not have been possible. I want to express my thanks to the group of Prof. Brian Walker and especially Dr. Ruth Morgan for their successful collaboration. I thank Dr. Klaus Seuwen for the collaboration in the oxysterol project. Additional thanks go my master students Murielle Bächler and Tanja Sommer for their work and contribution of important data. I thank my family for their continues support and finally also all members from the Molecular and Systems Toxicology group for their project suggestions, the discussions and the good time we had together.

7. References

- [1] Y. Kallberg, U. Oppermann, B. Persson, Classification of the short-chain dehydrogenase/reductase superfamily using hidden Markov models, *Febs J*, 277 (2010) 2375-2386.
- [2] H. Jornvall, J.O. Hoog, B. Persson, SDR and MDR: completed genome sequences show these protein families to be large, of old origin, and of complex nature, *FEBS Lett*, 445 (1999) 261-264.
- [3] C. Bhatia, S. Oerum, J. Bray, K.L. Kavanagh, N. Shafqat, W. Yue, U. Oppermann, Towards a systematic analysis of human short-chain dehydrogenases/reductases (SDR): Ligand identification and structure-activity relationships, *Chem Biol Interact*, 234 (2015) 114-125.
- [4] K.L. Kavanagh, H. Jornvall, B. Persson, U. Oppermann, Medium- and short-chain dehydrogenase/reductase gene and protein families: The SDR superfamily: Functional and structural diversity within a family of metabolic and regulatory enzymes, *Cell Mol Life Sci*, 65 (2008) 3895-3906.
- [5] A.M. Lesk, NAD-binding domains of dehydrogenases, *Curr Opin Struct Biol*, 5 (1995) 775-783.
- [6] I. Tsigelny, M.E. Baker, Structures important in NAD(P)(H) specificity for mammalian retinol and 11-Cis-retinol dehydrogenases, *Biochem Biophys Res Commun*, 226 (1996) 118-127.
- [7] I. Tsigelny, M.E. Baker, Structures important in mammalian 11 β - and 17 β -hydroxysteroid dehydrogenases, *J Steroid Biochem Mol Biol*, 55 (1995) 589-600.
- [8] M.J. Bennett, B.P. Schlegel, J.M. Jez, T.M. Penning, M. Lewis, Structure of 3 alpha-hydroxysteroid/dihydrodiol dehydrogenase complexed with NADP⁺, *Biochemistry*, 35 (1996) 10702-10711.
- [9] K.R. Beck, T. Kaserer, D. Schuster, A. Odermatt, Virtual screening applications in short-chain dehydrogenase/reductase research, *J Steroid Biochem Mol Biol*, 171 (2017) 157-177.
- [10] T. Kaserer, K.R. Beck, M. Akram, A. Odermatt, D. Schuster, Pharmacophore Models and Pharmacophore-Based Virtual Screening: Concepts and Applications Exemplified on Hydroxysteroid Dehydrogenases, *Molecules*, 20 (2015) 22799-22832.
- [11] B. Blumberg, T. Iguchi, A. Odermatt, Endocrine disrupting chemicals, *J Steroid Biochem Mol Biol*, 127 (2011) 1-3.
- [12] M.S. Attene-Ramos, N. Miller, R. Huang, S. Michael, M. Itkin, R.J. Kavlock, C.P. Austin, P. Shinn, A. Simeonov, R.R. Tice, M. Xia, The Tox21 robotic platform for the assessment of environmental chemicals - from vision to reality, *Drug Discov Today*, 18 (2013) 716-723.
- [13] F.M. Christensen, S.J. Eisenreich, K. Rasmussen, J.R. Sintes, B. Sokull-Kluettgen, E.J. Van de Plassche, European experience in chemicals management: integrating science into policy, *Environ Sci Technol*, 45 (2011) 80-89.
- [14] A.M. Richard, R.S. Judson, K.A. Houck, C.M. Grulke, P. Volarath, I. Thillainadarajah, C. Yang, J. Rathman, M.T. Martin, J.F. Wambaugh, T.B. Knudsen, J. Kancherla, K. Mansouri, G. Patlewicz, A.J. Williams, S.B. Little, K.M. Crofton, R.S. Thomas, ToxCast Chemical Landscape: Paving the Road to 21st Century Toxicology, *Chem Res Toxicol*, 29 (2016) 1225-1251.
- [15] W.L. Miller, R.J. Auchus, The molecular biology, biochemistry, and physiology of human steroidogenesis and its disorders, *Endocr Rev*, 32 (2011) 81-151.
- [16] J. Funder, K. Myles, Exclusion of corticosterone from epithelial mineralocorticoid receptors is insufficient for selectivity of aldosterone action: in vivo binding studies, *Endocrinology*, 137 (1996) 5264-5268.
- [17] J.L. Arriza, C. Weinberger, G. Cerelli, T.M. Glaser, B.L. Handelin, D.E. Housman, R.M. Evans, Cloning of human mineralocorticoid receptor complementary DNA: structural and functional kinship with the glucocorticoid receptor, *Science*, 237 (1987) 268-275.
- [18] Z.S. Krozowski, J.W. Funder, Renal mineralocorticoid receptors and hippocampal corticosterone-binding species have identical intrinsic steroid specificity, *Proc Natl Acad Sci U S A*, 80 (1983) 6056-6060.
- [19] C. Hellal-Levy, B. Couette, J. Fagart, A. Souque, C. Gomez-Sanchez, M. Rafestin-Oblin, Specific hydroxylations determine selective corticosteroid recognition by human glucocorticoid and mineralocorticoid receptors, *FEBS Lett*, 464 (1999) 9-13.

- [20] J.W. Funder, P.T. Pearce, R. Smith, A.I. Smith, Mineralocorticoid action: target tissue specificity is enzyme, not receptor, mediated, *Science*, 242 (1988) 583-585.
- [21] C.R. Edwards, P.M. Stewart, D. Burt, L. Brett, M.A. McIntyre, W.S. Sutanto, E.R. de Kloet, C. Monder, Localisation of 11 β -hydroxysteroid dehydrogenase - tissue specific protector of the mineralocorticoid receptor, *Lancet*, 2 (1988) 986-989.
- [22] P. Ferrari, The role of 11 β -hydroxysteroid dehydrogenase type 2 in human hypertension, *Biochim Biophys Acta*, 1802 (2010) 1178-1187.
- [23] M.I. New, L.S. Levine, E.G. Biglieri, J. Pareira, S. Ulick, Evidence for an unidentified steroid in a child with apparent mineralocorticoid hypertension, *J Clin Endocrinol Metab*, 44 (1977) 924-933.
- [24] T. Mune, F.M. Rogerson, H. Nikkila, A.K. Agarwal, P.C. White, Human hypertension caused by mutations in the kidney isozyme of 11 β -hydroxysteroid dehydrogenase, *Nat Genet*, 10 (1995) 394-399.
- [25] P.C. White, T. Mune, A.K. Agarwal, 11 beta-Hydroxysteroid dehydrogenase and the syndrome of apparent mineralocorticoid excess, *Endocr Rev*, 18 (1997) 135-156.
- [26] K.R. Beck, M. Bächler, A. Vuorinen, S. Wagner, M. Akram, U. Griesser, V. Temml, P. Klusonova, H. Yamaguchi, D. Schuster, A. Odermatt, Inhibition of 11 β -hydroxysteroid dehydrogenase 2 by the fungicides itraconazole and posaconazole, *Biochem Pharmacol*, 130 (2017) 93-103.
- [27] J.R. Seckl, Prenatal glucocorticoids and long-term programming, *Eur J Endocrinol*, 151 Suppl 3 (2004) U49-62.
- [28] J.L. Parker, S. Newstead, Membrane Protein Crystallisation: Current Trends and Future Perspectives, *Adv Exp Med Biol*, 922 (2016) 61-72.
- [29] T. Denolle, M. Azizi, C. Massart, M.C. Zennaro, Itraconazole: a new drug-related cause of hypertension, *Ann Cardiol Angeiol (Paris)*, 63 (2014) 213-215.
- [30] P.K. Sharkey, M.G. Rinaldi, J.F. Dunn, T.C. Hardin, R.J. Fetchick, J.R. Graybill, High-dose itraconazole in the treatment of severe mycoses, *Antimicrobial agents and chemotherapy*, 35 (1991) 707-713.
- [31] G.R. Thompson, 3rd, D. Chang, R.R. Wittenberg, I. McHardy, A. Semrad, In Vivo 11beta-Hydroxysteroid Dehydrogenase Inhibition in Posaconazole-Induced Hypertension and Hypokalemia, *Antimicrob Agents Chemother*, 61 (2017).
- [32] MSD-MERCK-SHARP&DOHME-AG, NOXAFIL Inf Konz 18 mg/ml drug safety sheet, (2014).
- [33] Janssen-Cilag-AG, Sporanox drug safety sheet, (2015).
- [34] G. Fanali, A. di Masi, V. Trezza, M. Marino, M. Fasano, P. Ascenzi, Human serum albumin: from bench to bedside, *Mol Aspects Med*, 33 (2012) 209-290.
- [35] O. Blennow, E. Eliasson, T. Pettersson, A. Pohanka, A. Szakos, I. El-Serafi, M. Hassan, O. Ringden, J. Mattsson, Posaconazole concentrations in human tissues after allogeneic stem cell transplantation, *Antimicrob Agents Chemother*, 58 (2014) 4941-4943.
- [36] L. Willems, R. van der Geest, K. de Beule, Itraconazole oral solution and intravenous formulations: a review of pharmacokinetics and pharmacodynamics, *J Clin Pharm Ther*, 26 (2001) 159-169.
- [37] D. Wexler, R. Courtney, W. Richards, C. Banfield, J. Lim, M. Laughlin, Effect of posaconazole on cytochrome P450 enzymes: a randomized, open-label, two-way crossover study, *Eur J Pharm Sci*, 21 (2004) 645-653.
- [38] A.H. Saad, D.D. DePestel, P.L. Carver, Factors influencing the magnitude and clinical significance of drug interactions between azole antifungals and select immunosuppressants, *Pharmacotherapy*, 26 (2006) 1730-1744.
- [39] A. Harris, J. Seckl, Glucocorticoids, prenatal stress and the programming of disease, *Horm Behav*, 59 (2011) 279-289.
- [40] C.S. Wyrwoll, J.R. Seckl, M.C. Holmes, Altered placental function of 11 β -hydroxysteroid dehydrogenase 2 knockout mice, *Endocrinology*, 150 (2009) 1287-1293.
- [41] J.R. Pace, A.M. DeBerardinis, V. Sail, S.K. Tacheva-Grigorova, K.A. Chan, R. Tran, D.S. Raccuia, R.J. Wechsler-Reya, M.K. Hadden, Repurposing the Clinically Efficacious Antifungal Agent Itraconazole as an Anticancer Chemotherapeutic, *J Med Chem*, 59 (2016) 3635-3649.
- [42] C.R. Chong, J. Xu, J. Lu, S. Bhat, D.J. Sullivan, Jr., J.O. Liu, Inhibition of angiogenesis by the antifungal drug itraconazole, *ACS Chem Biol*, 2 (2007) 263-270.

- [43] R. Del Carratore, A. Carpi, P. Befly, V. Lubrano, L. Giorgetti, B.E. Maserti, M.A. Carluccio, M. Simili, G. Iervasi, S. Balzan, Itraconazole inhibits HMEC-1 angiogenesis, *Biomed Pharmacother*, 66 (2012) 312-317.
- [44] V.M. Heine, D.H. Rowitch, Hedgehog signaling has a protective effect in glucocorticoid-induced mouse neonatal brain injury through an 11 β -HSD2-dependent mechanism, *J Clin Invest*, 119 (2009) 267-277.
- [45] J. Kim, J.Y. Tang, R. Gong, J.J. Lee, K.V. Clemons, C.R. Chong, K.S. Chang, M. Fereshteh, D. Gardner, T. Reya, J.O. Liu, E.H. Epstein, D.A. Stevens, P.A. Beachy, Itraconazole, a commonly used antifungal that inhibits Hedgehog pathway activity and cancer growth, *Cancer Cell*, 17 (2010) 388-399.
- [46] B. Chen, V. Trang, A. Lee, N.S. Williams, A.N. Wilson, E.H. Epstein, Jr., J.Y. Tang, J. Kim, Posaconazole, a Second-Generation Triazole Antifungal Drug, Inhibits the Hedgehog Signaling Pathway and Progression of Basal Cell Carcinoma, *Mol Cancer Ther*, 15 (2016) 866-876.
- [47] B.T. Heijmans, E.W. Tobi, A.D. Stein, H. Putter, G.J. Blauw, E.S. Susser, P.E. Slagboom, L.H. Lumey, Persistent epigenetic differences associated with prenatal exposure to famine in humans, *Proc Natl Acad Sci U S A*, 105 (2008) 17046-17049.
- [48] M.L. Lazo-de-la-Vega-Monroy, M.O. Solis-Martinez, G. Romero-Gutierrez, V.E. Aguirre-Arzola, K. Wrobel, K. Wrobel, S. Zaina, G. Barbosa-Sabanero, 11 β -hydroxysteroid dehydrogenase 2 promoter methylation is associated with placental protein expression in small for gestational age newborns, *Steroids*, 124 (2017) 60-66.
- [49] A.A. Appleton, D.A. Armstrong, C. Lesseur, J. Lee, J.F. Padbury, B.M. Lester, C.J. Marsit, Patterning in placental 11 β -hydroxysteroid dehydrogenase methylation according to prenatal socioeconomic adversity, *PLoS One*, 8 (2013) e74691.
- [50] X. Xiao, Y. Zhao, R. Jin, J. Chen, X. Wang, A. Baccarelli, Y. Zhang, Fetal growth restriction and methylation of growth-related genes in the placenta, *Epigenomics*, 8 (2016) 33-42.
- [51] A.J. Drake, R.C. McPherson, K.M. Godfrey, C. Cooper, K.A. Lillycrop, M.A. Hanson, R.R. Meehan, J.R. Seckl, R.M. Reynolds, An unbalanced maternal diet in pregnancy associates with offspring epigenetic changes in genes controlling glucocorticoid action and foetal growth, *Clin Endocrinol (Oxf)*, 77 (2012) 808-815.
- [52] C.J. Marsit, M.A. Maccani, J.F. Padbury, B.M. Lester, Placental 11-beta hydroxysteroid dehydrogenase methylation is associated with newborn growth and a measure of neurobehavioral outcome, *PLoS One*, 7 (2012) e33794.
- [53] A.J. Drake, B.R. Walker, J.R. Seckl, Intergenerational consequences of fetal programming by in utero exposure to glucocorticoids in rats, *Am J Physiol Regul Integr Comp Physiol*, 288 (2005) R34-38.
- [54] L.G. Nashev, D. Schuster, C. Laggner, S. Sodha, T. Langer, G. Wolber, A. Odermatt, The UV-filter benzophenone-1 inhibits 17 β -hydroxysteroid dehydrogenase type 3: Virtual screening as a strategy to identify potential endocrine disrupting chemicals, *Biochem. Pharmacol.*, 79 (2010) 1189-1199.
- [55] L. Wang, K. Kannan, Characteristic profiles of benzophenone-3 and its derivatives in urine of children and adults from the United States and China, *Environ. Sci. Technol.*, 47 (2013) 12532-12538.
- [56] L. Guo, S. Dial, L. Shi, W. Branham, J. Liu, J.L. Fang, B. Green, H. Deng, J. Kaput, B. Ning, Similarities and differences in the expression of drug-metabolizing enzymes between human hepatic cell lines and primary human hepatocytes, *Drug Metab Dispos*, 39 (2011) 528-538.
- [57] E.F. Brandon, C.D. Raap, I. Meijerman, J.H. Beijnen, J.H. Schellens, An update on in vitro test methods in human hepatic drug biotransformation research: pros and cons, *Toxicol Appl Pharmacol*, 189 (2003) 233-246.
- [58] K.R. Beck, T.J. Sommer, D. Schuster, A. Odermatt, Evaluation of tetrabromobisphenol A effects on human glucocorticoid and androgen receptors: A comparison of results from human- with yeast-based in vitro assays, *Toxicology*, 370 (2016) 70-77.
- [59] C.P. Wild, Complementing the genome with an "exposome": the outstanding challenge of environmental exposure measurement in molecular epidemiology, *Cancer Epidemiol Biomarkers Prev*, 14 (2005) 1847-1850.
- [60] C. Messerlian, R.M. Martinez, R. Hauser, A.A. Baccarelli, 'Omics' and endocrine-disrupting chemicals - new paths forward, *Nat Rev Endocrinol*, (2017).
- [61] Centers for Disease Control and Prevention, Exposome and Exposomics, <https://www.cdc.gov/niosh/topics/exposome/>, (2014).

- [62] D.G. DeBord, T. Carreon, T.J. Lentz, P.J. Middendorf, M.D. Hoover, P.A. Schulte, Use of the "Exposome" in the Practice of Epidemiology: A Primer on -Omic Technologies, *Am J Epidemiol*, 184 (2016) 302-314.
- [63] OECD, Guidance Document on Standardised Test Guidelines for Evaluating Chemicals for Endocrine Disruption - Series on Testing and Assessment No. 150, ENV/JM/MONO(2012)22, Environment Directorate Joint Meeting of the Chemicals Committee and the Working Party on Chemicals, Pesticides and Biotechnology, (2012).
- [64] M.J. Roelofs, M. van den Berg, T.F. Bovee, A.H. Piersma, M.B. van Duursen, Structural bisphenol analogues differentially target steroidogenesis in murine MA-10 Leydig cells as well as the glucocorticoid receptor, *Toxicology*, 329 (2015) 10-20.
- [65] G.A. Schoch, B. D'Arcy, M. Stihle, D. Burger, D. Bar, J. Benz, R. Thoma, A. Ruf, Molecular switch in the glucocorticoid receptor: active and passive antagonist conformations, *J Mol Biol*, 395 (2010) 568-577.
- [66] M.J. Garabedian, K.R. Yamamoto, Genetic dissection of the signaling domain of a mammalian steroid receptor in yeast, *Mol Biol Cell*, 3 (1992) 1245-1257.
- [67] D. Picard, M. Schena, K.R. Yamamoto, An inducible expression vector for both fission and budding yeast, *Gene*, 86 (1990) 257-261.
- [68] A. Kralli, S.P. Bohlen, K.R. Yamamoto, LEM1, an ATP-binding-cassette transporter, selectively modulates the biological potency of steroid hormones, *Proceedings of the National Academy of Sciences of the United States of America*, 92 (1995) 4701-4705.
- [69] A.C. Dankers, M.J. Roelofs, A.H. Piersma, F.C. Sweep, F.G. Russel, M. van den Berg, M.B. van Duursen, R. Masereeuw, Endocrine disruptors differentially target ATP-binding cassette transporters in the blood-testis barrier and affect Leydig cell testosterone secretion in vitro, *Toxicol Sci*, 136 (2013) 382-391.
- [70] J. Miao, Y. Cai, L. Pan, Z. Li, Molecular cloning and characterization of a MXR-related P-glycoprotein cDNA in scallop *Chlamys farreri*: transcriptional response to benzo(a)pyrene, tetrabromobisphenol A and endosulfan, *Ecotoxicol Environ Saf*, 110 (2014) 136-142.
- [71] D.L. Riggs, P.J. Roberts, S.C. Chirillo, J. Cheung-Flynn, V. Prapapanich, T. Ratajczak, R. Gaber, D. Picard, D.F. Smith, The Hsp90-binding peptidylprolyl isomerase FKBP52 potentiates glucocorticoid signaling in vivo, *Embo J*, 22 (2003) 1158-1167.
- [72] G.M. Nelson, V. Prapapanich, P.E. Carrigan, P.J. Roberts, D.L. Riggs, D.F. Smith, The heat shock protein 70 cochaperone hip enhances functional maturation of glucocorticoid receptor, *Mol Endocrinol*, 18 (2004) 1620-1630.
- [73] M. Carere, R. Kase, Science Policy Interface (SPI) action on "Effect-based and chemical analytical monitoring approaches for steroidal estrogens": project update and plans for NORMAN contribution in 2016, <http://www.normandata.eu/?q=node/285>, NORMAN 7th General Assembly Meeting PRESENTATIONS, Roma,, (2016).
- [74] T.B. Knudsen, D.A. Keller, M. Sander, E.W. Carney, N.G. Doerrer, D.L. Eaton, S.C. Fitzpatrick, K.L. Hastings, D.L. Mendrick, R.R. Tice, P.B. Watkins, M. Whelan, FutureTox II: in vitro data and in silico models for predictive toxicology, *Toxicol Sci*, 143 (2015) 256-267.
- [75] A. Covaci, S. Harrad, M.A. Abdallah, N. Ali, R.J. Law, D. Herzke, C.A. de Wit, Novel brominated flame retardants: a review of their analysis, environmental fate and behaviour, *Environ Int*, 37 (2011) 532-556.
- [76] T.T. Schug, R. Abagyan, B. Blumberg, T.J. Collins, D. Crews, P.L. DeFur, S.M. Dickerson, T.M. Edwards, A.C. Gore, L.J. Guillette, T. Hayes, J.J. Heindel, A. Moores, H.B. Patisaul, T.L. Tal, K.A. Thayer, L.N. Vandenberg, J. Warner, C.S. Watson, F.S. Saal, R.T. Zoeller, K.P. O'Brien, J.P. Myers, Designing Endocrine Disruption Out of the Next Generation of Chemicals, *Green Chem*, 15 (2013) 181-198.
- [77] M. Recanatini, G. Bottegoni, A. Cavalli, In silico antitarget screening, *Drug Discov Today Technol*, 1 (2004) 209-215.
- [78] A. Vuorinen, A. Odermatt, D. Schuster, In silico methods in the discovery of endocrine disrupting chemicals, *J Steroid Biochem Mol Biol*, 137 (2013) 18-26.
- [79] B. Persson, Y. Kallberg, J.E. Bray, E. Bruford, S.L. Dellaporta, A.D. Favia, R.G. Duarte, H. Jornvall, K.L. Kavanagh, N. Kedishvili, M. Kisiela, E. Maser, R. Mindnich, S. Orchard, T.M. Penning, J.M. Thornton, J. Adamski, U. Oppermann, The SDR (short-chain dehydrogenase/reductase and related enzymes) nomenclature initiative, *Chem Biol Interact*, 178 (2009) 94-98.

- [80] I. Beets, M. Lindemans, T. Janssen, P. Verleyen, Deorphanizing G protein-coupled receptors by a calcium mobilization assay, *Methods Mol Biol*, 789 (2011) 377-391.
- [81] E.P. Gomez-Sanchez, D.G. Romero, A.F. de Rodriguez, M.P. Warden, Z. Krozowski, C.E. Gomez-Sanchez, Hexose-6-phosphate dehydrogenase and 11 β -hydroxysteroid dehydrogenase-1 tissue distribution in the rat, *Endocrinology*, 149 (2008) 525-533.
- [82] A. Odermatt, P. Arnold, A. Stauffer, B.M. Frey, F.J. Frey, The N-terminal anchor sequences of 11 β -hydroxysteroid dehydrogenases determine their orientation in the endoplasmic reticulum membrane, *J Biol Chem*, 274 (1999) 28762-28770.
- [83] J. Ozols, Lumenal orientation and post-translational modifications of the liver microsomal 11 β -hydroxysteroid dehydrogenase, *J Biol Chem*, 270 (1995) 2305-2312.
- [84] A.G. Atanasov, L.G. Nashev, R.A. Schweizer, C. Frick, A. Odermatt, Hexose-6-phosphate dehydrogenase determines the reaction direction of 11 β -hydroxysteroid dehydrogenase type 1 as an oxoreductase, *FEBS Lett*, 571 (2004) 129-133.
- [85] G.G. Lavery, E.A. Walker, N. Draper, P. Jeyasuria, J. Marcos, C.H. Shackleton, K.L. Parker, P.C. White, P.M. Stewart, Hexose-6-phosphate dehydrogenase knock-out mice lack 11 β -hydroxysteroid dehydrogenase type 1-mediated glucocorticoid generation, *J Biol Chem*, 281 (2006) 6546-6551.
- [86] A.A. Dzyakanchuk, Z. Balazs, L.G. Nashev, K.E. Amrein, A. Odermatt, 11 β -Hydroxysteroid dehydrogenase 1 reductase activity is dependent on a high ratio of NADPH/NADP(+) and is stimulated by extracellular glucose, *Mol Cell Endocrinol*, 301 (2009) 137-141.
- [87] A.G. Atanasov, L.G. Nashev, L. Gelman, B. Legeza, R. Sack, R. Portmann, A. Odermatt, Direct protein-protein interaction of 11 β -hydroxysteroid dehydrogenase type 1 and hexose-6-phosphate dehydrogenase in the endoplasmic reticulum lumen, *Biochim Biophys Acta*, 1783 (2008) 1536-1543.
- [88] H. Masuzaki, J. Paterson, H. Shinyama, N.M. Morton, J.J. Mullins, J.R. Seckl, J.S. Flier, A transgenic model of visceral obesity and the metabolic syndrome, *Science*, 294 (2001) 2166-2170.
- [89] H. Masuzaki, H. Yamamoto, C.J. Kenyon, J.K. Elmquist, N.M. Morton, J.M. Paterson, H. Shinyama, M.G. Sharp, S. Fleming, J.J. Mullins, J.R. Seckl, J.S. Flier, Transgenic amplification of glucocorticoid action in adipose tissue causes high blood pressure in mice, *J. Clin. Invest.*, 112 (2003) 83-90.
- [90] R. Lathe, Y. Kotelevtsev, Steroid signaling: ligand-binding promiscuity, molecular symmetry, and the need for gating, *Steroids*, 82 (2014) 14-22.
- [91] R. Lathe, Steroid and sterol 7-hydroxylation: ancient pathways, *Steroids*, 67 (2002) 967-977.
- [92] S. Araya, D.V. Kratschmar, M. Tsachaki, S. Stucheli, K.R. Beck, A. Odermatt, DHRS7 (SDR34C1) - A new player in the regulation of androgen receptor function by inactivation of 5 α -dihydrotestosterone?, *J Steroid Biochem Mol Biol*, 171 (2017) 288-295.
- [93] A. Odermatt, L.G. Nashev, The glucocorticoid-activating enzyme 11 β -hydroxysteroid dehydrogenase type 1 has broad substrate specificity: Physiological and toxicological considerations, *J. Steroid Biochem. Mol. Biol.*, 119 (2010) 1-13.
- [94] F. Hoffmann, E. Maser, Carbonyl reductases and pluripotent hydroxysteroid dehydrogenases of the short-chain dehydrogenase/reductase superfamily, *Drug Metab Rev*, 39 (2007) 87-144.
- [95] A. Odermatt, T. Da Cunha, C.A. Penno, C. Chandsawangbhuwana, C. Reichert, A. Wolf, M. Dong, M.E. Baker, Hepatic reduction of the secondary bile acid 7-oxolithocholic acid is mediated by 11 β -hydroxysteroid dehydrogenase 1, *Biochem J*, 436 (2011) 621-629.
- [96] C.A. Penno, S.A. Morgan, A.J. Rose, S. Herzig, G.G. Lavery, A. Odermatt, 11 β -Hydroxysteroid dehydrogenase-1 is involved in bile acid homeostasis by modulating fatty acid transport protein-5 in the liver of mice, *Mol Metab*, 3 (2014) 554-564.
- [97] K.E. Chapman, A.E. Coutinho, Z. Zhang, T. Kipari, J.S. Savill, J.R. Seckl, Changing glucocorticoid action: 11 β -hydroxysteroid dehydrogenase type 1 in acute and chronic inflammation, *J Steroid Biochem Mol Biol*, 137 (2013) 82-92.
- [98] L. Zemanova, P. Kirubakaran, I.H. Pato, H. Stamberгова, J. Vondrasek, The identification of new substrates of human DHRS7 by molecular modeling and in vitro testing, *Int J Biol Macromol*, (2017).
- [99] A. Meyer, A. Vuorinen, A.E. Zielinska, P. Strajhar, G.G. Lavery, D. Schuster, A. Odermatt, Formation of threohydrobupropion from bupropion is dependent on 11 β -hydroxysteroid dehydrogenase 1, *Drug Metab Dispos*, 41 (2013) 1671-1678.

- [100] A. Vuorinen, L.G. Nashev, A. Odermatt, J.M. Rollinger, D. Schuster, Pharmacophore Model Refinement for 11 β -Hydroxysteroid Dehydrogenase Inhibitors: Search for Modulators of Intracellular Glucocorticoid Concentrations, *Mol Inform*, 33 (2014) 15-25.
- [101] P.C. Hawkins, A.G. Skillman, G.L. Warren, B.A. Ellingson, M.T. Stahl, Conformer generation with OMEGA: algorithm and validation using high quality structures from the Protein Databank and Cambridge Structural Database, *J Chem Inf Model*, 50 (2010) 572-584.
- [102] OMEGA2.2.3, OpenEye Scientific Software, Santa Fe, NM.
- [103] P.C. Hawkins, A. Nicholls, Conformer generation with OMEGA: learning from the data set and the analysis of failures, *J Chem Inf Model*, 52 (2012) 2919-2936.
- [104] G. Wolber, T. Langer, LigandScout: 3-D pharmacophores derived from protein-bound ligands and their use as virtual screening filters, *J Chem Inf Model*, 45 (2005) 160-169.
- [105] D.S. Wishart, T. Jewison, A.C. Guo, M. Wilson, C. Knox, Y. Liu, Y. Djoumbou, R. Mandal, F. Aziat, E. Dong, S. Bouatra, I. Sinelnikov, D. Arndt, J. Xia, P. Liu, F. Yallou, T. Bjorn Dahl, R. Perez-Pineiro, R. Eisner, F. Allen, V. Neveu, R. Greiner, A. Scalbert, HMDB 3.0--The Human Metabolome Database in 2013, *Nucleic Acids Res*, 41 (2013) D801-807.
- [106] D.S. Wishart, C. Knox, A.C. Guo, R. Eisner, N. Young, B. Gautam, D.D. Hau, N. Psychogios, E. Dong, S. Bouatra, R. Mandal, I. Sinelnikov, J. Xia, L. Jia, J.A. Cruz, E. Lim, C.A. Sobsey, S. Shrivastava, P. Huang, P. Liu, L. Fang, J. Peng, R. Fradette, D. Cheng, D. Tzur, M. Clements, A. Lewis, A. De Souza, A. Zuniga, M. Dawe, Y. Xiong, D. Clive, R. Greiner, A. Nazyrova, R. Shaykhtudinov, L. Li, H.J. Vogel, I. Forsythe, HMDB: a knowledgebase for the human metabolome, *Nucleic Acids Res*, 37 (2009) D603-610.
- [107] D.S. Wishart, D. Tzur, C. Knox, R. Eisner, A.C. Guo, N. Young, D. Cheng, K. Jewell, D. Arndt, S. Sawhney, C. Fung, L. Nikolai, M. Lewis, M.A. Coutouly, I. Forsythe, P. Tang, S. Shrivastava, K. Jeroncic, P. Stothard, G. Amegbey, D. Block, D.D. Hau, J. Wagner, J. Miniaci, M. Clements, M. Gebremedhin, N. Guo, Y. Zhang, G.E. Duggan, G.D. Macinnis, A.M. Weljie, R. Dowlatabadi, F. Bamforth, D. Clive, R. Greiner, L. Li, T. Marrie, B.D. Sykes, H.J. Vogel, L. Querengesser, HMDB: the Human Metabolome Database, *Nucleic Acids Res*, 35 (2007) D521-526.
- [108] M. Sud, E. Fahy, D. Cotter, A. Brown, E.A. Dennis, C.K. Glass, A.H. Merrill, Jr., R.C. Murphy, C.R. Raetz, D.W. Russell, S. Subramaniam, LMSD: LIPID MAPS structure database, *Nucleic Acids Res*, 35 (2007) D527-532.
- [109] E. Fahy, M. Sud, D. Cotter, S. Subramaniam, LIPID MAPS online tools for lipid research, *Nucleic Acids Res*, 35 (2007) W606-612.
- [110] G. Jones, P. Willett, R.C. Glen, A.R. Leach, R. Taylor, Development and validation of a genetic algorithm for flexible docking, *J Mol Biol*, 267 (1997) 727-748.
- [111] A. Vuorinen, R. Engeli, A. Meyer, F. Bachmann, U.J. Griesser, D. Schuster, A. Odermatt, Ligand-based pharmacophore modeling and virtual screening for the discovery of novel 17 β -hydroxysteroid dehydrogenase 2 inhibitors, *J Med Chem*, 57 (2014) 5995-6007.
- [112] A.G. Atanasov, A.A. Dzykanchuk, R.A. Schweizer, L.G. Nashev, E.M. Maurer, A. Odermatt, Coffee inhibits the reactivation of glucocorticoids by 11 β -hydroxysteroid dehydrogenase type 1: a glucocorticoid connection in the anti-diabetic action of coffee?, *FEBS Lett*, 580 (2006) 4081-4085.
- [113] D.V. Kratschmar, A. Vuorinen, T. Da Cunha, G. Wolber, D. Classen-Houben, O. Doblhoff, D. Schuster, A. Odermatt, Characterization of activity and binding mode of glycyrrhetic acid derivatives inhibiting 11 β -hydroxysteroid dehydrogenase type 2, *J Steroid Biochem Mol Biol*, 125 (2011) 129-142.
- [114] J.A. Doorn, E. Maser, A. Blum, D.J. Claffey, D.R. Petersen, Human carbonyl reductase catalyzes reduction of 4-oxonon-2-enal, *Biochemistry*, 43 (2004) 13106-13114.
- [115] U. Oppermann, Carbonyl reductases: the complex relationships of mammalian carbonyl- and quinone-reducing enzymes and their role in physiology, *Annu Rev Pharmacol Toxicol*, 47 (2007) 293-322.
- [116] A. Odermatt, P. Klusonova, 11 β -Hydroxysteroid dehydrogenase 1: Regeneration of active glucocorticoids is only part of the story, *J Steroid Biochem Mol Biol*, 151 (2015) 85-92.
- [117] M. Kanehisa, M. Furumichi, M. Tanabe, Y. Sato, K. Morishima, KEGG: new perspectives on genomes, pathways, diseases and drugs, *Nucleic Acids Res*, 45 (2017) D353-D361.
- [118] M. Kanehisa, Y. Sato, M. Kawashima, M. Furumichi, M. Tanabe, KEGG as a reference resource for gene and protein annotation, *Nucleic Acids Res*, 44 (2016) D457-462.

- [119] M. Kanehisa, S. Goto, KEGG: kyoto encyclopedia of genes and genomes, *Nucleic Acids Res*, 28 (2000) 27-30.
- [120] Tryptophan Metabolism, <http://www.genome.jp/kegg/pathway/map/map00380.html>, August 2017.
- [121] L.R. Kolodziej, E.M. Paleolog, R.O. Williams, Kynurenine metabolism in health and disease, *Amino Acids*, 41 (2011) 1173-1183.
- [122] T.W. Stone, N. Stoy, L.G. Darlington, An expanding range of targets for kynurenine metabolites of tryptophan, *Trends Pharmacol Sci*, 34 (2013) 136-143.
- [123] D.A. Bender, E.N. Njagi, P.S. Danielian, Tryptophan metabolism in vitamin B6-deficient mice, *Br J Nutr*, 63 (1990) 27-36.
- [124] K.A. Polyzos, D.F. Ketelhuth, The role of the kynurenine pathway of tryptophan metabolism in cardiovascular disease. An emerging field, *Hamostaseologie*, 35 (2015) 128-136.
- [125] G. Oxenkrug, Insulin resistance and dysregulation of tryptophan-kynurenine and kynurenine-nicotinamide adenine dinucleotide metabolic pathways, *Mol Neurobiol*, 48 (2013) 294-301.
- [126] P. Song, T. Ramprasath, H. Wang, M.H. Zou, Abnormal kynurenine pathway of tryptophan catabolism in cardiovascular diseases, *Cell Mol Life Sci*, 74 (2017) 2899-2916.
- [127] L. Zhang, O. Ovchinnikova, A. Jonsson, A.M. Lundberg, M. Berg, G.K. Hansson, D.F. Ketelhuth, The tryptophan metabolite 3-hydroxyanthranilic acid lowers plasma lipids and decreases atherosclerosis in hypercholesterolaemic mice, *Eur Heart J*, 33 (2012) 2025-2034.
- [128] J.E. Bray, B.D. Marsden, U. Oppermann, The human short-chain dehydrogenase/reductase (SDR) superfamily: a bioinformatics summary, *Chem Biol Interact*, 178 (2009) 99-109.
- [129] J.K. Seibert, L. Quagliata, C. Quintavalle, T.G. Hammond, L. Terracciano, A. Odermatt, A role for the dehydrogenase DHRS7 (SDR34C1) in prostate cancer, *Cancer Med*, 4 (2015) 1717-1729.
- [130] T.L. Romanuik, G. Wang, O. Morozova, A. Delaney, M.A. Marra, M.D. Sadar, LNCaP Atlas: gene expression associated with in vivo progression to castration-recurrent prostate cancer, *BMC Med Genomics*, 3 (2010) 43.
- [131] H. Stambergova, L. Skarydova, J.E. Dunford, V. Wsol, Biochemical properties of human dehydrogenase/reductase (SDR family) member 7, *Chem Biol Interact*, 207 (2014) 52-57.
- [132] H. Stambergova, L. Zemanova, T. Lundova, B. Malcekova, A. Skarka, M. Safr, V. Wsol, Human DHRS7, promising enzyme in metabolism of steroids and retinoids?, *J Steroid Biochem Mol Biol*, 155 (2016) 112-119.
- [133] A. Skarka, L. Skarydova, H. Stambergova, V. Wsol, Purification and reconstitution of human membrane-bound DHRS7 (SDR34C1) from Sf9 cells, *Protein Expr Purif*, 95 (2014) 44-49.
- [134] M. Biasini, S. Bienert, A. Waterhouse, K. Arnold, G. Studer, T. Schmidt, F. Kiefer, T. Gallo Cassarino, M. Bertoni, L. Bordoli, T. Schwede, SWISS-MODEL: modelling protein tertiary and quaternary structure using evolutionary information, *Nucleic Acids Res*, 42 (2014) W252-258.
- [135] F. Kiefer, K. Arnold, M. Kunzli, L. Bordoli, T. Schwede, The SWISS-MODEL Repository and associated resources, *Nucleic Acids Res*, 37 (2009) D387-392.
- [136] K. Arnold, L. Bordoli, J. Kopp, T. Schwede, The SWISS-MODEL workspace: a web-based environment for protein structure homology modelling, *Bioinformatics*, 22 (2006) 195-201.
- [137] N. Guex, M.C. Peitsch, T. Schwede, Automated comparative protein structure modeling with SWISS-MODEL and Swiss-PdbViewer: a historical perspective, *Electrophoresis*, 30 Suppl 1 (2009) S162-173.
- [138] Chemical Computing Group Inc., Montreal, QC, Canada (2011.10).
- [139] L.E. Olson, D. Bedja, S.J. Alvey, A.J. Cardounel, K.L. Gabrielson, R.H. Reeves, Protection from doxorubicin-induced cardiac toxicity in mice with a null allele of carbonyl reductase 1, *Cancer Res*, 63 (2003) 6602-6606.
- [140] P. Malatkova, E. Maser, V. Wsol, Human carbonyl reductases, *Curr Drug Metab*, 11 (2010) 639-658.
- [141] R.L. Bateman, D. Rauh, B. Tavshanjian, K.M. Shokat, Human carbonyl reductase 1 is an S-nitrosoglutathione reductase, *J Biol Chem*, 283 (2008) 35756-35762.
- [142] B. Wermuth, Purification and properties of an NADPH-dependent carbonyl reductase from human brain. Relationship to prostaglandin 9-ketoreductase and xenobiotic ketone reductase, *J Biol Chem*, 256 (1981) 1206-1213.
- [143] G.L. Forrest, B. Gonzalez, Carbonyl reductase, *Chem Biol Interact*, 129 (2000) 21-40.

- [144] S.M. Shi, L. Di, The role of carbonyl reductase 1 in drug discovery and development, *Expert Opin Drug Metab Toxicol*, 13 (2017) 859-870.
- [145] M.P. Jacobson, C. Kalyanaraman, S. Zhao, B. Tian, Leveraging structure for enzyme function prediction: methods, opportunities, and challenges, *Trends Biochem Sci*, 39 (2014) 363-371.
- [146] T. Kaserer, M. Höferl, K. Müller, S. Elmer, M. Ganzera, W. Jäger, D. Schuster, In silico predictions of drug-drug interactions caused by CYP1A2, 2C9, and 3A4 inhibition - a comparative study of virtual screening performance, *Mol. Inf.*, 34 (2015) 431– 457.
- [147] V. Temml, C.V. Voss, V.M. Dirsch, D. Schuster, Discovery of new liver X receptor agonists by pharmacophore modeling and shape-based virtual screening, *J. Chem. Inf. Model.*, 54 (2014) 367-371.
- [148] J.B. Cross, D.C. Thompson, B.K. Rai, J.C. Baber, K.Y. Fan, Y. Hu, C. Humblet, Comparison of several molecular docking programs: pose prediction and virtual screening accuracy, *Journal of chemical information and modeling*, 49 (2009) 1455-1474.
- [149] T. Miura, T. Nishinaka, T. Terada, Different functions between human monomeric carbonyl reductase 3 and carbonyl reductase 1, *Mol Cell Biochem*, 315 (2008) 113-121.
- [150] E.S. Pilka, F.H. Niesen, W.H. Lee, Y. El-Hawari, J.E. Dunford, G. Kochan, V. Wsol, H.J. Martin, E. Maser, U. Oppermann, Structural basis for substrate specificity in human monomeric carbonyl reductases, *PLoS One*, 4 (2009) e7113.
- [151] M.A. Koch, L.O. Wittenberg, S. Basu, D.A. Jeyaraj, E. Gourzoulidou, K. Reinecke, A. Odermatt, H. Waldmann, Compound library development guided by protein structure similarity clustering and natural product structure, *Proc. Natl. Acad. Sci. U. S. A.*, 101 (2004) 16721-16726.
- [152] Arachidonic Acid Metabolism, <http://www.genome.jp/kegg/pathway/map/map00590.html>, August 2017.